Toward Realistic Wireless Cooperative Communications Networks

Mohammed-Taha O. El Astal

June, 2015

University of Tasmania

School of Engineering
Faculty of Science, Engineering & Technology

Wireless Communications Engineering

Toward Realistic Wireless Cooperative Communications Networks

By

Mohammed-Taha O. El Astal

M.Sc. in Electrical Engineering/Communications Systems
B.Sc. in Electrical Engineering(Commun. and Control)

A thesis is submitted in fulfillment of the requirements for the degree of Doctor of Philosophy in Electrical Engineering/ Wireless Communications systems

Supervisor
Prof. J.C. Olivier

Revised June 20 2015
January 1 2015

Mohammed-Taha O. El Astal
Toward Realistic Wireless Cooperative Communications Networks
Wireless Communications Engineering, June, 2015
Supervisors: Prof. J.C. Olivier **University of Tasmania**
Electronics & Communication, Computer System Engineering
Faculty of Science, Engineering & Technology
School of Engineering
PrivateBag 65
7001 and Hobart

Declaration

Declaration of Originality

This thesis contains no material which has been accepted for a degree or diploma by the University or any other institution, except by way of background information and duly acknowledged in the thesis, and to the best of the my knowledge and belief no material previously published or written by another person except where due acknowledgment is made in the text of the thesis, nor does the thesis contain any material that infringes copyright.

Hobart, June, 2015

Mohammed-Taha O. El Astal

Authority of Access

Authority of Access

Hobart, June, 2015

Published works copyright

Statement regarding published work contained in thesis

The publishers of the papers comprising Chapters 3 to 7 hold the copyright for that content, and access to the material should be sought from the respective journals. The remaining non published content of the thesis may be made available for loan and limited copying and communication in accordance with the Copyright Act 1968."

Hobart, June, 2015

Abstract

Recently, the space-time block codes (STBCs) were suggested to use in wireless relaying networks (WRNs), denoted as distributed-STBCs (D-STBCs). This is to exploit effectively the spatial diversity and hence improve the link reliability. In addition, this usage may increase the network's spectrum efficiency as it allows concurrent transmission from the relaying nodes. However, these networks encounter numerous issues that limit their wide practical use. This thesis addresses three critical issues of WRNs, and proposes solutions for each part individually.

In Part I, WRNs are considered under imperfect synchronization. In the literature, most research tends to assume perfect synchronization among the cooperative relays. Unfortunately, this level of synchronization is almost impossible to achieve in real communication networks, and this introduces a significant performance degradation if imperfect synchronization is present in the network. This part includes mathematical models that are derived for WRNs, either one-way or two-way, under imperfect synchronisation conditions. Unlike existing models, this model provides a simple method of evaluating the problem for variant network configurations. In addition, this model considers the WRNs with N relays, each is equipped with R_a antennas, where $N, R_a \in \mathbb{N}^+$. With respect to current literature, the contributions of this part are : (1) both the existing PIC and SIC based detectors, which were proposed for specific network configurations instances, are extended here to work with the general model. (2) an enhanced interference cancellation based detector (EIC) is proposed. These proposed detectors shows significant performance improvement compared to the conventional detector under imperfect synchronisation conditions. In addition, the proposed EIC detector provides better improvement due to the designed interference cancellation process. It reduces the reliance on low-performance symbols and it benefits from interference components of currently-detected symbols using a modified maximum likelihood (ML) scheme. Accordingly, an extra performance improvement is achieved, particularly in the first iteration.

Part II considers the issue of designing D-STBCs for WRNs with an arbitrary number of relays. It has been shown that the reliability of WRNs increases by adding more relays as

a result of more communication paths becoming available. Unlike most existing D-STBCs, this part proposes two high rate coding schemes to accommodate an arbitrary number of relays, while retaining low decoding complexity at the destination. The first scheme, full-rate distributed space-time block coded-joint transmit/receive antenna diversity (D-STBC-JTRD), is proposed for AF WRNs. Its code rate is independent of the number of relays and hence no code rate loss is incurred as the relays number increases. In addition, this scheme deploys the same encoding matrices at every relay; this eliminates the need for additional network overhead to coordinate the code generation by the relays. In other words, there is no need to interrupt the transmission if a relay has been up/down. The second scheme aims to find a flexible trade-off between reliability and code-rate that can be offered by DF networks. Towards this end, a method to construct a D-STBC that is combined with spatial modulation (SM), denoted as D-STBC-SM, is proposed. This method is not restricted to a specific number of relays and can be constructed as necessary. In addition, a novel adaptive transmission protocol that uses the constructed codes, is proposed to achieve higher space diversity gain, even with relays equipped with a single antenna. Unlike most existing schemes, this protocol offers a throughput that increases as the number of relays increases. Moreover, the offered throughput is achieved using the same total average transmit energy, as only N_0 of the N available participating relays are active at any given time.

In Part III, the multi-user interference of WRNs is considered. Two transmission protocols with an interference cancellation scheme are proposed: the *concurrent*$_{S-R-D}$*-PIC*$_{R,D}$ protocol for DF WRNs and the *concurrent*$_{S-R-D}$*-PIC*$_{D}$ protocol for AF WRNs. Unlike existing protocols, these protocols allow the concurrent transmission in both phases of the transmission. Thus, high spectral efficiency is offered while maintaining low decoding complexity. This low decoding complexity is maintained due to the adaptation of the partial interference cancellation group decoding (PICGD) approach for WRNs, which was initially proposed by Guo, *et al.*, for point-to-point (P2P) communication link. For a WRN consisting of J users equipped each with J_a-antenna, a single half duplex (HD) R_a-antenna relay, and M-antenna destination, the *concurrent*$_{S-R-D}$*-PIC*$_{R,D}$ protocol achieves the *interference-free* diversity gain (i.e., $R_a \times \min\{J_a, M\}$) without imposing any conditions on a node's antenna number. The *interference-free* is the diversity gain achieved, assuming that each user in the network is transmitting solely without experiencing any interference from other users, hence it is considered as the natural upper bound of the diversity gain in multi-user WRNs. Similar to most exiting protocols, this protocol requires the CSI of the users-relay links at the relay. In contrast, the *concurrent*$_{S-R-D}$*-PIC*$_{R,D}$ protocol achieves a diversity gain of $J_a \times M$, given

that $R_a > 8$, while the CSI is required only at the destination. Although the diversity's upper bound is not achieved, this protocol uses a simple relay as no CSI or encoding is required at the relay. In addition, and unlike the existing protocols, the achievable diversity gain is determined by both J_a and M and it is not sacrificed while J is increased. This part also establishes sufficient conditions for an STBC to achieve the prior mentioned diversity gains, when the PICGD approach is employed by multi-users WRNs.

Dedicated

To my country, Palestine
Where I have grown.

To my parents
Who have given me endless support.

To my wife and sisters
Who encouraged me through this work.

To my daughters and son,
Arjan, Eliaan and Omar, for their lovely smiles.

Acknowledgement

I still remember the feeling of gladness, when I was accepted as a PhD student and was preparing to come to Australia for carrying out the studies in April 2012. Now this stunning journey is about to end and I am feeling very delighted that I have accomplished this period of life. Praise be to Allah Almighty, the most gracious and the most merciful, without his blessing and guidance my accomplishments would never have been possible. There is a long list of persons who have supported me during my PhD studies in different ways. I would like to take advantage of this opportunity to acknowledge them.

First and foremost, I would express my sincere gratitude supervisor Prof. J.C. Olivier, for providing me a chance to study as graduate student. I greatly appreciate his generosity in sharing his expertise and time in our frequent discussions which always help to clarify my thoughts and inspire me a lot. I would also like to thank Dr. Danchi Jiang, my secondary supervisor, and Dr. Brian Salmon for their technical inspiring discussion. I would like to extend my appreciation to Prof. Mohamed-Slim Alouini from KAUST university, Dr. Amr Ismail from Toshiba Telecommunications Research Laboratory (TRL) in UK and Dr. Ammar Abu-Hadrouss from IUG university for being coauthors in my publications, and spending time to review the work and adding the valuable comments. I would like to express my gratitude to Prof. Hassan S. Ashour and Eng. Obada Abdallah for their numerous technical discussions and suggestions that have found their way into this dissertation.

I am thankful to all my friends here and at home for their encouragement and help. I am extremely grateful to my bosses at my place of work at home, for allowing me to proceed for PhD studies abroad. My deepest gratitude and love belongs to my parents, sisters, my beloved wife and children, for their tremendous understanding, support, care, encouragement, and love during this long-term study.

Contents

List of Figures

List of Tables

List of Abbreviations

3GP-LTE	Third Generation Partnership Project
ADC	Analog-to-Digital Converter
AF	Amplify-and-Forward
APM	Amplitude/Phase Modulation
AWGN	Additive Wide Guassian Noise
BER	Bit Error Rate
BPSK	Binary Phase Shift Keying
CDF	Cumulative Distribution Function
CGD	Coding Gain Distance
CL-EO-STBC	Close Loop Extended Orthogonal STBC
CP	Cyclic Prefix
CRC	Cyclic Redundancy Check
CSI	Channel State Information
DAC	Digital-to-Analog Converter
D-CL-EO-STBC	Distributed CL-EO-STBC
DF	Decode-and-Forward
D-QO-STBC	Distributed-QO-STBC
D-STBC	Distributed STBC
D-STBC-JTRD	Distributed STBC-JTRD
D-STBC-SM	Distributed STBC-SM
DT	Direct Transmission
ECC	Error Control Code
EGC	Equal Gain Combining
EIC	Enhanced Interference Cancellation
FD	Full-Duplex
FDMA	Frequency Division Multiple Access

GSM	Global System for Mobile
HD	Half-Duplex
IC	INterference Cancellation
MAC	Multiple Access Control
MGF	Moment Generating Function
MIMO	Multiple-Input Multiple-Output
MISO	Multiple-Input Single-Output
ML	Maximum Likelihood
MLSE	Maximum Likelihood Sequence Estimation
MRC	Maximal Ratio Combining
OFDM	Orthogonal Frequency Division Multiplexing
OSTBC	Orthogonal STBC
OWRN	One-way Wireless Relaying Network
P2P	Point-to-Point
PDF	Probability Density Function
PEP	Pairwise Error Probability
PIC	Parallel Interference Cancellation
PICGD	Partial Interference Cancellation Group Decoding
PSD	Power Spectral Density
PSK	Phase Shift Keying
PSW	Pulse Shape Waveform
QAM	Quadrature Amplitude Modulation
QO-STBC	Quasi-Orthognal STBC
QPSK	Quadrature Phase Shift Keying
RC	Reduced Complexity
SAF	Selective Amplify-and-Forward
SDF	Selective Decode-and-Forward
SIC	Successive Interference Cancellation
SIMO	Single-Output Multiple-Input
SISO	Single-Output Single-Output
SNR	Signal-to-Noise Ratio
SSC	Selection and Stay Combining
STBC	Space-Time Block Code
STC	Space-Time Code
STTC	Space-Time Trellis Code

TDMA	Time Division Multiple Access
TWRN	Two-way Wireless Relaying Network
WRN	Wireless Relaying Network
ZF	Zero Forcing

Publication List

Journal articles:

- El Astal, M.-T. O.;Olivier, J.C.: "Improved Signal Detection for Two-Way Wireless Relaying Networks under Imperfect-Time Synchronisation," in **EURASIP Journal on Advances in Signal Processing**, 1, 2014, pp.-177. URL: click here.

- El Astal, M.-T. O.; Abu-Hudrouss, A.M.; Olivier, J.C.: "Improved Signal Detection of Wireless Relaying Networks employing Space-Time Block Codes under Imperfect Synchronization," in **Wireless Personal Communications**, Springer US, 2014, pp.1-18. DOI:10.1007/s11277-014-2239-4. URL: click here.

- El Astal, M.-T. O.; Salmon, B. P.; Olivier, J.C.: "Full-space diversity and full-rate distributed space–time block codes for amplify-and-forward relaying networks," in **IET Journal of Engineering**, IET, 2014, DOI: 10.1049/joe.2014.0063. URL: click here.

- El Astal, M.-T. O.; Abu-Hudrouss, A.M.; Salmon, B.P.; Olivier, J.C.: "An adaptive transmission protocol for exploiting diversity and multiplexing gains in wireless relaying networks," in **EURASIP Journal on Wireless Communications and Networking**,2015:1-15. URL: click here.

- El Astal, M.-T. O.; Ismail, A.; Alouini, M.-S. ; Olivier, J. C.: "Low-Complexity and Full-Diversity Partial Interference Cancellation for Multi-User Wireless Relaying Networks," *re-submitted* in **IEEE Transactions on Vehicular Technology**.

Conference articles:

- El Astal, M.-T. O.; Salmon, B.P.;Olivier, J.C.: "Distributed Space-Time Block Coding for Two-Way Wireless Relaying Networks: Improved Performance under Imperfect

Synchronization," in **IEEE Wireless Communications and Networking conference (WCNC)**, Istanbul, Turkey, pp.1176 - 1181, 6-9 Apr. 2014. URL: click here.

- El Astal, M.-T.O.; Salmon, B.P.;Olivier, J.C.: "Distributed Space-Time Codes for Amplify-and-Forward Relaying Networks," in **IEEE Wireless Communications and Networking conference (WCNC)**, Istanbul, Turkey, pp.1166-1169, 6-9 Apr. 2014. URL: click here.

- El Astal, M.-T.; Ismail, A.; Alouini, M.-S. ; Olivier, J. C.: "Full-diversity partial interference cancellation for multi-user wireless relaying networks," in the **7th International Conference on Signal Processing and Communication Systems-ICSPCS 2013**, Gold coast, Australia, pp.1-6,16-18 Dec. 2013. URL: click here.

- El Astal, M.-T. O.; Olivier, J.C.: "Distributed Closed-Loop Extended Orthogonal STBC: Improved performance in imperfect synchronization," in **IEEE 24th International Symposium on Personal Indoor and Mobile Radio Communications (PIMRC)**, London, UK, pp.1941-1945, 8-11 Sept. 2013. URL: click here.

- El Astal, M.-T. O.; Olivier, J.C.: "Distributed orthogonal STBC for amplify and forward cooperative network under imperfect synchronization," in **IEEE 14th International Conference on Communication Technology (ICCT)**, Chengdu, China, pp.364-368, 9-11 Nov. 2012. URL: click here.

1 Introduction

> *Excellence is not a skill. It is an attitude.*
>
> **— Ralph Marston**
>
> (Writer)

1.1 Introduction and Motivation

The introduction of wireless communication networks during the last decade of the previous century changed the way modern society works and lives, and has impacted most social and economical aspects of the modern world. Besides traditional communication services, the pervasive use of wireless communication networks has improved people's well-being through a range of applications that are available today. Nevertheless, a remaining challenge in wireless communication systems design is the provision of high reliability and throughput given limited wireless channel resources. Demand for various emergent services, such as broadband Internet and media streaming has consistently been increasing over the last 20 years and thus the current need for reliable and high-rate wireless communications systems is more important than ever. For example, the IEEE 802.20 standard [1] requires rates of 260 Mbps and 60 Mbps for the down- link and the uplink, respectively.

While propagating through the channel, the signal arrives at the destination via multiple paths, and each signal component generally experiences a different propagation channel. These multi-path signals can be destructive and may result in a significant performance degradation and low data rate and is referred to as signal fading [2, 3]. Hence diversity schemes have been introduced to combat the signal fading in a wireless channel. The basic idea is to receive a number of independent (uncorrelated) faded copies of the transmitted signal hoping that jointly processing the received signals can lead to reliable detection. The diversity schemes include spatial diversity, time diversity and frequency diversity. It is also possible to combine two or more of the mentioned diversity schemes in order to further improve the achieved performance [2, 3]. Space diversity has seen much research interest

in the last few decades due to expectations of reliability and rate improvement. These methods use multiple antennas at the transmitter and/or receiver to provide multiple uncorrelated received signals at the destination. This technology is referred to as multiple-input multiple-output (MIMO) schemes.

However, size and cost limitations may make the deployment of multiple antennas impractical in many wireless communications systems. Therefore, a new transmission scheme has been proposed to overcome these limitations [4, 5]. This scheme encourages neighbouring multiple client apparatus to share their resources cooperatively with the transmitter in order to construct a distributed antenna array. Accordingly, multiple signal copies that are affected by different independent fading paths can be received by the destination, hence *virtual* MIMO scheme is created without facing the difficulties of physical deployment. As with other diversity schemes, the destination then tries to combine all the received signals in order to enhance the detection performance. Networks that use this diversity scheme are referred to as cooperative communication networks or wireless relaying networks (WRNs) [4–7]. Generally, WRNs consists of a source, N relays, and a destination. These nodes are equipped with J_a, R_a, and M antenna, respectively, where $N, R_a, M \in \mathbb{N}^+$. The networks are classified according to the protocol type that is followed by the relays. Two cooperative (relaying) protocols that are extensively studied in the literature are: amplify-and-forward (AF) and decode-and-forward (DF) [4–9]. With AF, relays receive noisy versions of the source's signal, then amplify and re-transmit to the destination. With DF, relays decode the source's data, re-encode and re-transmit to the destination. In [6], the idea of space-time block coding (STBC) devised for MIMO was applied to the problem of communication over WRNs. This is known as a Distributed STBC (D-STBC), as the STBC is conducted in a distributive manner [6]. It has been shown that the D-STBCs have high potential to both exploit the diversity gain inherent in a wireless relaying communication channel, and to provide a notable coding gain [6, 10, 11]. For example, with two single-antenna relays and single-antenna destination, an achieved pairwise error probability (PEP) inversely proportional to square of signal-to-noise ratio (SNR^2) is obtained if Alamouti's STC scheme of [12] is used, where the achieved PEP is inversely proportional to SNR when no coding scheme is used [13].

In this thesis, three problems of WRNs that delimit their ability to be established in a wide manner are investigated. In Part I, three enhanced detectors are proposed to combat the experienced performance degradation due to imperfect synchronisation. Part II proposes two high rate coding schemes to accommodate an arbitrary number of relays while retaining low decoding complexity at the destination. Finally, two full-diversity transmission protocols

for multi-users WRNs are introduced. Unlike existing protocols, these protocols offer high spectral efficiency while maintaining low decoding complexity.

1.2 Problem statements

This thesis investigates three problems of WRNs and hence three statements are introduced

1. **Part I problem statement**: In WRNs, the assumed perfect synchronisation among the random-located cooperative relays is unlikely to be achieved [14, 15]. This lack of common timing reference badly influences system performance as the orthogonality of used D-STBC's is compromised at the destination.

2. **Part II problem statement**: A trade-off in D-STBC design is between a decrease in the code rate and the need to retain the single-symbol decoding complexity when more relays are need to be utilised.

3. **Part III problem statement**: The use of concurrent transmissions is needed in multi-user WRNs in order to offer high bandwidth efficiency. However, the resulting multi-user interference may cause a significant performance degradation.

1.3 Thesis Contributions

Analysis, illustrations and results are provided separately for each issue. In Part I, the WRNs, either one-way or two-way networks, are considered under the assumption of imperfect-time synchronisation conditions. Part II consider the scalability issue of the WRNs. Finally, the multi-user interference issue of either AF or DF WRNs, while maintaining high performance is considered in Part III.

In the following, a brief summary on the contribution of each part will be described.

1.3.1 Part I: Wireless Relaying Networks under Imperfect Synchronisation

In this part, the WRNs are considered under imperfect synchronisation conditions. Mathematical models are derived for WRNs, either one-way or two-way. Unlike the literature, this model provides a simple method of evaluating the problem for variant network configurations. With respect to current literature, the contributions of this part are : (1) both the existing PIC and SIC based detectors, which were proposed for specific network configurations instances, are extended here to work with the general model. (2) an enhanced interference cancellation based detector (EIC) is proposed. These proposed detectors shows significant performance improvement compared to the conventional detector under imperfect synchronisation conditions.

Part I publications:

- El Astal, M.-T. O.; Olivier, J.C.: "Improved Signal Detection for Two-Way Wireless Relaying Networks under Imperfect-Time Synchronisation," in **EURASIP Journal on Advances in Signal Processing**, 1, 2014, pp. 177.

- El Astal, M.-T. O.; Abu-Hudrouss, A.M.; Olivier, J.C.: "Improved Signal Detection of Wireless Relaying Networks employing Space-Time Block Codes under Imperfect Synchronisation," in **Wireless Personal Communications**, Springer US, 2014, pp.1-18. DOI:10.1007/s11277-014-2239-4.

- El Astal, M.-T. O. ; Salmon, B.P.; Olivier, J.C.: "Distributed Space-Time Block Coding for Two-Way Wireless Relaying Networks: Improved Performance under Imperfect Synchronisation," 2014 **IEEE Wireless Communications and Networking conference (WCNC)**, Istanbul, Turkey, pp.1176 - 1181, 6-9 Apr. 2014.

- El Astal, M.-T. O.; Olivier, J.C.: "Distributed Closed-Loop Extended Orthogonal STBC: Improved performance in imperfect synchronisation," 2013 **IEEE 24th International Symposium on Personal Indoor and Mobile Radio Communications (PIMRC)**, London, UK, pp.1941-1945, 8-11 Sept. 2013.

- El Astal, M.-T. O.; Olivier, J.C.: "Distributed orthogonal STBC for amplify and forward cooperative network under imperfect synchronisation," 2012 **IEEE 14th In-**

ternational Conference on Communication Technology (ICCT), Chengdu, China, pp.364-368, 9-11 Nov. 2012.

1.3.2 Part II: Scalable Wireless Relaying Networks

Unlike most existing D-STBCs, this part proposes two high rate coding schemes to accommodate an arbitrary number of relays, while retaining low decoding complexity at the destination. The first scheme, full-rate distributed space-time block coded-joint transmit/receive antenna diversity (D-STBC-JTRD), is proposed for AF WRNs. Its code rate is independent of the number of relays and hence no code rate loss is incurred as the relays' number increases. In addition, this scheme deploys the same encoding matrices at every relay; this eliminates the need for additional network overhead to coordinate the code generation by the relays. In other words, there is no need to interrupt the transmission if a relay has been up/down.

The second scheme aims to find a flexible trade-off between reliability and code-rate that can be offered by DF networks. Towards this end, a method to construct a D-STBC that is combined with spatial modulation (SM), denoted as D-STBC-SM, is proposed. This method is not restricted to a specific number of relays and can be constructed as necessary. In addition, a novel adaptive transmission protocol that uses the constructed codes, is proposed to achieve higher space diversity gain, even with relays equipped with a single antenna. Unlike most existing schemes, this protocol offers a throughput that increases as the number of relays increases. Moreover, the offered throughput is achieved using the same total average transmit energy, as only N_0 of the N available participating relays are active at any given time.

Part II publications: Part II contributions are published as

- El Astal, M.-T. O.; Salmon, B.P.; Olivier, J.C.: "Full-space diversity and full-rate distributed space–time block codes for amplify-and-forward relaying networks," in **IET Journal of Engineering**, 2014, DOI: 10.1049/joe.2014.0063.

- El Astal, M.-T. O.; Abu-Hudrouss, A.M.; Salmon, B.P.; Olivier, J.C.: "An adaptive transmission protocol for exploiting diversity and multiplexing gains in wireless relaying networks," in **EURASIP Journal on Wireless Communications and Networking**, 2015:1-15

- El Astal, M.-T. O.; Salmon, B.P.; Olivier, J.C., "Distributed Space-Time Codes for Amplify-and-Forward Relaying Networks," in **IEEE Wireless Communications and Networking conference (WCNC)**, Istanbul, Turkey, pp.1166-1169 , 6-9 Apr. 2014.

1.3.3 Part III: Multi-User interference in Wireless Relaying Networks

In this part, the multi-user interference of WRNs is considered. Two transmission protocols with an interference cancellation scheme are proposed: the *concurrent*$_{S-R-D}$*-PIC*$_{R,D}$ protocol for DF WRNs and the *concurrent*$_{S-R-D}$*-PIC*$_{D}$ protocol for AF WRNs. Unlike existing protocols, these protocols allow the concurrent transmission in both phases of the transmission. Thus, high spectral efficiency is offered while maintaining low decoding complexity. This low decoding complexity is maintained due to the adaptation of the partial interference cancellation group decoding (PICGD) approach for WRNs, which was initially proposed by Guo, *et al.*, for point-to-point (P2P) communication link. For a WRN consists of J users equipped each with J_a-antenna, a single half duplex (HD) R_a-antenna relay, and M-antenna destination, the *concurrent*$_{S-R-D}$*-PIC*$_{R,D}$ protocol achieves the *interference-free* diversity gain (i.e., $R_a \times \min\{J_a, M\}$) without imposing any conditions on a node's antenna number. The *interference-free* is the diversity gain achieved, assuming that each user in the network is transmitting solely without experiencing any interference from other users, hence it is considered as the natural upper bound of the diversity gain in multi-user WRNs. Similar to most exiting protocols, this protocol requires the CSI of the users-relay links at the relay. In contrast, the *concurrent*$_{S-R-D}$*-PIC*$_{R,D}$ protocol achieves a diversity gain of $J_a \times M$, given that $R_a > 8$, while the CSI is required only at the destination. Although the diversity's upper bound is not achieved, this protocol uses a simple relay as no CSI or encoding is required at the relay. In addition, and unlike the existing protocols, the achievable diversity gain is determined by both J_a and M and it is not sacrificed while J is increased. This part also establishes sufficient conditions for an STBC to achieve the prior mentioned diversity gains, when the PICGD approach is employed by multi-users WRNs.

Part III publications:

- El Astal, M.-T. O.; Ismail, A.; Alouini, M.-S. ; Olivier, J. C.: " Full-diversity partial interference cancellation for multi-user wireless relaying networks," in the **7th IEEE**

International Conference on Signal Processing and Communication Systems (ICSPCS), Gold coast, Australia, pp.1-6,16-18 Dec. 2013.

- El Astal, M.-T.; Ismail, A.; Alouini, M.-S. ; Olivier, J. C.: "Low-Complexity and Full-Diversity Partial Interference Cancellation for Multi-User Wireless Relaying Networks," *re-submitted to* in **IEEE Transactions on Vehicular Technology**.

1.4 Thesis organization

This thesis is organised as follows: In part I, the issue of imperfect synchronisation is considered and three enhanced detectors are proposed. Chapter 3 considers the one-way case while the two-way case is considered in Chapter 4. Then, Part II proposes two high-rate coding schemes for WRNs with an arbitrary number of relays, while retaining low decoding complexity at the destination. The D-STBC-JTRD and D-STBC-SM coding schemes are introduced in Chapter 5 and Chapter 6, respectively. The last part consider the issue of multi-user interference. Two transmission protocols are proposed for multi-users WRNs: the *concurrent*$_{S-R-D}$*-PIC*$_{R,D}$ protocol for DF WRNs and the *concurrent*$_{S-R-D}$*-PIC*$_{D}$ protocol for AF WRNs.

1.5 Thesis notation

Hereafter, small letters, bold small letters and bold capital letters will designate scalars, vectors and matrices, respectively. If $\mathbf{A}$ is a matrix, then $\mathbf{A}^H$, $\mathbf{A}^T$,and $\mathbf{A}^\dagger$ denote the hermitian, the transpose, and the pseudo-inverse of $\mathbf{A}$, respectively. Also, $\Psi_1(\mathbf{A}, a, b)$ denotes the result of shifting down each b row of $\mathbf{A}$ by a rows individually with zero padding. Similarly, $\Psi_2(\mathbf{A}, a, b)$ denotes the result of shifting $\mathbf{A}$ as with $\Psi_1(\mathbf{A}, a, b)$ but in an upward direction. For a vector $\mathbf{v}$, $\bar{\mathbf{v}} = [\Re(\mathbf{v})^T, \Im(\mathbf{v})^T]^T$. $\Re(.)$ and $\Im(.)$ indicates the real and imaginary part, respectively. We define $\mathcal{M}(\mathbf{A})$ to be the vector space spanned by the columns of $\mathbf{A}$ and the vec$(.)$ as the operator which, when applied to a $m \times n$ matrix, transforms it into a $mn \times 1$ vector by simply concatenating vertically the columns of the corresponding matrix. The

$\otimes$ operator is the Kronecker product. The operator blkdiag$(\mathbf{A}_1, \mathbf{A}_2, ..., \mathbf{A}_n)$ outputs a block diagonal matrix of the form

$$\text{blkdiag}(\mathbf{A}_1, \mathbf{A}_2, \mathbf{A}_3, \ldots, \mathbf{A}_n) = \begin{bmatrix} \mathbf{A}_1 & \mathbf{0} & \mathbf{0} & \mathbf{0} \\ \mathbf{0} & \mathbf{A}_2 & \mathbf{0} & \mathbf{0} \\ \vdots & \ldots & \ddots & \vdots \\ \mathbf{0} & \mathbf{0} & \mathbf{0} & \mathbf{A}_n \end{bmatrix},$$

A Gaussian distribution is denoted by $\mathcal{CN}(\mu, \Gamma^2)$, with corresponding mean μ and diagonal covariance matrix Γ^2 with value σ^2.

2

Background and Related Literature

> *In order to carry a positive action we must develop here a positive vision.*
>
> **— Dalai Lama**
> (Tibetan Leader)

2.1 Introduction

In the last decade, the demand for speedy wireless communications systems has grown due to emergent services, such as mobile multimedia and the Internet, which require a high rate of transmission. In addition, wireless transmissions experience fundamental performance limitations due to impairments of the radio propagation channel, such as reflection, diffraction, and scattering [3]. Accordingly, offering high data rates while maintaining reliable transmissions over wireless propagation channels is a major challenge for communications engineers [16].

Compared to the single-input single-output (SISO) scheme, MIMO scheme was shown to have the potential to increase the data rate and reliability of transmission [17–21]. In addition, STBCs have been suggested in order to efficiently exploit MIMO scheme resources. However, MIMO schemes assume that a rich scattering propagation channel exists to provide uncorrelated signal paths. Moreover, there are variety of communications systems that cannot support the physical deployment of multiple antennas due to cost and size limitations [13]. To overcome these issues, cooperative communication system was proposed in [7], where the transmitter tries to utilise neighbour clients to act as multiple distributed antennas . Due to the random locations of the neighbour clients, the signal paths to the destination are more likely to be uncorrelated. Thus, the SISO schemes are transformed into a virtual

MIMO scheme without the difficulties that associated with multi-antennas deployment [7, 22, 23].

This chapter provides the background required throughout this work. It is organised as follows: Firstly, the general block diagram of wireless communications systems is introduced along with a brief description of .each block. Then, discussions regarding wireless channel characteristics are presented, followed by a description of the modulation schemes used throughout this work. Then, the background of both the cooperative communications networks and STBC are briefly reviewed.

2.2 Overview of Wireless Communications Systems

In this section, the general block diagram of wireless communication systems is presented along with a brief description of each block. Generally, communication systems aim to convey information from a given source to a particular destination through a propagation channel. The source can be a microphone within a client's mobile while the destination can be a speaker. Many operations are applied to the source information in order to receive it at the destination correctly and in an efficient way. The block diagram is depicted in Fig. 2.1.

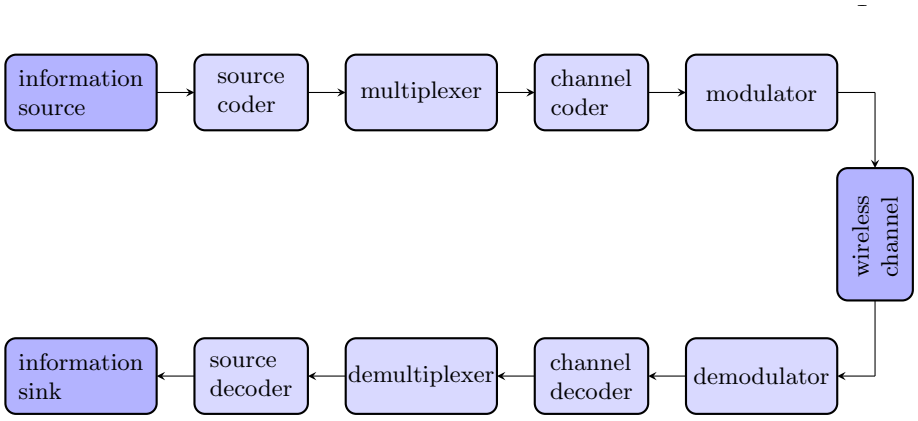

Fig. 2.1: Block diagram of a wireless communication system.

- **Information source**: It might be an analog or digital information source; a sequence of symbols (i.e. a computer file) is provided by digital sources while an analog waveform (i.e. voice signal from a microphone) is generated by analog sources. The analog to digital converter (ADC) is combined with the analog sources in order to digitise the signal. This ADC device converts the signal into a digital data stream at a

certain sampling rate and resolution. For numerical simulation purposes, a sample function of random processes is used to model the information provided from the source, whatever the type of the source. This is also used throughout this work.

- **Source coder**: To use the system's resources efficiently, the source coder tries to reduce any redundancy in the source signal in order to reduce the required time and/or bandwidth of the transmitting signal.

- **Channel coder**: This device adds redundancy bits to the source coder output in order to protect data against transmission errors that result from any impairment of the channel. This increases the redundancy in the baseband signal and hence a higher data rate is required at the channel coder output.

- **Multiplexer**: This combines data from a different number of users, if needed, in order to be transmitted through the propagation channel; this operation is called multiplexing. Signalling information is also multiplexed.

- **Modulator**: The modulator firstly assigns a symbol, drawn from the modulation constellation, to each specific number of information bits. This number is determined by the order of the used modulation scheme. Then, these assigned symbols often (but not always) modulated to a higher frequency carrier signal in order to be transmitted via radio frequencies. Refer to Section 2.4 for further detail regarding the modulation scheme used throughout this work.

- **Propagation channel**: It represents the medium where the modulator output is conveyed from the transmitter side to the receiver side. The type of medium and other factors determine the impairments that the channel introduces to the transmitted signal. It may attenuate, reflect and diffract the signal. Section 2.3 shows further details.

- **Diversity combiner**: This device is required when one of diversity schemes is employed by the system (see Section 2.5). It either selects the best signal from antennas for further processing, i.e. selection and stay combining (SSC), or tries to combine all of them in an innovative way, i.e. maximum ratio combining (MRC) [3]. In addition, the signals can be transmitted directly to a "joint" demodulator that can make use of information from the different antennas jointly. Better performance is achieved through the joint demodulator, but higher decoding complexity is reported.

- **Demodulator**: It obtains soft-decision data from the received signal and hands it over to the decoder. According to the considered system, the demodulator can be an optimum, coherent, or differential demodulator. This device may include further signal processing like equalisation.

- **Channel decoder**: It reverses the operation of the channel coder by using the soft estimates from the demodulator output to find the original multiplexed data. In un-coded systems, the decoder is just a threshold (hard-decision) device, while the maximum likelihood sequence estimators (MLSEs) are used, for example, in the systems where convolution codes are used. Other channel coding schemes were introduced in the literature, such as STCs.

- **De-multiplexer**: As the name indicates, this separates the user's data. It should be noted that the de-multiplexer can be placed earlier; its optimum placement depends on the specific multiplexing and multi-access scheme used by the system.

- **Source decoder**: According to the rules of the source coding schemes employed at the transmitter, the source decoder reconstructs the source signal from the output of the channel decoder. If the source data is digital, the output signal is transferred to the destination. Otherwise, the data are transferred to the digital to analog (DAC) device, which converts the received information into an analog signal and hands it over to the analog destination (i.e. a speaker).

2.3 Wireless propagation channel

As mentioned in Section 2.2, the propagation channel is the physical medium linking the source and the sink, where the signal is moving from one place to another. This medium can be a physical wire, like twisted pair wire and coaxial cable, or a wireless medium like free space. The channel causes noise, attenuation and distortion which may result in interference that causes error reception at the destination. It is essential to understand the wireless propagation channel behaviour, along with its key parameters, in order to determine how specific wireless systems will behave.

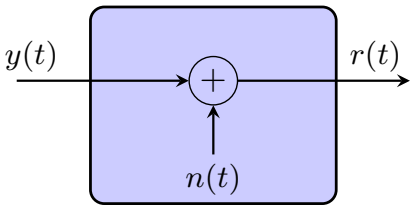

Fig. 2.2: The AWGN channel model.

2.3.1 Additive Wide Gaussian Noise

Additive white Gaussian noise (AWGN) is a basic noise model used in the simulation of communications systems to emulate the thermal noise that occurs in nature, either in channels or even in the receiving device itself [3, 24]. As the name indicates, the AWGN noise effect is added to the original transmitted signal. Also, 'white' refers to the idea that its energy is equal and uniform over the whole frequency spectrum, actually to 10^{12} Hz. This is similar to the white colour which has uniform emissions across the whole visible spectrum. The AWGN is referred to as 'Gaussian' because its distribution follows the normal distribution which is given by

$$f_{\mathbf{n}}(t) = \frac{1}{\sqrt{2\pi\sigma^2}} \exp\left(\frac{-\mathbf{n}^2}{2\sigma^2}\right) \tag{2.1}$$

where σ^2 is the variance (power) of the noise $\mathbf{n}$.

The AWGN model does not account for multi-path fading, path loss or the reflection and diffraction of the wireless channel. However, it is used as a simple and tractable mathematical tool to gain insight into the underlying behaviour of a system before these other phenomena are considered. This work considers the band limited AWGN. It means that the amplitudes of the real and imaginary noise contributions are independent variables and it follow the Gaussian distribution model. When combined, the resultant effect amplitude is a Rayleigh distributed random variable while the phase is uniformly distributed from 0 to 2π.

2.3.2 Multi-path fading channel

The transmitting signal interacts with many obstacles in the surrounding environment while propagates to the destination from the source through multiple paths. This results in a number of different reflected and diffracted signals. These signals are combined at the receiver and hence a wide-varying signal, in term of amplitude and phase, is received (see Fig. 2.3). This effect is called multi-path fading. The fading that may be experienced by the signal is affected by (1) multi-path propagation due to scattered obstacles, (2) the bandwidth of the transmitted signal, (3) the relative motion speed between the transmitter and the receiver and (4) the speed of surrounding objects, if they are moving [24].

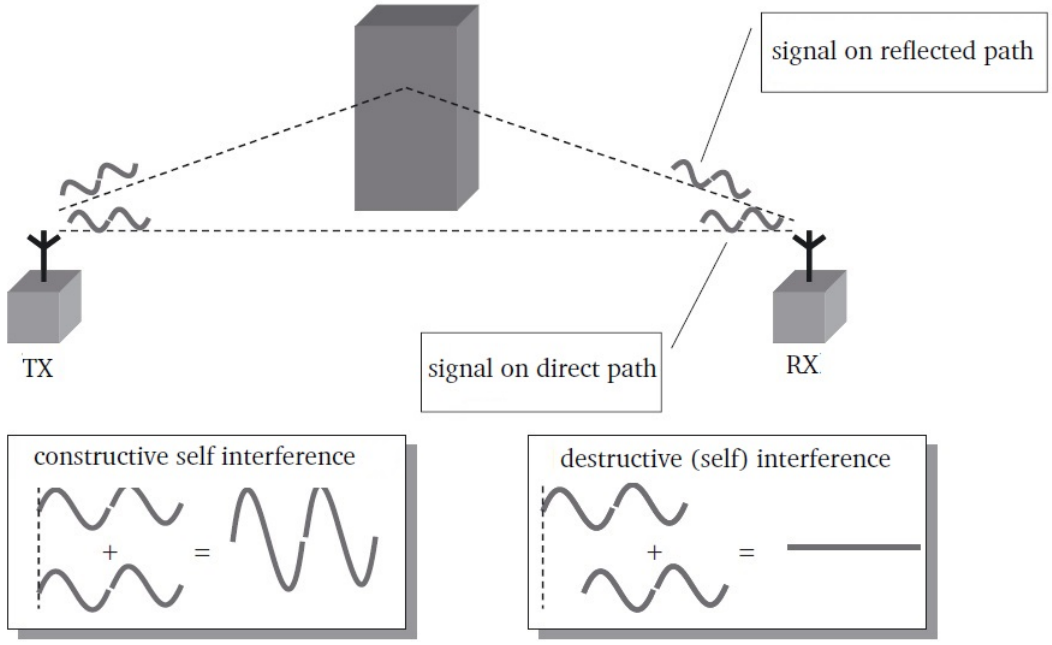

Fig. 2.3: Principle of small-scale fading [16].

The fading effects that the signal experiences through propagation via the wireless channel is classified into (illustrated in Fig. 2.4):

- Large-scale fading: It includes the variations in signal that results from path loss and shadowing, which may happen by large obstacles. This fading can be modelled by a ratio between the transmitted and received signal power, measured in decibels (dB) [3].

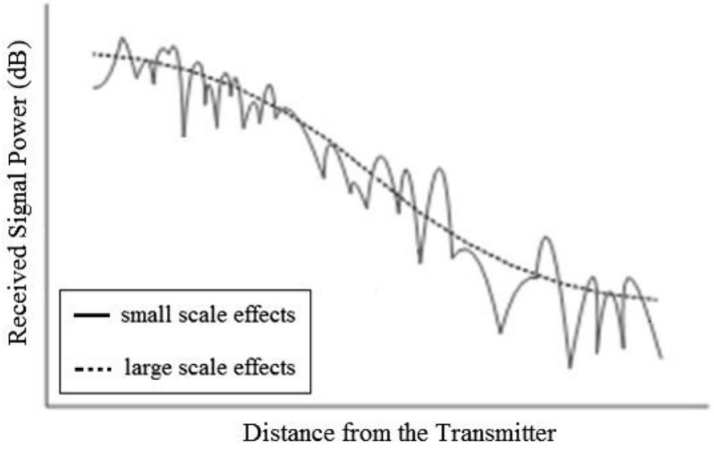

Fig. 2.4: Signal is experiencing multi-path fading effects [25].

- Small-scale fading: This fading type includes the variations that result due to the constructive and destructive nature of the received multi-path signals. This is due to the fact that the received multi-path signals experience different random reflectors, scatters, and attenuators (see Fig. 2.3) [3, 16, 24]).

Multi-path channel impulse response

It has been shown that the multi-path fading channel can be modelled as a time-varying linear filter [24]. The filter's impulse response reflects the influences of the amplitude and delay parameters of the channel components. Assuming that the transmitting signal is denoted as $y(t)$, the channel output signal can be modelled as

$$r(t) = y(t) \otimes h(t, \tau), \tag{2.2}$$

with

$$h(t, \tau) = \Re(h_b(t, \tau) \exp(j2\pi f_c t)), \tag{2.3}$$

where $h(t, \tau)$ is the channel impulse response, τ is the experienced time-delay, f_c is the used carrier frequency and $\otimes$ represents a continuous time convolution operator. Assuming a channel with L multi-path components, $h(t, \tau)$ can be written as

$$h_b(t, \tau) = \sum_{i=1}^{L} \beta_i(t, \tau) \delta(\tau - \tau_i(t)) \exp\left(j\phi_i(t, \tau)\right) \tag{2.4}$$

where $\beta_i(t,\tau)$, $\tau_i(t)$ and $\phi_i(t,\tau)$ are the instantaneous amplitude, time delay and phase associated with the i^{th} multi-path component of the channel, respectively.

Given that the time delay $\tau_i(t)$ remains constant for each multi-path component and the channel is wide sense stationary over a small time interval,

$$h_b(\tau) = \sum_{i=1}^{L} \bar{\beta}_i(t)\delta(\tau - \tau_i(t)) \exp\left(j\bar{\phi}_i(t)\right), \tag{2.5}$$

where $\bar{\beta}_i$ and $\bar{\phi}_i$ is the average amplitude and phase values associated with the i^{th} multi-path component of the channel, respectively.

It is worth noting that the power delay profile $P(\tau)$ is a common tool that is used to show the distribution of a received signal's power over multi-path component delays. The plot of $P(\tau)$ shows the signal power of each multi-path component against its respective propagation delays.

Multi-path channel parameters

In this section, the defining parameters of the wireless multi-path fading channel are defined and discussed. [3, 24].

Definition 2.1. *The channel Doppler spread (B_D) is a measure of how much the signal spectral components have been broadened due to propagating through the communicating channel. In addition, it defines the range of frequencies over which the Doppler spectrum components are received.* ■

Definition 2.2. *The channel coherence time (T_c) is the time duration over which the channel impulse response is considered to be not varying.* ■

Definition 2.3. *The channel delay spread (T_d) is a measure of how much the signal time components have been delayed due to propagating through the communicating channel. Also, it defines the difference in propagation time between the longest and shortest path.* ■

Definition 2.4. *The coherence bandwidth (B_c) defines the range of frequencies over which the propagation channel are likely to experience comparable or correlated amplitude fading.* ■

Multi-path channel Classification

The multi-path fading is influenced by both the nature of the transmitting signal (bandwidth, etc.) and the channel parameters (delay and Doppler spread). Accordingly, the wireless channel is classified into

- **Slow or Fast fading channel**:

  If T_c is much smaller than the delay requirement of the system (T), the channel is a fast fading channel. Otherwise, it is a slow fading channel. This means that one transmitted symbol will experience multiple fades in the fast fading channel, while multiple symbols will experience identical fading in a slow fading channel.

- **Flat or Frequency-selective fading channel**:

  The channel is referred as a flat fading channel if the system's bandwidth is considerably less than the channel coherence bandwidth B_c. This means that all spectral components of the transmitting signal will undergo the same fading effects. In this case, the delay spread (T_d) is much less than the symbol time of the system, and a single-tap channel model is sufficient to represent the channel. In contrast, the channel is said to be frequency-selective if the transmitting signal bandwidth is much larger than the channel coherence bandwidth B_c. In other words, all transmitted signal spectral components are affected by different amplitude gains and phase shifts. Accordingly, the channel has to be represented by multiple taps.

The wireless channel types are summarised in Tab. 2.1.

Channel type	Description
Slow-fading channel	$T_c \gg$system delay requirements
Fast-fading channel	$T_c \ll$system delay requirements
Flat-fading channel	$B_c \gg$system bandwidth requirements
Frequency selective-fading channel	$B_c \ll$system bandwidth requirements

Tab. 2.1: Wireless channel types parameters.

It is worth noting that the channel can be classified also according to the fading distribution. For example, Nakagami distribution, Rayleigh distribution, Rician distribution and Weibull distribution [26].

2.3.3 The used wireless channel model

A slow flat-fading channel model with a Rayleigh distribution is used throughout this work. This model is sufficient when the surrounding environment of the source and/or destination has many scatterers obstructing the transmission and there is no line of sight between the source and destination. For example, it has been shown by experimental work that Manhattan city exhibits a near-Rayleigh fading channel [27].

2.4 Modulation schemes

The modulator is responsible for converting the input bit sequence into a waveform that is suitable for transmission over the used communication channel. On the receiver side, the demodulator is responsible for converting the received waveform into the corresponding input sequence of bits. Three processes are conducted by the modulator/demodulator [28]. These processes depend on the modulation scheme employed by the system (see next subsections). However, their functions can be described as follow (shown in Fig. 2.5):

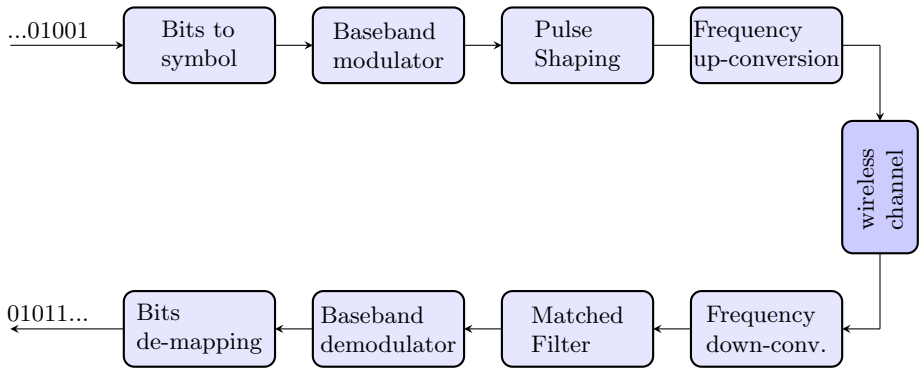

Fig. 2.5: Signal is experiencing multi-path fading effects [25].

Firstly, a bit sequence is mapped into a (complex) symbol drawn from a finite number of symbols, called modulation constellation. The number of bits (n) in each sequence that represent a symbol depends on the size (order) of the used constellation (M), where $M = 2^n$. Modulators usually (but not always) include an additional layer, which maps a baseband waveform into a passband waveform centred on a given carrier frequency f_c. Pulse shaping changes the transmitted waveform to a form which makes the transmitted signal better suited the undergoing channel [29]. Thus, the inter symbol interference caused by the

channel can be kept in control. In wireless communication, this process is essential for making the signal fit in its frequency band. At the receiver side, the passband waveform is mapped back to the baseband, then the corresponding sequence of bits is estimated.

Two common modulation schemes are used throughout the chapters of this work: phase shift keying (PSK); and quadrature amplitude modulation (QAM).

2.4.1 Phase shift keying (PSK) modulation

As the name indicates, the PSK is a digital modulation scheme that conveys bits by modifying the phase angle of the used waveform [28]. Like any other digital modulation, the PSK uses a finite number of distinct waveforms to represent the input data. Specifically, a determinant number of phase angles are used to assign a unique pattern of bits sequence. This number is determined by the modulation order. The PSK modulation order can be either $2, 4, 8,$ ..., or 2^n, which are denoted as 'BPSK', 'QPSK', 8-PSK',..., or M-ary PSK, respectively. In general, higher order forms allow higher data rates but lower performance is reported. In the demodulator, the phase of the received signal is determined and mapped back to the corresponding symbol, hence the transmitted bits can be estimated. Usually, the modulation schemes are presented by the constellation diagram as shown in Fig. 2.6. This shows the constellation symbols in the complex plane where, in this context, the real and imaginary axes are termed the in-phase and quadrature axes, respectively.

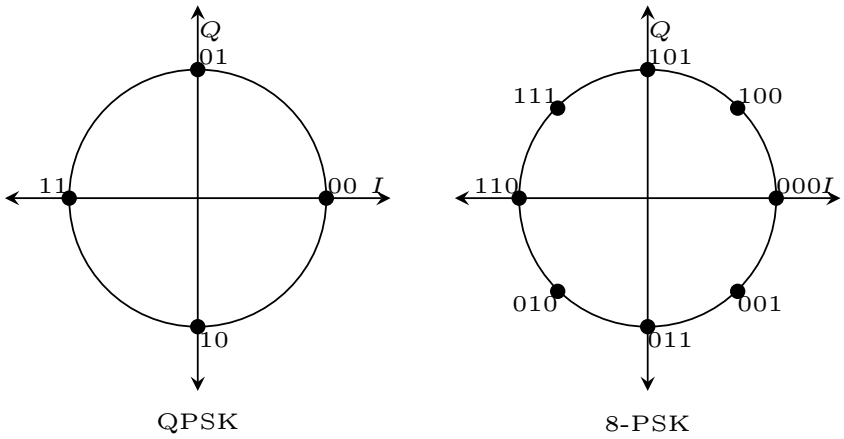

Fig. 2.6: Constellation diagram of QPSK and 8-PSK modulation scheme.

It is worth noting that the Gray code is used to arrange the represented bits of each symbol (as shown in Fig. 2.6) to achieve higher performance in term of BER [29].

2.4.2 Quadrature amplitude modulation (QAM)

Unlike PSK, the QAM scheme conveys the transmitted bits by modifying both the amplitude and the phase angle of the used waveform [28]. Each combination represents a symbol which represents a bit sequence (see Fig. 2.7). Due to proved performance improvement, the QAM is used by a variety of communication systems, i.e. 802.11b wireless Ethernet standard and digital video broadcast (DVB). In the literature, different QAM designs were introduced, each with positive and negative aspects (i.e. the star QAM). The star QAM design is used in Chapter 6 and thus its definition is given below.

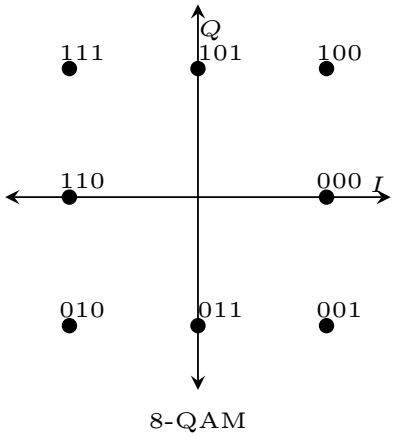

Fig. 2.7: Constellation diagram of 8-QAM scheme.

Definition 2.5. *A two-tier star M-ary QAM modulation has its constellation points distributed over two amplitude levels a and b. There are $\frac{M}{2}$ constellation points on each amplitude level with a phase difference ϕ [30], as depicted in Fig. 2.8. Both a and ϕ should be optimised to*

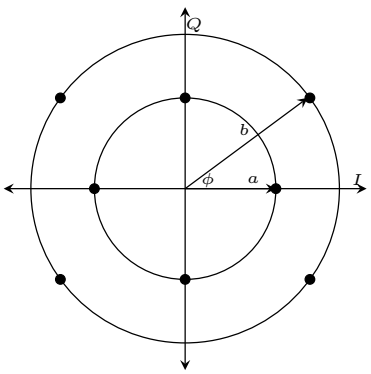

Fig. 2.8: Two-tier Star M-ary QAM constellation.

maximise codeword differences. $b = \sqrt{2 - a^2}$ *must hold to ensure a unity average transmitted power.* ■

2.5 Diversity in Wireless Channel

Due to numerous reflectors and obstacles in the surrounding communication environment, multiple different fading copies of the transmitted signal are received at the destination. As mentioned in Section 2.3, this may result a wide-varying receiving signal, and thus performance degradation may be introduced [3, 24]. However, diversity techniques were proposed to mitigate this degradation [3, 24, 31]. Generally, these techniques aim to receive the same original information through multiple fading-independent channels. This can be obtained via transmitting and/or receiving through either antennas, time-slots or frequencies. Thus, by using a proper combining technique, the multi-path variations can be reduced, and the reliability can be improved. For example, a switch and stay combining (SSC) technique instantaneously selects the highest-power replica. Other enhanced schemes were introduced, i.e. equal gain combining (EGC) and maximal ratio combining (MRC) [3, 24, 31].

2.5.1 Space (Spatial) diversity

In space diversity schemes, the transmitter and/or receiver is equipped with multiple antennas (see Fig. 2.9). These antennas are physically enough separated in order to receive uncorrelated replicas of the transmitted signal. Nowadays, this diversity is employed in many established communication networks, i.e. base station (BS) in GSM system is typically equipped with two receive antennas. The system is referred to as MIMO when a combination of a transmit and receive diversity is employed. The MIMO technology has become a cornerstone of many wireless communication system standards, i.e., IEEE 802.20 [1]. As mentioned, this is because it has the potential to achieve high reliability and can offer higher data-rate compared to SISO systems.

As a result, two performance measures are related to the MIMO systems, the diversity gain and the multiplexing gain. The multiplexing gain is directly related to the data rate offered by the system while the diversity gain is related to the performance improvement which can be achieved (see Definition 2.6). It should be noted that there is a trade-off between the diversity gain and the multiplexing gain offered by the MIMO technology. [3].

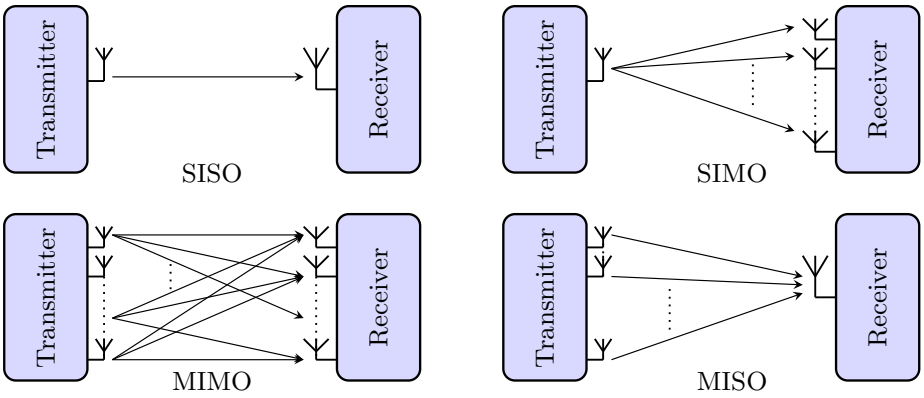

Fig. 2.9: SISO, SIMO, MISO and MIMO technology

Definition 2.6. *Space-diversity order (gain) of wireless communications network:*
The wireless communications network is said to achieve a space-diversity order of d *if the average error probability* $\mathbb{P}$ *decays as the inverse of the* d^{th} *power of SNR (*γ*). This is stated mathematically as*

$$\mathbb{P}(\gamma) \leq b\gamma^{-d}, \tag{2.6}$$

where $b > 0$ *is a constant independent of* γ.

2.5.2 Other diversity schemes

Different diversity schemes were introduced to achieve the same objective, for example, time diversity and frequency diversity [3]. As the name indicates, time diversity can be implemented by transmitting multiple copies of the source signal in different time slots, each separated at least by the channel coherence time (T_c). As a result, multiple uncorrelated signals are received. The reliability of the data is improved, but at the cost of data rate. In frequency diversity, multiple copies of the transmitter's signal are transmitted on different frequencies, each separated at least by the channel coherence bandwidth (B_c). Accordingly, uncorrelated multi-path signals are received via these different frequencies by the destination. Other diversity schemes exist in the literature, such as polarisation and angle diversity schemes. In addition, some hybrid schemes were introduced where two of the mentioned diversity schemes were combined to acquire higher diversity gain (see Fig. 2.10) and hence better performance can be achieved [3].

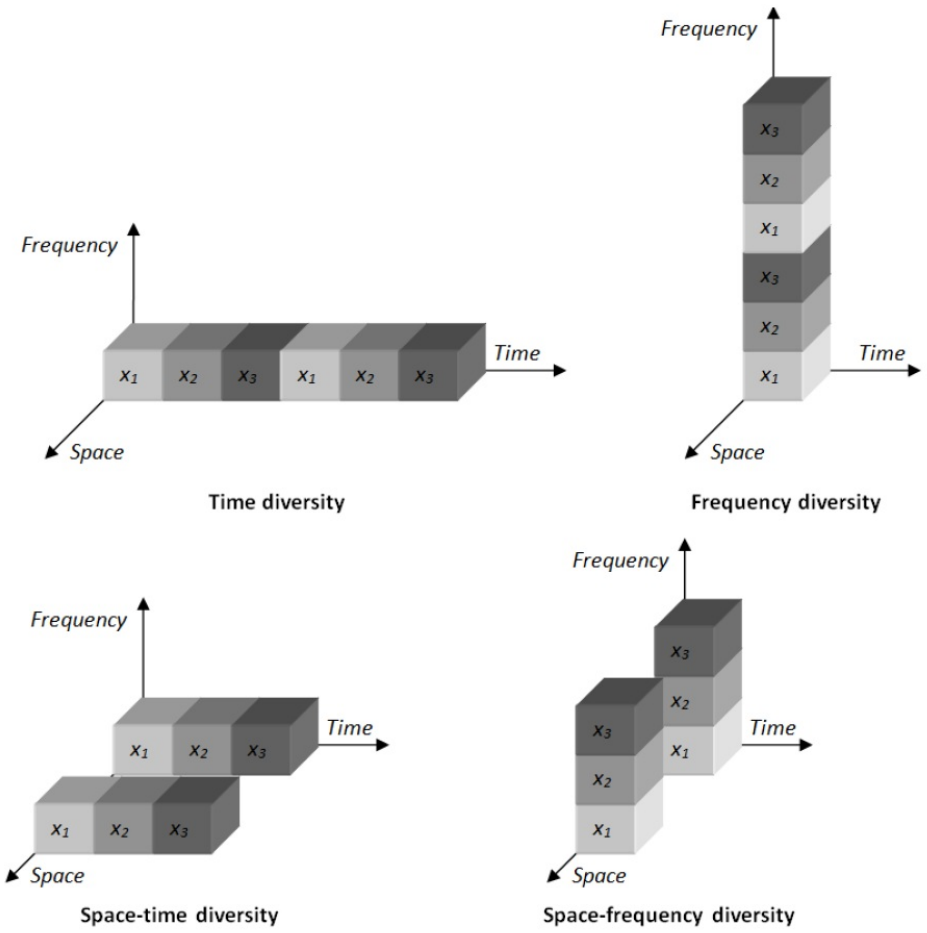

Fig. 2.10: Most common diversity schemes [32].

2.6 Background of Cooperative Communications Networks

Compared to SISO systems, the MIMO systems are shown to have the ability to increase the system's reliability and capacity [3]. However, these improvements may not be applicable to all systems as they either cannot support multiple physical antenna deployment, or the propagation channel cannot feature this technology. The channel can delimit the MIMO deployment when the received signal replicas are highly correlated [24]. Recently, cooperative communications have been introduced to create a *virtual* MIMO system. This is by encouraging neighbouring multiple client apparatus to share their resources cooperatively with the transmitter in order to construct a distributed antenna array (see Fig. 2.11). Due to the random location of neighbour nodes, uncorrelated signal paths are likely to be received.

Consequently, the reception reliability and the data-rate can be improved, like MIMO schemes but without physical multiple-antenna deployment [13]. The communication networks that are employing the cooperative transmission scheme are referred to in the literature as cooperative communications networks or wireless relaying networks (WRNs). Therefore, these names can be used interchangeably in this work.

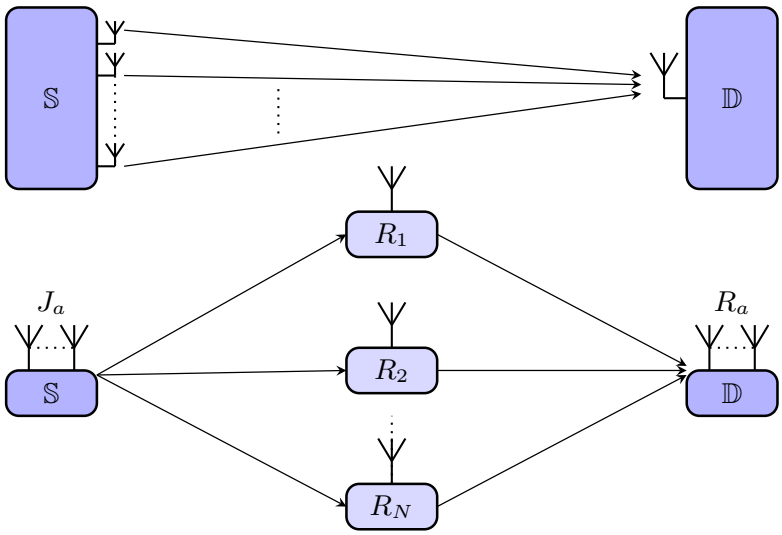

Fig. 2.11: WRNs versus conventional MIMO P2P networks.

The full diversity gain (see Definition 2.6) is adapted here for WRNs [33] as,

Definition 2.7. *Full-space diversity gain of wireless relaying networks:*

Consider a cooperative communication network comprised of a source equipped with J_a antennas, N single-antenna relays and a destination with N_r antennas; in this case the network is said to have achieved full-space diversity if its diversity gain is equal to

$$d = \min(J_a \times N, N \times N_r). \tag{2.7}$$

In most WRNs, either with TDMA or FDMA, the transmission is conducted via

- **Phase 1 (Broadcasting phase)**: The source transmits M-ary modulated symbols denoted by $\mathbf{s}(i) = [s(1,i), \ldots, s(J,i)]^T$, where i denotes the information block index and J is the number of symbols in the broadcasting phase. Thus, the relays, but not

always the destination, receive the source's signal. The transmission link with the destination is known as a direct transmission (DT) link.

- **Phase 2 (Relaying or Cooperative phase)**: As the name indicates, each relay receiving the transmission is encouraged to relay and forward the signal to the destination. According to the used relaying protocol, the relays amplify or decode the received data prior to relaying them to the destination. For further detail, refer to Section 2.6.1.

2.6.1 Relaying Protocols

According to the literature, the relaying protocols are sorted into two categories, namely, fixed or adaptive relaying protocols. In fixed relaying protocols, the system resources are divided between the two transmission phases into a pre-determined manner. For example, each phase has its own transmission dedicated time-slots; if TDMA is used by the network. Although the fixed type protocols are easy to implement due to the systematic sharing nature, they may lead to error propagation and low bandwidth efficiency. Error propagation is experienced as the relays are constantly forwarding their signal to the destination even though their received signals may be distorted significantly. Low bandwidth efficiency results as the network resources are shared with the relays even though the information is received correctly through the first phase of the transmission. In contrast, the resources in the adaptive relaying protocols are shared in an adaptive manner to overcome the mentioned disadvantages of the fixed relaying protocols. For example, the relaying phase of the incremental relaying protocol is initiated only if the broadcasting phase fails. In addition, a relay's selection scheme can be employed by the relaying protocols to avoid error propagation. This protocol category is refered to as selective relaying protocol. A brief description of each of relaying protocols used throughout this work is given below.

- Amplify-and-forward (AF) relaying protocol:
  With AF protocols, the relays are required to amplify their received signals, construct encoded versions and then forward them to the destination. Therefore, this protocol is desirable for the WRNs with simple-design relays. Two forms of this protocol are used: the fixed AF protocol and the selective AF protocol. In the fixed AF protocol, termed simply AF protocol, all receiving relays participate in the cooperation phase, while the selective AF (SAF) activates only a selected subset of the relays to work in the cooperation phase. One of the existing selection criteria is the SNR threshold-based

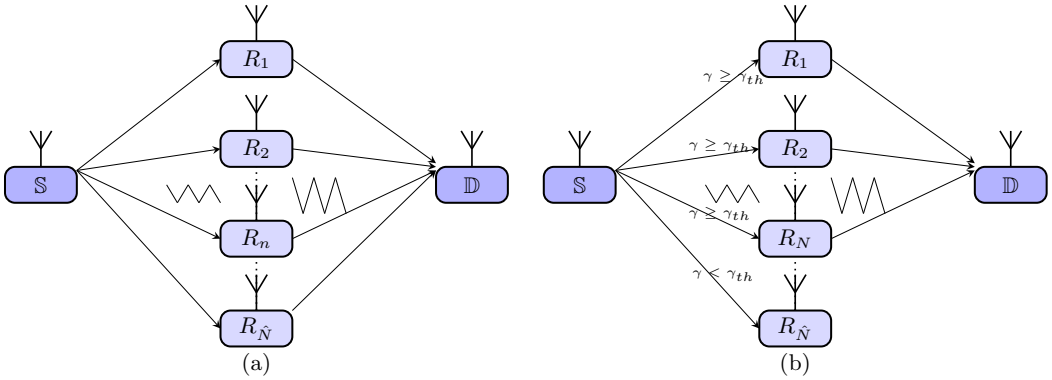

Fig. 2.12: (a) AF relaying protocol and (b) SAF relaying protocol.

criterion, where only relays with $SNR \geq SNR_{threshold}$ participate in the next phase of transmission.

- Decode-and-Forward (DF) Relaying protocol:

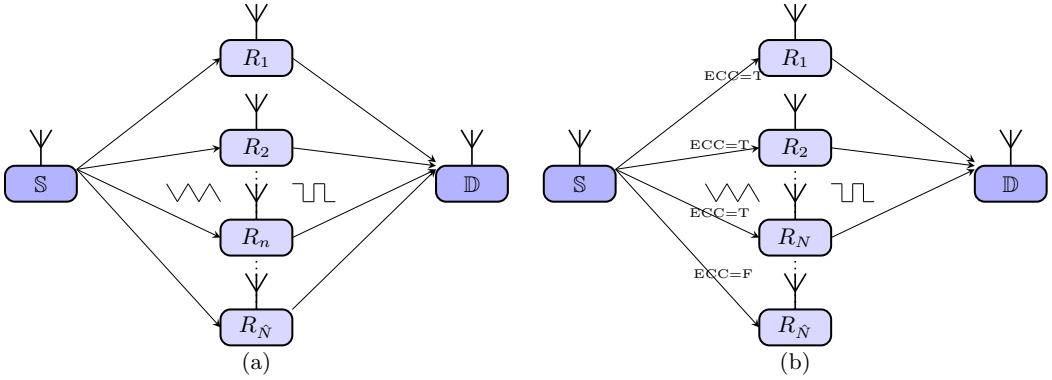

Fig. 2.13: (a) DF relaying protocol and (b) SDF relaying protocol.

The DF relays firstly decode their received signal, then encode their detected data according to the employed code and finally forward the resulting encoded data to the destination. In fixed type, termed simply (DF), all of the available relays participate in the cooperation phase while only a selected subset of the relays is active if the selective DF (SDF) is employed. A possible selection criteria is to use an error control code (ECC). Thus, each relay can determine if it will or will not partake in this phase. This can be done by letting the source to add a sufficient level of redundancy ECC bits to its original data. These bits can be used by the relays to determine if their received symbols can be correctly detected. To limit the discussion, it is assumed in this work that a fixed number N out of $\hat{N}$ relays will always partake in the relaying phase if selective relaying protocol is used.

Other relaying protocols were proposed in the literature, such as compress-and-forward relaying protocol and coded cooperation relaying protocol [13]. As their names indicate, the relay transmits a quantised and compressed version of the received message in the compress-and-forward protocol in order to reduce the required bandwidth, while the relay adds redundancy bits in the coded cooperation in order to further improve the transmission reliability.

2.7 Background of Distributed Space-Time Block Codes

2.7.1 Space-time coding review

Motivated by the hybrid diversity schemes, space time coding (STC) was introduced [31]. It aims to improve reliability through exploiting both the multiple antennas and time-slots of the system [34]. As the name indicates, it transmits a number of encoded data copies through multiple time-slots and antennas, hoping that some of them may be received in a good enough state to allow reliable decoding. For example, in a MIMO system with two transmit antennas and one receive antenna, the achieved PEP is inversely proportional to SNR^2 if Alamouti STC scheme is used. In contrast, the achieved PEP is inversely proportional to SNR (not SNR^2 as of Alamouti STC scheme), if identical signals are transmitted from the transmitters' antennas simultaneously. Due to proved performance improvement, numerous STC classes were introduced. There are two main categories of STC schemes: space time trellis coding (STTC) schemes, where the data are encoded using a trellis code and then transmitted over antennas and time-slots; and space time block coding (STBC) where the encoding process is conducted in a block by block manner [31]. Also, the STC schemes can be categorised into coherent and non-coherent coding schemes. In coherent STC schemes, the receiver knows the instantaneous channel parameters, but in non-coherent STC schemes, the receiver only knows the channel distribution. In differential STC schemes, neither the channel parameters nor the channel statistics are available at the receiver. This work is concerned with the coherent STBC schemes. It is worth noting that the STBC scheme is modelled by the coding matrix ($\mathcal{X}$) as shown below.

Definition 2.8. *The STBC scheme is represented by a matrix expressed as*

$$\underset{L\times N}{\mathcal{X}} = \begin{bmatrix} x_{1,1} & x_{1,2} & \cdots & x_{1,N} \\ x_{2,1} & x_{2,2} & \cdots & x_{2,N} \\ \vdots & \vdots & \cdots & \vdots \\ x_{L,2} & x_{L,2} & \cdots & x_{L,N} \end{bmatrix}, \tag{2.8}$$

where the columns represent the encoded L time-slots sequences that should be transmitted by the N transmitting antennas of the source. If n_s denotes the number of encoded symbols, then the code rate r of the used STBC is defined as $r = \frac{n_s}{L}$. ■

For illustration purpose, the Alamouti STBC encoding process is considered below,

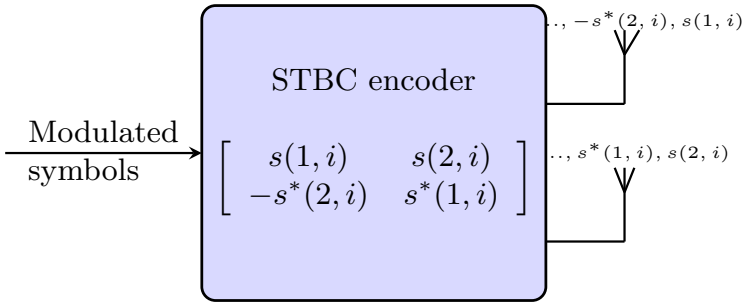

Fig. 2.14: The Alamouti STBC encoder.

The Alamouti STBC matrix is given by

$$\mathcal{X} = \begin{bmatrix} s(1,i) & s(2,i) \\ -s^*(2,i) & s^*(1,i) \end{bmatrix}. \tag{2.9}$$

Accordingly, for the information block (i), the encoding process is simultaneously conducted as follows:

- From the first antenna, transmit $s(1,i)$ over the first time-slot and then transmit $-s^*(2,i)$ over the second time-slot of the transmission.

- From the second antenna, transmit $s(2,i)$ over the first time-slot and then transmit $s(1,i)^*$ over the second time-slot of the transmission.

In the same manner, repeat the former steps for the next information block $(i+1)$.

By using proper decoding the system performance is significantly improved (see Section 2.7.2). The decoding process varies according to the STBC employed by the network and hence each chapter contains a unique decoding method.

2.7.2 Distributed STBCs

The adaptation of STBC schemes to work via distributed manner for WRNs was termed as distributed STBC (D-STBC) (see Definition 2.9) [35]. Using a distributed version of STBC, the relays' signal can be transmitted simultaneously to the destination. This is due to orthogonality existing among the D-STBC sequences. The D-STBCs have been extensively studied for their ability to exploit the diversity inherent in a wireless communication channel in order to improve signal quality and hence increased the spectral efficiency [6, 35–37]. In what follows, some of common STBCs that are used throughout this work listed below with their D-STBC encoding matrices. Finally, an example of D-STBC is further studied to illustrate the encoding, decoding and detection process.

Definition 2.9. *The D-STBC is an STBC generated in a distributive manner via WRN, where each relay is responsible for generating one column of the STBC matrix $\mathcal{X}$. It is mathematically represented by the encoding matrices of $\mathcal{X}$, $\boldsymbol{A}_n$ and $\boldsymbol{B}_i, \forall n = 1, \cdots, N$, where $\boldsymbol{A}_n$ and $\boldsymbol{B}_n$ are the matrices belonging to the relay R_n that are responsible for generating the un-conjugated and conjugated symbols of the n^{th} column of $\mathcal{X}$. The vector generated by the relay R_n is determined by*

$$\boldsymbol{t}_n(i) = \boldsymbol{A}_n \boldsymbol{s}(i) + \boldsymbol{A}_n \boldsymbol{s}^*(i), \tag{2.10}$$

where $\boldsymbol{t}_n(i)$ is the vector generated by the relay R_n. ■

Common D-STBCs

This section shows some of common D-STBCs that are used across the thesis.

- **Orthogonal STBCs**:
  1. **Alamouti STBC** of [12]: This code is commonly used in the literature, as it results

a single-symbol decoding complexity due to orthogonality. In addition, it is a full-rate code. It suits WRNs with two single-antenna relays. It is given by

$$\mathcal{X} = \begin{bmatrix} s(i,1) & -s^*(i,2) \\ s(i,2) & s(i,1)^* \end{bmatrix} \tag{2.11}$$

. It should be noted that (2.11) is equivalent to that was shown in (2.9). This can be resulted by letting $s_2 = s^*(2,i)$ and it facilitates the design of encoding matrices which are given by: $\mathbf{A}_1 = \mathbf{I}_2, \mathbf{B}_1 = \mathbf{0}_2, \mathbf{A}_2 = \mathbf{0}_2$, and $\mathbf{B}_2 = \begin{bmatrix} 0 & -1 \\ 1 & 0 \end{bmatrix}$. It was shown in [38] that no STBC scheme can be designed for WRN with more than two relays while offering the full-rate feature and maintaining the orthogonality of the code.

- The **3/4 OSTBC** of [10]: The best-rate orthogonal code designed for four relays is modelled by

$$\mathcal{X} = \begin{bmatrix} s(i,1) & s(i,2) & s(i,3) & 0 \\ -s^*(i,2) & {}^*s(i,1) & 0 & s(i,3) \\ s^*(i,3) & 0 & -s^*(i,1) & s(i,2) \\ 0 & s^*(i,3) & -s^*(i,2) & -s(i,1) \end{bmatrix}, \tag{2.12}$$

with encoding matrices given as

$$\mathbf{A}_1 = \begin{bmatrix} 1 & 0 & 0 \\ 0 & 0 & 0 \\ 0 & 0 & 0 \\ 0 & 0 & 0 \end{bmatrix}, \mathbf{A}_2 = \begin{bmatrix} 0 & 1 & 0 \\ 0 & 0 & 0 \\ 0 & 0 & 0 \\ 0 & 0 & 0 \end{bmatrix}, \mathbf{A}_3 = \begin{bmatrix} 0 & 0 & 1 \\ 0 & 0 & 0 \\ 0 & 0 & 0 \\ 0 & 0 & 0 \end{bmatrix},$$

$$\mathbf{A}_4 = \begin{bmatrix} 0 & 0 & 0 \\ 0 & 0 & 1 \\ 0 & 1 & 0 \\ -1 & 0 & 0 \end{bmatrix}, \mathbf{B}_1 = \begin{bmatrix} 0 & 0 & 0 \\ 0 & -1 & 0 \\ 0 & 0 & 1 \\ 0 & 0 & 0 \end{bmatrix}, \mathbf{B}_2 = \begin{bmatrix} 0 & 0 & 0 \\ 1 & 0 & 0 \\ 0 & 0 & 0 \\ 0 & 0 & 1 \end{bmatrix},$$

$$\mathbf{B}_3 = \begin{bmatrix} 0 & 0 & 0 \\ 0 & 0 & 0 \\ -1 & 0 & 0 \\ 0 & -1 & 0 \end{bmatrix}, \text{ and } \mathbf{B}_4 = \mathbf{0}_{4\times 3}.$$

This code can be used in WRNs with three relays by simply omitting the fourth columns of (2.12) and hence their encoding matrices $\mathbf{A}_4$ and $\mathbf{B}_4$ should not be used.

3. **Closed-loop extended orthogonal STBC (CL-EO-STBC)** of [39]: At the cost of using a two-bits feedback channel, a full-rate code was proposed in [39] for WRN with four relays, each equipped with a single antenna. The two-bits (U_1 and U_2) are used by the first and third relay to maximise the received SNR at the destination and hence achieve better performance. This code matrix is given by

$$\mathcal{X} = \begin{bmatrix} U_1 s(i,1) & s(i,1) & U_2 s(i,2) & s(i,2) \\ -U_1 s^*(i,2) & -U_2 s^*(i,2) & s^*(i,1) & s^*(i,1) \end{bmatrix}, \tag{2.13}$$

with encoding matrices given by

$$\mathbf{A}_1 = \mathbf{A}_2 \begin{bmatrix} 1 & 0 \\ 0 & 0 \end{bmatrix}, \mathbf{A}_3 = \mathbf{A}_4 = \begin{bmatrix} 0 & 1 \\ 0 & 0 \end{bmatrix},$$

$$\mathbf{B}_1 = \mathbf{B}_2 = \begin{bmatrix} 0 & 0 \\ 0 & -1 \end{bmatrix} \text{and} \mathbf{B}_3 = \mathbf{B}_4 = \begin{bmatrix} 0 & 0 \\ 1 & 0 \end{bmatrix}$$

- **Quasi-orthogonal D-STBCs**:

  1. **The QO-STBC** of [10]: This QO-STBC was designed for WRNs with four relays. Each is equipped with a single-antenna. The coding matrix is given by

$$\mathcal{X} = \begin{bmatrix} s(i,1) & -s^*(i,2) & -s^*(i,3) & s(i,4) \\ s(i,2) & s^*(i,1) & -s^*(i,4) & -s(i,3) \\ s(i,3) & -s^*(i,4) & s^*(i,1) & -s(i,2) \\ s(i,4) & s^*(i,3) & s^*(i,2) & s(i,1) \end{bmatrix}, \tag{2.14}$$

with encoding matrices as $\mathbf{A}_1 = \mathbf{I}_4, \mathbf{A}_2 = \mathbf{0}_4, \mathbf{A}_3 = \mathbf{0}_4, \mathbf{B}_1 = \mathbf{0}_4, \mathbf{B}_4 = \mathbf{0}_4,$

$$\mathbf{A}_4 = \begin{bmatrix} 0 & 0 & 0 & 1 \\ 0 & 0 & -1 & 0 \\ 0 & -1 & 0 & 0 \\ 1 & 0 & 0 & 0 \end{bmatrix}, \mathbf{B}_2 = \begin{bmatrix} 0 & -1 & 0 & 0 \\ 1 & 0 & 0 & 0 \\ 0 & 0 & 0 & -1 \\ 0 & 0 & 1 & 0 \end{bmatrix} \text{ and } \mathbf{B}_3 = \begin{bmatrix} 0 & 0 & -1 & 0 \\ 0 & 0 & 0 & -1 \\ 1 & 0 & 0 & 0 \\ 0 & 1 & 0 & 0 \end{bmatrix}$$

2. **The QO-STBC** of [40]: This code is designed for double dual-antenna relay networks. It is given by

$$\mathcal{X} = \begin{bmatrix} (s(i,1)+s^*(i,2))+(s(i,1)-s^*(i,2)) & (s(i,3)+s^*(i,4))+(s(i,3)-s^*(i,4)) \\ (s(i,2)-s^*(i,1))+(s(i,2)+s^*(i,1)) & (s(i,4)-s^*(i,3))+(s(i,4)+s^*(i,3)) \\ (s(i,3)+s^*(i,4))+(s(i,3)-s^*(i,4)) & (s(i,1)+s^*(i,2))+(s(i,1)-s^*(i,2)) \\ (s(i,4)-s^*(i,3))+(s(i,4)+s^*(i,3)) & (s(i,2)-s^*(i,1))+(s(i,2)+s^*(i,1)) \end{bmatrix}, \tag{2.15}$$

with encoding matrices as $\mathbf{A}_{1,1} = \mathbf{A}_{1,2} = \mathbf{I}_4$,

$$\mathbf{A}_{2,1} = \mathbf{A}_{2,2} = \begin{bmatrix} 0 & 0 & 1 & 0 \\ 0 & 0 & 0 & 1 \\ 1 & 0 & 0 & 0 \\ 0 & 1 & 0 & 0 \end{bmatrix}, \tag{2.16}$$

$$\mathbf{B}_{1,1} = -\mathbf{B}_{1,2} = \begin{bmatrix} 0 & 1 & 0 & 0 \\ -1 & 0 & 0 & 0 \\ 0 & 0 & 0 & 1 \\ 0 & 0 & -1 & 0 \end{bmatrix}, \tag{2.17}$$

and

$$\mathbf{B}_{2,1} = -\mathbf{B}_{2,2} = \begin{bmatrix} 0 & 0 & 0 & 1 \\ 0 & 0 & -1 & 0 \\ 0 & 1 & 0 & 0 \\ -1 & 0 & 0 & 0 \end{bmatrix}. \tag{2.18}$$

The encoding matrices are with double subscript as the relays are equipped with double antennas, meaning that $\mathbf{A}_{n,l}$ denotes the encoding matrix $\mathbf{A}_n$ of the l^{th} antenna of R_n.

Illustrative Example

In this section, an illustrative example is given to show how the transmission is conducted when the D-STBC is employed by a WRN. The network includes a source ($\mathbb{S}$), two half-duplex

(HD) DF relays (R_1 and R_2) and a destination ($\mathbb{D}$). For simplicity, all nodes are assumed to have a single-antenna. As mentioned, the transmission in WRN is conducted through two phases

- **Broadcasting phase**: given that the Alamouti STBC is employed by the network, the source $\mathbb{S}$ broadcasts a symbol vector $\mathbf{y}(i) = [y(i,1), y(i,2)]^T$. Accordingly, the received signal at the relay R_n and $\mathbb{D}$ can be modelled as

$$\underset{J\times 1}{\mathbf{r}_n(i)} = h_n \underset{J\times 1}{\mathbf{y}(i)} + \underset{J\times 1}{\mathbf{v}_n(i)}, \tag{2.19}$$

and

$$\underset{J\times 1}{\mathbf{r}_{DT}(i)} = f \underset{J\times 1}{\mathbf{y}(i)} + \underset{J\times 1}{\boldsymbol{\delta}(i)}, \tag{2.20}$$

respectively, where $J = 2$ is the signalling period in the broadcasting phase. h_n and f ($h_n, f \sim \mathcal{CN}(0,1)$) are the channel coefficients for the $\mathbb{S}$-R_n link and the $\mathbb{S}$-$\mathbb{D}$ link, respectively. $\mathbf{v}_n$ and $\boldsymbol{\delta}(i)$ with entries $v_{n,j}$ and $\delta_j \sim \mathcal{CN}(0, N_0/2)$ are the noise vectors at R_n and the $\mathbb{D}$, respectively.

The symbols received by the $\mathbb{D}$ as a result of direct transmission can be detected using

$$\hat{\mathbf{y}}_{DT}(i,j) = \underset{y\epsilon\mathcal{S}^{1\times 1}}{\operatorname{argmin}} |f^H \mathbf{r}_{DT}(i,j) - |f|^2 y|^2, \forall j. \tag{2.21}$$

- **Relaying phase**: Each relay decodes its received symbols and then these detected symbols are encoded using the Alamouti STBC scheme. To limit the discussion, it has been assumed that the relays are detecting their received symbols successfully (see Section 2.6.1) and hence $\hat{\mathbf{y}}_n(i) = \mathbf{y}(i), \forall n = 1,2$. The resulting encoding symbol vectors of the relay R_1 and R_2 are determined by (2.10) as

$$\begin{aligned} \mathbf{t}_1(i) &= \mathbf{A}_1 \hat{\mathbf{y}}_1(i) + \mathbf{B}_1 \hat{\mathbf{y}}_1^*(i) \\ &= \mathbf{A}_1 \mathbf{y}_1(i) + \mathbf{B}_1 \mathbf{y}_1^*(i) \\ &= \begin{bmatrix} \mathbf{y}(i,1) \\ -\mathbf{y}^*(i,2) \end{bmatrix}, \end{aligned} \tag{2.22}$$

and

$$\begin{aligned}\mathbf{t}_2(i) &= \mathbf{A}_2\hat{\mathbf{y}}_2(i) + \mathbf{B}_2\hat{\mathbf{y}}_2^*(i)\\ &= \mathbf{A}_2\mathbf{y}_2(i) + \mathbf{B}_2\mathbf{y}_2^*(i)\\ &= \begin{bmatrix} \mathbf{y}(i,2) \\ \mathbf{y}^*(i,1) \end{bmatrix},\end{aligned} \tag{2.23}$$

, respectively. It can be seen by comparing (2.22) and (2.23) with (2.11) that the columns of the Alamouti STBC matrix are generated in a distributive manner due to the design of the encoding matrices $\mathbf{A}_n$ and $\mathbf{B}_n$, where $n = 1 - 2$.

Thus, the received signal at the destination $\mathbb{D}$ is given by

$$\underset{L\times N_r}{\mathbf{Z}(i)} = \sum_{n=1}^{N} \underset{L\times 1}{\mathbf{t}_n(i)}\ \underset{1\times N_r}{\mathbf{g}_n} + \underset{L\times N_r}{\boldsymbol{\eta}(i)}, \tag{2.24}$$

where $L = 2$ is the codeword signalling period in the relaying phase, $\mathbf{g}$ is the channel coefficient vector from the relay $\mathbb{R}_n$ to the destination's antennas, with entries $g_j \sim \mathcal{CN}(0,1)$. $\boldsymbol{\eta}(i)$ is the noise matrix at the destination with entries $\eta_{ij} \sim \mathcal{CN}(0, N_0/2)$. It can be seen from (2.19) and (2.24) that $J = L$; this is because the employed STBC is a full-rate coding scheme.

Substituting (2.22) and (2.23) in to (2.24), the received signal can be re-written equivalently as

$$\mathbf{z}(i) = \mathcal{H}\mathbf{y}(i) + \boldsymbol{\eta}(i), \tag{2.25}$$

where $\mathcal{H}$ is the equivalent channel matrix structured according to the Alamouti STBC matrix [12].

One of the key features of the Alamouti STBC scheme is that the code is orthogonal. Thus, a decomposition of the received symbols can be conducted and therefore the detection can be carried out symbol by symbol using

$$\hat{y}(i,j) = \underset{y\in\mathcal{S}^{1\times 1}}{\operatorname{argmin}} |\bar{\mathbf{u}}(i,j) - \lambda y|^2. \tag{2.26}$$

where $\bar{\mathbf{u}} = \mathcal{H}^H\mathbf{z}(i)$ and $\mathcal{H}^H\mathcal{H} = \lambda\mathbf{I}_2$.

As mentioned, the non-orthogonal STBCs (i.e. quasi-orthogonal STBCs of Section 2.7.2) lead to higher decoding complexity. In other words, the search field ($\mathcal{S}^{1\times 1}$) over the modulation

constellation will not be with one-by-one dimension. Its order depends on the level of orthogonality existing in the used STBC.

To show the achieved performance improvement, numerical simulations are provided in Fig. 2.15 in terms of BER. For comparison purposes, the performance of the receiving diversity scheme and the SISO scheme (no diversity is used) are included in the shown figure. All simulations are conducted on a Rayleigh faded channel, and the BPSK modulation scheme is used by the system.

From the shown figure, it can be observed what performance level is achieved if the Alamouti STBC is employed compared to the 'no diversity' scheme. Due to transmission power division, the received diversity scheme outperforms the Alamouti scheme by nearly $3dB$ SNR gain. However, the same diversity gain is achieved while no multiple-antennas are installed. In other words, the D-STBC can avoid the deployment difficulties of multiple-antenna.

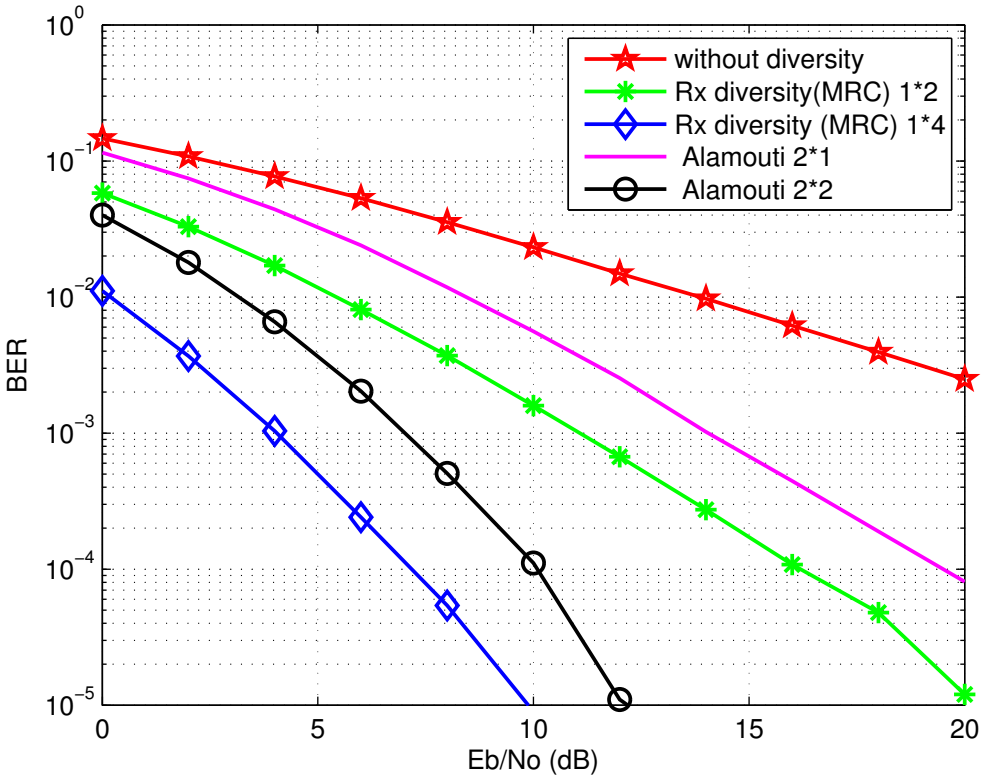

Fig. 2.15: Performance comparison of of receiver space diversity (MRC), SISO scheme and the Alamouti's STBC scheme

2.8 General related literature

Although each thesis part has its own literature review section, some general key researches related to the cooperative communication networks are listed in this section. This is to show how the cooperative communications networks research field has grown over time, due to its novel features. The basic concept of cooperative communication was introduced in [41], where the concept of a relaying channel was discussed. This channel's properties were studied later in [42]. These pioneering researches derived the maximum achievable rate for a basic model of a single source, HD relay and a destination. In [4, 5, 43], the idea of the relay channel was extended in order to improve both the capacity and the outage probability in the uplink transmissions. These works introduced cooperative protocols to allow two users to receive the broadcasting data and retransmit this data back. This results in the diversity gain improving, as uncorrelated paths to the destination are obtained. Later, the cooperation concept was extended in [7, 22], where energy efficient multiple access protocols based on DF and AF relaying protocols were designed. Accordingly, better performance was reported compared to the direct transmission schemes. In [7], an outage probability analysis was shown for the designed proposed protocols. In order to reduce the experienced error-rates, distributed codes were suggested for use by the relays [44–46], including repetition coding [47, 48] and space time coded cooperation [6, 49]. Accordingly, significant performance improvement has been reported, while allowing simultaneous transmission among the relays in the second phase of transmission.

2.9 Conclusion

The background are required for the remaining chapters of this work were introduced in this chapter. In particular, this chapter mainly discussed the cooperative communications networks and the STBC schemes basics. It started by introducing the general block diagrams of wireless communications systems along with a brief description of each block. Then, a general discussion regarding characteristics of wireless propagation channels was presented, followed by the used modulation schemes throughout this work. In addition, the relaying protocols and the most common D-STBC schemes used by cooperative communications were discussed. This discussion included a general related literature review and an illustrative example of a particular WRN along with simulation results. It was shown how much performance improvement was achieved through the cooperative scheme compared with

the SISO scheme. However, the cooperative communication networks still have some issues that limit their ability to be established widely. In the next parts of this work, three issues are considered and some interesting solutions are proposed.

Part I

Wireless Relaying Networks under Imperfect Synchronization

Part 1: Abstract

This part considers WRNs under imperfect synchronization. In the literature, most research tends to assume perfect synchronization among the cooperative relays. Unfortunately, this level of synchronization is almost impossible to achieve in real communication networks, and this introduces a significant performance degradation if imperfect synchronization is present in the network. This part includes mathematical models that are derived for WRNs, either one-way or two-way, under imperfect synchronisation conditions. Unlike existing models, this model provides a simple method of evaluating the problem for variant network configurations. In addition, this model considers the WRNs with N relays, each equipped with R_a antennas, where $N, R_a \in \mathbb{N}^+$. With respect to current literature, the contributions of this part are : (1) both the existing PIC and SIC based detectors, which were proposed for specific network configurations instances, are extended here to work with the general model, and (2) an enhanced interference cancellation based detector (EIC) is proposed. These proposed detectors show significant performance improvement compared to the conventional detector under imperfect synchronisation conditions. In addition, the proposed EIC detector provides better improvement due to the designed interference cancellation process. It reduces the reliance on low-performance symbols and it benefits from interference components of currently-detected symbols using a modified maximum likelihood (ML) scheme. Accordingly, an extra performance improvement is achieved, particularly in the first iteration.

Part I: Publication List

Publications List

- El Astal, M.O.;Olivier, J.C.: "Improved Signal Detection for Two-Way Wireless Relaying Networks under Imperfect-Time Synchronisation," in **EURASIP Journal on Advances in Signal Processing**, 1, 2014, pp.-177. URL: click here.
- El Astal, M.-T. O.; Abu-Hudrouss, A.M.; Olivier, J.C.: "Improved Signal Detection of Wireless Relaying Networks employing Space-Time Block Codes under Imperfect Synchronization," **Wireless Personal Communications**, Springer US, 2014, pp.1-18. DOI:10.1007/s11277-014-2239-4. URL: click here.
- El Astal, M.-T. O.; Salmon, B.P.;Olivier, J.C.: "Distributed Space-Time Block Coding for Two-Way Wireless Relaying Networks: Improved Performance under Imperfect Synchronization," 2014 **IEEE Wireless Communications and Networking conference (WCNC)**, Istanbul, Turkey, pp.1176 - 1181, 6-9 Apr. 2014. URL: click here.
- El Astal, M.-T. O.; Olivier, J.C.: "Distributed Closed-Loop Extended Orthogonal STBC: Improved performance in imperfect synchronization," 2013 **IEEE 24th International Symposium on Personal Indoor and Mobile Radio Communications (PIMRC)**, London, UK, pp.1941-1945, 8-11 Sept. 2013. URL: click here.
- El Astal, M.-T. O.; Olivier, J.C.: "Distributed orthogonal STBC for amplify and forward cooperative network under imperfect synchronization," 2012 **IEEE 14th International Conference on Communication Technology (ICCT)**, Chengdu, China, pp.364-368, 9-11 Nov. 2012. URL: click here.

3 One-way WRNs under Imperfect Synchronisation

> *Nothing is impossible, the word itself says 'I'm possible'!*
>
> **— Audrey Hepburn**

3.1 Introduction

In [6, 11], the idea of space-time coding devised for multiple-antenna systems was applied to the problem of communication over WRNs. This is known as a D-STBC [6]. It has been shown that the D-STBCs have the potential to exploit the diversity gain inherent in a wireless relaying communication channel and provide a notable coding gain [6, 10, 11, 50]. Compared with STBC schemes, D-STBC creates a virtual antenna array by using neighbouring relays to assist the transmission of the source to the destination [7, 13]. This means that reliability can be improved, while the deployment difficulties are avoided. However, most existing research assumes that the relays are perfect synchronised. This means that all the relays' transmitted sequences have the same timing and the same propagation delay when received by the destination [14, 15, 36, 37]. Unfortunately, this assumption is unrealistic or, at the very least, it imposes conditions that are difficult or even impossible to achieve in real world networks [14, 15, 51]. The lack of a common timing reference negatively impacts the network's performance [36]. In this chapter, a brief discussion of the majority of the existing schemes used to mitigate the effects of asynchronism is introduced. This is followed by a mathematical model which is derived under a condition of imperfect synchronisation for one-way WRNs. Then, both the existing PIC and SIC based detectors are extended to work for the derived model. These detectors show a better performance improvement compared to the conventional detectors. In addition, an enhanced interference cancellation based detector (EIC) is proposed. This detector conducts an innovative iterative interference cancellation process. Also, it reduces the reliance on low-performance symbols and tries to

benefit from the interference components of currently-detected symbols. Accordingly, an extra performance improvement is achieved, particularly in the first iteration, compared to the extended detectors.

3.2 Prior Works

It would appear that limited research has been done on addressing the imperfect synchronisation of D-STBC networks, while maintaining the low-decoding complexity. This section briefly addresses the few elements of research that exist in this field. This brief is shown in details in our work of [52], which offers an overview of the methodology, features, drawbacks, and assumptions of these few elements of research. The existing research works can be categorized into: detectors based on iterative interference cancellation, detector based on OFDM schemes, and Miscellaneous detector schemes.

3.2.1 Detectors based on Iterative Interference Cancellation

The articles in this group involve adapting one of the iterative interference cancellation techniques in order to design a detector that has ability to mitigate the experienced performance degradation. In fact, these articles either employ a PIC or a SIC. The resulting schemes retain the key features of D-STBC: simplicity and optimality. However, these detectors were designed for specific network configurations. A general description is provided below, where the related articles are compared in Tab. 4.2.

Detectors based on PIC:

Researchers who use the iterative PIC based detectors have created a model of the interference terms, denoted here as $\mathbf{q}(i)$, and then try to cancel these terms in an iterative manner. Initially, the interference model ($\mathbf{q}(i)$) is fed by the detected symbols of the DT-link (see (3.2)), then the detector use this interference-cancelled received signal to estimate the transmitted data. The result of this detection is fed back to the detector which then conducts a new iteration. Usually, the PIC detectors converge in 3-4 iterations in order to achieve a performance close to that of conditions under perfect-synchronisation. Although the PIC based detector is model dependent, most PIC based detectors use the procedures illustrated in Fig. 3.1. In this figure, the received signal at the destination is denoted as $\mathbf{z}(i)$.

$\mathbf{q}(i)$ denotes the interference model and $\hat{\mathbf{y}}(i)$ denotes the detection result. The interference model is initialised by the DT-link result $\hat{\mathbf{y}}_{DT}$.

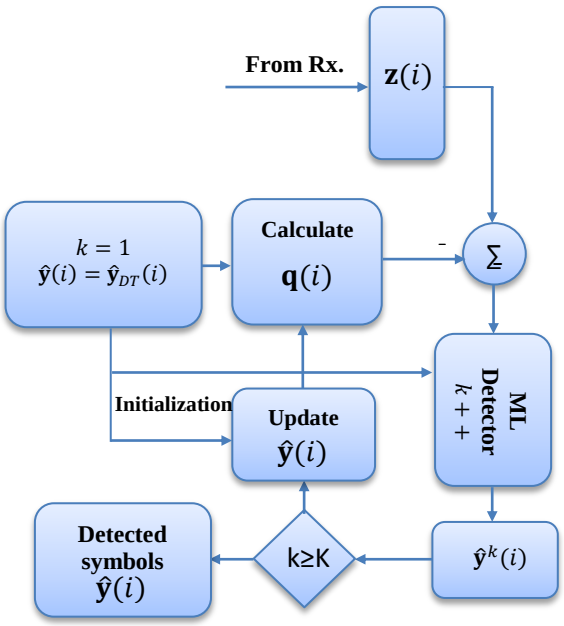

Fig. 3.1: D-STBC PIC based detectors approach.

Detectors based on SIC:

In [37], the authors propose a new approach wherein the PIC can be enhanced to converge quickly. It operates by rephrasing the interference model ($\mathbf{q}(i)$) in terms of the original transmitting symbols. This is to order the cancellation and decoding process according to the interference amount seen on each slot. The result of the entire detection is fed back to the detector so that a new iteration can be conducted (see Fig. 3.2). The SIC detectors usually converge in two-three iterations and achieve a performance closer to that under perfect-synchronisation conditions than what can be achieved using the PIC detector.

In the shown figure, $\mathbf{G}_q$ denotes the channel matrix of $\mathbf{q}(i)$ while $\mathbf{q}_{eq}(\ell, i)$ denotes the equalised interference time-slot ℓ.

3.2.2 Detector based on OFDM schemes

The orthogonal frequency division multiplexing (OFDM) enables D-STBC networks to counter the imperfect synchronisation issue [53]. In [54, 55], a novel transmission scheme

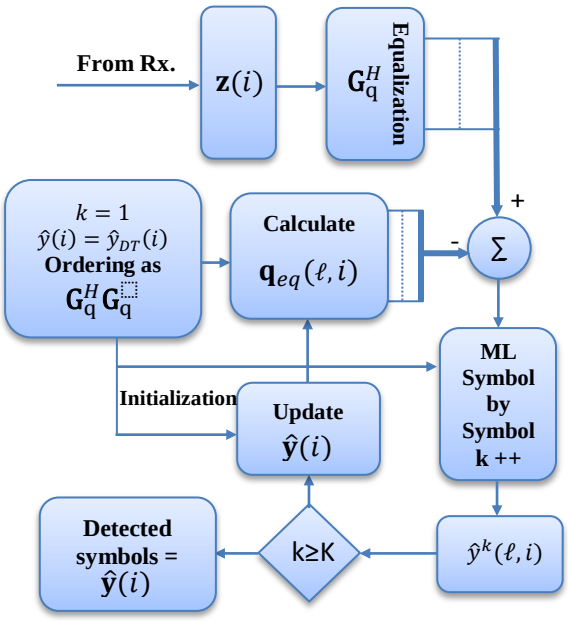

Fig. 3.2: D-STBC SIC based detectors approach

was proposed for asynchronous WRNs with 3-4 AF relays. This scheme uses the cyclic prefix of the OFDM along with a low-rate feedback channel to provide robustness to counter the time misalignment among the relays. The research presented by [56] considered the case of WRNs with high number of relays. It focused on both timing and carrier frequency misalignments among the relay transmissions. In [57], the time delay issue of AF D-STBC networks, where there is only one relay, was studied over frequency-selective channels. In addition, an equalization scheme based on an inter-block interference cancellation (IBIC) and a cyclic prefix reconstruction of [58] was proposed to suppress the effects of imperfect synchronisation. This is while making no additional demands on the 3GPP-LTE up-link frame structure. It is worth noting that the research in this section requires an additional level of computational complexity at both the transmitter and receiver. This is to deal with the OFDM transmission scheme and the used feedback channel.

3.2.3 Miscellaneous detector schemes

There is some research that focuses on neither iterative based nor OFDM based detectors, but rather on changing the transmission scheme. In [59], a near-optimum detector was proposed to deal with asynchronism in the WRNs, but it is restricted to just two-relays DF WRNs. This detector is mainly based on the PIC concept, but without iterations. This is because three out of four interference terms can be completely cancelled if a proper initialization is used.

The fourth term can be counteracted by ordering the detection process to hone firstly on the second symbol and then return to the first symbol. This detector uses the DT-link symbols of phase 1 in order to enhance system performance by employing the MRC approach. Its performance is very close to that of perfect synchronisation conditions, only needing M/2 additional multiplications per symbol in order to achieve this state. A transmission scheme to deal with both imperfect synchronisation and channel dispersion on the D-STBC networks was proposed by [60]. This scheme was designed only for P2P systems as it does not take into account the existence of multiple users.

3.3 Network Modelling

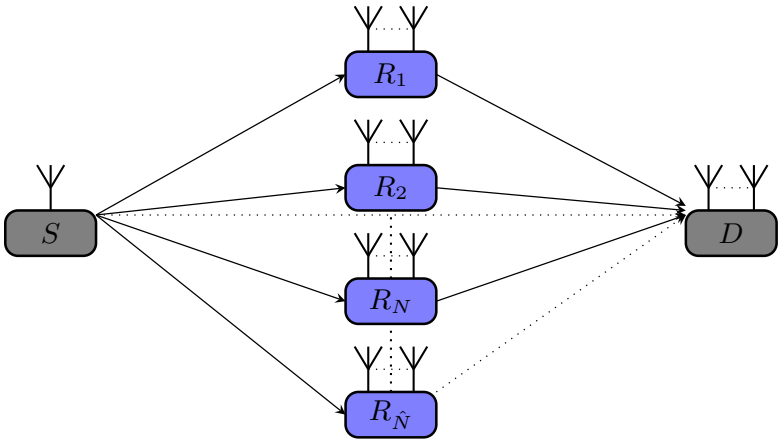

Fig. 3.3: One-way Wireless Relaying Networks Model

The network is comprised of a source S, a number $\hat{N}$ of HD relays $R_1, \ldots, R_N$, and a destination D (as shown in Fig. 3.3). Note that both the source and destination are single-antenna nodes while relays are equipped each with R_a HD antennas; this configuration is described afterwards by $\left(1 \rightarrow R_a^{\hat{N}} \rightarrow 1\right)$. This model can be straightforwardly extended to a multiple-antenna destination scenario. The channel is assumed to be a Quasi-static Rayleigh fading channel, and perfect channel state information (CSI) is assumed to be known only at the decoding node. The total transmission power dedicated to the entire network is denoted as P, and divided between both phases of the transmission according to the used power loading scheme. The communication through the network is conducted in two phases as

Phase 1 (Broadcasting phase): During this phase, the source broadcasts its J symbols $\mathbf{y}(i) = [y(i,1)\dots y(i,J)]^T$ to both the relays and destination. Their receiving signals can be represented by

$$\underset{(R_a\times J)\times 1}{\mathbf{r}_n(\mathrm{i})} = \sqrt{P_1}\ \underset{(R_a\times J)\times J}{\mathbf{H}_n}\ \underset{J\times 1}{\mathbf{y}(\mathrm{i})} + \underset{J\times 1}{\mathbf{v}_n(\mathrm{i})}, \tag{3.1}$$

and

$$\underset{J\times 1}{\mathbf{r}_{DT}(\mathrm{i})} = \sqrt{P_1} f \underset{J\times 1}{\mathbf{y}(\mathrm{i})} + \underset{J\times 1}{\boldsymbol{\delta}(\mathrm{i})}, \tag{3.2}$$

where $\mathbf{r}_{DT}$ and $\mathbf{r}_n$ are the received signals during the broadcasting phase at the relay R_n and at the destination (denoted as DT signal), respectively. P_1 is the power dedicated for the first phase of transmission. Here, $\mathbf{H}_n = \mathbf{I}_J \otimes \mathbf{h}_n$ and $\mathbf{h}_n = [\ h_{n,1}\quad h_{n,2}\quad \cdots\quad h_{n,R_a}\ ]^T$ is the channel coefficient matrix for the S-R_n link with entries $h_{n,i} \sim \mathcal{CN}(0,1)$. $f \sim \mathcal{CN}(0,1)$ is the channel coefficient for the $S-D$ link. The $h_{n,i}$ and f are assumed to remain constant for every J consecutive channel used. Both $\mathbf{v}_n$ and $\boldsymbol{\delta}$ are the AWGN noise vectors at the relay R_n and the destination with entries $n_{n,i}$ and $v_i \sim \mathcal{CN}(0,1)$, respectively.

The detection of the broadcasting phase symbols, which are available at the destination and denoted as DT results, can be carried out using

$$\widehat{\mathbf{y}}_{DT}(i,j) = \arg\min_{y\in\mathcal{S}^{1\times 1}} \|\mathbf{r}_{DT}(\mathrm{i},\mathrm{j}) - fy\|^2 \tag{3.3}$$

where $j = 1\dots J$ and J is the number of symbols contained in $\mathbf{y}$. This detection result is used by a network to enhance performance through MRC [59], or here to initialize the interference cancellation process (to be shown later).

Phase 2 (Relaying phase): To minimise error propagation, certain relaying protocols assume that only the relays which satisfy a selection performance criteria will be participating in this phase (see Section 2.6.1). To limit the discussion, it has been assumed here that N out of $\hat{N}$ relays are participating. In the selective protocols $\hat{N} \leq N$ while $\hat{N} = N$ for the non-selective relaying protocol. During this phase, the participating relays will process, encode, and forward their received symbols to the destination. This process varies according to the employed relaying protocol. As shown in Section 2.7.2, the encoding matrices $\mathbf{A}_n^{(\ell)}$ and $\mathbf{B}_n^{(\ell)}$ with $\ell = 1,\dots,L$, are used by R_n to generate its portion of the particular used $L \times (R_a \times \hat{N})$ STBC coding matrix ($\mathcal{X}_k$), wherein k is the number of data symbols embedded

in the code matrix. The code rate is given as $r = k/L$. To avoid the necessity of buffering, $J = k$ should be hold. Generally, the R_n's transmitted signal can be written as

$$\mathbf{t}_n(i,\ell) = \sqrt{P_2}\beta\left(\mathbf{A}_n^{(\ell)}\mathbf{r}_n(\mathrm{i}) + \mathbf{B}_n^{(\ell)}\mathbf{r}_n^*(\mathrm{i})\right) \tag{3.4}$$

where P_2 is the power dedicated to the relaying phase, and β is the scaling factor required by particular types of relaying protocol, i.e., a power amplification factor in the AF relaying protocol.

These signals are forwarded from all participating nodes ($\hat{N}$) to the destination simultaneously. Due to numerous factors such as different propagation delays, the relays' transmission will arrive at the destination D with a different time misalignment τ_n as illustrated in Fig. 3.4. It is essential that the handshaking among the relays is used as infrequently as possible to save energy and bandwidth. Therefore, perfect synchronisation among them is difficult or even impossible to achieve [14, 15]. However, an assumption of quasi-synchronisation can be made [36, 37, 59, 61, 62]. It states that $0 \le \tau_n \le 0.5T$, where T is the symbol period. Otherwise (which is the case of $kT \le \tau_n \le (k+1)T$, where $k = 1, 2, ...$), the time advanced node can simply be forced to delay its transmission by kT. Such process can be carried out during the link set-up and channel estimation stage [36]. Due to sampling or matched filtering (whatever kind of pulse shaping is used) [37], τ_n still cause inter-symbol interference (ISI). Without loss of generality, the destination is assumed to be synchronised perfectly with

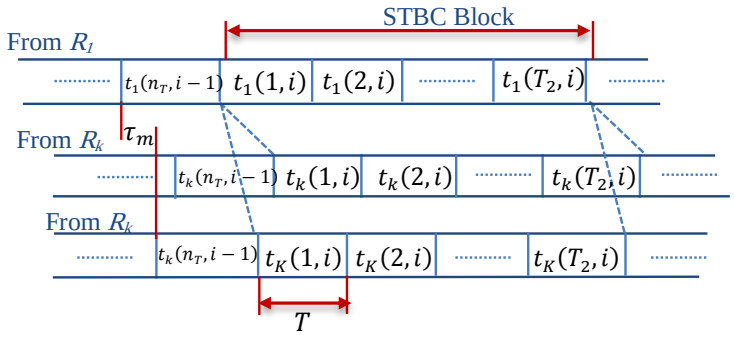

Fig. 3.4: Received signal at the destination under imperfect synchronisation conditions.

the relay R_1. Accordingly, the received signal at the destination can be modelled as

$$\mathbf{z}(i,1) = \sqrt{P_2}\beta\sum_{n=1}^{N}\mathbf{g}_{n^{(0)}}\mathbf{t}_n(i,1) + \sqrt{P_2}\beta\sum_{n=2}^{N}\mathbf{g}_{n^{(1)}}\mathbf{t}_n(i-1,L) + \boldsymbol{\eta}(i,1) \tag{3.5}$$

and

$$\mathbf{z}(i,\ell) = \sqrt{P_2}\beta \sum_{n=1}^{N} \mathbf{g}_{n^{(0)}} \mathbf{t}_n(i,\ell) + \sqrt{P_2}\beta \sum_{n=2}^{N} \mathbf{g}_{n^{(1)}} \mathbf{t}_n(i,\ell-1) + \boldsymbol{\eta}(i,\ell), \tag{3.6}$$

where $\boldsymbol{\eta}$ is the noise vector at the destination with entries $\eta_i \sim \mathcal{CN}(0,1)$. $\mathbf{g}_{n^{(0)}} = [g_{n,1^{(0)}}, \ldots, g_{n,R_a{}^{(0)}}]^T$ is the current time slot channel coefficient vectors for the R_n-and-D link; $\mathbf{g}_{n^{(\nu)}}$ for $\nu = 1, \ldots, \infty$ represent the composite effects of time delay and the pulse shaping waveform (PSW) for the mentioned link. As they are much less dominant, $\mathbf{g}_{n^{(\nu)}}$ for $\nu = 2, \ldots, \infty$ can be truncated [36]. The strength of $\mathbf{g}_{n^{(1)}}$ can be represented by

$$\alpha_n = \frac{\|\mathbf{g}_{n^{(1)}}\|^2}{\|\mathbf{g}_{n^{(0)}}\|^2}. \tag{3.7}$$

Its value depends upon the time misalignment and the PSW used. Regardless of which PSW is used, it is worth noting that $\alpha_n = 0$ for $\tau_n = 0$ and $\alpha_n = 1(0dB)$ for $\tau_n = 0.5T$. This is due to symmetry in the PSW.

Substituting (3.4) into (3.5) and (3.6), signal components of $\mathbf{z}(i,\ell)$ can be written in term of $\mathbf{y}(i)$ as

$$\underset{L\times 1}{\mathbf{z}(i)} = \sqrt{P_1 P_2}\beta \left(\underbrace{\mathbf{A}_{g^{(0)}} \mathbf{H}\mathbf{y}(i)}_{\mathbf{C}_1} + \underbrace{\mathbf{B}_{g^{(0)}} \mathbf{H}^* \mathbf{y}^*(i)}_{\mathbf{D}_1} \right) + \mathbf{q}(i) + \boldsymbol{\zeta}(i), \tag{3.8}$$

where

$$\underset{L\times(J\times N\times R_a)}{\mathbf{A}_{g^{(0)}}} = \begin{bmatrix} \mathbf{g}_1^T \mathbf{A}_1^{(1)} & \mathbf{g}_{2\,(0)}^T \mathbf{A}_2^{(1)} & \cdots & \mathbf{g}_{N^{(0)}}^T \mathbf{A}_N^{(1)} \\ \mathbf{g}_1^T \mathbf{A}_1^{(2)} & \mathbf{g}_{2\,(0)}^T \mathbf{A}_2^{(2)} & \cdots & \mathbf{g}_{N^{(0)}}^T \mathbf{A}_N^{(2)} \\ \vdots & \ddots & \ddots & \vdots \\ \mathbf{g}_1^T \mathbf{A}_1^{(L)} & \mathbf{g}_{2\,(0)}^T \mathbf{A}_2^{(L)} & \cdots & \mathbf{g}_{N^{(0)}}^T \mathbf{A}_N^{(L)} \end{bmatrix},$$

$$\underset{L\times(J\times N\times R_a)}{\mathbf{B}_{g^{(0)}}} = \begin{bmatrix} \mathbf{g}_1^T \mathbf{B}_1^{(1)} & \mathbf{g}_{2\,(0)}^T \mathbf{B}_2^{(1)} & \cdots & \mathbf{g}_{N^{(0)}}^T \mathbf{B}_N^{(1)} \\ \mathbf{g}_1^T \mathbf{B}_1^{(2)} & \mathbf{g}_{2\,(0)}^T \mathbf{B}_2^{(2)} & \cdots & \mathbf{g}_{N^{(0)}}^T \mathbf{B}_N^{(2)} \\ \vdots & \ddots & \ddots & \vdots \\ \mathbf{g}_1^T \mathbf{B}_1^{(L)} & \mathbf{g}_{2\,(0)}^T \mathbf{B}_2^{(L)} & \cdots & \mathbf{g}_{N^{(0)}}^T \mathbf{B}_N^{(L)} \end{bmatrix},$$

$$\underset{(J\times N\times R_a)\times J}{\mathbf{H}} = \begin{Bmatrix} \begin{bmatrix} \mathbf{H}_1^T, & \ldots, & \mathbf{H}_N^T \end{bmatrix}^T & \text{for AF protocols family} \\ \frac{1}{\sqrt{P_1}} \begin{bmatrix} \mathbf{I}_J, & \ldots, & \mathbf{I}_J \end{bmatrix}^T & \text{for DF protocols family} \end{Bmatrix}, \tag{3.9}$$

and $\mathbf{q}(i) = \mathbf{q}_0(i) + \mathbf{q}_1(i)$. With

$$\underset{L\times 1}{\mathbf{q}_0(i)} = \sqrt{P_1 P_2}\beta \left(\underbrace{\Psi_1(\mathbf{A}_{g(1)}, 1)\mathbf{H}}_{\mathbf{C}_2}\mathbf{y}(i) + \underbrace{(\Psi(\mathbf{B}_{g(1)}, 1)\mathbf{H}^*}_{\mathbf{D}_2}\mathbf{y}^*(i) \right), \tag{3.10}$$

and

$$\underset{L\times 1}{\mathbf{q}_1(i)} = \sqrt{P_1 P_2}\beta \left(\Psi_2(\mathbf{A}_{g(1)}, L-1)\mathbf{H}\mathbf{y}(i-1) + \Psi_2\mathbf{B}_{g(1)}\mathbf{H}^*\mathbf{y}^*(i-1)\right), \tag{3.11}$$

where $\mathbf{A}_{g(1)}$ and $\mathbf{B}_{g(1)}$ are formed with $\mathbf{g}_n(1)$ instead of $\mathbf{g}_{n(0)}$, given that $\mathbf{g}_{1(1)} = \mathbf{0}_{R_a\times 1}$ as follows:

$$\underset{L\times(J\times N\times R_a)}{\mathbf{A}_{g(1)}} = \begin{bmatrix} \mathbf{0}_{1\times J} & \mathbf{g}_2^T(1)\mathbf{A}_2^{(1)} & \cdots & \mathbf{g}_N^T(1)\mathbf{A}_N^{(1)} \\ \mathbf{0}_{1\times J} & \mathbf{g}_2^T(1)\mathbf{A}_2^{(2)} & \cdots & \mathbf{g}_N^T(1)\mathbf{A}_N^{(2)} \\ \vdots & \ddots & \ddots & \vdots \\ \mathbf{0}_{1\times J} & \mathbf{g}_2^T(1)\mathbf{A}_2^{(L)} & \cdots & \mathbf{g}_N^T(1)\mathbf{A}_N^{(L)} \end{bmatrix}$$

and

$$\underset{L\times(J\times N\times R_a)}{\mathbf{B}_{g(1)}} = \begin{bmatrix} \mathbf{0}_{1\times J} & \mathbf{g}_2^T(1)\mathbf{B}_2^{(1)} & \cdots & \mathbf{g}_N^T(1)\mathbf{B}_N^{(1)} \\ \mathbf{0}_{1\times J} & \mathbf{g}_2^T(1)\mathbf{B}_2^{(2)} & \cdots & \mathbf{g}_N^T(1)\mathbf{B}_N^{(2)} \\ \vdots & \ddots & \ddots & \vdots \\ \mathbf{0}_{1\times J} & \mathbf{g}_2^T(1)\mathbf{B}_2^{(L)} & \cdots & \mathbf{g}_N^T(1)\mathbf{B}_N^{(L)} \end{bmatrix}.$$

The noise terms accumulated at the destination are modelled as

$$\begin{aligned} \underset{L\times 1}{\zeta(i)} = \sqrt{\beta}\,\big(&(\mathbf{A}_{g(0)} + \Psi_1(\mathbf{A}_{g(1)}, 1))\,\mathbf{v}(i) + \Psi_2(\mathbf{A}_{g(1)}, L-1)\mathbf{v}(i-1) \\ &+ (\mathbf{B}_{g(0)} + \Psi_1(\mathbf{B}_{g(1)}, 1))\,\mathbf{v}^*(i) + \Psi_2(\mathbf{B}_{g(1)}, L-1)\mathbf{v}^*(i-1)) + \boldsymbol{\eta}(i) \end{aligned} \tag{3.12}$$

where $\mathbf{v} = \left[\mathbf{v}_1^T, \ldots, \mathbf{v}_N^T\right]^T$ and $\boldsymbol{\eta} \in \mathcal{CN}(0, 1)$. This noise model of (3.12) is for the case of AF network while $\zeta(i) = \boldsymbol{\eta}(i)$ is in the case of DF networks.

With some more algebraic manipulations, equation (3.8) can be rearranged and rewritten for detection as

$$\underset{2L\times 1}{\bar{\mathbf{z}}(i)} = \sqrt{P_1}\beta\mathbf{G}_{\mathbf{H}}\underset{2L\times 1}{\bar{\mathbf{y}}(i)} + \mathbf{G}_{\mathbf{q}}\underset{2L\times 1}{\bar{\mathbf{y}}(i)} + \underset{2L\times 1}{\bar{\mathbf{q}}_1(i)} + \underset{2L\times 1}{\bar{\boldsymbol{\zeta}}(i)}, \tag{3.13}$$

where

$$\underset{2L\times 2J}{\mathbf{G_H}} = \begin{bmatrix} \Re(\mathbf{C}_1+\mathbf{D}_1) & \Im(-\mathbf{C}_1+\mathbf{D}_1) \\ \Im(\mathbf{C}_1+\mathbf{D}_1) & \Re(\mathbf{C}_1-\mathbf{D}_1) \end{bmatrix}, \tag{3.14}$$

and

$$\underset{2L\times 2J}{\mathbf{G_q}} = \begin{bmatrix} \Re(\mathbf{C}_2+\mathbf{D}_2) & \Im(-\mathbf{C}_2+\mathbf{D}_2) \\ \Im(\mathbf{C}_2+\mathbf{D}_2) & \Re(\mathbf{C}_2-\mathbf{D}_2) \end{bmatrix}. \tag{3.15}$$

It is worth noting that the interference term $\mathbf{q}_0(i)$ is written in terms of $\mathbf{y}(i)$ as the proposed detector requires this form. Now, the derived mathematical model is evaluated for a few instances of one-way WRN configurations. These instances are used for evaluating the proposed improved detection methods shown later. It will become clear how this general model eases the modelling process of any instances of WRN configurations.

3.3.1 Four-relay AF WRN using 3/4 OSTBC

An one-way WRN with four relays ($N = 4$) is considered. These relays are employing a non-selective AF protocol, hence $\hat{N} = N$. The network uses the OSTBC of Section 2.7.2, it assumes that $J = k = 3$ and $L = 4$. The encoding matrices are shown in Section 2.7.2. These configurations refered to as Network I. The used power loading scheme is

$$P_1 = \frac{P_t + L/J - \sqrt{(P_t+L/J)(P_t+2)L/J/2}}{2(1-L/J/2)},$$
$$P_2 = \frac{(P_t-2P_1)J}{4L} \text{and} \beta = \frac{P_2 L}{(P_1+1)J}.$$

Accordingly, the components of (3.13) for Network I can be modelled as

$$\mathbf{C}_1 = \begin{bmatrix} g_1 h_1 & g_{2^{(0)}} h_2 & g_{3^{(0)}} h_3 \\ 0 & 0 & g_{4^{(0)}} h_4 \\ 0 & g_{4^{(0)}} h_4 & 0 \\ -g_{4^{(0)}} h_4 & 0 & 0 \end{bmatrix}, \mathbf{D}_1 = \begin{bmatrix} 0 & 0 & 0 \\ g_{2^{(0)}} h_2^* & -g_1 h_1^* & 0 \\ -g_{3^{(0)}} h_3^* & 0 & g_1 h_1^* \\ 0 & -g_{3^{(0)}} h_3^* & g_{2^{(0)}} h_2^* \end{bmatrix},$$

$$\mathbf{C}_2 = \begin{bmatrix} 0 & 0 & 0 \\ 0 & g_{2^{(1)}} h_2 & g_{3^{(1)}} h_3 \\ 0 & 0 & g_{4^{(1)}} h_4 \\ 0 & g_{4^{(1)}} h_4 & 0 \end{bmatrix}, \mathbf{D}_2 = \begin{bmatrix} 0 & 0 & 0 \\ 0 & 0 & 0 \\ g_{2^{(1)}} h_2^* & 0 & 0 \\ -g_{3^{(1)}} h_3^* & 0 & 0 \end{bmatrix},$$

and

$$\mathbf{q}_1(i) = \begin{bmatrix} -g_{4(1)}h_4\mathbf{y}(i,1) - g_{3(1)}h_3^*\mathbf{y}^*(i,2) + g_{2(1)}h_2^*\mathbf{y}^*(i,3) \\ 0 \\ 0 \\ 0 \end{bmatrix}.$$

3.3.2 Four-relay DF WRN using CL-EO-STBC

An one-way network with four relays employing a selective DF protocol is considered. This means that $N = \hat{N} = 4$. This network uses the CL-EO-STBC of Section 2.7.2, it assumes $J = L = 2$. The corresponding encoding matrices are shown in Section 2.7.2. This scheme achieves full diversity gain and offers a full code-rate, even when using four relays. However, a *two-bit* feedback channel is required, U_1 and U_2. The used power loading scheme is shown below.

$$P_1 = \frac{P_t}{2},\ P_2 = \frac{P_t}{8} \text{ and } \beta = 1.$$

Accordingly, the components of (3.13) for these shown configurations (refered to as Network II) can be simplified as

$$\mathbf{C}_1 = \begin{bmatrix} g_1U_1 + g_2(0) & g_{3(0)}U_2 + g_{4(0)} \\ 0 & 0 \end{bmatrix}, \mathbf{D}_1 = \begin{bmatrix} 0 & 0 \\ g_{3(0)}U_2 + g_{4(0)} & -g_1U_1 - g_{2(0)} \end{bmatrix},$$

$$\mathbf{C}_2 = \begin{bmatrix} 0 & 0 \\ g_{2(1)} & g_{3(1)}U_2 + g_{4(1)} \end{bmatrix}, \mathbf{D}_2 = \mathbf{0}_2 \text{ and}$$

$$\mathbf{q}_1(i) = \begin{bmatrix} (U_2g_3(1) + h_4(1))\mathbf{y}(i-1,1) + g_2(1)f_3\mathbf{y}(i-1,2) \\ 0 \end{bmatrix}.$$

3.4 Detection methods

As mentioned, Tab. 4.2 presents the full picture of what research has been done; hence it can be used to identify what is still lacking. It can be seen that both the PIC and SIC based detectors vary according to the network configuration, including relaying protocol, coding

scheme, relays number, and network type. Therefore, there is a need to extend both of these existing detectors in order to adapt the varying of network configurations.

Accordingly, these ideas are extended in this part of the thesis. In addition, an enhanced detector is proposed which shows better performance improvement. To avoid repetition, the conventional, extended and proposed detectors are shown in Section 4.4. This is because that they are designed for either for one-way or two-way WRNs.

3.5 Simulation Results and Discussion

In terms of BER, the simulation results of using the proposed EIC and PIC detectors in Network II are provided under different conditions of imperfect synchronisation. This network uses the CL-EO-STBC of Section 2.7.2. For clarity, the SIC is not included in the shown figures. This is because there is no noticeable performance difference between EIC and SIC detector in the case of $L = 2$. The simulations are conducted over a Rayleigh block fading channel and using 8-PSK Gray coded modulation. For comparison purposes, these results include the BER of the conventional detector assuming both perfect and imperfect synchronisation. It should be noted that this specific PIC detector instance, was proposed in [55].

In Fig. 3.5, the performance of the conventional detector is simulated under different amounts of imperfect synchronisation which range from very little to severely imperfect synchronisation. This figure shows that even under low levels of imperfect synchronisation, the conventional detector leads to a significant performance degradation. It means that the conventional detector is very sensitive to time misalignments. This figures includes also the performance of OSTBC of [36, 37] to show why the CL-EO-STBC is interesting. This code achieves 3 dB SNR gain better than the STBC of [36, 37]. Moreover, this code can offer a full code-rate even with four relay one-way WRNs.

In Fig. 3.6, the network is simulated with $\alpha = -3dB$. This value is seen as a moderate condition of imperfect synchronisation. It can be observed that a performance improvement can be achieved when the PIC detector is used, and even more by using the proposed detector (EIC). Specifically, one iteration of the EIC based detector offers a performance better than two iterations of the PIC based detector. By one more iteration, a performance close to the perfect synchronisation case can be achieved. To show the effectiveness of the

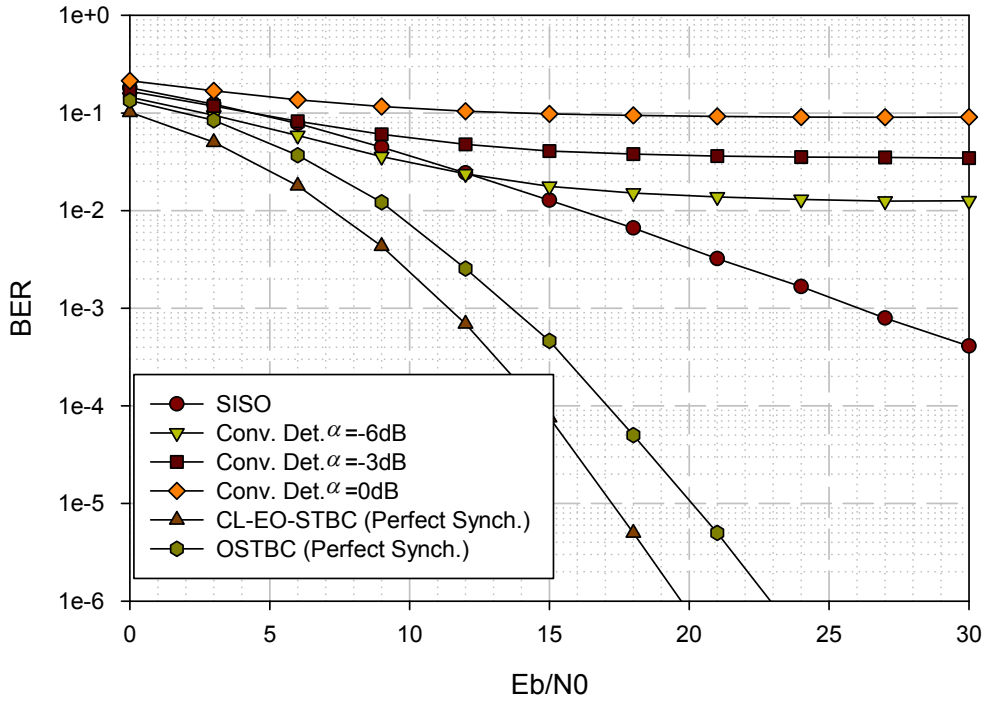

Fig. 3.5: The BER performance of using a conventional detector in Network II under different α values

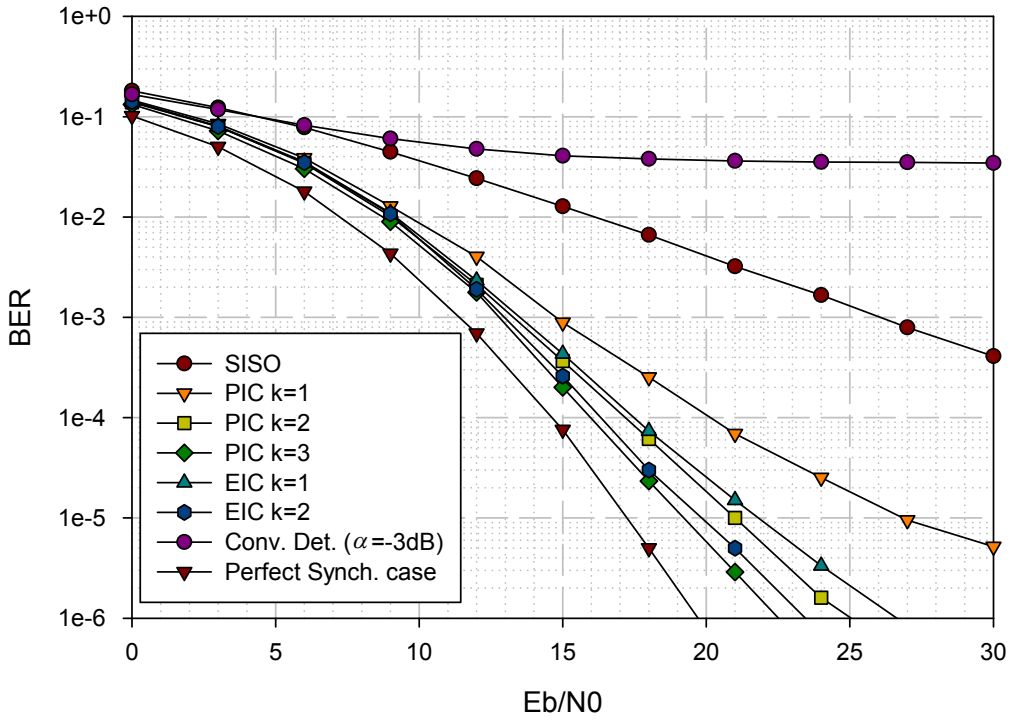

Fig. 3.6: The BER performance by using an EIC and PIC detector in Network II when $\alpha = -3dB$

EIC detector, the Network II is simulated with $\alpha = 0dB$ and shown in Fig. 3.7. It can be seen that the proposed detector still has its key features, even under severe conditions of imperfect synchronisation. Its first iteration is still better than the two iterations of the PIC based detector, and it achieves the perfect synchronisation case in two iterations only.

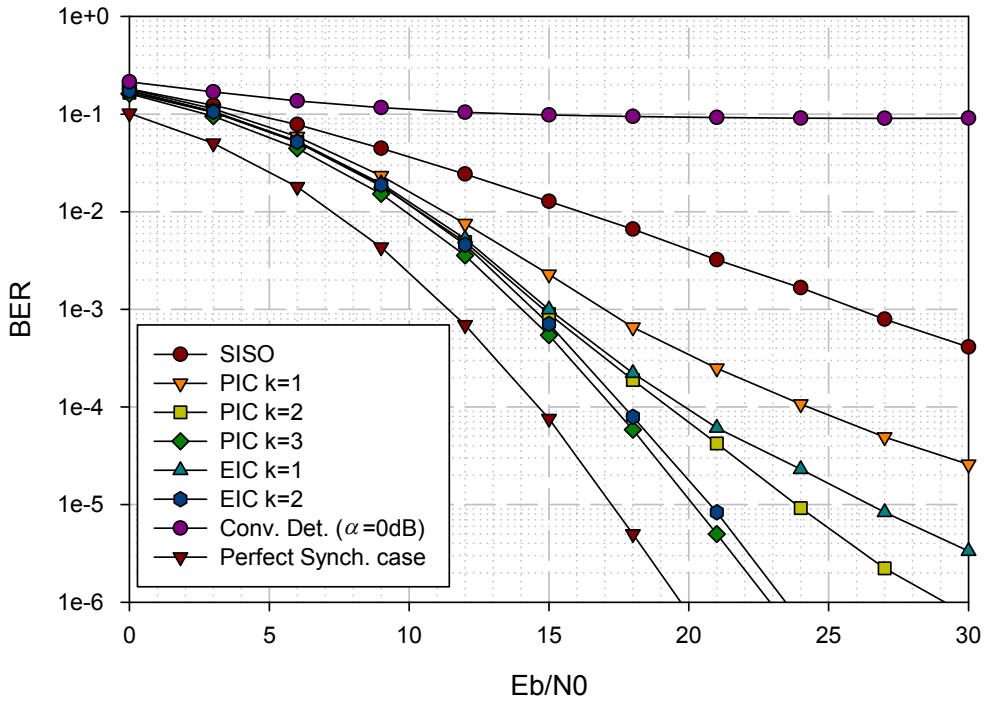

Fig. 3.7: The BER performance by using an EIC and PIC detector in Network II when $\alpha = 0dB$

3.6 Conclusion

It has been shown that the D-STBC has the ability to both exploit the diversity gain inherent in a wireless relaying communication channel and provide a notable coding gain. However, most of the existing research assumes a perfect synchronisation among the relays with reference to the destination, which is difficult or even impossible to achieve in real world networks. This lack of a common timing reference negatively impacts the network's performance. This chapter considered the case of one-way networks. It provides a brief discussion of the majority of the existing schemes. In addition, a mathematical model was derived for WRNs with arbitrary number of relays. Then, both the existing PIC and SIC based detectors were extended to work for the general derived model under imperfect synchronisation conditions. They showed a better performance improvement compared to

the conventional detector. Finally, an enhanced interference cancellation based detector (EIC) was proposed to mitigate the experienced performance degradation. This detector showed higher performance, particularly in the first iteration. This is because it reduces the reliance on low-performance symbols and benefits from interference components of currently-detected symbols.

4 Two-way WRNs under Imperfect Synchronisation

> *Innovation distinguishes between a leader and a follower.*
>
> **— Steve Jobs**
> (CEO Apple Inc.)

4.1 Introduction

As mentioned in Chapter 2, the potential spatial diversity that arises from the presence of multiple distributed nodes in a network can be exploited if suitable cooperation is arranged among these nodes [7]. This creates a virtual MIMO network. In [6], the use of D-STBCs was suggested to exploit the spatial diversity effectively and hence improve the link reliability. In addition, the use of D-STBC increases the network's spectrum efficiency as it allows simultaneous transmission from relays. However, this network is still limited by half-duplex constraints. In other words, to exchange a data packet between the connection terminals, four time-slots are required. In contrast, two-way wireless relaying networks (TWRNs) have been proposed to halve this required number of time slots by allowing also the terminals to transmit simultaneously [63].

Due to promising bandwidth efficiency, the TWRN has attracted interest in the literature [40, 64–67]. Most research reported in the literature assume perfect timing synchronisation at the receiver. The fact that in practice the timing is non-perfect introduces an impairment at the receiver and negatively impacts the network performance due to inter-symbol interference (ISI). Unlike one-way WRNs, two forms of ISI exist in TWRNs due to the dispersed nature of both the terminals and relays. It arises between the terminals' signals in the first phase of transmission as well as among the relays in the next phase of transmission. Similar to one-way WRNs in chapter 3, the contributions with respect to current literature are: (1) a

mathematical model is derived under a condition of imperfect synchronisation for TWRNs with N relays, each being equipped with R_a-antenna, where $N, R_a \in \mathbb{N}^+$. This model can be used easily to evaluate any variant of TWRN configurations; (2) both the existing PIC and SIC based detectors of [36, 37], which were introduced for specific one-way WRNs configurations, are extended here to work in TWRNs. They show a better performance improvement compared to the conventional detector; (3) an enhanced interference cancellation based detector (EIC) is proposed. Unlike [36, 37], this detector shows better performance, particularly in the first iteration, as it reduces the reliance on low-performance symbols. Moreover, the EIC benefits from interference components of currently-detected symbols using a modified maximum likelihood (ML) scheme. As mentioned in Chapter 3, the extended and proposed detectors are designed to work in both the one-way and two-way networks.

4.2 Prior Work

Unlike one-way WRNs, two forms of imperfect time synchronisation exist in TWRNs due to the dispersed nature of both the terminals and relays. These different timing errors are introduced between the received signals of terminals at the relays and also among the received signals of relays at the terminals. In [68], the authors considered the timing error among the terminals and concluded that a significant performance degradation was introduced but no mitigation strategy was offered. In [69], a preamble structure was proposed for efficient synchronisation among the terminals only. A delay-tolerant distributed space-time trellis code was proposed to conserve high performance, even under imperfect synchronisation in [70]. However, this code functions in the binary field, meaning it cannot be employed in AF TWRNs. In [61, 71–73], robust schemes against the relays' timing error were proposed. These schemes depend on using a sufficient cyclic prefix and/or performing physical-layer network coding to combat the performance degradation. They involve much higher complexity, introduce an extra control overhead and feedback channels were sometimes needed. In addition, the inter-block interference among the relays was not considered. As shown in Chapter 3, a number of low-complexity methods have been proposed for one-way WRNs, notably PIC and SIC [36, 37]. Although the timing error among the terminals is a unique issue for TWRNs and never occurs in one-way networks, these methods can be extended to TWRNs. In [61, 62], the authors considered specific TWRN instances, two-relay networks use Alamouti's STBC and four-relay networks use

EOSTBC, under imperfect synchronisation, and extended the design of the PIC detector to deal with the interference terms that are found in both phases. Similar to what is discussed in Section 3.2, there is a high potential to model a general case of TWRN under imperfect synchronisation given various network configurations. In addition, an extended version of the existing IC detectors is required.

4.3 Network Modelling

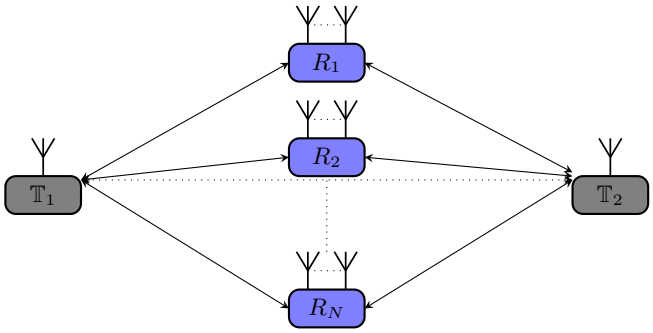

Fig. 4.1: Two-way Relaying network (TWRN) model.

A TWRN consists of two terminals $\mathbb{T}_1$ and $\mathbb{T}_2$ that exchange data through N relay nodes (R_n, $n = 1 \cdots N$) is considered. The terminals are single-antenna nodes while the relays are equipped each with $R_a, R_a \in \mathbb{N}^+$. The channel of the network is assumed to be a quasi-static Rayleigh fading channel. The relays are assumed to be completely blind while perfect CSI is assumed only at the terminals. In this section, the TWRN is generally modelled under imperfect synchronisation. Then, instances of the general model are evaluated for: (1) two dual-antenna relays using QO-STBC; (2) two single-antenna relays using orthogonal STBC (Alamouti's STBC); and (3) four single-antenna relays using the novel QO-STBC of [40]. These models are used later to examine the effectiveness of the proposed detectors.

In TWRNs, the transmission is conducted through

Broadcasting phase: the terminals simultaneously transmit their M-ary PSK/QAM modulated symbols, which are denoted by $\mathbf{x}(i) = [x(i,1), \ldots, x(i,J)]^T$ and $\mathbf{y}(i) = [y(i,1), \ldots, y(i,J)]^T$, where i denotes the information block index and J is the number of symbols of each terminal. Due to different timing and propagation delays, the transmitting symbols reach the relays

with a different delay (τ_n). Similar to [36, 37], a condition of $\tau_n \in [0, 0.5T]$ is assumed, where T is the symbol signalling period. Thus, the received vector at R_n is

$$\underset{(R_a\times J)\times 1}{\mathbf{r}_n(i)} = \sqrt{P_1}\ \underset{(R_a\times J)\times J}{\mathbf{G}_{n(0)}}\ \underset{J\times 1}{\mathbf{x}(i)} + \sqrt{P_2}\ \underset{(R_a\times J)\times J}{\mathbf{H}_{n(0)}}\ \underset{J\times 1}{\mathbf{y}(i)} + \underset{(R_a\times J)\times 1}{\mathbf{q}_n(i)} + \underset{(R_a\times J)\times 1}{\mathbf{v}_n(i)}\ , \tag{4.1}$$

with

$$\mathbf{q}_n(i) = \sqrt{P_1}\left(\mathbf{g}_{n(1)} \otimes (\mathbf{Q}\mathbf{x}(i) + \mathbf{N}\mathbf{x}(i-1))\right) + \sqrt{P_2}\left(\mathbf{h}_{n(1)} \otimes (\mathbf{Q}\mathbf{y}(i) + \mathbf{N}\mathbf{y}(i-1))\right), \tag{4.2}$$

where P_1 and P_2 are the power dedicated for $\mathbb{T}_1$ and $\mathbb{T}_2$, respectively.

$$\underset{J\times J}{\mathbf{Q}} = \begin{bmatrix} \mathbf{0}_{1\times(J-1)} & 0 \\ \mathbf{I}_{J-1} & \mathbf{0}_{(J-1)\times 1} \end{bmatrix} \text{and } \underset{J\times J}{\mathbf{N}} = \begin{bmatrix} \mathbf{0}_{1\times(J-1)} & 1 \\ \mathbf{0}_{(J-1)\times(J-1)} & \mathbf{0}_{(J-1)\times 1} \end{bmatrix}.$$

$\mathbf{G}_{n(0)} = \mathbf{I}_J \otimes \mathbf{g}_{n(0)}$, $\mathbf{H}_{n(0)} = \mathbf{I}_J \otimes \mathbf{h}_{n(0)}$. Both $\mathbf{g}_{n(0)} = [g_{n,1(0)}, \ldots, g_{n,R_a(0)}]^T$ and $\mathbf{h}_{n(0)} = [h_{n,1(0)}, \ldots, h_{n,R_a(0)}]^T$ are the current time slot channel coefficient vectors for the $\mathbb{T}_1$-and-R_n and $\mathbb{T}_2$-and-R_n links, respectively; $\mathbf{g}_{n(\nu)}$ and $\mathbf{h}_{n(\nu)}$ for $\nu = 1, \ldots, \infty$ represent the composite effects of time delay and the PSW for the mentioned links. The strength of $\mathbf{g}_{n(1)}$ or $\mathbf{h}_{n(1)}$ is represented by (3.7). Assuming full-duplex terminals, DT links between the terminals exist. It is not common in TWRNs, hence it is considered here as an optional case. These links are modelled as

$$\underset{J\times 1}{\mathbf{r}_{DT,1}(i)} = \sqrt{P_1} f\ \underset{J\times 1}{\mathbf{y}}\ (i) + \underset{J\times 1}{\boldsymbol{\delta}_1}\ (i), \tag{4.3}$$

and

$$\underset{J\times 1}{\mathbf{r}_{DT,2}(i)} = \sqrt{P_2} f\ \underset{J\times 1}{\mathbf{x}}\ (i) + \underset{J\times 1}{\boldsymbol{\delta}_2}\ (i), \tag{4.4}$$

where f ($f \sim \mathcal{CN}(0,1)$) is the channel coefficient of the $\mathbb{T}_1$ and $\mathbb{T}_2$ link. The vector δ_k, $\delta_k \sim \mathcal{CN}(0,1)$ is the noise vector at $\mathbb{T}_k$. The detection results of (4.3) or (4.4) can be carried through a conventional ML detector [10, 37], denoted by $\hat{\mathbf{x}}_{DT}(i)$ and $\hat{\mathbf{y}}_{DT}(i)$, respectively.

Relaying phase (phase 2): according to the used code, each relay converts the received symbol vector into new transmitting symbols $R_a \times J$ vector $\mathbf{t}_n(i)$ using

$$\mathbf{t}_n(i,j) = \beta \left(\underset{R_a\times(R_a\times J)}{\mathbf{A}_n^{(j)}}\ \underset{(R_a\times J)\times 1}{\mathbf{r}_n(i)} + \underset{R_a\times(R_a\times J)}{\mathbf{B}_n^{(j)}}\ \underset{(R_a\times J)\times 1}{\mathbf{r}_n^*(i)} \right), \forall j = 1, \ldots, J, \tag{4.5}$$

where $\mathbf{A}_n^{(\ell)}$ and $\mathbf{B}_n^{(\ell)}$ are the encoding matrices (each is of $R_a \times J$ size) that are used by R_n to construct its corresponding part of the particular $L \times (R_a \times N)$ STBC coding matrix ($\mathcal{X}_k$) in a distributive manner, wherein k is the number of data symbols embedded in the code

matrix. The code rate is given as $R = k/L$. To avoid the necessity of buffering, $J = k$ should be hold. β is such an amplification gain that let the average power per antenna of each relay is P_r, where P_r is the power dedicated by network for each relay in the relaying phase. These resulting symbols are then forwarded simultaneously from all participating relays to the terminals. Again, interference terms due to imperfect time synchronisation among relays arise at the terminals (see Fig. 4.2). Due to similarity, only the received signal at $\mathbb{T}_1$ is considered. It can be modelled as

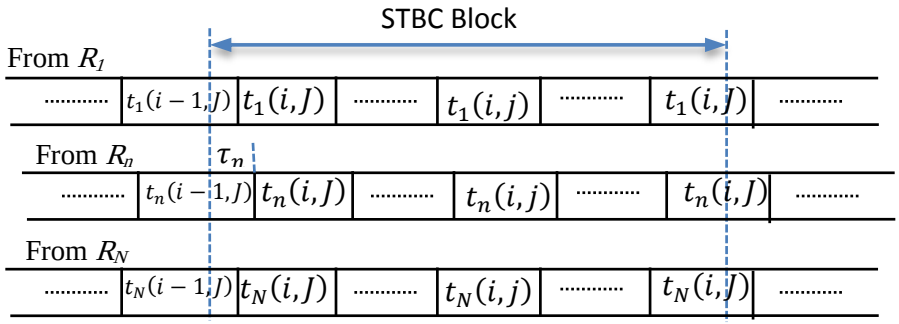

Fig. 4.2: The relay signal under imperfect synchronisation.

$$\begin{aligned}\underset{L\times 1}{\mathbf{z}_1(i)} =& \sqrt{P_1}\beta\left(\overbrace{\mathbf{A}_{g(0)}\mathbf{G}(0)}^{\mathbf{C}_0}\mathbf{x}(i) + \overbrace{\mathbf{B}_{g(0)}\mathbf{G}^*(0)}^{\mathbf{D}_0}\mathbf{x}^*(i)\right)\\ &+\sqrt{P_2}\beta\left(\overbrace{\mathbf{A}_{g(0)}\mathbf{H}(0)}^{\mathbf{C}_1}\mathbf{y}(i) + \overbrace{\mathbf{B}_{g(0)}\mathbf{H}^*(0)}^{\mathbf{D}_1}\mathbf{y}^*(i)\right) + \mathbf{q}_{\mathbb{T}_1}(i) + \boldsymbol{\zeta}_1(i),\end{aligned} \tag{4.6}$$

where

$$\underset{L\times(J\times N\times R_a)}{\mathbf{A}_{g(0)}} = \begin{bmatrix} \mathbf{g}_1^T(0)\mathbf{A}_1^{(1)} & \mathbf{g}_2^T(0)\mathbf{A}_2^{(1)} & \cdots & \mathbf{g}_N^T(0)\mathbf{A}_N^{(1)} \\ \mathbf{g}_1^T(0)\mathbf{A}_1^{(2)} & \mathbf{g}_2^T(0)\mathbf{A}_2^{(2)} & \cdots & \mathbf{g}_N^T(0)\mathbf{A}_N^{(2)} \\ \vdots & \ddots & \ddots & \vdots \\ \mathbf{g}_1^T(0)\mathbf{A}_1^{(L)} & \mathbf{g}_2^T(0)\mathbf{A}_2^{(L)} & \cdots & \mathbf{g}_N^T(0)\mathbf{A}_N^{(L)} \end{bmatrix},$$

$$\underset{L\times(J\times N\times R_a)}{\mathbf{B}_{g(0)}} = \begin{bmatrix} \mathbf{g}_1^T(0)\mathbf{B}_1^{(1)} & \mathbf{g}_2^T(0)\mathbf{B}_2^{(1)} & \cdots & \mathbf{g}_N^T(0)\mathbf{B}_N^{(1)} \\ \mathbf{g}_1^T(0)\mathbf{B}_1^{(2)} & \mathbf{g}_2^T(0)\mathbf{B}_2^{(2)} & \cdots & \mathbf{g}_N^T(0)\mathbf{B}_N^{(2)} \\ \vdots & \ddots & \ddots & \vdots \\ \mathbf{g}_1^T(0)\mathbf{B}_1^{(L)} & \mathbf{g}_2^T(0)\mathbf{B}_2^{(L)} & \cdots & \mathbf{g}_N^T(0)\mathbf{B}_N^{(L)} \end{bmatrix},$$

$\mathbf{G}(0) = \left[\mathbf{G}_1^T(0), \quad \ldots, \quad \mathbf{G}_N^T(0) \right]^T$, and $\mathbf{H}(0) = \left[\mathbf{H}_1^T(0), \quad \ldots, \quad \mathbf{H}_N^T(0) \right]^T$. The noise terms $\zeta_1(i)$ can be modelled equivalently as

$$\underset{L\times 1}{\zeta_1(i)} = \beta\left(\left(\mathbf{A}_{g(0)} + \Psi_1(\mathbf{A}_{g(1)}, 1)\right)\mathbf{v}(i) + \left(\mathbf{B}_{g(0)} + \Psi_1(\mathbf{B}_{g(1)}, 1)\right)\mathbf{v}^*(i)\right) + \boldsymbol{\eta}_1(i), \tag{4.7}$$

where $\mathbf{v}(i) = \left[\mathbf{v}_1^T(i), \ldots, \mathbf{v}_N^T(i)\right]^T$ and $\boldsymbol{\eta}_1 \in \mathcal{CN}(0,1)$. Both $\mathbf{A}_{g(1)}$ and $\mathbf{B}_{g(1)}$ are formed using $\mathbf{g}_n(1)$ instead of $\mathbf{g}_n(0)$ as follows:

$$\underset{L\times(J\times N\times R_a)}{\mathbf{A}_{g(1)}} = \begin{bmatrix} \mathbf{g}_1^T(1)\mathbf{A}_1^{(1)} & \mathbf{g}_2^T(1)\mathbf{A}_2^{(1)} & \cdots & \mathbf{g}_N^T(1)\mathbf{A}_N^{(1)} \\ \mathbf{g}_1^T(1)\mathbf{A}_1^{(2)} & \mathbf{g}_2^T(1)\mathbf{A}_2^{(2)} & \cdots & \mathbf{g}_N^T(1)\mathbf{A}_N^{(2)} \\ \vdots & \ddots & \ddots & \vdots \\ \mathbf{g}_1^T(1)\mathbf{A}_1^{(L)} & \mathbf{g}_2^T(1)\mathbf{A}_2^{(L)} & \cdots & \mathbf{g}_N^T(1)\mathbf{A}_N^{(L)} \end{bmatrix},$$

and

$$\underset{L\times(J\times N\times R_a)}{\mathbf{B}_{g(1)}} = \begin{bmatrix} \mathbf{g}_1^T(1)\mathbf{B}_1^{(1)} & \mathbf{g}_2^T(1)\mathbf{B}_2^{(1)} & \cdots & \mathbf{g}_N^T(1)\mathbf{B}_N^{(1)} \\ \mathbf{g}_1^T(1)\mathbf{B}_1^{(2)} & \mathbf{g}_2^T(1)\mathbf{B}_2^{(2)} & \cdots & \mathbf{g}_N^T(1)\mathbf{B}_N^{(2)} \\ \vdots & \ddots & \ddots & \vdots \\ \mathbf{g}_1^T(1)\mathbf{B}_1^{(L)} & \mathbf{g}_2^T(1)\mathbf{B}_2^{(L)} & \cdots & \mathbf{g}_N^T(1)\mathbf{B}_N^{(L)} \end{bmatrix}.$$

All interference terms received at $\mathbb{T}_1$ that resulted due to imperfect synchronisation can be modelled as $\mathbf{q}_{\mathbb{T}_1}(i) = \mathbf{q}_{0,x}(i) + \mathbf{q}_{1,x}(i) + \mathbf{q}_{0,y}(i) + \mathbf{q}_{1,y}(i)$, with

$$\begin{aligned}\underset{L\times 1}{\mathbf{q}_{0,x}(i)} =& \sqrt{P_1}\beta\left(\left(\mathbf{A}_{g(0)}\Psi_1(\mathbf{G}(1), R_a) + \Psi_1(\mathbf{A}_{g(1)}, 1)\left(\mathbf{G}(0) + \Psi_1(\mathbf{G}(1), R_a)\right)\right)\mathbf{x}(i)\right. \\ &\left. + \left(\mathbf{B}_{g(0)}\Psi_1(\mathbf{G}^*(1), R_a) + \Psi_1(\mathbf{B}_{g(1)}, 1)\left(\mathbf{G}^*(0) + \Psi_1(\mathbf{G}^*(1), R_a)\right)\right)\mathbf{x}^*(i)\right),\end{aligned} \tag{4.8}$$

$$\begin{aligned}\underset{L\times 1}{\mathbf{q}_{1,x}(i)} =& \sqrt{P_1}\beta\left(\left(\mathbf{A}_{g(0)}\Psi_2(\mathbf{G}(1), L - R_a) + \Psi_2(\mathbf{A}_{g(1)}, L-1)\mathbf{G}(0)\right)\mathbf{x}(i-1)\right. \\ &+ \Psi_2(\mathbf{A}_{g(1)}, L-1)\Psi_2(\mathbf{G}(1), L - R_a)\mathbf{x}(i-1) \\ &+ \Psi_2(\mathbf{B}_{g(1)}, L-1)\Psi_2(\mathbf{G}^*(1), L - R_a)\mathbf{x}^*(i-2) \\ &\left. + \left(\mathbf{B}_{g(0)}\Psi_2(\mathbf{G}^*(1), L - R_a) + \Psi_2(\mathbf{B}_{g(1)}, L-1)\mathbf{G}^*(0)\right)\mathbf{x}^*(i-1)\right),\end{aligned} \tag{4.9}$$

$$\begin{aligned}\underset{L\times 1}{\mathbf{q}_{0,y}(i)} =& \sqrt{P_2}\beta\left(\overbrace{\left(\mathbf{A}_{g(0)}\Psi_1(\mathbf{H}(1), R_a) + \Psi_1(\mathbf{A}_{g(1)}, 1)\left(\mathbf{H}(0) + \Psi_1(\mathbf{H}(1), R_a)\right)\right)}^{\mathbf{C}_2}\mathbf{y}(i)\right. \\ &\left. + \overbrace{\left(\mathbf{B}_{g(0)}\Psi_1(\mathbf{H}^*(1), R_a) + \Psi_1(\mathbf{B}_{g(1)}, 1)\left(\mathbf{H}^*(0) + \Psi_1(\mathbf{H}^*(1), R_a)\right)\right)}^{\mathbf{D}_2}\mathbf{y}^*(i)\right),\end{aligned} \tag{4.10}$$

and

$$\begin{aligned}\underset{L\times 1}{\mathbf{q}_{1,y}(i)} =& \sqrt{P_2}\beta\left(\left(\mathbf{A}_{g(0)}\Psi_2(\mathbf{H}(1), L-R_a) + \Psi_2(\mathbf{A}_{g(1)}, L-1)\mathbf{H}(0)\right)\mathbf{y}(i-1)\right.\\ &+ \Psi_2(\mathbf{A}_{g(1)}, L-1)\Psi_2(\mathbf{H}(1), L-R_a)\mathbf{y}(i-2)\\ &+ \Psi_2(\mathbf{B}_{g(1)}, L-1)\Psi_2(\mathbf{H}^*(1), L-R_a)\mathbf{y}^*(i-2)\\ &\left.+ \left(\mathbf{B}_{g(0)}\Psi_2(\mathbf{H}(1), L-R_a) + \Psi_2(\mathbf{B}_{g(1)}, L-1)\mathbf{H}^*(0)\right)\mathbf{y}^*(i-1)\right), \end{aligned} \tag{4.11}$$

where $\mathbf{G}(1) = \begin{bmatrix} \mathbf{G}_1^T(1) & ,\cdots & ,\mathbf{G}_N^T(1) \end{bmatrix}^T$, $\mathbf{H}(1) = \begin{bmatrix} \mathbf{H}_1^T(1) & ,\cdots & ,\mathbf{H}_N^T(1) \end{bmatrix}^T$, $\mathbf{G}_n(1) = \mathbf{I}_J \otimes \mathbf{g}_n(1)$, and $\mathbf{H}_n(1) = \mathbf{I}_J \otimes \mathbf{h}_n(1)$.

With some algebraic manipulations, equation (4.6) can be rewritten as

$$\underset{2L\times 1}{\bar{\mathbf{z}}_1(i)} = \sqrt{P_1}\beta\mathbf{G}_{\mathbf{G}}\underset{2J\times 1}{\bar{\mathbf{x}}(i)} + \sqrt{P_2}\beta\mathbf{G}_{\mathbf{H}}\underset{2J\times 1}{\bar{\mathbf{y}}(i)} + \mathbf{G}_{\mathbf{q}}\underset{2J\times 1}{\bar{\mathbf{y}}(i)} + \underset{2J\times 1}{\bar{\mathbf{q}}_{1,y}(i)} + \underset{2L\times 1}{\bar{\mathbf{q}}_{0,x}(i)} + \underset{2L\times 1}{\bar{\mathbf{q}}_{1,x}(i)} + \underset{2L\times 1}{\bar{\boldsymbol{\zeta}}_1(i)}, \tag{4.12}$$

where $\mathbf{G}_{\mathbf{H}}$ and $\mathbf{G}_{\mathbf{q}}$ are shown in (3.14) and (3.15), respectively, while

$$\underset{2L\times 2J}{\mathbf{G}_{\mathbf{G}}} = \begin{bmatrix} \Re(\mathbf{C}_0 + \mathbf{D}_0) & \Im(-\mathbf{C}_0 + \mathbf{D}_0) \\ \Im(\mathbf{C}_0 + \mathbf{D}_0) & \Re(\mathbf{C}_0 - \mathbf{D}_0) \end{bmatrix}. \tag{4.13}$$

Now, this derived general mathematical model is evaluated for specific network configurations which will be used in Section 4.5 to evaluate the extended and proposed detectors.

4.3.1 Two dual-antenna relay TWRNs using QO-STBC

In [40], a novel class of D-QO-STBC was proposed for TWRNs with a number N of dual-antenna relays. This class is promising as it can achieve the maximum coding gain and the optimal diversity gain while maintaining low decoding complexity. Using this code, the general model is evaluated in the case of two dual-antenna relays, meaning that $R_a = 2$ and $N = 2$. The used encoding matrices are shown in Section 2.7.2. The data exchanged through the network is $\mathbf{x}(i) = [\mathbf{x}(i,1), \ldots, \mathbf{x}(i,4)]^T$ from $\mathbb{T}_1$ and $\mathbf{y}(i) = [\mathbf{y}(i,1), \ldots, \mathbf{y}(i,4)]^T$ from $\mathbb{T}_2$. The model instance can be represented as

$$\mathbf{C}_0 = \begin{bmatrix} \mathbf{g}_1^T(0)\mathbf{g}_1(0) & 0 & \mathbf{g}_2^T(0)\mathbf{g}_2(0) & 0 \\ 0 & \mathbf{g}_1^T(0)\mathbf{g}_1(0) & 0 & \mathbf{g}_2^T(0)\mathbf{g}_2(0) \\ \mathbf{g}_2^T(0)\mathbf{g}_2(0) & 0 & \mathbf{g}_1^T(0)\mathbf{g}_1(0) & 0 \\ 0 & \mathbf{g}_2^T(0)\mathbf{g}_2(0) & 0 & \mathbf{g}_1^T(0)\mathbf{g}_1(0) \end{bmatrix}, \mathbf{D}_0 = \begin{bmatrix} 0 & \mathbf{g}_1^T(0)\mathbf{J}\mathbf{g}_1^*(0) & 0 & \mathbf{g}_2^T(0)\mathbf{J}\mathbf{g}_2^*(0) \\ \mathbf{g}_1^H(0)\mathbf{J}\mathbf{g}_1(0) & 0 & \mathbf{g}_2^H(0)\mathbf{J}\mathbf{g}_2(0) & 0 \\ 0 & \mathbf{g}_2^T(0)\mathbf{J}\mathbf{g}_2^*(0) & 0 & \mathbf{g}_1^T(0)\mathbf{J}\mathbf{g}_1^*(0) \\ \mathbf{g}_2^H(0)\mathbf{J}\mathbf{g}_2(0) & 0 & \mathbf{g}_1^H(0)\mathbf{J}\mathbf{g}_1(0) & 0 \end{bmatrix}, \tag{4.14}$$

$$\mathbf{C}_1 = \begin{bmatrix} \mathbf{g}_1^T(0)\mathbf{h}_1(0) & 0 & \mathbf{g}_2^T(0)\mathbf{h}_2(0) & 0 \\ 0 & \mathbf{g}_1^T(0)\mathbf{h}_1(0) & 0 & \mathbf{g}_2^T(0)\mathbf{h}_2(0) \\ \mathbf{g}_2^T(0)\mathbf{h}_2(0) & 0 & \mathbf{g}_1^T(0)\mathbf{h}_1(0) & 0 \\ 0 & \mathbf{g}_2^T(0)\mathbf{h}_2(0) & 0 & \mathbf{g}_1^T(0)\mathbf{h}_1(0) \end{bmatrix}, \mathbf{D}_1 = \begin{bmatrix} 0 & \mathbf{g}_1^T(0)\mathbf{J}\mathbf{h}_1^*(0) & 0 & \mathbf{g}_2^T(0)\mathbf{J}\mathbf{h}_2^*(0) \\ \mathbf{h}_1^H(0)\mathbf{J}\mathbf{g}_1(0) & 0 & \mathbf{h}_2^H(0)\mathbf{J}\mathbf{g}_2(0) & 0 \\ 0 & \mathbf{g}_2^T(0)\mathbf{J}\mathbf{h}_2^*(0) & 0 & \mathbf{g}_1^T(0)\mathbf{J}\mathbf{h}_1^*(0) \\ \mathbf{h}_2^H(0)\mathbf{J}\mathbf{g}_2(0) & 0 & \mathbf{h}_1^H(0)\mathbf{J}\mathbf{g}_1(0) & 0 \end{bmatrix}, \tag{4.15}$$

and

$$\mathbf{C}_2 = \begin{bmatrix} 0 & \mathbf{g}_2^T(0)\mathbf{h}_2(1) & 0 & 0 \\ (\mathbf{g}_1^T(0)\mathbf{h}_1(1) + \mathbf{g}_1^T(1)\mathbf{h}_1(0)) & \mathbf{g}_2^T(1)\mathbf{h}_2(1) & (\mathbf{g}_2^T(0)\mathbf{h}_2(1) + \mathbf{g}_2^T(1)\mathbf{h}_2(0)) & 0 \\ \mathbf{g}_1^T(1)\mathbf{h}_1(1) & (\mathbf{g}_1^T(0)\mathbf{h}_1(1) + \mathbf{g}_1^T(1)\mathbf{h}_1(0)) & \mathbf{g}_2^T(1)\mathbf{h}_2(1) & \mathbf{g}_2^T(1)\mathbf{h}_2(0) \\ (\mathbf{g}_2^T(0)\mathbf{h}_2(1) + \mathbf{g}_2^T(1)\mathbf{h}_2(0)) & \mathbf{g}_1^T(1)\mathbf{h}_1(1) & (\mathbf{g}_1^T(0)\mathbf{h}_1(1) + \mathbf{g}_1^T(1)\mathbf{h}_1(0)) & 0 \end{bmatrix}, \mathbf{D}_2 = \begin{bmatrix} \mathbf{g}_1^T(0)\mathbf{J}\mathbf{h}_1^*(1) & 0 & \mathbf{g}_2^T(0)\mathbf{J}\mathbf{h}_2^*(1) & 0 \\ \mathbf{g}_1^T(1)\mathbf{J}\mathbf{h}_1^*(1) & (\mathbf{g}_1^T(1)\mathbf{J}\mathbf{h}_1^*(0) - \mathbf{g}_2^T(0)\mathbf{J}\mathbf{h}_2^*(1)) & \mathbf{g}_2^T(1)\mathbf{J}\mathbf{h}_2^*(1) & \mathbf{g}_2^T(1)\mathbf{J}\mathbf{h}_2(0) \\ (\mathbf{h}_1^H(0)\mathbf{J}\mathbf{g}_1(1) + \mathbf{g}_2^T(0)\mathbf{J}\mathbf{h}_2^*(1)) & \mathbf{h}_2^H(1)\mathbf{J}\mathbf{g}_2(1) & (\mathbf{g}_1^T(0)\mathbf{J}\mathbf{h}_1^*(1) - \mathbf{g}_2^T(1)\mathbf{J}\mathbf{h}_2^*(0)) & 0 \\ \mathbf{g}_2^T(1)\mathbf{J}\mathbf{h}_2^*(1) & (\mathbf{h}_1^H(1)\mathbf{J}\mathbf{g}_1(0) + \mathbf{g}_2^T(1)\mathbf{J}\mathbf{h}_2^*(0)) & \mathbf{g}_1^T(1)\mathbf{J}\mathbf{h}_1^*(1) & \mathbf{g}_1^T(1)\mathbf{J}\mathbf{h}_1^*(0) \end{bmatrix}, \tag{4.16}$$

where $\mathbf{J} = \begin{bmatrix} 0 & 1 \\ -1 & 0 \end{bmatrix}$. The values of $\mathbf{q}_{1,x}, \mathbf{q}_{1,y}$, and $\mathbf{q}_{0,x}$ are given by

$$\underset{4\times 1}{\mathbf{q}_{1,x}(i)} = \begin{bmatrix} (2\mathbf{g}_1^T(0)\mathbf{g}_1(0)\mathbf{x}(i-1,4) + \mathbf{g}_2^T(0)\mathbf{g}_2(1)\mathbf{x}(i-1,2) - \mathbf{g}_1^T(1)\mathbf{J}\mathbf{g}_1^*(0)\mathbf{x}^*(i-1,3) \\ -\mathbf{g}_2^T(1)\mathbf{J}\mathbf{g}_2^*(0)\mathbf{x}^*(i-1,1) - \mathbf{g}_2^T(1)\mathbf{J}\mathbf{g}_2^*(1)\mathbf{x}^*(i-2,4)) \\ -\mathbf{g}_1^T(0)\mathbf{J}\mathbf{g}_1^*(1)\mathbf{x}^*(i-1,4) \\ \mathbf{g}_2^T(0)\mathbf{g}_2(1)\mathbf{x}(i-1,4) \\ -\mathbf{g}_2^T(0)\mathbf{J}\mathbf{g}_2^*(1)\mathbf{x}^*(i-1,4) \end{bmatrix}, \tag{4.17}$$

$$\underset{4\times 1}{\mathbf{q}_{1,y}(i)} = \begin{bmatrix} (\mathbf{g}_2^T(1)\mathbf{h}_2(0)\mathbf{x}(i-1,2) - \mathbf{g}_1^T(1)\mathbf{J}\mathbf{h}_1^*(0)\mathbf{x}^*(i-1,3) - \mathbf{g}_2^T(1)\mathbf{J}\mathbf{h}_2^*(0)\mathbf{x}^*(i-1,1) \\ -\mathbf{g}_2^T(1)\mathbf{J}\mathbf{h}_2^*(1)\mathbf{x}^*(i-2,4) + (\mathbf{g}_2^T(0)\mathbf{h}_1(1) + \mathbf{g}_1^T(0)\mathbf{h}_1(1))\mathbf{x}(i-1,4)) \\ -\mathbf{g}_1^T(0)\mathbf{J}\mathbf{h}_1^*(1)\mathbf{x}^*(i-1,4) \\ \mathbf{g}_2^T(0)\mathbf{h}_2(1)\mathbf{x}(i-1,4) \\ -\mathbf{g}_2^T(0)\mathbf{J}\mathbf{h}_2^*(1)\mathbf{x}^*(i-1,4) \end{bmatrix}, \tag{4.18}$$

and $\mathbf{q}_{0,x}(i) = \begin{bmatrix} \mathbf{q}_{0,x}(i,1) & \mathbf{q}_{0,x}(i,2) & \mathbf{q}_{0,x}(i,3) & \mathbf{q}_{0,x}(i,4) \end{bmatrix}$, where

$$\mathbf{q}_{0,x}(i,1) = \mathbf{g}_2^T(0)\mathbf{g}_1(1)\mathbf{x}(i,2) + \mathbf{g}_1^T(0)\mathbf{J}\mathbf{g}_1^*(1)\mathbf{x}^*(i,1) + \mathbf{g}_2^T(0)\mathbf{J}\mathbf{g}_2^*(1)\mathbf{x}^*(i,3), \tag{4.19}$$

$$\begin{aligned} \mathbf{q}_{0,x}(i,2) = {} & 2\mathbf{g}_1^T(0)\mathbf{g}_1(1)\mathbf{x}(i,1) + 2\mathbf{g}_2^T(0)\mathbf{g}_2(1)\mathbf{x}(i,3) + \mathbf{g}_2^T(1)\mathbf{J}\mathbf{g}_2^*(0)\mathbf{x}^*(i,4) \\ & + \mathbf{g}_1^T(1)\mathbf{J}\mathbf{g}_1^*(1)\mathbf{x}^*(i,1) + \mathbf{g}_2^T(1)\mathbf{J}\mathbf{g}_2^*(1)\mathbf{x}^*(i,3) \\ & + \mathbf{g}_2^T(1)\mathbf{g}_2(1)\mathbf{x}(i,2) + (\mathbf{g}_1^T(1)\mathbf{J}\mathbf{g}_1^*(0) - \mathbf{g}_2^T(0)\mathbf{J}\mathbf{g}_2^*(1))\mathbf{x}^*(i,2), \end{aligned} \tag{4.20}$$

$$\mathbf{q}_{0,x}(i,3) = 2\mathbf{g}_1^T(0)\mathbf{g}_1(1)\mathbf{x}(i,2) + \mathbf{g}_2^T(0)\mathbf{g}_2(1)\mathbf{x}(i,4) - \mathbf{g}_2^T(1)\mathbf{J}\mathbf{g}_2^*(1)\mathbf{x}^*(i,2)$$
$$+ \mathbf{g}_1^T(1)\mathbf{g}_1(1)\mathbf{x}(i,1) - (\mathbf{g}_1^T(1)\mathbf{J}\mathbf{g}_1^*(0) - \mathbf{g}_2^T(0)\mathbf{J}\mathbf{g}_2^*(1))\mathbf{x}^*(i,2)$$
$$+ \mathbf{g}_2^T(1)\mathbf{g}_2(1)\mathbf{x}(i,3) + (\mathbf{g}_1^T(0)\mathbf{J}\mathbf{g}_1^*(1) - \mathbf{g}_2^T(1)\mathbf{J}\mathbf{g}_2^*(0))\mathbf{x}^*(i,3), \tag{4.21}$$

and

$$\mathbf{q}_{0,x}(i,4) = 2\mathbf{g}_1^T(0)\mathbf{g}_1(1)\mathbf{x}(i,3) + 2\mathbf{g}_2^T(0)\mathbf{g}_2(1)\mathbf{x}(i,1) + \mathbf{g}_1^T(1)\mathbf{J}\mathbf{g}_1^*(0)\mathbf{x}^*(i,4)$$
$$+ \mathbf{g}_1^T(1)\mathbf{J}\mathbf{g}_1^*(1)\mathbf{x}^*(i,3) + \mathbf{g}_1^T(1)\mathbf{g}_1(1)\mathbf{x}(i,2)$$
$$+ \mathbf{g}_2^T(1)\mathbf{J}\mathbf{g}_2^*(1)\mathbf{x}^*(i,1) - (\mathbf{g}_1^T(0)\mathbf{J}\mathbf{g}_1^*(1) - \mathbf{g}_2^T(1)\mathbf{J}\mathbf{g}_2^*(0))\mathbf{x}^*(i,2). \tag{4.22}$$

4.3.2 Two-relay TWRNs using Alamouti's STBC

Another instance is shown here - it is for a case of two single-antenna relay TWRNs. This means that $R_a = 1$ and $N = 2$. This instance uses Alamouti's STBC of [12]. The encoding matrices used by these relays are shown in Section 2.7.2. The data exchanged through the network is $\mathbf{x}(i) = [\mathbf{x}(i,1), \mathbf{x}(i,2)]^T$ and $\mathbf{y}(i) = [\mathbf{y}(i,1), \mathbf{y}(i,2)]^T$. Accordingly, the model instance can be represented as

$$\mathbf{C}_0 = \begin{bmatrix} g_1^2(0) & 0 \\ 0 & g_1^2(0) \end{bmatrix}, \mathbf{D}_0 = \begin{bmatrix} 0 & -|g_2|^2(0) \\ |g_2|^2(0) & 0 \end{bmatrix}, \tag{4.23}$$

$$\mathbf{C}_1 = \begin{bmatrix} g_1(0)h_1(0) & 0 \\ 0 & g_1(0)h_1(0) \end{bmatrix}, \mathbf{D}_1 = \begin{bmatrix} 0 & -g_2(0)h_2^*(0) \\ g_2(0)h_2^*(0) & 0 \end{bmatrix} \text{ and} \tag{4.24}$$

$$\mathbf{C}_2 = \begin{bmatrix} 0 & 0 \\ g_1(0)h_1(1) + g_1(1)h_1(0) & 0 \end{bmatrix}, \mathbf{D}_2 = \begin{bmatrix} -g_2(0)h_2^*(1) & 0 \\ -g_2(1)h_2^*(1) & -g_2(1)h_2^*(0) \end{bmatrix}. \tag{4.25}$$

The values of $\mathbf{q}_{1,x}, \mathbf{q}_{1,y}$, and $\mathbf{q}_{0,x}$ are given by

$$\underset{2\times 1}{\mathbf{q}_{1,x}(i)} = \begin{bmatrix} (|g_2(1)|^2\mathbf{x}^*(i-2,2) + g_2(1)g_2^*(0)\mathbf{x}^*(i-1,1) \\ +2g_1(0)g_1(1)\mathbf{x}(i-1,2)) \\ g_2(0)g_2^*(1)\mathbf{x}^*(i-1,2) \end{bmatrix}, \tag{4.26}$$

$$\underset{2\times 1}{\mathbf{q}_{1,y}(i)} = \begin{bmatrix} ((g_1(0)h_1(1) + g_1(1)h_1(0))\mathbf{x}(i-1,2) \\ +g_2(1)h_2(0)\mathbf{x}^*(i-1,1) + g_2(1)h_2(1)\mathbf{x}^*(i-2,2)) \\ g_2(0)h_2^*(1)\mathbf{x}^*(i-1,2) \end{bmatrix}, \tag{4.27}$$

and

$$\underset{2\times 1}{\mathbf{q}_{0,x}(i)} = \begin{bmatrix} -g_2(0)g_2^*(1)\mathbf{x}^*(i,1) \\ (2g_1(0)g_1(1)\mathbf{x}(i,1) - g_2(1)g_2^*(0)\mathbf{x}^*(i,2) \\ -|g_2(1)|^2\mathbf{x}^*(i,1)) \end{bmatrix}. \tag{4.28}$$

4.3.3 Four-relay TWRNs using QO-STBC:

This section shows the model evaluation for a TWRN with four relays. These relays are single-antenna nodes and they use the QO-STBC of Section 2.7.2. Thus, $R_a = 1$, $N = 4$ and $J = 4$. The model instance can be represented as

$$\mathbf{C}_0 = \begin{bmatrix} g_1^2(0) & 0 & 0 & g_4^2(0) \\ 0 & g_1^2(0) & -g_4^2(0) & 0 \\ 0 & -g_4^2(0) & g_1^2(0) & 0 \\ g_4^2(0) & 0 & 0 & g_1^2(0) \end{bmatrix}, \quad \mathbf{D}_0 = \begin{bmatrix} 0 & -|g_2(0)|^2 & -|g_3(0)|^2 & 0 \\ |g_2(0)|^2 & 0 & 0 & -|g_3(0)|^2 \\ |g_3(0)|^2 & 0 & 0 & -|g_2(0)|^2 \\ 0 & |g_3(0)|^2 & |g_2(0)|^2 & 0 \end{bmatrix}, \tag{4.29}$$

$$\mathbf{C}_1 = \begin{bmatrix} g_1(0)h_1(0) & 0 & 0 & g_4(0)h_4(0) \\ 0 & g_1(0)h_1(0) & -g_4(0)h_4(0) & 0 \\ 0 & -g_4(0)h_4(0) & g_1(0)h_1(0) & 0 \\ g_4(0)h_4(0) & 0 & 0 & g_1(0)h_1(0) \end{bmatrix}, \mathbf{D}_1 = \begin{bmatrix} 0 & -g_2(0)h_2^*(0) & -g_3(0)h_3^*(0) & 0 \\ g_2(0)h_2^*(0) & 0 & 0 & -g_3(0)h_3^*(0) \\ g_3(0)h_3^*(0) & 0 & 0 & -g_2(0)h_2^*(0) \\ 0 & g_3(0)h_3^*(0) & g_2(0)h_2^*(0) & 0 \end{bmatrix}, \tag{4.30}$$

and

$$\mathbf{C}_2 = \begin{bmatrix} 0 & 0 & g_4(0)h_4(1) & 0 \\ (g_1(0)h_1(1) & -g_4(0)h_4(1) & g_4(1)h_4(1) & g_4(1)h_4(0) \\ +g_1(1)h_1(0)) & & & \\ (g_1(1)h_1(1) & (g_1(0)h_1(1) & & \\ -g_4(0)h_4(1)) & +g_1(1)h_1(0) & -g_4(1)h_4(0) & 0 \\ & -g_4(1)h_4(1)) & & \\ -g_4(1)h_4(1) & (g_1(1)h_1(1) & (g_1(0)h_1(1) & 0 \\ & -g_4(1)h_4(0)) & +g_1(1)h_1(0)) & \end{bmatrix}, \mathbf{D}_2 = \begin{bmatrix} -g_2(0)h_2^*(1) & -g_3(0)h_3^*(1) & 0 & 0 \\ -g_2(1)h_2^*(1) & (-g_2(1)h_2^*(0) & (-g_3(1)h_3^*(1) & 0 \\ & -g_3(1)h_3^*(1)) & -g_3(1)h_3^*(0)) & \\ g_2(1)h_2^*(0) & 0 & (-g_2(0)h_2^*(1) & -g_3(1)h_3^*(0) \\ & & -g_3(1)h_1^*(1)) & \\ g_3(0)h_3^*(1) & (g_3(0)h_3^*(1) & -g_2(0)h_2^*(1) & -g_2(1)h_2^*(0) \\ & +g_3(1)h_3^*(0)) & & \end{bmatrix}. \tag{4.31}$$

The values of $\mathbf{q}_{1,x}, \mathbf{q}_{1,y}$, and $\mathbf{q}_{0,x}$ are given by

$$\underset{4\times 1}{\mathbf{q}_{1,x}(i)} = \begin{bmatrix} (g_4^2(1)\mathbf{x}(i-2,4) + g_4(0)g_4(1)\mathbf{x}(i-1,1) + g_2(1)g_2^*(0)\mathbf{x}^*(i-1,3) \\ +g_3(1)g_3^*(0)\mathbf{x}^*(i-1,2) + 2g_1(0)g_1(1)x(i-1,4)) \\ g_2(0)g_2^*(1)\mathbf{x}^*(i-1,4) \\ g_3(0)g_3^*(1)\mathbf{x}^*(i-1,4) \\ g_4(0)g_4(1)\mathbf{x}(i-1,4) \end{bmatrix}, \tag{4.32}$$

$$\underset{4\times1}{\mathbf{q}_{1,y}(i)} = \begin{bmatrix} ((g_1(0)h_1(1) + g_1(1)h_1(0))\mathbf{x}(i-1,4) + g_2(1)h_2^*(0)\mathbf{x}^*(i-1,3) \\ +g_3(1)h_3^*(0)\mathbf{x}^*(i-1,2) + g_4(1)h_4(0)\mathbf{x}(i-1,1) + g_4(1)h_4(1)x(i-2,4)) \\ g_2(0)h_2^*(1)\mathbf{x}^*(i-1,4) \\ g_3(0)h_3^*(1)\mathbf{x}^*(i-1,4) \\ g_4(0)h_4(1)\mathbf{x}(i-1,4) \end{bmatrix}, \quad (4.33)$$

and $\mathbf{q}_{0,x}(i) = \begin{bmatrix} \mathbf{q}_{0,x}(i,1) & \mathbf{q}_{0,x}(i,2) & \mathbf{q}_{0,x}(i,3) & \mathbf{q}_{0,x}(i,4) \end{bmatrix}$. With

$$\mathbf{q}_{0,x}(i,1) = g_4(0)g_4(1)\mathbf{x}(i,3) - g_3(0)g_3^*(1)\mathbf{x}^*(i,2) - g_2(0)g_2^*(1)\mathbf{x}^*(i,1), \quad (4.34)$$

$$\begin{aligned}\mathbf{q}_{0,x}(i,2) = &-|g_2(1)|^2\mathbf{x}^*(i,1) - (|g_3(1)|^2 + g_2(1)g_2^*(0))\mathbf{x}^*(i,2) - (g_3(0)g_3^*(1) + g_3(1)g_3^*(0))\mathbf{x}^*(i,3) \\ &+ g_4^2(1)\mathbf{x}(i,3) + 2g_1(0)g_1(1)\mathbf{x}(i,1) - g_4(0)g_4(1)x(i,2) + g_4(0)g_4(1)\mathbf{x}(i,4), \quad (4.35)\end{aligned}$$

$$\begin{aligned}\mathbf{q}_{0,x}(i,3) = &(-g_4^2(1) + 2g_1(0)g_1(1))\mathbf{x}(i,2) - (g_4(0)g_4(1) - g_1^2(1))\mathbf{x}(i,1) + g_2(1)g_2^*(0)\mathbf{x}^*(i,1) \\ &- (g_2(0)g_2^*(1) + g_3(1)g_3^*(1))\mathbf{x}^*(i,3) - g_3(1)g_3^*(0)\mathbf{x}^*(i,4) - g_4(0)g_4(1)\mathbf{x}(i,3), \quad (4.36)\end{aligned}$$

and

$$\begin{aligned}\mathbf{q}_{0,x}(i,4) = &(g_3(0)g_3^*(1) + g_3(1)g_3^*(0))\mathbf{x}^*(i,1) - (g_4(0)g_4(1) - g_1^2(1))\mathbf{x}(i,2) + g_2(0)g_2^*(1)\mathbf{x}^*(i,2) \\ &- g_4^2(1)\mathbf{x}(i,1) - g_2(1)g_2^*(0)\mathbf{x}^*(i,4) - |g_2(1)|^2\mathbf{x}^*(i,3) + 2g_1(0)g_1(1)\mathbf{x}(i,3). \quad (4.37)\end{aligned}$$

4.4 Detection methods

The conventional detector is outlined here, then the two existing detectors of [36, 37] are extended for the derived general model. In addition, an enhanced detector (EIC) is proposed. Unlike existing research, our proposed designs of these detectors work for both TWRNs and one-way WRNs. It should be noted that the information block index (i) is omitted for clarity in the current section.

4.4.1 Conventional Detector

Assuming perfect synchronisation, the detection is carried out conventionally from (4.6) through the following steps:

1. Self-interference cancellation:

$$\widetilde{\bar{\mathbf{z}}}(i) = \begin{cases} \bar{\mathbf{z}}(i) & \text{1-WRNs} \\ \bar{\mathbf{z}}_1(i) - \sqrt{P_1}\beta \mathbf{G}_\mathbf{G}\bar{\mathbf{x}}(i) & \text{TWRNs.} \end{cases} \tag{4.38}$$

2. Equalization process: obtain the equalised vector $\mathbf{u}$ by calculating

$$\begin{aligned} \mathbf{u} &= \mathbf{G}_\mathbf{H}^H \widetilde{\bar{\mathbf{z}}} \\ &= \begin{cases} \sqrt{P_2}\beta\boldsymbol{\mathcal{H}}\bar{\mathbf{y}} + \sqrt{P_2}\beta\boldsymbol{\mathcal{B}}\bar{\mathbf{y}} + \mathbf{G}_\mathbf{H}^H\bar{\mathbf{q}}_1 + \mathbf{G}_\mathbf{H}^H\bar{\boldsymbol{\zeta}} & \text{1-WRNs} \\ \sqrt{P_2}\beta\boldsymbol{\mathcal{H}}\bar{\mathbf{y}} + \sqrt{P_2}\beta\boldsymbol{\mathcal{B}}\bar{\mathbf{y}} + \mathbf{G}_\mathbf{H}^H(\bar{\mathbf{q}}_{1,y} + \bar{\mathbf{q}}_{0,x} + \bar{\mathbf{q}}_{1,x}) + \mathbf{G}_\mathbf{H}^H\bar{\boldsymbol{\zeta}}_1 & \text{TWRNs} \end{cases}, \end{aligned} \tag{4.39}$$

   where $\boldsymbol{\mathcal{H}} = \mathbf{G}_\mathbf{H}^H\mathbf{G}_\mathbf{H}$ and $\boldsymbol{\mathcal{B}} = \mathbf{G}_\mathbf{H}^H\mathbf{G}_q$.

3. Group decoding: assuming a code with C decoding groups have been used, the decoding can be carried using

$$\widehat{\mathbf{y}}_c = \underset{\mathbf{y}_c \in \mathcal{S}^{(J/C)\times 1}}{\operatorname{argmin}} \|\mathbf{d}_c - \boldsymbol{\mathcal{H}}_c\bar{\mathbf{y}}_c|^2\}, \forall c = 1, \ldots, C, \tag{4.40}$$

   where $\widehat{\mathbf{y}}_c$ is the vector contained the estimation result of symbols belongs to the group c. It worth noting that if the used code is fully orthogonal, then $C = J$ (refer to [10]). Both $\mathbf{d}_c$ and $\boldsymbol{\mathcal{H}}_c$ are the corresponding elements of the group c of the $\mathbf{u}$ and $\boldsymbol{\mathcal{H}}$, respectively. For example, for the code of Section 4.3.1 that has $C = 2$ and $\mathbf{s}_1 = [1, 3]$ and $\mathbf{s}_2 = [2, 4]$, $\widehat{\mathbf{y}} = [\widehat{\mathbf{y}}_1(1), \widehat{\mathbf{y}}_2(1), \widehat{\mathbf{y}}_1(2), \widehat{\mathbf{y}}_2(2)]^T$,

$$\mathbf{d}_1 = \begin{bmatrix} \mathbf{u}(1) \\ \mathbf{u}(3) \end{bmatrix} + 1i \begin{bmatrix} \mathbf{u}(5) \\ \mathbf{u}(7) \end{bmatrix}, \mathbf{d}_2(i) = \begin{bmatrix} \mathbf{u}(2) \\ \mathbf{u}(4) \end{bmatrix} + 1i \begin{bmatrix} \mathbf{u}(6) \\ \mathbf{u}(8) \end{bmatrix},$$

$$\boldsymbol{\mathcal{H}}_1 = \begin{bmatrix} h_{11} & h_{12} & h_{13} & h_{14} \\ h_{31} & h_{32} & h_{33} & h_{34} \\ h_{51} & h_{52} & h_{53} & h_{54} \\ h_{71} & h_{72} & h_{73} & h_{74} \end{bmatrix} \text{ and } \boldsymbol{\mathcal{H}}_2 = \begin{bmatrix} h_{21} & h_{22} & h_{23} & h_{24} \\ h_{41} & h_{42} & h_{43} & h_{44} \\ h_{61} & h_{62} & h_{53} & h_{64} \\ h_{81} & h_{82} & h_{83} & h_{84} \end{bmatrix}.$$

Due to the interference components in (4.39), the code matrix is compromised. Unless an IC is used, a significant performance degradation is introduced (see Section 4.5).

4.4.2 Extending IC detectors

As mentioned, the PIC and SIC based detectors were proposed for specific instances of one-way WRNs [36, 37, 55, 74–76]. Here, these detectors are extended for the derived general model, either one-way WRNs or TWRNs. Unlike existing detectors, the extending detectors work for networks either if orthogonal or quasi-orthogonal STBC is employed. In addition, they work with AF and DF networks and with an arbitrary number of relays.

Logically, the IC detectors first tries to eliminate the known interference terms. In one-way networks, it can be noticed that $\mathbf{q}_1(i)$ can be cancelled completely if the transmission has been initialized properly [36]. Similarly, $\mathbf{q}_{1,y}(i)$ term in TWRNs can also be cancelled. In addition, the terms from the current processing terminals $\mathbf{q}_{0,x}(i)$ and $\mathbf{q}_{1,x}(i)$, are known to the terminal and hence they both can be eliminated completely. This is conducted through a modified version of the self-interference cancellation step

$$\widetilde{\bar{\mathbf{z}}}^0 = \begin{cases} \bar{\mathbf{z}} - \bar{\mathbf{q}}_1 = \sqrt{P_2}\beta \mathbf{G}_\mathbf{H}\bar{\mathbf{y}} + \bar{\mathbf{q}}_0 + \bar{\boldsymbol{\zeta}} & \text{1-WRNs} \\ \bar{\mathbf{z}}_1 - \mathbf{G}_\mathbf{G}\bar{\mathbf{x}} - \bar{\mathbf{q}}_{0,x} - \bar{\mathbf{q}}_{1,x} - \bar{\mathbf{q}}_{1,y} = \sqrt{P_2}\beta \mathbf{G}_\mathbf{H}\bar{\mathbf{y}} + \bar{\mathbf{q}}_{0,y} + \bar{\boldsymbol{\zeta}}_1 & \text{TWRNs} \end{cases}, \tag{4.41}$$

Most IC detectors differ in how they deal with the current-block interference term ($\mathbf{q}_0$ or $\mathbf{q}_{0,y}$). However, they are all reliant on initializing the interference cancellation process by the low-performance DT detected symbols and feeding the results into a new iteration of the cancellation and decoding process [36, 37]. In addition to the mentioned difference between the one-way and two-way networks, the DT link is not commonly feasible in the TWRNs as it requires full-duplex terminals.

The extended PIC and SIC based detectors are shown in Algorithm 1 and Algorithm 2, respectively.

Algorithm 1 Extended PIC based detector

1. Set $k = 0$ and then initialise $\mathbf{y}^{(k)}$ to the DT detection results $\widehat{\mathbf{y}}_{\mathrm{DT}}$ if the DT link exists (see (3.2) for one-way WRNs and either (4.3) or (4.4) for TWRNs). Otherwise, initialise $\mathbf{y}^{(k)}$ to the result of the conventional detector of Section 4.4.1 applied to $\widetilde{\mathbf{z}}^0$ of (4.41).

2. Remove more ISI by calculating

$$\widetilde{\mathbf{z}}^{0,(k+1)} = \begin{cases} \widetilde{\mathbf{z}}^0 - \bar{\mathbf{q}}_0^{(k)} & \text{1-WRNs} \\ \widetilde{\mathbf{z}}^0 - \bar{\mathbf{q}}_{0,y}^{(k)} & \text{TWRNs} \end{cases}, \tag{4.42}$$

   where $\mathbf{q}_0^{(k)}$ and $\mathbf{q}_{0,y}^{(k)}$ are evaluated through (1.11) and (4.10), respectively, using the current value of $\mathbf{y}^{(k)}$.

3. Update $\mathbf{y}^{(k)}$ to the current result of the conventional detector of Section 4.4.1 applied to $\widetilde{\mathbf{z}}^{0,(k+1)}$.

4. Go back to step 3 till $k \geq K$.

Algorithm 2 Extended SIC based detector for TWRN.

1. Do step 1 of Algorithm 1.

2. Assuming a C-decoding group STBC is employed, determine the detection order $\mathbf{w}$ by comparing $\|\boldsymbol{\mathcal{B}}_c\|^2, \forall c = 1, \ldots, C$. For example, for the network of Section 4.3.1, set $\mathbf{w} = [1, 2]$ if $\|\boldsymbol{\mathcal{B}}_1\|^2 \leq \|\boldsymbol{\mathcal{B}}_2\|^2$. Otherwise, set $\mathbf{w} = [2, 1]$.

3. Set w value to the first value in the order vector $\mathbf{w}$.

4. Remove more ISI by calculating $\mathbf{u}^{0,(k+1)} = \mathbf{G}_{\mathbf{H}}^H \widetilde{\mathbf{z}}^0 - \boldsymbol{\mathcal{B}}\left(\bar{\mathbf{y}}^{(k)}\right)$ using the current available detected symbols ($\mathbf{y}^{(k)}$).

5. Estimate the symbols within the group w ($\widehat{\mathbf{y}}_w$) using the group-decoding step of Section (4.4.1) applied to $\mathbf{u}_w^{0,(k+1)}$.

6. Update the corresponding symbols of the group w in $\mathbf{y}^{(k)}$.

7. Set w value to the next value of the order vector $\mathbf{w}$. Otherwise, set $w = 0$.

8. If $w = 0$ go to step 9. Otherwise, go back to step 4.

9. Go back to step 3 until $k \geq K$.

4.4.3 Proposed Detector

In this section, the idea behind the new detector is explained and then its steps are designed. Unlike the extending detectors, the proposed detector tries to cancel only the interference terms that must be eliminated and benefits from the other terms in an innovative manner. Accordingly, the achieved performance is enhanced, particularly in the first iteration of the detection process. The explanation is conducted based on the network of Section 4.3.1. Rewriting (4.41) for illustration purposes as

$$\widetilde{\bar{\mathbf{z}}}^0 = \sqrt{P_2\beta}\mathbf{G_H}\bar{\mathbf{y}} + \sqrt{P_2\beta}\mathbf{G_q}\widetilde{\bar{\mathbf{y}}} + \bar{\zeta}_1, \tag{4.43}$$

and assuming, that the 2^{nd}, 4^{th},6^{th}, and 8^{th} columns of $\mathbf{G_q}$ are zeros, then the equalization process $\mathbf{u} = \mathbf{G}_\mathbf{H}^H\widetilde{\bar{\mathbf{z}}}^0$ leads to (ignoring non-important terms):

$$\mathbf{u} = \begin{bmatrix} h_{11} & 0 & h_{12} & 0 & h_{13} & 0 & h_{14} & 0 \\ 0 & h_{21} & 0 & h_{22} & 0 & h_{23} & 0 & h_{24} \\ h_{31} & 0 & h_{32} & 0 & h_{33} & 0 & h_{34} & 0 \\ 0 & h_{41} & 0 & h_{42} & 0 & h_{43} & 0 & h_{44} \\ h_{51} & 0 & h_{52} & 0 & h_{53} & 0 & h_{54} & 0 \\ 0 & h_{61} & 0 & h_{62} & 0 & h_{63} & 0 & h_{64} \\ h_{71} & 0 & h_{72} & 0 & h_{73} & 0 & h_{74} & 0 \\ 0 & h_{81} & 0 & h_{82} & 0 & h_{83} & 0 & h_{84} \end{bmatrix} \bar{\mathbf{y}} + \begin{bmatrix} b^1_{11} & 0 & b^1_{12} & 0 & b^1_{13} & 0 & b^1_{14} & 0 \\ b^1_{21} & 0 & b^1_{22} & 0 & b^1_{23} & 0 & b^1_{24} & 0 \\ b^1_{31} & 0 & b^1_{32} & 0 & b^1_{33} & 0 & b^1_{34} & 0 \\ b^1_{41} & 0 & b^1_{42} & 0 & b^1_{43} & 0 & b^1_{44} & 0 \\ b^1_{51} & 0 & b^1_{52} & 0 & b^1_{53} & 0 & b^1_{54} & 0 \\ b^1_{61} & 0 & b^1_{62} & 0 & b^1_{63} & 0 & b^1_{64} & 0 \\ b^1_{71} & 0 & b^1_{72} & 0 & b^1_{73} & 0 & b^1_{74} & 0 \\ b^1_{81} & 0 & b^1_{82} & 0 & b^1_{83} & 0 & b^1_{84} & 0 \end{bmatrix} \bar{\mathbf{y}} \tag{4.44}$$

Notice that all of the 1^{st}, 3^{rd}, 5^{th}, and 7^{th} time-slots of $\mathbf{u}$ are independent of $\bar{\mathbf{y}}(2)$, $\bar{\mathbf{y}}(4)$, $\bar{\mathbf{y}}(6)$ and $\bar{\mathbf{y}}(8)$. Therefore, the first group of symbols ($\mathbf{y}_1 = [\mathbf{y}(1), \mathbf{y}(3)]^T$) can be detected independently through these mentioned slots of $\mathbf{u}$ (denoted as $\mathbf{u}_1$). Similarly,

$$\mathbf{u} = \begin{bmatrix} h_{11} & 0 & h_{12} & 0 & h_{13} & 0 & h_{14} & 0 \\ 0 & h_{21} & 0 & h_{22} & 0 & h_{23} & 0 & h_{24} \\ h_{31} & 0 & h_{32} & 0 & h_{33} & 0 & h_{34} & 0 \\ 0 & h_{41} & 0 & h_{42} & 0 & h_{43} & 0 & h_{44} \\ h_{51} & 0 & h_{52} & 0 & h_{53} & 0 & h_{54} & 0 \\ 0 & h_{61} & 0 & h_{62} & 0 & h_{63} & 0 & h_{64} \\ h_{71} & 0 & h_{72} & 0 & h_{73} & 0 & h_{74} & 0 \\ 0 & h_{81} & 0 & h_{82} & 0 & h_{83} & 0 & h_{84} \end{bmatrix} \bar{\mathbf{y}} + \begin{bmatrix} 0 & b^2_{11} & 0 & b^2_{12} & 0 & b^2_{13} & 0 & b^2_{14} \\ 0 & b^2_{21} & 0 & b^2_{22} & 0 & b^2_{23} & 0 & b^2_{24} \\ 0 & b^2_{31} & 0 & b^2_{32} & 0 & b^2_{33} & 0 & b^2_{34} \\ 0 & b^2_{41} & 0 & b^2_{42} & 0 & b^2_{43} & 0 & b^2_{44} \\ 0 & b^2_{51} & 0 & b^2_{52} & 0 & b^2_{53} & 0 & b^2_{54} \\ 0 & b^2_{61} & 0 & b^2_{62} & 0 & b^2_{63} & 0 & b^2_{64} \\ 0 & b^2_{71} & 0 & b^2_{72} & 0 & b^2_{73} & 0 & b^2_{74} \\ 0 & b^2_{81} & 0 & b^2_{82} & 0 & b^2_{83} & 0 & b^2_{84} \end{bmatrix} \bar{\mathbf{y}} \tag{4.45}$$

if the 1^{st}, 3^{rd},5^{th} and 7^{th} columns of $\mathbf{G_q}$ are zeros. This means that ($\mathbf{y}_2 = [\mathbf{y}(2), \mathbf{y}(4)]^T$) can be detected independently through 2^{nd}, 4^{th}, 6^{th} and 8^{th} time slots of $\mathbf{u}$ (denoted as $\mathbf{u}_2$).

Assuming that the mentioned assumptions hold, the detection can be carried out using

$$\widehat{\mathbf{y}}_c = \underset{\mathbf{y}_c \in \mathcal{S}}{\operatorname{argmin}} \left| \bar{\mathbf{u}}_c - \left(\boldsymbol{\mathcal{H}}_c \bar{\mathbf{y}}_c + \mathcal{B}_c \bar{\mathbf{y}}_c \right) \right|^2, \tag{4.46}$$

where $\boldsymbol{\mathcal{H}} = \mathbf{G}_{\mathbf{H}}^H \mathbf{G}_{\mathbf{H}}$ and $\mathcal{B} = \mathbf{G}_{\mathbf{H}}^H \mathbf{G}_{\mathbf{q}}$. $\boldsymbol{\mathcal{H}}_c$ and $\boldsymbol{\mathcal{B}}_c$ are the matrices that contained the corresponding elements of the group c from $\mathcal{H}$ and $\mathcal{B}$, respectively. For example, for (4.43):

$$\boldsymbol{\mathcal{H}}_1 = \begin{bmatrix} h_{11} & h_{12} & h_{13} & h_{14} \\ h_{31} & h_{32} & h_{33} & h_{34} \\ h_{51} & h_{52} & h_{53} & h_{54} \\ h_{71} & h_{72} & h_{73} & h_{74} \end{bmatrix}, \boldsymbol{\mathcal{B}}_1 = \begin{bmatrix} b_{11}^1 & b_{12}^1 & b_{13}^1 & b_{14}^1 \\ b_{31}^1 & b_{32}^1 & b_{33}^1 & b_{34}^1 \\ b_{51}^1 & b_{52}^1 & b_{53}^1 & b_{54}^1 \\ b_{71}^1 & b_{72}^1 & b_{73}^1 & b_{74}^1 \end{bmatrix}, \tag{4.47}$$

and

$$\boldsymbol{\mathcal{H}}_2 \begin{bmatrix} h_{21} & h_{12} & h_{23} & h_{24} \\ h_{41} & h_{42} & h_{43} & h_{44} \\ h_{61} & h_{62} & h_{63} & h_{64} \\ h_{81} & h_{82} & h_{83} & h_{84} \end{bmatrix}, \boldsymbol{\mathcal{B}}_2 = \begin{bmatrix} b_{21}^2 & b_{22}^2 & b_{23}^2 & b_{24}^2 \\ b_{41}^2 & b_{42}^2 & b_{43}^2 & b_{44}^2 \\ b_{61}^2 & b_{62}^2 & b_{63}^2 & b_{64}^2 \\ b_{81}^2 & b_{82}^2 & b_{83}^2 & b_{84}^2 \end{bmatrix}. \tag{4.48}$$

Now, a method for cancelling these columns and the order of the cancellation is considered. Similar to all IC based detectors, a subtraction of interference terms of the corresponding time slots is used. Logically, the ordering should be carried out according to the ordering of reliability of available detected symbols. This can be achieved by estimating which time slots have a better instantaneous SNR. The estimation of SNR values can be done through a two-phase training pilot sequence for TWRN channel estimation [77, 78] and traditionally as proposed in [79, 80] if the DT link exists or one-way WRNs. Consequently, better performance is achieved, particularly in the first iteration of the proposed detector, and hence faster convergence is achieved in the subsequent iteration, see Section 4.5. Algorithm 3 includes the steps of the EIC detector.

Algorithm 3 EIC based detector for TWRNs.

1. Set $k = 0$ and then initialise $\mathbf{y}^{(k)}$ to the DT detection results $\widehat{\mathbf{y}}_{\mathrm{DT}}$ if the DT link exists (see (3.2) for one-way WRNs and either (4.3) or (4.4) for TWRNs). Otherwise, initialise $\mathbf{y}^{(k)}$ to the result of the conventional detector of Section 4.4.1 applied to $\widetilde{\widetilde{\mathbf{z}}}^{0}$ of (4.41).

2. Assuming a C-decoding groups STBC is employed, determine the detection order $\mathbf{w}$ by comparing the estimating SNR values, $\forall c = 1, \ldots, C$. For example, for the network of Section 4.3.1, set $\mathbf{w} = [1, 2, 0]$ if $\gamma_1 \leq \gamma_2$. Otherwise, set $\mathbf{w} = [2, 1, 0]$. If a DT link exists, the detection order of the first iteration is determined through the DT link symbols rather than the second phase symbols.

3. Set w value to the first value of the order vector ($\mathbf{w}$).

4. For the current processing group w, remove more ISI by calculating

$$\widetilde{\widetilde{\mathbf{z}}}^{0,(k)} = \begin{cases} \widetilde{\widetilde{\mathbf{z}}}^{0} - \bar{\mathbf{q}}_{0}^{(k)} & \text{1-WRNs} \\ \widetilde{\widetilde{\mathbf{z}}}^{0} - \bar{\mathbf{q}}_{0,y}^{(k)} & \text{TWRNs} \end{cases}. \tag{4.49}$$

   Both $\mathbf{q}_{0}^{(k)}$ and $\mathbf{q}_{0,y}^{(k)}$ are evaluated using the current value of $\mathbf{y}^{(k)}$, and by setting the corresponding columns of the other groups in $\mathbf{G_q}$ to zeros (i.e., for the network in Section 4.3.1, these columns are the 2$^{\text{nd}}$, 4$^{\text{th}}$, 6$^{\text{th}}$, and 8$^{\text{th}}$ column if $w = 1$ and 1$^{\text{st}}$, 3$^{\text{rd}}$, 5$^{\text{th}}$ and 7$^{\text{th}}$ column when $w = 2$).

5. Estimate the symbols of the current-processing group through the modified ML shown in (4.46) using the last recent value of $\widetilde{\widetilde{\mathbf{z}}}^{0,(k)}$, where $c = w$.

6. Update the corresponding symbols of the group w in $\mathbf{y}^{(k)}$ by the result obtained in the previous step.

7. Set w to the next value of the order vector $\mathbf{w}$.

8. If $w = 0$ go to step 9. Otherwise, go back to step 4.

9. Go back to step 3 till $k \geq K$.

4.5 Simulation Results and Discussion

In terms of BER, simulation results are presented below to demonstrate the performance of the proposed detectors under different conditions of imperfect synchronisation. The simulation used 4-QAM Gray coded modulation over a Rayleigh fading channel. The simulated network configurations are shown in Tab. 4.1. The used power loading schemes are similar to that used under perfect synchronisation conditions (refer to the corresponding references).

Denoted by	Used code	Network configurations
Network 1	QO-STBC of [40]	TWRN with two dual-antenna relays; terminals are half-duplex nodes.
Network 2	Novel QO-STBC of [40]	TWRN with two dual-antenna relays; terminals are full-duplex nodes.
Network 3	Alamouti's STBC of[12, 66]	TWRN with two single-antenna relays; terminals are half-duplex nodes.
Network 4	QO-STBC of[67]	TWRN with four single-antenna relays; terminals are half-duplex nodes.

Tab. 4.1: The configurations of the simulated Networks.

Network 1 is simulated under a condition of $\alpha = -5dB$ and $-3dB$ in Fig. 4.3 and Fig. 4.4, respectively. Fig. 4.3 shows that even under a limited condition of imperfect synchronisation, much performance degradation is experienced if the conventional detector is used. This degradation can be mitigated if the extended PIC and SIC based detectors are used and to an even greater degree when the proposed EIC detector is used. Due to the novel cancellation process designed, one iteration of EIC can offer a performance close (less than 3dB) to the performance of two iterations of either the PIC or SIC detector. Specifically, it offers a 3 and 4 SNR gain to get a BER of 10^{-3} over the SIC and PIC detector, respectively. Fig. 4.4 shows the performance of the extended detectors is degraded but they are still effective compared to the conventional detector. In contrast, the EIC detector outperforms the extended detectors and shows a performance closer to the perfect synchronisation condition.

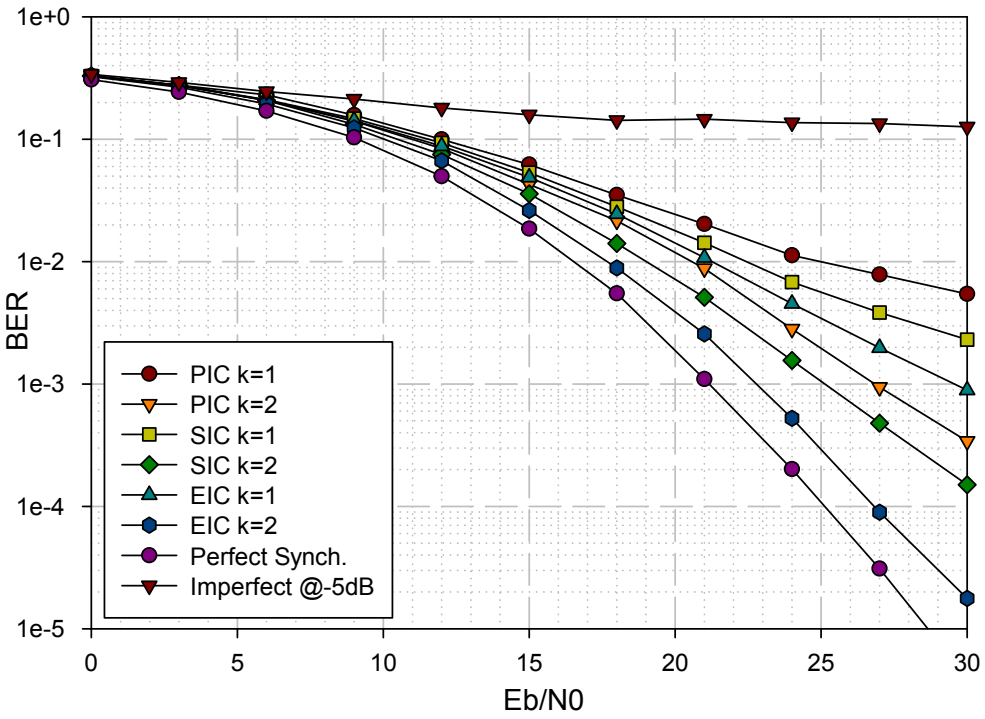

Fig. 4.3: The BER using PIC, SIC and EIC detectors under $-5dB$.

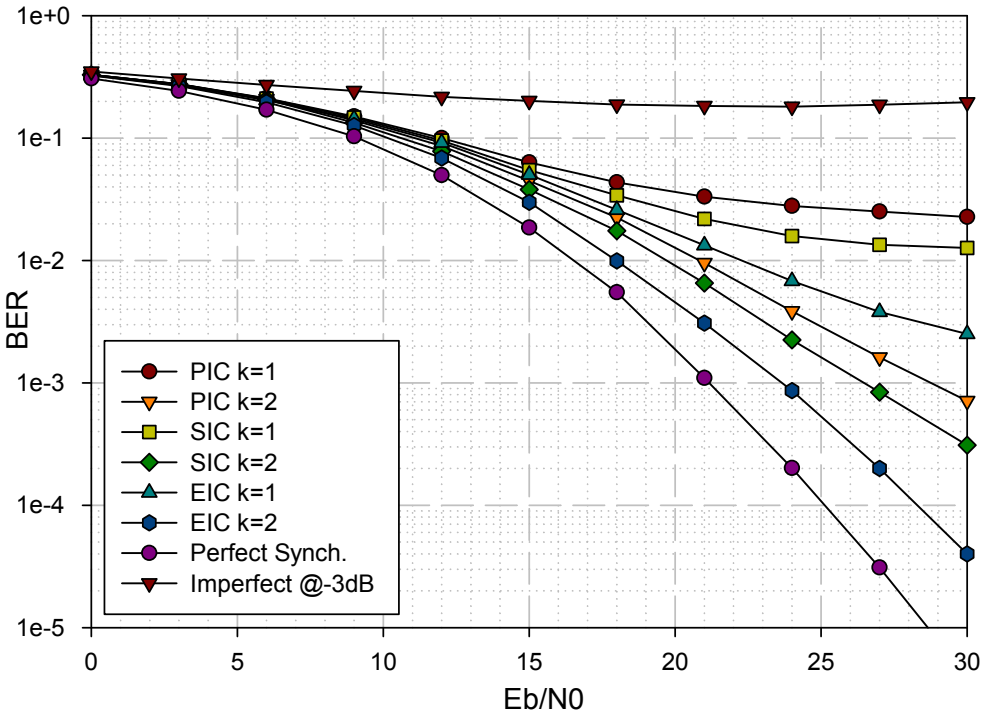

Fig. 4.4: The BER using PIC, SIC and EIC detectors under $-3dB$.

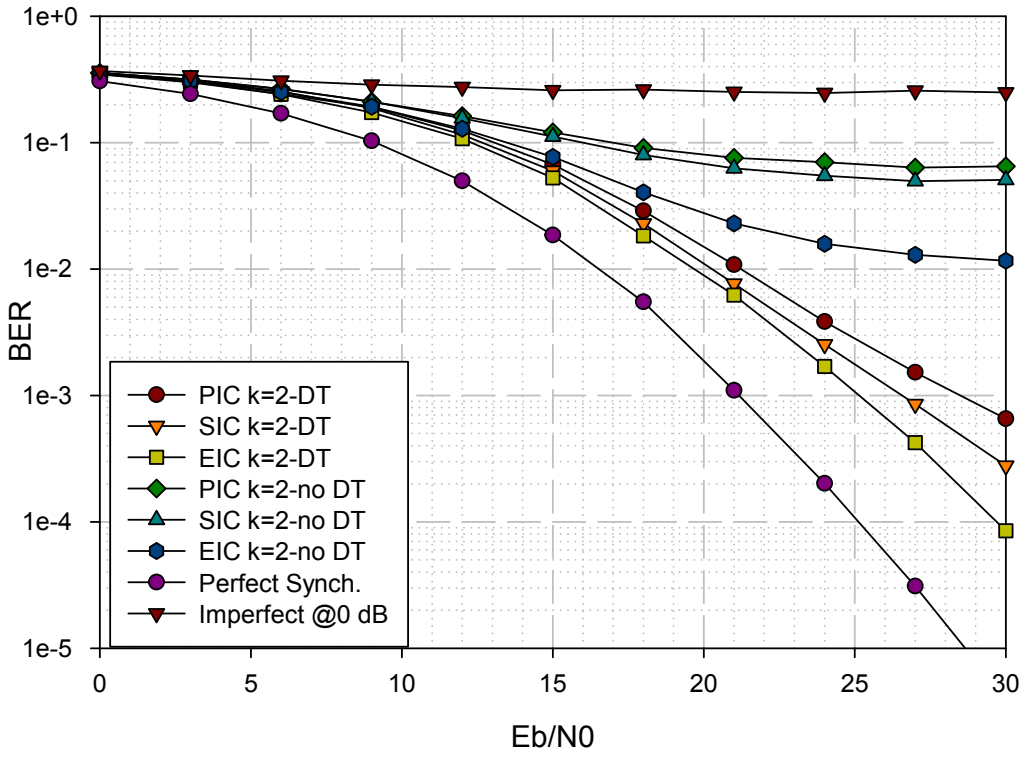

Fig. 4.5: The BER using PIC, SIC and EIC detectors under $0dB$.

To show the effectiveness of the proposed detectors, Network 1 and Network 2 are simulated under a condition of α = 0dB in Fig. 4.5. This condition corresponds to the most severe value of time misalignment. In spite of severe timing errors, the proposed detector still outperforms the extended ones and performs much better than the conventional detector. It is worth noting that the EIC detector fails to achieve performance close to perfect synchronisation under this severe condition in the event of no DT link but is still effective in the case where it exists.

The simulation results of using the proposed detectors by Network 3 and Network 4 are shown in Fig. 4.6 and Fig. 4.7, respectively. This shows that these detectors are designed not only for particular networks as in [36, 37] but also for any TWRN and one-way WRN. In addition, they can be used for an orthogonal or quasi-orthogonal linear dispersion STBC. From the shown figures, it can be concluded that the EIC detector outperforms the extended detectors and these extended detectors are still effective compared to the conventional detector.

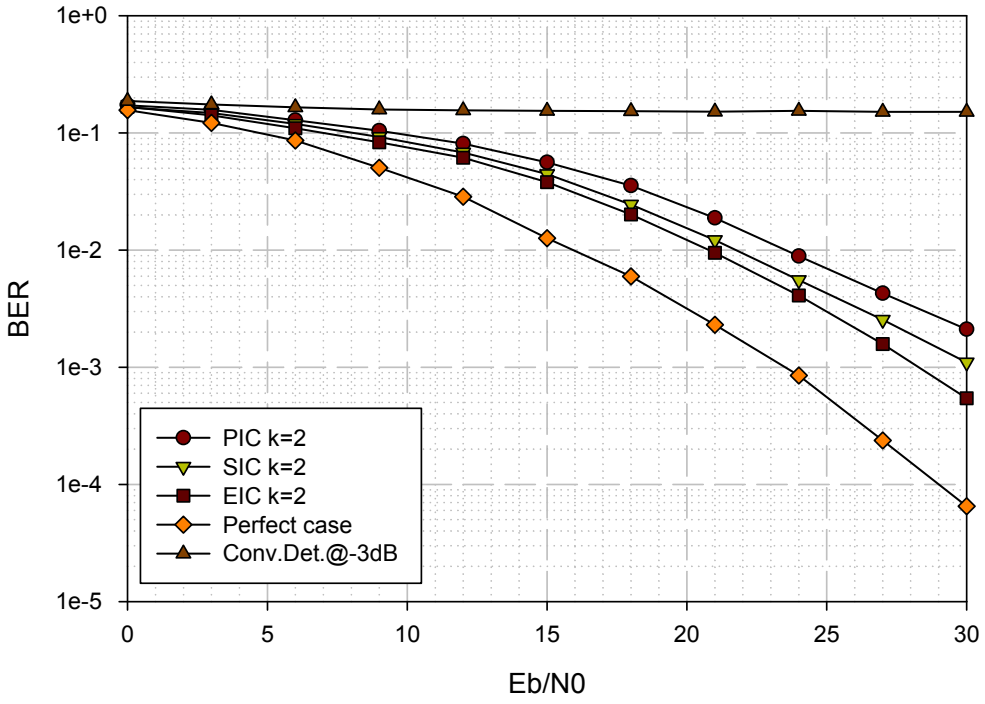

Fig. 4.6: The BER using PIC, SIC and EIC detectors under $-3dB$ in Network 3.

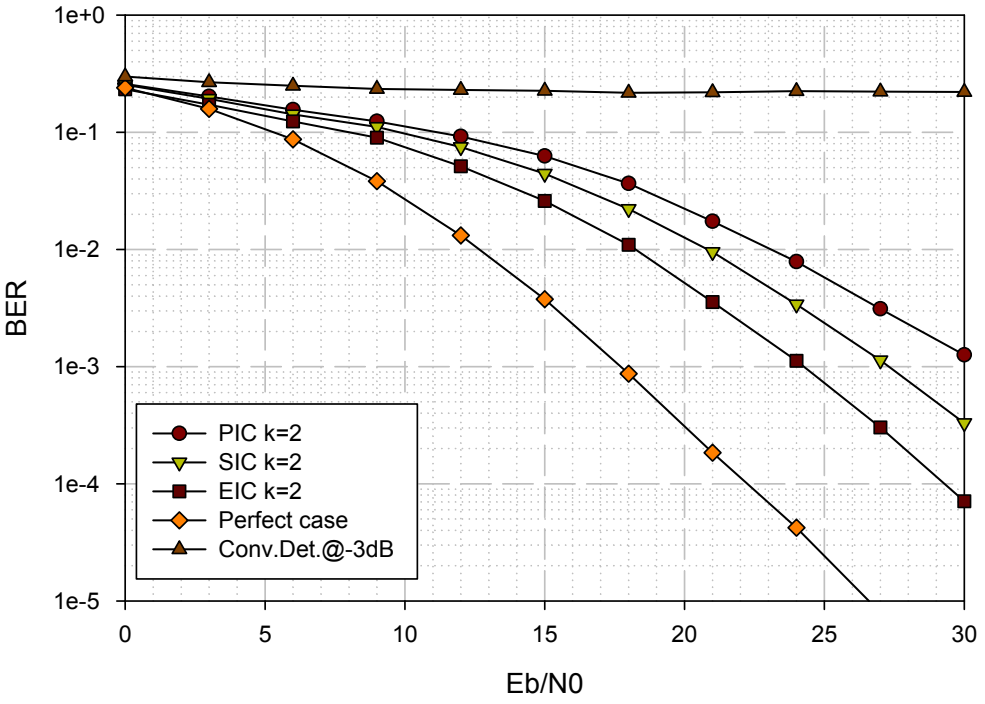

Fig. 4.7: The BER using PIC, SIC and EIC detectors under -3dB in Network 4.

4.6 Conclusion

This chapter considered the issue of imperfect synchronisation in TWRNs. The considered network consists of two terminals exchanging data through N relays, equipped each with R_a antennas. A general model was derived for the considered network and then instances were evaluated for a number of network configurations. Both the existing PIC and SIC based detectors were extended here for the derived general model. Unlike the literature, these extended detectors work for networks with either quasi-orthogonal or orthogonal STBCs. This chapter proposed an enhanced detector (EIC) detector while maintaining low computational complexity. This detector shows better performance improvement due to the designed iterative cancellation process. It reduces the dependency on low-performance symbols and befits from the interference that belong to the current-detecting symbols. The simulation results showed that significant improvement can be gained compared to the conventional detector if these proposed detectors are used.

Tab. 4.2: Summary of Literature regarding the D-STBC Networks under Imperfect Synchronisation

Ref.	Relaying b network Type	Sys. trans. Type	Main scheme used to over-come asynchro-nism	Used Code type	# relays	relaying protocol used	Channel Model	Further important details
[59, 81, 82]	1-way	P2P	Optimum PIC	Alamouti	2	DF	Block Flat Fading	NA
[36, 83]	1-way	P2P	PIC	orthogonal STBC	3 or 4	DF	as above	MRC enhancement
[55]	1-way	P2P	PIC	Extended STBC	4	DF	as above	require feedback ch.
[84]	1-way	P2P	PIC	Quasi-Orthogonal	4	DF	as above	require feedback ch.
[85]	1-way	MA	PIC merged with j-STBC	joint STBC	2	AF	as above	NA
[76]	1-way	P2P	GPIC	Systematic STBC	any	DF	as above	NA
[74]	1-way	P2P	PIC	Alamouti	2	incremental DF	as above	MRC enhancement
[75]	1-way	P2P	PIC	Alamouti	2	AF	as above	NA
[62]	TWRN	P2P	PIC	Alamouti	2	AF	as above	NA
[37]	1-way	P2P	SIC	orthogonal STBC	4	DF	as above	NA
[54]	1-way	P2P	OFDM with CP & 2-bits feedback	EO-STBC	3 or 4	AF	as above	need just 2 time slots
[61]	TWRN	P2P	OFDM with CP& 2-bits feedback	EO-STBC	3 or 4	AF	as above	same as above
[56]	1-way	P2P	OFDM with CP	Orthogonal STBC	any	DF	as above	deal with ICI issues
[57]	1-way	P2P	IBIC and CPR	Orthogonal STBC	1	AF	Frequency-Selective	Mainly designed for 3GPP-LTE
[86]	1-way	P2P	PIC	Alamouti	2	DF	Block Flat Fading	Cellular scheme deal with CCI
[60]	1-way	P2P	Novel transmis-sion scheme	Orthogonal STBC	any	DF	as above	NA

Part II

Scalable Wireless Relaying Networks

Part 2: Abstract

This part considers the issue of designing D-STBCs for WRNs with an arbitrary number of relays. It has been shown that the reliability of WRNs increases by adding more relays as a result of more communication paths becoming available. Unlike most existing D-STBCs, this part proposes two high rate coding schemes to accommodate an arbitrary number of relays, while retaining low decoding complexity at the destination. The first scheme, full-rate distributed space-time block coded-joint transmit/receive antenna diversity (D-STBC-JTRD), is proposed for AF WRNs. Its code rate is independent of the number of relays and hence no code rate loss is incurred as the relays number increases. In addition, this scheme deploys the same encoding matrices at every relay; this eliminates the need for additional network overhead to coordinate the code generation by the relays. In other words, there is no need to interrupt the transmission if a relay has been up/down. The second scheme aims to find a flexible trade-off between reliability and code-rate that can be offered by DF networks. Towards this end, a method to construct a D-STBC that is combined with spatial modulation (SM), denoted as D-STBC-SM, is proposed. This method is not restricted to a specific number of relays and can be constructed as necessary. In addition, a novel adaptive transmission protocol that uses the constructed codes, is proposed to achieve higher space diversity gain, even with relays equipped with a single antenna. Unlike most existing schemes, this protocol offers a throughput that increases as the number of relays increases. Moreover, the offered throughput is achieved using the same total average transmit energy, as only N^0 of the N available participating relays are active at any given time.

Part II: Publication List

Publications List

- El Astal, Mohammed-Taha O.; Salmon, Brian P.; Olivier, Jan Corné:"Full-space diversity and full-rate distributed space–time block codes for amplify-and-forward relaying networks," in **IET Journal of Engineering**, IET, 2014, DOI: 10.1049/joe.2014.0063. URL: click here.
- El Astal, M.-T. O.; Abu-Hudrouss, A.M.; Salmon, B.P.; Olivier, J.C.: "An adaptive transmission protocol for exploiting diversity and multiplexing gains in wireless relaying networks," in **EURASIP Journal on Wireless Communications and Networking**,2015:1-15. URL: click here.
- El Astal, M.-T.O.; Salmon, B.P.;Olivier, J.C.: "Distributed Space-Time Codes for Amplify-and-Forward Relaying Networks," in **IEEE Wireless Communications and Networking conference (WCNC)**, Istanbul, Turkey, pp.1166-1169, 6-9 Apr. 2014. URL: click here.

5

Full-Diversity and Full-Rate D-STBCs for AF WRNs

> *Genius might be the ability to say a profound thing in a simple way.*
>
> — **Charles Bukowski**
> (American author)

5.1 Introduction

It has been shown that D-STBCs have the potential to exploit the space diversity gain inherent in WRNs in order to improve signal quality [6, 35, 87, 88]. It is known that the diversity gain is further improved when the number of relays is increased [7, 89–92]. However, a trade off in code design is between a decrease in the code rate and the need to retain the single-symbol decoding complexity at the receiver when more relays are utilised. Another factor is how well the network deals with the addition and removal of relays and what this entails for the generation of the used D-STBC. This is important as incorporating more relays can improve the diversity gain. However, treating all relays as permanent connections is impractical as these relays may be clients' apparatus and may not always be available. Most D-STBCs require additional network overhead when additional relays become available. This is because there is a need to pass along all information necessary to generate the used STBC to all relays. Potentially, this overhead could degrade the expected performance gain due to limited network resources.

In this chapter, the STBC scheme of [93, 94], that was initially proposed for conventional P2P MIMO networks, is introduced to the problem of WRNs. Unlike most existing D-STBCs, the proposed scheme can accommodate an arbitrary number of relays while full-rate and single symbol decoding complexity are offered. Specifically, its rate is independent of the number of relays, hence there is no code rate loss experienced when the number of relays increases.

In addition, this scheme deploys the same encoding matrices at every relay. This eliminates the need for additional network overhead to coordinate the code generation by the relays. This means there is no prior set-up steps are required for code-generation coordination process when relays de/activate. Also, there is no need to interrupt the transmission if a relay has been down. The only restrictions for the proposed scheme is that the destination must be equipped with two antennas and that there is a reliance on global knowledge of the CSI at the relays. These constraints are inherited from the original code's design. This is not seen as a severe limitation as most modern receivers have two or more antennas.

5.2 Prior Work

The overall interest in this field of research lies in the construction of a high-rate D-STBC that has the ability to utilize any arbitrary number of relays [33, 95]. It would appear that research has had limited success in designing high-rate codes while maintaining a single-symbol decodability at the destination. In [96], the authors proposed systematic construction steps of a row-monomial D-STBC with a code rate bounded by $2/(2+N)$, where N denotes the number of relays. In [97], a new code class called semi-orthogonal precoded distributed single-symbol decodable STBC (Semi-PD-SSD-STBCs) was proposed. It has the advantage of performing precoding on the information symbols, which in turn doubles the achieved code rate. Although these codes were designed for an arbitrary number of relays, it may be preferable to use them only in WRNs with a few numbers of relays. This is because the code rate decreases dramatically as the number of relays increases. In [98], a coding scheme, with a code rate of $\frac{1}{4}$, was proposed to operate in WRNs of high number of relays. However, this scheme has a high decoding delay, as the required transmission time increases exponentially with the number of relays. In [99], an adjustable full-rate STBC matrix was designed, but it requires a feedback channel to adjust the code. This creates additional network overhead that inherently reduces the achieved diversity gain. In [100–102], the generalised ABBA code (GABBA) of [103] was adapted for AF WRNs to offer a full-rate while maintaining single-symbol decodability. However the resulting D-GABBA scheme has some constraints: (1) the number of symbols per block (T) should be expressible as a power of two, and (2) the number of available relays (N) should be smaller or equal to T ($N \leq T$).

In conclusion, and to best of the author's knowledge, most D-STBCs that were proposed to accommodate an arbitrary number of relays have constraints that limit the variety of applications that can use them. In addition, they all require that the utilised relays

remain permanent throughout the communication. Furthermore, they need an exchange of additional control information overhead among the relays to generate the code used. As mentioned, the cost of this overhead has the potential to reduce the performance.

5.3 Network Model

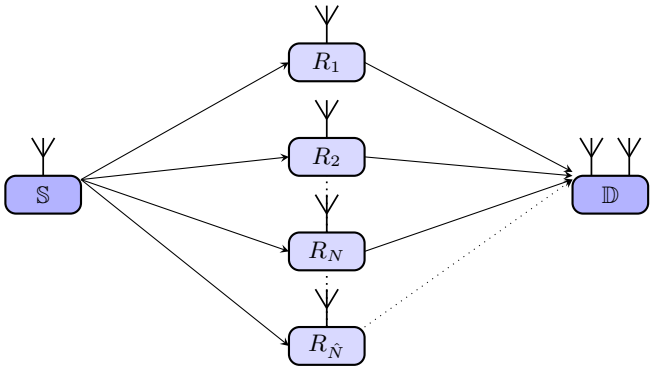

Fig. 5.1: The Network model.

The network is comprised of a source (S), $\hat{N}$ relays ($R_1, \ldots, R_{\hat{N}}$), and a destination (D), as depicted in Fig. 5.1. It has been assumed that all nodes are single-antenna nodes, except the destination which is equipped with two antennas ($N_r = 2$). The network employs the selective AF (SAF) relaying protocol (see Section 2.6.1). The total transmission power dedicated for the entire network is denoted by P, and is evenly divided between the two phases. The channel is assumed to be a quasi-static Rayleigh fading channel. Both the source and the destination are completely blind, while perfect and global CSI is known only at the relays.

As with most WRNs, the transmission through the network is conducted via two phases: the first phase is when the source broadcasts its information to the relays; in the second phase, the participating relays amplify and forward a linear combination of scaled versions of their received symbols to the destination.

Assuming that the source transmits M-ary modulated symbols denoted by $\mathbf{y}(i) = [y(1,i), \ldots, y(J,i)]^T$, the received symbols at the relay R_n is given by

$$\underset{J\times 1}{\mathbf{r}_n(i)} = \sqrt{P_1} h_n \underset{J\times 1}{\mathbf{y}(i)} + \underset{J\times 1}{\mathbf{v}_n(i)}, \tag{5.1}$$

where i denotes the information block index and J is the number of symbols in the broadcasting phase. $J = 2$. $P_1 = P/2$ is the power dedicated for phase 1, $h_n \sim \mathcal{CN}(0,1)$ is the channel coefficient for the link between the source and the relay R_n. $\mathbf{v}_n(i)$ denotes the AWGN noise vector at the relay R_n with entries $v_{nj} \sim \mathcal{CN}(0,1)$.

As mentioned, the network employs the SAF relaying protocol. This means that only relays that are satisfying a selection performance based criteria will participate in the relaying phase. This is to avoid error propagation in the network. As mentioned in Section 2.6.1, the SNR can be used as a criterion to determine whether a relay is participating or not in this phase (i.e., $\gamma_n \geq \gamma_{th}$, where γ_n is the SNR at relay R_n and γ_{th} is a threshold that is optimally designed according to the definition of the protocol). To limit the discussion, it is assumed directly that N out of $\hat{N}$ relays satisfies the criterion. Without loss of generality, these N participating relays are mentioned as relays throughout this chapter.

The relays R_n has to scale their received signals as

$$\mathbf{s}_n(i) = \rho_n \mathbf{r}_n(i), \tag{5.2}$$

where ρ_n is the scaling factor at R_n and it is computed as

$$\rho_n = \sqrt{\frac{1}{C_n}} \underbrace{\sqrt{\frac{P_2}{N(P_1+1)}}}_{\rho}, \tag{5.3}$$

with

$$C_n = \sum_{m=1}^{2} |g_{mn}|^2, \tag{5.4}$$

where $P_2 = P_1 = \frac{P}{2}$, as the total network power P is evenly divided between the two phases of transmission. $g_{mn} \sim \mathcal{CN}(0,1)$ denotes the channel coefficient for the link between the relay R_n and the destination's antenna m.

Each relay then simultaneously forwards its amplified received symbols ($\mathbf{s}_n(i)$) to the destination after encoding them according to the constructed D-STBC ($\mathbf{X}$) (see Section 5.4). Accordingly, the received symbol at the destination can be modelled as

$$\underset{L\times N_r}{\mathbf{Z}(i)} = \underset{L\times N}{\mathbf{X}(i)} \underset{N\times N_r}{\mathbf{G}} + \underset{L\times N_r}{\boldsymbol{\eta}(i)}, \tag{5.5}$$

where L is the signalling period of phase 2. Here $L = J = 2$ as the proposed code is a full-rate code. The matrix $\mathbf{G}$ denotes the channel coefficients matrix for the links between the relays and the destination with entries $g_{mn} \sim \mathcal{CN}(0,1)$. The matrix $\boldsymbol{\eta}(i)$ is the noise matrix at the destination with entries $\eta_{ik} \sim \mathcal{CN}(0,1)$.

5.4 D-STBC Design with JTRD

In this section, the STBC-JTRD of [93, 94] is adapted to operate for AF WRNs. The resulting distributed coding scheme (denoted as D-STBC-JTRD) can accommodate an arbitrary number of relays while offering full-space diversity gain and retaining a full-rate with single-symbol complexity decoding at the destination. In addition, it deploys the same encoding matrices at all relays which avoids the need for extra network overhead. This section shows the code construction and the used decoding algorithm.

5.4.1 Code Construction

For clarity, the information block index (i) can be omitted and thus the source data can be denoted simply by y_1 and y_2. Accordingly, the code of [93, 94] for the case of double-antenna destination is given by

$$\mathbf{X} = \begin{bmatrix} y_1 \\ -y_2^* \end{bmatrix} \otimes \mathbf{g}_1^* + \begin{bmatrix} y_2 \\ y_1^* \end{bmatrix} \otimes \mathbf{g}_2^*, \tag{5.6}$$

where $\mathbf{X}$ is the general code matrix that it should be totally generated in a distributive manner by the relays. The vector $\mathbf{g}_m = [g_{m,1}, g_{m,2}, \ldots, g_{m,N}]$ and it denotes the channel coefficient vector for the links between the receiving antenna m of the destination and the relays $(R_1, \ldots, R_N)$.

Towards this end, each relay should encode its received symbols using

$$\mathbf{x}_n = \begin{bmatrix} d_n(1) \\ -d_n^*(2) \end{bmatrix} \times g_{1,n}^* + \begin{bmatrix} d_n(2) \\ d_n^*(1) \end{bmatrix} \times g_{2,n}^*, \tag{5.7}$$

where $\mathbf{x}_n$ is the encoding output that the relay R_n should generate to construct $\mathbf{X}$ of (5.6) in distributive manner. The scalars d_1 and d_2 are computed as

$$\mathbf{d}_n = \begin{bmatrix} d_n(1) \\ d_n(2) \end{bmatrix} = \frac{h_n^H}{\|h_n^H\|^2} \times \mathbf{s}_n(i). \tag{5.8}$$

From (5.7), it can be concluded that the encoding matrices within each relay is a combination of

$$\mathbf{A} = \begin{bmatrix} 1 & 0 \\ 0 & 1 \end{bmatrix} \tag{5.9}$$

and

$$\mathbf{B} = \begin{bmatrix} 0 & -1 \\ 1 & 0 \end{bmatrix}. \tag{5.10}$$

Thus, each relay should transmit

$$\mathbf{t}_n = \dot{\mathbf{G}}_{1,n}^{*}\mathbf{A}\mathbf{d}_n + \dot{\mathbf{G}}_{2,n}^{*}\mathbf{B}\mathbf{d}_n^{*}, \tag{5.11}$$

where

$$\dot{\mathbf{G}}_{1,n} = \begin{bmatrix} g_{1,n} & g_{2,n} \\ 0 & 0 \end{bmatrix} \tag{5.12}$$

and

$$\dot{\mathbf{G}}_{2,n} = \begin{bmatrix} 0 & 0 \\ g_{1,n} & g_{2,n} \end{bmatrix}. \tag{5.13}$$

In a conventional D-STBC network, a coordinating process must be used to assist each relay to generate its portion of the general code matrix. In contrast, the proposed scheme does not require this process. This can be observed from (5.11) where the constructed code uses the same two encoding matrices at all relays to generate the general code matrix of (5.6). Thus, there is no control information overhead is required to arrange which relay should generate the certain portion of the code. Implicitly, this means that the proposed scheme can add/remove any number of relays during transmission without interruption or the need of connection re-set-up for the code generation coordination process. This feature is desirable in a variety of communications networks, especially where fast varying channels occur.

5.4.2 Decoding Algorithm

To show how the optimal decoding can be carried out, the received signal is firstly modelled. Substituting equation (5.1) and (5.2) into (5.8) yields

$$\begin{pmatrix} d_n(1) \\ d_n(2) \end{pmatrix} = \rho\sqrt{\frac{P_1}{C_n}}\mathbf{y} + \rho\frac{1}{\sqrt{C_n}}\frac{h_n^H}{\|h_n^H\|^2}\mathbf{v}_n, \tag{5.14}$$

and then substituting equation (5.14) into (5.11) results

$$\mathbf{t}_n = \rho\frac{1}{\sqrt{C_n}}(\dot{\mathbf{G}}^*_{1,n}\mathbf{A}_1(\sqrt{P_1}\mathbf{y} + \frac{h_n^H}{\|h_n^H\|^2}\mathbf{v}_n) + \dot{\mathbf{G}}^*_{2,n}\mathbf{B}_1(\sqrt{P_1}\mathbf{y} + \underbrace{\frac{h_n^T}{\|h_n^H\|^2}}_{\alpha_n^*}\mathbf{v}_n)^*). \tag{5.15}$$

Through the links to the destination, each relay's symbol ($\mathbf{t}_n$) experience a multi-path fading channel (modelled by the matrix $\mathbf{G}$) and they are collated then at the destination. Thus, (5.5) can be rewritten using (5.15) as

$$\mathbf{Z}^1 = \rho\sum_{n=1}^{N}\frac{\mathbf{G}_{n,1}}{\sqrt{C_n}}\left(\sqrt{P_1}\mathbf{y} + \alpha\mathbf{v}_n\right) + \boldsymbol{\eta}^1, \tag{5.16}$$

$$\mathbf{Z}^2 = \rho\sum_{n=1}^{N}\frac{\mathbf{G}_{n,2}}{\sqrt{C_n}}\left(\sqrt{P_1}\mathbf{y}^* + \alpha^*\mathbf{v}_n^*\right) + \boldsymbol{\eta}^2, \tag{5.17}$$

where superscript denote the column of the matrix, e.g. Z^l is the l-th column of the matrix Z,

$$\mathbf{G}_{n,1} = \begin{bmatrix} |g_{1,n}|^2 & g_{1,n}g_{2,n}^* \\ g_{1,n}g_{2,n}^* & |g_{2,n}|^2 \end{bmatrix}$$

and

$$\mathbf{G}_{n,2} = \begin{bmatrix} g_{1,n}g_{2,n}^* & |g_{1,n}|^2 \\ |g_{2,n}|^2 & -g_{1,n}^*g_{2,n} \end{bmatrix}.$$

Now, using

$$\begin{pmatrix} \mathbf{u}(1) \\ \mathbf{u}(2) \end{pmatrix} = \begin{pmatrix} \mathbf{Z}^{1,1} + \left(\mathbf{Z}^{2,2}\right)^* \\ \mathbf{Z}^{1,2} - \left(\mathbf{Z}^{2,1}\right)^* \end{pmatrix}, \tag{5.18}$$

where $\mathbf{Z}^{k,l}$ denotes the element (k,l) of a matrix $\mathbf{Z}$, the former derivation concludes that

$$\begin{pmatrix} \mathbf{u}(1) \\ \mathbf{u}(2) \end{pmatrix} = \rho\sqrt{2CP_1}\begin{pmatrix} \mathbf{y}(1) \\ \mathbf{y}(2) \end{pmatrix} + \underbrace{\frac{\rho}{\sqrt{C}}\sum_{n=1}^{N}\alpha_n\left(|g_{1,n}|^2 + |g_{2,n}|^2\right)\mathbf{v}_n + \begin{bmatrix} \eta^{1,1} + \eta^{2,2*} \\ \eta^{2,1} - \eta^{1,2*} \end{bmatrix}}_{\zeta}, \tag{5.19}$$

The mean and variance of the noise terms of (5.19) (denoted as $\boldsymbol{\zeta}$) are given by

$$E[\boldsymbol{\zeta}] = \mathbf{0} \tag{5.20}$$

and

$$\sigma_{\boldsymbol{\zeta}}^2 = \left(\sigma_\eta^2 + \frac{\sigma_{\mathbf{v}}^2 \rho^2 C}{\left(\sum_{n=1}^{N} |h_n|^2\right)}\right) I_T \tag{5.21}$$

, respectively, where $\sigma_\eta^2 = 1$.

Thus, $\hat{\mathbf{u}}$ is a Gaussian random vector. Accordingly, the decoding can be conducted optimally using

$$\hat{\mathbf{y}}(j) = \underset{y \in \mathcal{S}^{1\times 1}}{\operatorname{argmin}} \left\{ |\mathbf{u}(j) - \lambda y|^2 \right\}, \forall j = 1, 2, \tag{5.22}$$

where $\mathcal{S}$ is the used modulation constellation and $\lambda = \rho\sqrt{CP_1}$.

It can be observed that the decoding is carried out symbol-by-symbol through each received equalised time-slots.

5.5 Performance analysis

In this section, the proposed scheme is evaluated in term of the diversity gain, decoding delay and complexity. This analysis shows that the proposed scheme can achieve the full-space diversity gain while maintaining single-symbol decoding complexity at the destination. Unlike the existing schemes, a low decoding delay is experienced and it is independent of the number of relays.

5.5.1 Decoding delay and complexity analysis

Let us define some definitions for our discussion.

Definition 5.1. *Single-Symbol ML Decodable: A code or a scheme is said to be single-symbol ML decodable if its ML decoding metric can be written as a sum of several terms, each of which depends at most on one transmitted symbol [104].*

Definition 5.2. *The decoding Delay is the time that the destination has to wait, starting from the time of transmission from the source, before it can start decoding the symbols that it receives [98].*

It can be observed from (5.19) and (5.22), that each equalised time-slot depends only on one transmitted symbol. This means that the proposed scheme is a single-symbol ML decodable scheme. In addition, the decoding delay of the proposed scheme is four time-slots. This is because the destination has to wait for two time slots on each transmission phase before starting the decoding process. Unlike the methods proposed in [98, 104], it is worth noting that the proposed scheme's decoding delay is independent of the relays number.

5.5.2 Diversity gain Analysis

According to Definition 2.6, the diversity gain that a network can achieve is determined by the SNR of the ML estimate. For the proposed scheme (see (5.22), it can be expressed as

$$\gamma = \frac{2CP_1\rho^2}{2\sigma_\eta^2 + \frac{2\sigma_{\mathbf{v}}^2\rho^2 C}{(\sum_{n=1}^{N}|h_n|^2)}}. \tag{5.23}$$

According to [105] and given that the SNR between the relays and destination is high, the following relationship holds

$$2\sigma_\eta^2 + \frac{2\sigma_{\mathbf{v}}^2\rho^2 C}{\left(\sum_{n=1}^{N}|h_n|^2\right)} = \frac{2\sigma_{\mathbf{v}}^2\rho^2 C}{\left(\sum_{n=1}^{N}|h_n|^2\right)}, \tag{5.24}$$

Thus, the SNR in (5.23) is approximated as

$$\gamma = \gamma_0 \sum_{n=1}^{N} |h_n|^2, \tag{5.25}$$

where $\gamma_0 = P_1/\sigma_{\mathbf{v}}^2$ is the nominal SNR in the network.

From (5.25), it can be concluded that the maximum diversity gain can be achieved is bounded by $d = N$. This is as the total SNR is affected by N channel coefficients. To determine the achieved diversity gain, the average error probability ($\mathbb{P}$) should be determined. Generally, it is defined as

$$\mathbb{P}(\gamma, u_0) = \mathrm{E}_{\mathbf{h},\mathbf{g}}\left(Q\left(\sqrt{u_0\gamma}\right)\right), \tag{5.26}$$

where $\mathbf{h} = [h_1, h_2, \ldots, h_N]^T$, $\mathbf{g} = vec(\mathbf{G})$ and u_0 is a constant scalar that depends on the used modulation constellation.

Using the Craig formula for the Q-function [106], the $\mathbb{P}(\gamma, u_0)$ of (5.26) can be rewritten as

$$\mathbb{P}(\gamma, u_0|\mathbf{h}) = \frac{1}{\pi}\int_0^{\frac{\pi}{2}} \exp\left(-\frac{u_0\gamma}{2sin^2\theta}\right) d\theta. \tag{5.27}$$

Using Lemma 1 of [106], the averaging over $\mathbf{h}$ gives that

$$\begin{aligned}\mathbb{P}(\gamma, u_0) =& \frac{1}{\pi}\int_0^{\frac{\pi}{2}} \prod_{n=1}^{N} \frac{1}{1+\frac{u_0\gamma_0}{2\sin^2\theta}} d\theta \\ \backsimeq& \frac{1}{\pi}\int_0^{\frac{\pi}{2}} \frac{1}{\left(\frac{u_0\gamma_0}{2\sin^2\theta}\right)^N} d\theta \backsimeq b.\gamma_0^{-N}\end{aligned} \tag{5.28}$$

From (5.28), it can be concluded that the space-diversity gain of the network (d) is N. Thus, the network is said to achieve the full-space diversity gain as $d = \min(1 \times N, N \times 2)) = N$ (see Definition 2.7).

5.6 Simulation Results and Discussion

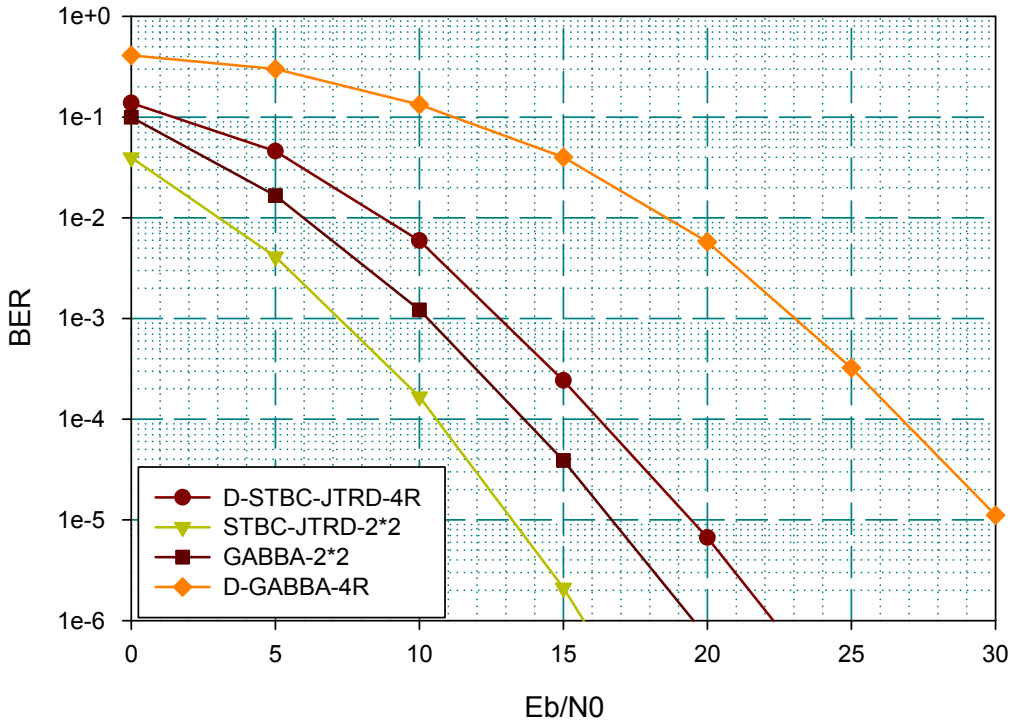

Fig. 5.2: BER of GABBA and STBC-JTRD (P2P and Distributed AF network)

In this section, the performance results of the proposed scheme (D-STBC-JTRD) for different number of relays N are presented. Specifically, the spatial diversity gain is investigated by utilising 2, 3, 5 and 6 relays. This is to illustrate the increase in diversity gain. The

QPSK modulation was used and the performance is reported in terms of BER. A slow and non-selective frequency Rayleigh fading channel was used, which resulted in a fixed fading coefficient over a fixed number of $J = L = T = 2$. From the shown figures, it can be observed that higher space-diversity gains were achieved. This is while retaining a fixed full-rate and single-symbol decoding complexity.

In Fig. 5.2, the BER of the proposed scheme is compared to the D-GABBA scheme of [102], where four relays are utilised ($N = 4$). Also, this figure includes the performance of the MIMO P2P version of 2×2 GABBA and 2×2 STBC-JTRD. This to show the performance degradation due to adapting to a distributed AF network [93, 94, 103]. Like the proposed code, the D-GABBA code is chosen here as it offers full-rate for an arbitrary number of relays. From Fig. 5.2, it is observed that both the proposed code and the existing D-GABBA code achieves the full-space diversity gain ($d = \min(1 \times 4, 4 \times 2) = 4$). However, the proposed code shows better performance and less performance degradation due to the adaptation for WRNs. In addition and unlike the D-GABBA code, there is no need to adjust the coding scheme which reduces the network overhead [102].

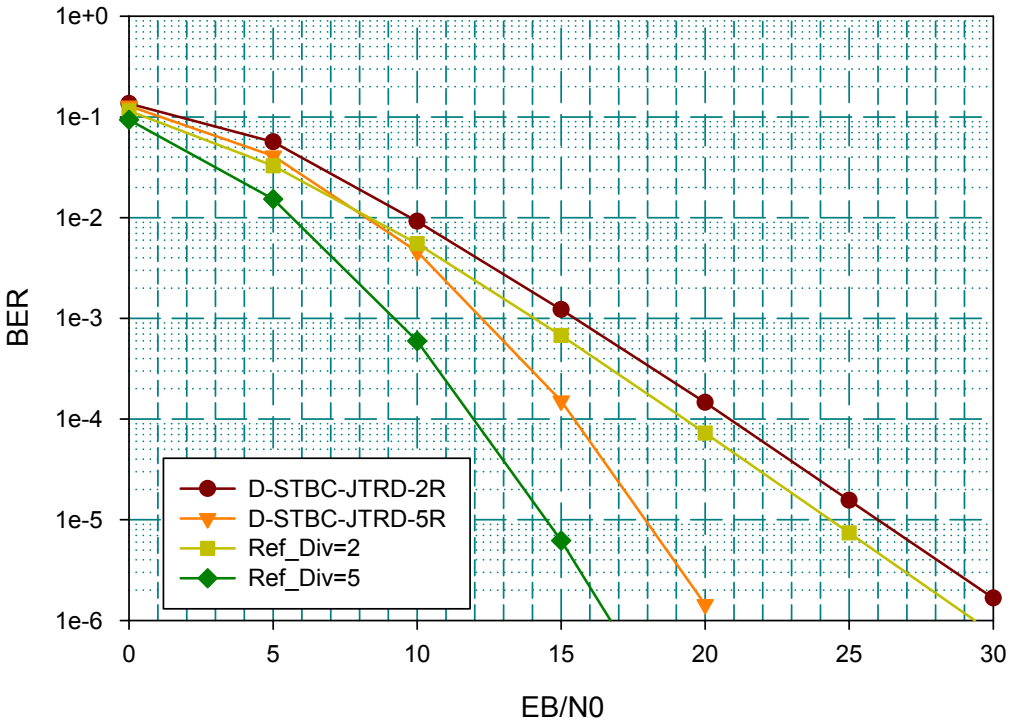

Fig. 5.3: BER of $1 \times 2 \times 2$ and $1 \times 5 \times 2$ D-STBC-JTRD scheme

Fig. 5.3 shows the space-diversity gain that can be achieved by the proposed scheme (D-STBC-JTRD), when two and four relays are utilized. For comparison purposes, the diversity gain reference curves of $d = 2$ and $d = 5$ are included. As discussed in Section 5.4, it is shown

that full-space diversity gain is achieved as the BER curve approximates the reference curves in high SNR values range.

Similarly, the BER in the cases of three and six relays are simulated in Fig. 5.4 to show the diversity gain achieved when more relays are available for utilization.

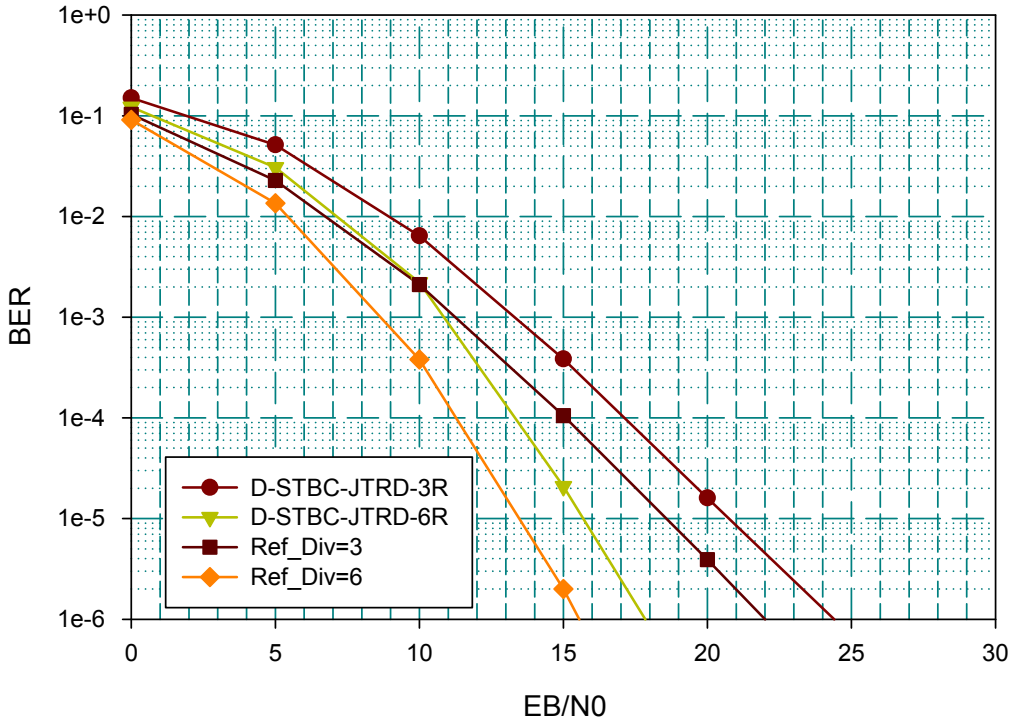

Fig. 5.4: BER of $1 \times 3 \times 2$ and $1 \times 6 \times 2$ D-STBC-JTRD scheme

5.7 Conclusion

As mentioned, it is known that the diversity gain is further improved when the number of relays is increased. However, in most existing code design, there is a trade-off between a decrease in the code rate and the need to retain the single-symbol decoding complexity at the receiver when more relays are utilised. This chapter proposed the D-STBC-JTRD scheme which has the ability to accommodate an arbitrary number of relays. This is while maintaining both the full-rate transmission and the single-symbol decoding complexity. Unlike most existing D-STBCs, the offered code rate is independent of the number of relays and hence there is no code rate loss as the number of relays increases. In addition, this scheme uses the same encoding matrices at every relay. Thus, it eliminates the need for additional network overhead to coordinate the code generation by the relays. This means that there is no need to interrupt the transmission if a relay has been down/up. These

mentioned features have value in many communication applications, particularly where the communications system is varying rapidly (sometimes 2 relays and sometimes 6 relays...etc.) due to busy or on call status (or other reasons).

6 D-STBC-SM scheme for DF WRNs

> *Intelligence without ambition is a bird without wings.*
>
> **— Salvador Dali**
> (Spanish artist)

6.1 Introduction

As mentioned in Chapter 5, a major challenge in a WRN is to coordinate an arbitrary number of relay transmissions while maintaining full diversity gain and offering high rates with low decoding complexity at the destination. Using a combination of STBC and spatial modulation (SM), it is expected that high throughput and high transmit diversity gain is possible. In general such combinations are achieved using MIMO systems. This allows the construction of a fixed STBC-SM code as the number of antennas at the transmitter is fixed [107–111]. Moreover, these designs are bounded by a transmit-diversity gain of two. To the best of the author's knowledge, there is no existing research addressing distributed STBC-SM (D-STBC-SM). With respect to the current literature, this chapter presents:

- An adaptive transmission protocol for DF WRNs proposed to accommodate an arbitrary number of relays. Unlike [107–111], this protocol offers a transmit-diversity gain of N^0 ($N \geq N^0 \geq 1$) because of the possibility of activating an N^0 number of relays simultaneously. Given some control information, the protocol can be adapted easily to transmit through any given number of relays (N^0). This means it can work with a varying number of N^0, which is a desirable feature for networks that experience imperfect time synchronisation [36, 37].

- An algorithm to construct D-STBC-SM codes. Unlike [96, 97, 100–102], this algorithm offers a rate that increases as the number of relays increases. Specifically, it can offer

a rate of $r_0 \log_2 M_2 + \frac{1}{T_2}\log_2 c$ bpcu instead of $r_0 \log_2 M_2$ bpcu, where $c = \left\lfloor \begin{pmatrix} N \\ N^0 \end{pmatrix} \right\rfloor_{2^p}$ is the number of possible relay combinations, r_0 is the code-rate of the used STBC, M_2 is the order of modulation that is used by the relays and $\lfloor . \rfloor$ represents the floor integer operator. A promising feature is that an increase in throughput is achieved using the same total average transmitting energy. This is as only N^0 of the N available participating relays are active at any given time. Moreover, the proposed algorithm uses multi-level optimization processes and hence the constructed code outperforms the few existing STBC-SM codes.

- An optimal and suboptimal reduced-complexity decoder provided for the proposed protocol. The orthogonal property of the used STBC allows a decoding complexity reduction to $\mathcal{O}(cn_s M_2)$ instead of $\mathcal{O}(cM_2^{n_s})$, where n_s is the number of symbols per information block of transmission. Using the sub-optimal decoder, this decoding-complexity can be further reduced to $\mathcal{O}(c + n_s M_2)$ with some performance penalty. This makes it suitable to acquire higher throughput.

- Theoretical analysis of diversity gain, coding gain and required decoding complexity of the proposed protocol. Also, these claims are backed up by numerical simulations.

This chapter is organised as follows: First, the network model is described. Then, the proposed transmission protocol is introduced and more details of designing the STBC-SM code are provided. This is followed by a theoretical analysis of performance and complexity. Last, empirical results to back up the claims are presented.

6.2 Prior Work

The overall interest in this field of research lies in the construction of a high-rate D-STBC that has the ability to utilize any arbitrary number of relays [33, 95]. It would appear that research has had limited success in designing high-rate codes while maintaining a single-symbol decodability at the destination. In [96], the authors proposed systematic construction steps of a row-monomial D-STBC with a code rate bounded by $2/(2+N)$, where N denotes the number of relays. In [97], a new code class called semi-orthogonal precoded distributed single-symbol decodable STBC (Semi-PD-SSD-STBCs) was proposed. It has the advantage of performing precoding on the information symbols, which in turn doubles the

achieved code rate. Although these codes were designed for an arbitrary number of relays, it may be preferable to use them only in WRNs with a few numbers of relays. This is because the code rate decreases dramatically as the number of relays increases. In [98], a coding scheme, with a code rate of $\frac{1}{4}$, was proposed to operate in WRNs of high number of relays. However, this scheme has a high decoding delay, as the required transmission time increases exponentially with the number of relays. In [99], an adjustable full-rate STBC matrix was designed, but it requires a feedback channel to adjust the code. This creates additional network overhead that inherently reduces the achieved diversity gain. In [100–102], the generalised ABBA code (GABBA) of [103] was adapted for AF WRNs to offer a full-rate while maintaining single-symbol decodability. However the resulting D-GABBA scheme has some constraints: (1) the number of symbols per block (T) should be expressible as a power of two, and (2) the number of available relays (N) should be smaller or equal to T ($N \leq T$). These constraints were resolved by utilising global knowledge of channel state information (CSI) of the entire WRN at the relays [112].

Spatial modulation (SM) was developed to improve the throughput of MIMO systems and was initially extended for WRNs in [113–115]. The intention was to add the spatial dimension to the modulated signal constellation; this allowed information to be transmitted not only using amplitude/phase modulation (APM) but also using the relay indices. This offers higher throughput due to multiplexing data via different relays [114, 116]. However, the overall achieved diversity gain was limited to the number of receive antennas, as only one relay was active for any given transmission. This was partially solved for WRNs by employing SM specifically at the source node and leaving the full diversity gain to be achieved between the relays and the destination [115, 117, 118]. In these research studies, the effective use of SM was still bounded by the number of antennas available at the source node. Due to size, cost and hardware limitations, the availability of multiple antenna may not be feasible in many systems [7]. In [119, 120], transmit-diversity gain can be achieved at the expense of orthogonal channel resources. In conclusion, existing research uses relays only either to offer high throughput using SM or to achieve transmit diversity gain using D-STBC in an WRN with an arbitrary number of relays and a source equipped with a single antenna.

6.3 Network Model

A WRN is comprised of a source $\mathbb{S}$, a $\hat{N}$ number of HD relays $R_1, \ldots, R_{\hat{N}}$ and a destination $\mathbb{D}$ (depicted in Fig. 6.1). Let the source and relays each be equipped with a single antenna

and the destination with $N_r, N_r \in \mathbb{N}^+$. This configuration is denoted by $\left(\hat{N}, N_r\right)$. The transmission through the network is conducted in two phases. In the first phase, the information is broadcast from the source to the relays. In the second phase, each relay decodes its received symbols which are then only encoded and transmitted to the destination if received correctly. The total transmission power for the entire network is denoted by P and is evenly divided between both phases. The channel through the network is assumed to be a quasi-static Rayleigh fading channel. The source is assumed to be completely blind, while perfect CSI is assumed only at the decoding nodes.

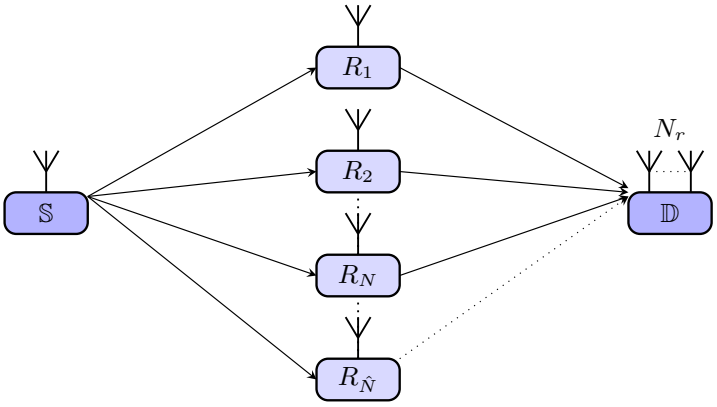

Fig. 6.1: Wireless relaying network model.

6.4 The Proposed Transmission Protocol

In this chapter, an adaptive protocol that uses an efficient combination of D-STBC and SM is proposed to obtain better cooperative diversity gain and higher overall throughput. This will be supported by a mathematical evaluation and an empirical comparison to existing protocols on BER graphs.

6.4.1 Protocol Description

For a network configuration of $\left(\hat{N}, N_r\right)$, the transmission through the network is conducted in two phases:

Broadcasting Phase: The source transmits M_1-ary PSK/QAM modulated symbols denoted by $\mathbf{s}(i) = [s(i,1), \ldots, s(i,J)]^T$, where i denotes the information block index and J is the number of symbols in the broadcasting phase. To maximise the number of participating

relays, the source ($\mathbb{S}$) uses an error control code (ECC) to mitigate all errors. This is as relays are only allowed to transmit if no error is present (see IEEE 802.16j standard). Thus, the received vector at R_n is

$$\underset{J\times 1}{\mathbf{r}_n(i)} = g_n \underset{J\times 1}{\mathbf{y}(i)} + \underset{J\times 1}{\mathbf{v}_n(i)}, \tag{6.1}$$

where g_n ($g_n \sim \mathcal{CN}(0,1)$) is the channel coefficient for the link between $\mathbb{S}$ and R_n. The vector $\mathbf{v}_n$ is the noise at R_n with entries $v_n \sim \mathcal{CN}(0, \sqrt{\frac{2}{P}})$.

Multiplexing and Relaying Phase: To match the proposed modifications, this phase's name is changed to 'multiplexing and relaying phase' rather than 'relaying phase'. As stated previously, a relay will not partake in this phase if it detects an error. To limit the discussion, it is assumed that a fixed number N out of $\hat{N}$ relays will always have no errors (see Section 2.6.1). The participating N relays will each conduct the following on its $K = J\log_2 M_1$ received bits (illustrated in Fig. 6.2):

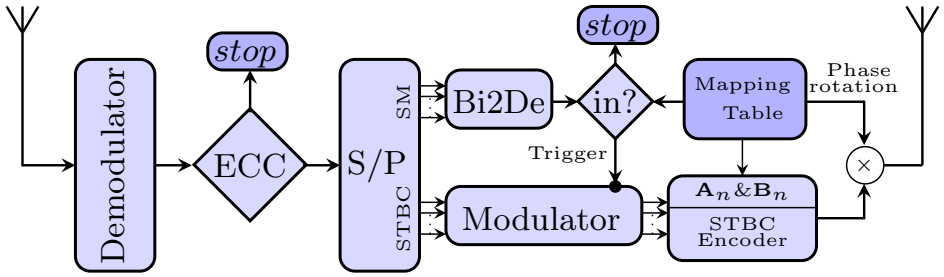

Fig. 6.2: Multiplexing and relaying phase for a given relay node.

1. The K decoded bits are divided into two groups. The first group contains K_1 bits and it is multiplexed to determine the relays that will be used to transmit the second group of K_2 bits. These K_2 bits are modulated and then encoded with the D-STBC. If $K \neq K_1 + K_2$, the excess bits must be buffered. The values of K_1 and K_2 are chosen according to Section 6.4.2.

2. The binary sequence of the first group is converted to a decimal value ℓ. This value is used to determine if the relay is allowed to transmit and what it should transmit. The second group of K_2 bits is modulated to a symbol vector $\mathbf{y}_2(i) = [\mathbf{y}_2(1,i), \ldots, \mathbf{y}_2(n_s,i)]^T$ using a two-tier star M_2-ary QAM modulator (see Section 6.4.2).

3. Given ℓ, the relay R_n encodes its second group of K_2 bits with a column of the D-STBC. The column index is obtained from the entries given in the code-mapping table. This encoding process is expressed as

$$\underset{L\times 1}{\mathbf{t}_n(i)} = \underset{L\times n_s}{\mathbf{A}_{n_\ell}}\ \underset{n_s\times 1}{\mathbf{y}_2(i)} + \underset{L\times n_s}{\mathbf{B}_{n_\ell}}\ \underset{n_s\times 1}{\mathbf{y}_2^*(i)}, \tag{6.2}$$

where $L = n_s/r_0$ and r_0 is the code rate of the code used. n_ℓ is the logic index used to identify the encoding matrices that should be used at relay R_n. Both $\mathbf{A}_{n_\ell}$ and $\mathbf{B}_{n_\ell}$ are the encoding matrices responsible for generating the column n_ℓ of the D-STBC matrix. All of $\mathbf{A}_{n_\ell}$ and $\mathbf{B}_{n_\ell}$ ($n_\ell = 1 \dots N^0$) are characterized the D-STBC matrix and are used to construct the code in a distributive manner (see Section (2.7.2)) [7, 10]. It is worth noting that many existing D-STBC matrix can be used, given the number of relays and the extent of the diversity gain required (N^0). This will be discussed in detail in Section 6.4.2.

4. The vector $\mathbf{t}_n(i)$ is then phase-rotated. This results in the transmitted vector given as $\mathbf{t}_n^\theta(i) = \exp(j\theta_i)\mathbf{t}_n(i)$, where θ_i, $\theta_i \in [0, \pi]$ are provided by the code-mapping table.

Accordingly, the received symbol matrix at destination $\mathbb{D}$ is given by

$$\underset{L\times N_r}{\mathbf{Z}(i)} = \sum_{n=1}^{N^0} \underset{L\times 1}{\mathbf{t}_n^\theta(i)}\ \underset{1\times N_r}{\mathbf{h}_n} + \underset{L\times N_r}{\boldsymbol{\eta}(i)}, \tag{6.3}$$

where $\mathbf{h}_n = [h_{n,1}, \dots, h_{n,N_r}]^T$ is the channel coefficient vector from the relay R_n to the destination with entries $h_{n,j} \sim \mathcal{CN}(0,1)$. The matrix $\boldsymbol{\eta}$ is the noise at the destination with entries $\eta_{ij} \sim \mathcal{CN}(0, \sqrt{\frac{2}{P}})$.

The received signal matrix of (6.3) can be rewritten using (6.2) as

$$\mathbf{z}(i) = \boldsymbol{\mathcal{H}}_\ell \mathbf{y}_2(i) + \boldsymbol{\eta}(i), \tag{6.4}$$

where $\boldsymbol{\mathcal{H}}_\ell$ is the equivalent channel matrix that encapsulates both the rotation employed and the channel coefficients of the relay set ℓ used for transmission.

6.4.2 D-STBC-SM System Design and Optimization

Review of Conventional STBC-SM

Recently, the design of STBC-SM codes has drawn research attention because of the promising improvements shown [107–111]. In this section, some basics and definitions of STBC-SM that are needed to work for D-STBC-SM are shown.

Definition 6.1. *Let $\boldsymbol{X}$ denote the STBC matrix (see Definition 2.8) and the STBC-SM code word denoted by $\boldsymbol{X}_{i,j}$ [107]. An STBC-SM codebook $\mathcal{X}_d$ is defined as a set of $n_{\boldsymbol{X}}$ STBC-SM code words. The STBC-SM code $\mathcal{X}$ is, thus, formally defined as a set of $n_{\mathcal{X}}$ codebooks.* ■

Definition 6.2. *Let $\mathcal{X}$ be an STBC-SM code with $n_{\mathcal{X}}$ codebooks and each has $n_{\boldsymbol{X}}$ code words. The minimum coding gain distance (CGD) is defined by*

$$\alpha(\mathcal{X}) = \min_{i,j} \gamma_{\min}(\mathcal{X}_i, \mathcal{X}_j), \tag{6.5}$$

where $i, j = 1 \ldots n_{\mathcal{X}}$ and $\gamma_{\min}(\mathcal{X}_i, \mathcal{X}_j)$ is the minimum CGD between two codebooks given by

$$\gamma_{\min}(\mathcal{X}_i, \mathcal{X}_j) = \min_{k,l} \boldsymbol{H}_{\lambda}(\boldsymbol{X}_{ik}, \hat{\boldsymbol{X}}_{jl} | i \neq j \& k \neq l). \tag{6.6}$$

The variables $l, k = 1 \ldots n_{\boldsymbol{X}}$, $\boldsymbol{H}_{\lambda}(\boldsymbol{X}_{ik}, \hat{\boldsymbol{X}}_{jl})$ are the harmonic mean of the non-zero eigenvalues of $\boldsymbol{A}(\boldsymbol{X}_{ik}, \hat{\boldsymbol{X}}_{jl}) = \Delta(\boldsymbol{X}_{ik}, \hat{\boldsymbol{X}}_{jl}) \Delta^H(\boldsymbol{X}_{ik}, \hat{\boldsymbol{X}}_{jl})$, and $\Delta(\boldsymbol{X}, \hat{\boldsymbol{X}}) = \boldsymbol{X} - \hat{\boldsymbol{X}}$. ■

The STBC-SM code exploits the properties of SM by distributing the STBC code word over a subset of the number of antennas at the transmitter. The number of antennas at the transmitter is fixed. This allows the construction only of a fixed STBC-SM code. For example, code words of an STBC-SM code ($\mathcal{X}$) proposed in [107] based on the Alamouti's STBC for a 4×1 MIMO system are expressed as

$$\mathcal{X}_1 = \{\mathbf{X}_{11}, \mathbf{X}_{12}\} = \left\{ \begin{pmatrix} \mathbf{y}(1) & \mathbf{y}(2) & 0 & 0 \\ -\mathbf{y}^*(2) & \mathbf{y}^*(1) & 0 & 0 \end{pmatrix}, \begin{pmatrix} 0 & 0 & \mathbf{y}(1) & \mathbf{y}(2) \\ 0 & 0 & -\mathbf{y}^*(2) & \mathbf{y}^*(1) \end{pmatrix} \right\} \tag{6.7}$$

$$\mathcal{X}_2 = \{\mathbf{X}_{21}, \mathbf{X}_{22}\} = \left\{ \begin{pmatrix} 0 & \mathbf{y}(1) & \mathbf{y}(2) & 0 \\ 0 & -\mathbf{y}^*(2) & \mathbf{y}^*(1) & 0 \end{pmatrix}, \begin{pmatrix} \mathbf{y}(2) & 0 & 0 & \mathbf{y}(1) \\ \mathbf{y}^*(1) & 0 & 0 & -\mathbf{y}^*(2) \end{pmatrix} \right\} e^{j\theta}. \tag{6.8}$$

In this STBC-SM design, the first two bits are used to decide on selecting the code word $\mathbf{X}_{ij}$. These bits define the set of antennas to transmit the remaining encoded bits ($\mathbf{y}(1)$ and $\mathbf{y}(2)$).

It should be noted that each code word $\mathbf{X}_{ij}$ uses a unique antenna mapping pattern. The phase rotation θ_i is set to avoid rank deficiency among codebooks to mitigate diversity gain loss. The designs of a more complex STBC-SM in a MIMO system have shown promising improvements and recently have started to attract attention [107–111].

D-STBC-SM Code Construction

In a conventional MIMO system, the number of antennas at both the receiver and transmitter is fixed. However, the number of transmitting antennas is determined by the number of available relays in WRNs. The number of relays can differ for each initiated transmission, a variation that equates to the need for a distributed STBC-SM (D-STBC-SM) code to operate over a distributed network. In this section, an algorithm is defined to construct D-STBC-SM codes to work in WRNs. Two examples of constructing a D-STBC-SM code for given WRNs are also provided.

The construction of an optimal D-STBC-SM code relies on the proper selection of a relays indices pattern that maximises the CGD. To reduce the search space for the optimised codebooks, the inner and mutual CGDs are formally defined:

Definition 6.3. *For a given $\mathcal{X}$, the inner CGD ($\varphi_{\min}(\mathcal{X})$) and the mutual CGD ($\delta_{\min}(\mathcal{X})$) are given by*

$$\varphi_{\min}(\mathcal{X}) = \min_{i} \gamma_{\min}(\mathcal{X}_i, \mathcal{X}_i) \tag{6.9}$$

and

$$\delta_{\min}(\mathcal{X}) = \min_{i,j} \gamma_{\min}(\mathcal{X}_i, \mathcal{X}_j) \forall\ i \neq j, \tag{6.10}$$

respectively.■

Another two important metrics in the construction of the code are how the relays patterns are chosen, namely the indexing distance and the Hamming distance. Both are used in the shown algorithm and are formally defined as

Definition 6.4. *Let $\{R_i\}$ and $\{R_j\}$, iand $j \in \mathbb{N}$, denote two sets of relays. Then, $\rho : \mathbb{N} \rightarrow |(\{R_i\} \cap \{R_j\})|$ defines the indexing distance. This computes the size of the intersection between these two sets.* ■

Definition 6.5. *Let $\{R_i\}$ and $\{R_j\}$, iand $j \in \mathbb{N}$, denote two sets of relays with similar cardinality. Then, $d_{min} : \mathbb{N} \rightarrow (\{R_i\}, \{R_j\})$ defines the Hamming distance between the two sets of relays.* ■

To maximise the BER performance, the proposed algorithm is designed to construct code words with minimal indexing distance ρ and maximum Hamming distance d_{min}. This design can operate on the common modulation schemes (see Section 2.4), but an additional improvement was observed using star QAM. The star QAM relies on two parameters that are also optimised in the algorithm as an additional step and, for completeness, are defined in Definition (2.5).

Now with the necessary definitions, the proposed algorithm can be described in detail in Algorithm 4. Two examples are provided to illustrate how the algorithm operates. The codes shown below follow step by step in its construction phase. The algorithm shown are offering a code rate of

$$r = r_0 \log_2 M_2 + \log_2 c, \tag{6.11}$$

where r and r_0 is the code rate offered of the constructed D-STBC-SM and the STBC used, respectively.

The offered overall rate increases as the number of relays increases. This can be seen while examining (6.11) for a number of participating relays as shown in Tab. 6.1.

N^0	r_0	N	c	r
2	1	3	2	$0.5 + \log_2 M_2$
		4	4	$1 + \log_2 M_2$
		5	8	$1.5 + \log_2 M_2$
3	$\frac{3}{4}$	4	4	$0.5 + \frac{3}{4}\log_2 M_2$
		5	8	$\frac{3}{4} + \frac{3}{4}\log_2 M_2$
		6	16	$1 + \frac{3}{4}\log_2 M_2$

Tab. 6.1: The offered code rate for a different number of relays

Example 6.1. *Let $N^0 = 2$ and $N = 4$, then the number of possible combinations is $c = 4$. A D-STBC-SM is constructed based on the proposed algorithm while using the Alamouti's STBC shown in Section (2.7.2). For illustration purposes, the optimisation process results are shown below. The STBC-SM proposed in [107] that was originally designed for a conventional MIMO*

Algorithm 4 D-STBC-SM Code Design Procedures.

1. In a WRN, a network protocol uses several metrics to determine which relays can participate in the communication to the destination. Let N denote the number of relays available to the WRN and let N^0 denote the number of relays assigned by the network protocol to transmit simultaneously ($N^0 < N$). The number N^0 is determined when the transmission flow is initiated by higher layer functions within the WRN. Based on network constraints (desired code rate, latency, etc.), select from the existing $L \times N^0$ MIMO STBC codes ($\mathcal{X}$), e.g. several are suggested in [7, 10].

2. Determine $K_1 = \log_2(c)$, where $c = \left\lfloor \binom{N}{N^0} \right\rfloor_{2^p}$ denotes the number of possible relay combinations for the transmission of the STBC code word and $p \in \mathbb{N}$.

3. Generate a list of all possible combinations of relays while avoiding inner and outer repetition [121–123].

4. Pick unique c combinations while
   - maximising $d_{\min}$,
   - minimising ρ,
   - and minimising $n_{\mathcal{X}}$.

5. Create a code-mapping table by reordering and labelling the c combinations to minimise the number of $n_{\mathcal{X}}$, e.g. see Tab. 6.2 and Tab. 6.3. Each row in the mapping table represents one code word of the new D-STBC-SM code.

6. As an optional step, the parameters $\{a, b\}$, and ϕ for a M_2-ary star-QAM modulation can be optimised, if this modulation is used, by

$$[a, \phi] = \underset{r_i \in (0,2), \phi \in [0, \frac{\pi}{4}]}{\operatorname{argmax}} \varphi_{\min}, \tag{6.12}$$

   where $\varphi_{\min}$ is defined in (6.9) and $b = \sqrt{2 - a^2}$.

7. Assuming $\theta_1 = 0$, optimise the set of phase rotation angles $\{\theta_i\}_{i=2}^{i=n_{\mathcal{X}}}$ that maximise $\delta_{\min}(\mathcal{X})$ expressed as $[\theta_2 \dots \theta_{n_{\mathcal{X}}}] = \operatorname{argmax}_{\theta_i \in [0,\pi]} \delta_{\min}$.

system can be used on this WRN, but Section 6.6 shows an improvement when using the proposed algorithm. The final constructed code-mapping table is given in Tab. 6.2.

	ℓ	R_1	R_2	R_3	R_4	θ
$\mathcal{X}_1$	0 (00)	1	2	0	0	0
	1 (01)	0	0	1	2	
$\mathcal{X}_2$	2 (10)	0	1	2	0	0.96
	3 (11)	2	0	0	1	
Star-QAM parameters :a = 0.8245 and ϕ = 0.7854.						

Tab. 6.2: The code-mapping table for Example 6.1.

***Optimisation process of Example 6.1 code**: The resulting figures of the optimization process of Example 6.1 code are shown here for illustration purposes. First, the parameters set $\{a, \phi\}$ for a M_2-ary star-QAM modulation is chosen to maximise the inner CGD for the given code. In Fig. 6.3, the inner CGD is shown over search ranges of a and ϕ. The values for the example was a = 0.65 and ϕ = 0.78 which provided a maximum inner CGD of 0.70. Another optimization*

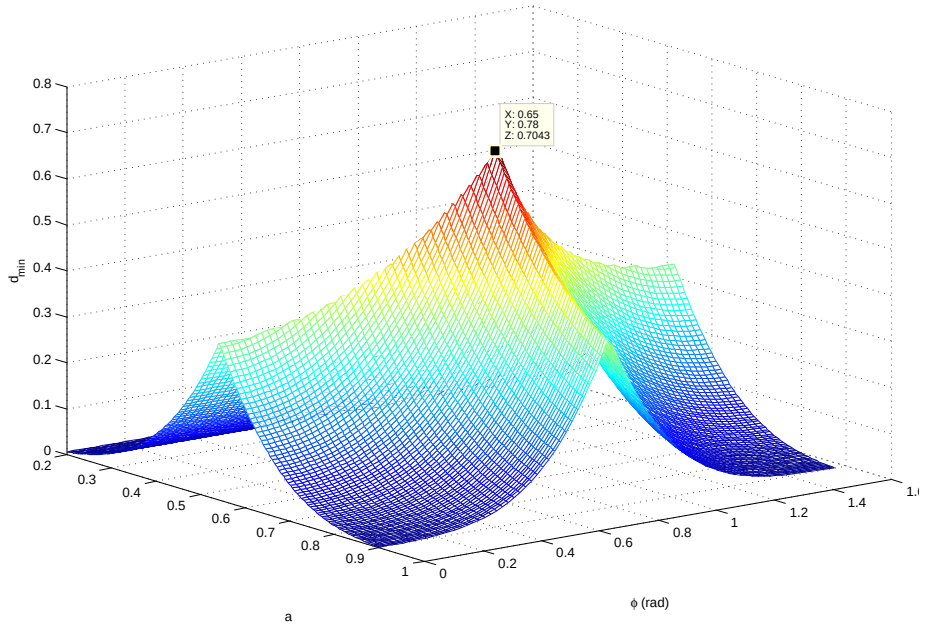

Fig. 6.3: The optimization of a and ϕ value of the Example 6.1 network.

which is crucial is to determine the correct phase rotation θ_i for each codebook. This is to avoid rank deficiency among codebooks to mitigate diversity gain loss. This is accomplished by choosing the set $\{\theta_i\}$ to maximise the mutual CGD. In Fig. 6.4, the mutual CGD is shown for Example 6.1 for the search range of θ. ■

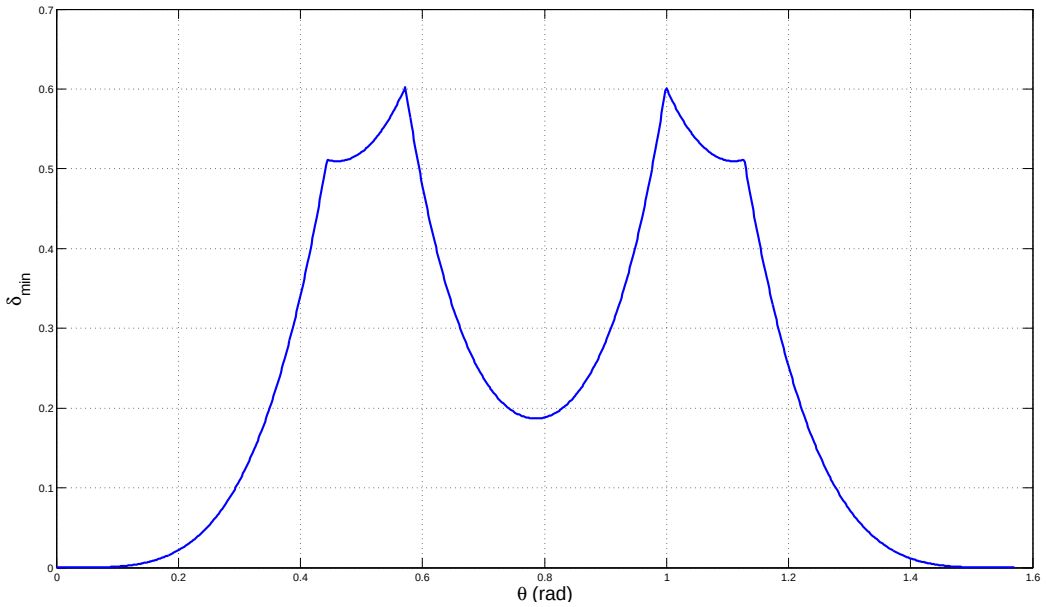

Fig. 6.4: The optimization of θ values for the Example 6.1 network.

Example 6.2. *Let $N^0 = 3$ and $N = 6$, then the number of possible combinations is $c = 8$. A D-STBC-SM is constructed using the STBC (with code rate $\frac{3}{4}$) of Section (2.7.2). The constructed code-mapping table is given in Tab. 6.3. To avoid repetition, the illustration of optimization*

	ℓ	R_1	R_2	R_3	R_4	R_5	R_6	θ
$\mathcal{X}_1$	0 (000)	1	0	0	0	3	2	0
	1 (001)	0	3	2	1	0	0	
$\mathcal{X}_2$	2 (010)	0	1	0	0	2	3	0.6
	3 (011)	3	0	1	2	0	0	
$\mathcal{X}_3$	4 (100)	0	2	3	0	1	0	0.35
	5 (101)	2	0	0	3	0	1	
$\mathcal{X}_4$	6 (110)	0	2	1	0	3	0	1.1
	7 (111)	1	0	0	2	0	3	
Star-QAM parameters :$a = 0.75$ and $\phi = 0.393$.								

Tab. 6.3: The code-mapping table for Example 6.2.

process for this code is omitted. ■

6.4.3 Decoding Methods

The growing demand for more complex WRN transmissions requires more complex decoders at the receiving node. In this section, an optimal ML decoder for the transmission protocol is described, followed by proposing a reduced-complexity decoder. **Optimal ML Decoder**

The ML decoder considers an exhaustive search trying to estimate the transmitted data. This is expressed as

$$\left[\hat{\ell}, \hat{\mathbf{y}}_2\right] = \underset{\ell \in \{0,\ldots c-1\}, \mathbf{y}_2 \in \mathcal{S}_2^{n_s}}{\operatorname{argmin}} \|\mathbf{z} - \boldsymbol{\mathcal{H}}_\ell \mathbf{y}_2\|^2, \tag{6.13}$$

where $\mathcal{S}_2$ is the M_2-ary star-QAM modulation used by the relays.

This equates to searching over all $cM_2^{n_s}$ permutations. Assuming an orthogonal STBC (OSTBC) is used, the received matrix can be decomposed into

$$\hat{\mathbf{y}}_2^\ell(m) = \underset{y_2 \in \mathcal{S}_2}{\operatorname{argmin}} \|\mathbf{u}(m) - \beta y_2\|^2, \forall m = 1, \ldots, n_S, \tag{6.14}$$

and

$$\hat{\ell} = \underset{\ell}{\operatorname{argmin}} \left\{ \sum_{m=1}^{n_s} \left(\min_{y_2 \in \mathcal{S}_2} \|\mathbf{u}(m) - \beta y_2\|^2 \right) \right\}, \tag{6.15}$$

where $\mathbf{u} = [\mathbf{u}(1), \mathbf{u}(2), \ldots, \mathbf{u}(n_S)]^T = \boldsymbol{\mathcal{H}}_\ell^H \mathbf{y}_d$ and $\boldsymbol{\mathcal{H}}_\ell^H \boldsymbol{\mathcal{H}}_\ell = \beta \mathbf{I}_{n_s}$.

This simplification based on the orthogonality property reduces the complexity of the decoder from $cM_2^{n_S}$ to $n_s cM_2$.

Proposed Reduced-Complexity (RC) Decoder

A further reduction in decoding-complexity can be made using two sequential steps, with an accepted loss in BER performance. The first step determines the set of relays used in the relaying phase. This is accomplished by using a projection matrix $\mathbf{P}_\ell$ with condition that $\mathbf{P}_\ell \boldsymbol{\mathcal{H}}_\ell = 0$. This projection matrix maps the received vector $\mathbf{y}_d$ to an orthogonal subspace $\boldsymbol{\mathcal{H}}_{\hat{\ell}} = \left[\begin{array}{cccc} \boldsymbol{\mathcal{H}}_1 \ldots & \boldsymbol{\mathcal{H}}_{\ell-1} & \boldsymbol{\mathcal{H}}_{\ell+1} & \ldots \boldsymbol{\mathcal{H}}_c \end{array} \right]$. The projection matrix is computed as

$$\mathbf{P}_\ell = \mathbf{I} - \boldsymbol{\mathcal{H}}_{\hat{\ell}} \left(\left(\boldsymbol{\mathcal{H}}_{\hat{\ell}}\right)^H \boldsymbol{\mathcal{H}}_{\hat{\ell}} \right)^{-1} \left(\boldsymbol{\mathcal{H}}_{\hat{\ell}}\right)^H. \tag{6.16}$$

This matrix projects the received vector $\mathbf{y}_d$ to the space of $\boldsymbol{\mathcal{H}}_\ell$, which results in a product of zero for the correct set of relays if $N_r \geq N^0$ and has no channel impairments. However, in the presence of channel impairments, the projection of the received vector $\mathbf{z}$ is altered and the decoder decides on the set of relays by

$$\hat{\ell} = \underset{\ell}{\operatorname{argmin}} \|\mathbf{P}_\ell \mathbf{z}\|^2. \tag{6.17}$$

The second step of this decoder is conducted using a traditional OSTBC decoder which computes [10]

$$\hat{\mathbf{y}}_2(m) = \underset{y \in \mathcal{S}_2^{1\times 1}}{\operatorname{argmin}} \|\mathbf{u}(m) - \beta y\|^2, \tag{6.18}$$

where $\mathbf{u} = \boldsymbol{\mathcal{H}}_{\hat{\ell}}^H \mathbf{z}$, and $\boldsymbol{\mathcal{H}}_{\hat{\ell}}^H \boldsymbol{\mathcal{H}}_\ell = \beta \mathbf{I}_{n_s}$ and $\mathbf{I}_{n_s}$ is $n_s \times n_s$ identity matrix.

Thus, it can be observed that the number of all possible combinations for an ML search diminishes from cn_sM_2 to $(c + n_sM_2)$.

6.5 Performance Analysis

In this section, the proposed transmission protocol is evaluated theoretically in term of diversity gain, coding gain and the decoding complexity.

6.5.1 Diversity gain Analysis

The diversity gain of a DF WRN is determined by the broadcasting or relaying phase that offers the lowest diversity gain individually (see Definition 2.7). The scope of this work is focused on the diversity gain in the relaying phase. This section shows analysis of the diversity gain in the case of the optimal ML decoder and then in the case of the RC decoder.

ML decoder Diversity analysis

It will be shown below that if the diversity gain of an STBC code is $N^0 \times N_r$, then the D-STBC-SM constructed using on Algorithm 4 based on this STBC will also have a diversity gain of $N^0 \times N_r$, if the ML decoder of Section 6.4.3 is used at the destination.

According to Definition 2.6, a wireless communication system achieves a space-diversity gain of d if the average error probability $\mathbb{P}$ is upper bounded in the high SNR range by $\mathbb{P} \leq \alpha\gamma^{-d}$, where $\alpha \in \mathbb{R}^+$ and it is independent of γ. γ is the SNR. Assuming that a code word $\mathbf{X}$ is transmitted through the relays, then (6.4) is equivalently written for a single-antenna receiver as

$$\mathbf{z} = \mathbf{X}\mathbf{h} + \boldsymbol{\eta}, \tag{6.19}$$

where $\mathbf{h}$ is the relays-destination channel vector. Thus, the conditional pairwise error probability (PEP) of the WRN (see Section 6.3) can be computed as [26]

$$\mathbb{P}(\mathbf{X} \to \hat{\mathbf{X}}|\mathbf{h}) = Q\left(\sqrt{\frac{\gamma\|\Delta\mathbf{X}\mathbf{h}\|^2}{2}}\right), \tag{6.20}$$

where $Q(x) = \int_x^\infty e^{-y^2/2}\mathrm{d}y$. The error matrix is denoted by $\Delta\mathbf{X} = \mathbf{X} - \hat{\mathbf{X}}$.

Equation (6.20) can be expanded as

$$\mathbb{P}(\mathbf{X} \to \hat{\mathbf{X}}|\mathbf{h}) = Q\left(\sqrt{\frac{\gamma\left\|\tilde{\mathbf{h}}^H\Lambda\tilde{\mathbf{h}}\right\|^2}{2}}\right), \tag{6.21}$$

where $\Lambda = \mathrm{diag}(\lambda_1^2, \ldots, \lambda_N^2)$ and λ_n denotes the singular values of $\Delta\mathbf{X}$. $\mathbf{V}$ is a unitary matrix and $\tilde{\mathbf{h}} = \mathbf{V}\mathbf{h}$. It is worth noting that there is no rank deficiency in Λ due to using of the phase rotation(see Appendix 6.8.1).

Equation (6.21) can be simplified and bounded as

$$\begin{aligned}\mathbb{P}(\mathbf{X} \to \hat{\mathbf{X}}) =& \mathbb{E}_{\mathbf{h}}\left(Q\left(\sqrt{\frac{\gamma\sum_{i=1}^{N^0}\lambda_i^2\left\|\tilde{\mathbf{h}}(i)\right\|^2}{2}}\right)\right)\\ \leq& \mathbb{E}_{\mathbf{h}}\left(\exp\left(\sqrt{\frac{\gamma\sum_{i=1}^{N^0}\lambda_i^2\left\|\tilde{\mathbf{h}}(i)\right\|^2}{4}}\right)\right).\end{aligned}$$

Given that the former code construction steps are followed, the rank of N^0 is preserved (see Appendix 6.8.1). Thus, according Lemma 1 of [106], the unconditional PEP is determined by

$$\mathbb{P}(\mathbf{X} \to \hat{\mathbf{X}}) \leq \prod_{n=1}^{N^0}\frac{1}{1+\gamma\frac{\lambda_n^2}{4}}, \tag{6.22}$$

which can be approximated for high SNR values as

$$\mathbb{P}(\mathbf{X} \to \hat{\mathbf{X}}) \lesssim \left(\frac{4}{\gamma}\right)^{N^0} \frac{1}{\prod_{n=1}^{N^0} \lambda_n^2}. \tag{6.23}$$

This concludes that a transmit diversity gain of N^0 is achieved. As the equivalent channel matrix is a concatenation of the equivalent channel matrices of each receive antenna, it suffices to check the diversity gain for only one receiver antenna. This results in a diversity gain of $N^0 \times N_r$ for a code employed with an N_r-antennas destination.

Diversity analysis of RC decoder

It was shown that the designed D-STBC-SM code achieves the full diversity gain if the ML decoder is used. However, the RC decoder of Section 6.4.3 has limited diversity gain encapsulated in (6.17). It is limited by the relays combination detection step, which has an error probability $\mathbb{P}_c$ of

$$\begin{aligned}
\mathbb{P}_{c|\mathbf{H}} &= 1 - \mathbb{P}(\nu_\ell > \nu_{\hat{\ell}_1}, \ldots, \nu_\ell > \nu_{\hat{\ell}_{c-1}} | \ell, \mathbf{H}) \\
&= 1 - \mathbb{P}(\nu_\ell - \nu_{\hat{\ell}_1} = 0 | \ell, \mathbf{H})^{c-1} \\
&= 1 - \left(\int_0^\infty f_{\nu_\ell - \nu_{\hat{\ell}_1}}(x) \mathrm{d}x \right)^{c-1} \qquad (6.24) \\
&= \left(Q\left(\frac{\mu_\ell - \mu_{\hat{\ell}_1}}{\sqrt{\sigma_\ell^2 + \sigma_{\hat{\ell}_1}^2}} \right) \right)^{c-1}. \qquad (6.25)
\end{aligned}$$

where with $\sigma_i^2 = \sigma_i^2 \left\| \mathbf{P}_\ell \right\|^2$, $\mu_i = \mathbf{P}_\ell \mathbf{H}$ and

$$f_{\nu_\ell - \nu_{\hat{\ell}_1}}(x) = \frac{1}{\sqrt{2\pi \left(\sigma_\ell^2 + \sigma_{\hat{\ell}_1}^2 \right)}} \exp\left(- \frac{\left(x - \mu_\ell - \mu_{\hat{\ell}_1} \right)^2}{2 \left(\sigma_\ell^2 + \sigma_{\hat{\ell}_1}^2 \right)} \right)$$

This holds assuming that $\nu_\ell = \|\mathbf{P}_\ell \mathbf{z}\|^2$ and information bits are independent and equiprobable.

By applying the Chernoff bound to (6.25), we can rewrite as

$$\mathbb{P}_{c|\mathbf{F}} \leq \frac{1}{2^{c-1}} \exp\left(- \frac{c-1}{2} \frac{\left\| \boldsymbol{\mathcal{H}}_\ell \right\|^2}{\sigma^2} \right). \tag{6.26}$$

Averaging over $\mathbf{H}$, the relay combination detection error can be determined as

$$\begin{aligned}\mathbb{P}_c &\leq \int_0^{\infty} \frac{1}{2^{c-1}} \exp\left(-\frac{c-1}{2}\frac{x}{\sigma^2}\right) f_{\|\boldsymbol{\mathcal{H}}_\ell\|^2}(x)\mathrm{dx} \\ &= \frac{1}{2^{c+N_r-1}\Gamma(N_r)} \int_0^{\infty} \exp\left(-\frac{(c+\sigma^2-1)x}{2\sigma^2}\right) x^{N_r-1}\mathrm{dx} \\ &\leq \left(\frac{\sigma^2}{\sigma^2+c-1}\right)^{N_r} \\ &\leq \left(\frac{1}{(c-1)\,\gamma}\right)^{N_r}. \end{aligned} \tag{6.27}$$

From (6.27), it can be concluded that the two-step decoder can achieve only the full-receive diversity gain N_r. Therefore, the complexity-reduction is at the expense of transmit diversity gain.

6.5.2 Coding Gain Analysis

The coding gain of the proposed D-STBC-SM code is improved by maximising the CGD. The inner and mutual CGD of the code designed in Example 6.1 is compared with the code of [107] under the assumption of using an 8-ary modulation.

STBC-SM of [107]		Proposed	
$d_{\min}(\mathcal{X})$	$\delta_{\min}(\mathcal{X})$	$d_{\min}(\mathcal{X})$	$\delta_{\min}(\mathcal{X})$
0.44	0.32	0.71	0.51

Tab. 6.4: CGD values of the proposed code and [107].

Thus, it can be observed that the proposed STBC-SM has a larger inner and mutual CGD than the code proposed in [107] and, hence better performance can be achieved.

6.5.3 Complexity Analysis

The complexity order is defined here as the number of iterations needed to find the optimal estimate for (6.4). The complexity order of the optimal ML decoder is $\mathcal{O}(cM_2^{n_s})$, where n_s is the number of symbols per code word and M_2 is the order of the modulation used. This order is reduced to $\mathcal{O}(cM_2n_s)$ when orthogonality of STBC used is preserved. This is as orthogonality allows linear decomposition of the symbols. In contrast, the complexity-order of the proposed RC decoder is further reduced to $\mathcal{O}(c+M_2n_s)$. This is because the set of

transmitting relays is firstly identified. A comparison of the complexity order is shown in Fig. 6.5 in term of the number of relays, for the configuration used in Example 6.1. The offered bits per channel use (bpcu) is also shown; this is determined by the number of relays and the modulation scheme. From Fig. 6.5, it is observed that the complexity of the RC decoder increases marginally with the number of relays when compared to the complexity of the optimal ML decoder. The advantage of using the RC decoder is that the throughput can be increased from 3 to 4.5 bpcu for a 4-ary modulation scheme without complexity increasing at a cost of minor loss in performance.

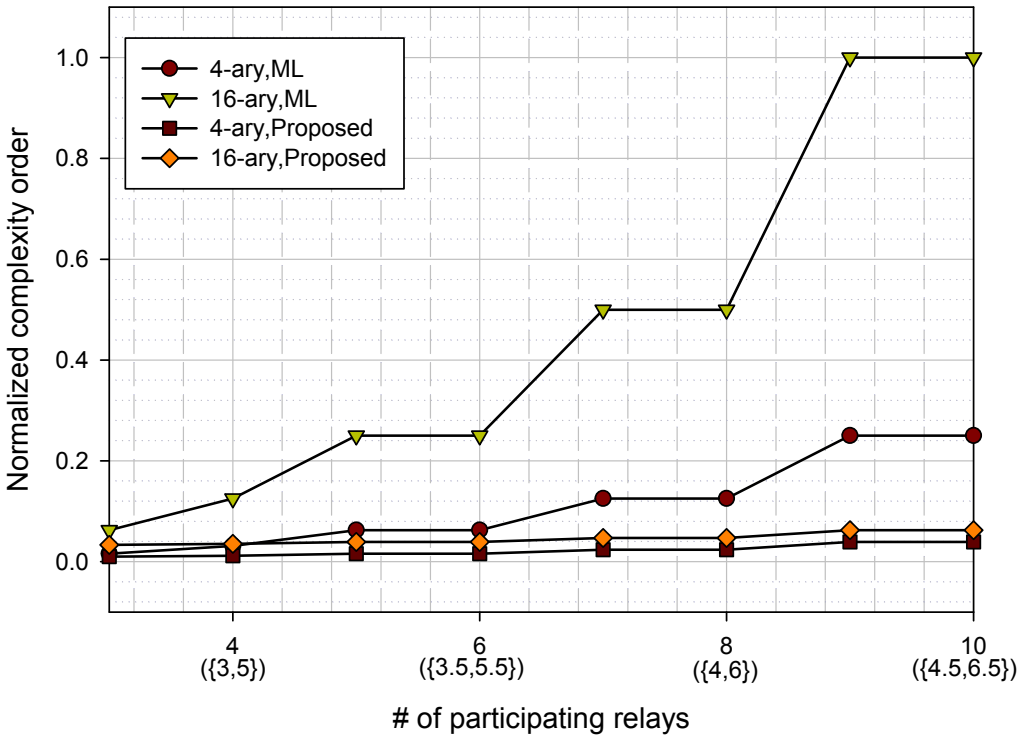

Fig. 6.5: Normalised complexity order versus the number of relays. Also, the offered bpcu is given in parentheses; the first value corresponds to an 8-ary case while the second value corresponds to a 16-ary case.

6.6 Simulation Results and Discussion

Numerical simulations are shown here in terms of BER to back up the theoretical claims of the proposed protocol. First, Example 6.1 and 6.2 networks are simulated and compared with a number of existing systems in Fig. 6.6 and Fig. 6.7, respectively. This is to show how the proposed protocol and the constructed codes outperform the existing systems. Tab. 6.5 and Tab. 6.6 summarise the simulation parameters used for the existing systems. This

section shows also a comparison of using the optimal ML decoder and the RC decoder for different network configurations (shown in Fig. 6.8). All simulations were conducted on a Rayleigh faded channel and it was assumed that the total transmission power is evenly distributed between the transmission phases. For comparison purposes, the shown figures include two slope diversity gain reference curves for cases of $(N \times N_r)$ and $(N^0 \times N_r)$.

Code	Network	Broadcast phase	Relaying phase
Alamouti's STBC [106, 124]	$(2^2, 4)$	J = 2(16-QAM)	n_S = 2(16-QAM)
$\frac{3}{4}$-OSTBC [10]	$(4^4, 4)$	J = 3(32-QAM)	n_S = 4(32-QAM)
ABBA code [102]	$(4^4, 4)$	J = 4(16-QAM)	n_S = 4(16-QAM)
SM of [113, 125]	$(4^1, 4)$	J = 1(16-QAM)	n_S = 1(4-QAM)
D-STBC-SM (Example 6.1)	$(4^2, 4)$	J = 2(16-QAM)	n_S = 2(8-*QAM)

Tab. 6.5: Simulation parameters used in Fig. 6.6

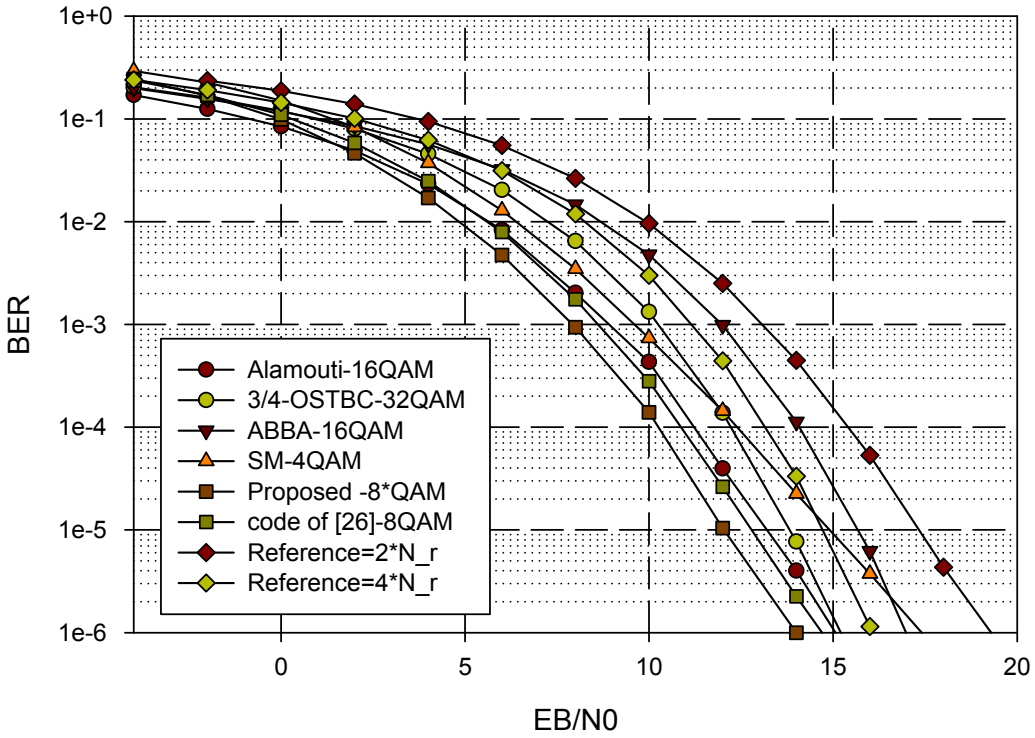

Fig. 6.6: BER performance result of Example 6.1 Network.

In Fig. 6.6, the proposed transmission protocol (using the code in Example 6.1 on a $(4^2, 4)$ network) is compared to the Alamouti's STBC, the $\frac{3}{4}$-OSTBC, the ABBA code and the traditional SM. The Alamouti's STBC is limited to only two relays and can achieve a transmit-diversity gain of two ($N^0 = 2$), while both the $\frac{3}{4}$-OSTBC and the ABBA code constantly utilise all four relays and achieve a transmit diversity gain of $N^0 = N = 4$. However, they lose the throughput that can be offered by SM. The traditional SM offers better throughput at the cost of not using an STBC, which results in a loss of transmit diversity gain and a coding gain. For a fair comparison in this experiment, no constraint was imposed on the modulation order used and that the resulting system was required to provide a bpcu of 2. With reference to Fig. 6.6, it is observed that the proposed protocol reports an improved BER performance. Specifically, it results in performance gains of 1.3 dB, 2.3 dB and 3.6 dB over networks employing Alamouti's STBC, $\frac{3}{4}$-OSTBC and ABBA code, respectively. In addition, a gain of 1 dB was achieved over the STBC-SM of [107] because of the unique selection of the c code words and the using of optimised star-QAM modulation. It should be noted that this STBC-SM code of [107] was originally designed for a conventional MIMO system and was extended here to operate on the WRN for the purpose of this comparison.

The proposed protocol was simulated in Fig. 6.7 for another network configuration of $(6^3, 4)$ to investigate the ability to achieve higher diversity gain and to offer higher throughput. It was compared to an ABBA system which offers a transmit diversity gain of $N^0 = N = 6$ by using all the available relays but without throughput improvement. A simulation of the traditional SM was included again to illustrate how the throughput can be maximised. It was observed that the proposed protocol had the lowest BER in this experiment with a diversity gain of $(N^0 = 3) \times (N_r = 4)$. It provides an SNR gain of 1.2 dB and 2.8 dB over networks employing the ABBA code and SM, respectively.

Code	Network	Broadcast phase	Relaying phase
SM of [113, 125]	$(6^1, 4)$	$J = 1$(16-QAM)	$n_S = 1$(4-QAM)
ABBA code [102]	$(6^6, 4)$	$J = 6$(16-QAM)	$n_S = 6$(16-QAM)
D-STBC-SM (Example 6.2)	$(6^3, 4)$	$J = 3$(32-QAM)	$n_S = 4$(16-*QAM)

Tab. 6.6: Simulation parameters used in Fig. 6.7

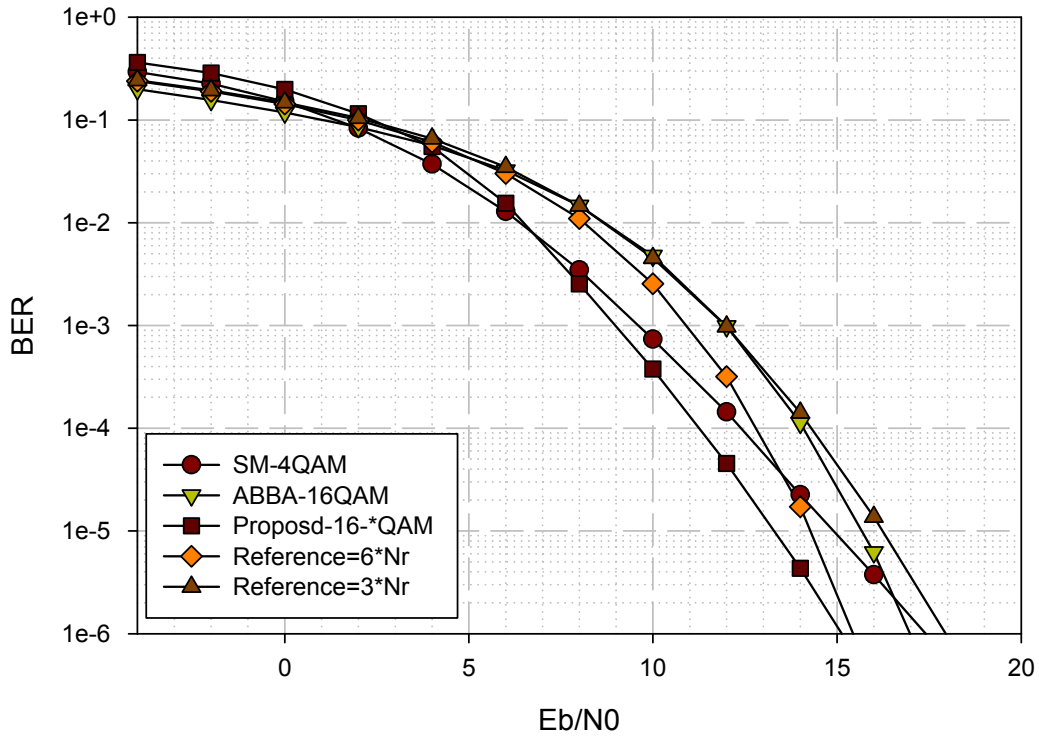

Fig. 6.7: BER performance result of Example 6.2 Network.

In the next experiment, the loss in performance in the case of using the RC decoder was investigated in Fig. 6.8. It was compared to the optimal ML decoder in WRNs of $(3^2, 4)$, $(5^2, 4)$ and $(8^2, 4)$. It should be noted that a reduction in complexity is ideal in certain applications when higher throughput is needed. In this experiment, it was observed that the optimal ML decoder achieved a diversity gain of $(2 \times N_r = 8)$, while the RC decoder had a reduced diversity gain of $N_r = 4$.

6.7 Conclusion

Motivated by the developments in spatial modulation, an adaptive transmission protocol was proposed for WRNs to exploit the potential space-diversity gain while obtaining higher spectral efficiency. Unlike the existing literature, this protocol can accommodate an arbitrary number of relays while improving the overall throughput and maintaining the same achieved space-diversity gain. In addition, an algorithm to generate D-STBC-SM codes to be used by this protocol was shown. The achieved performance of the resulting codes is better than that of many existing codes because the criteria are designed to choose the code words and to

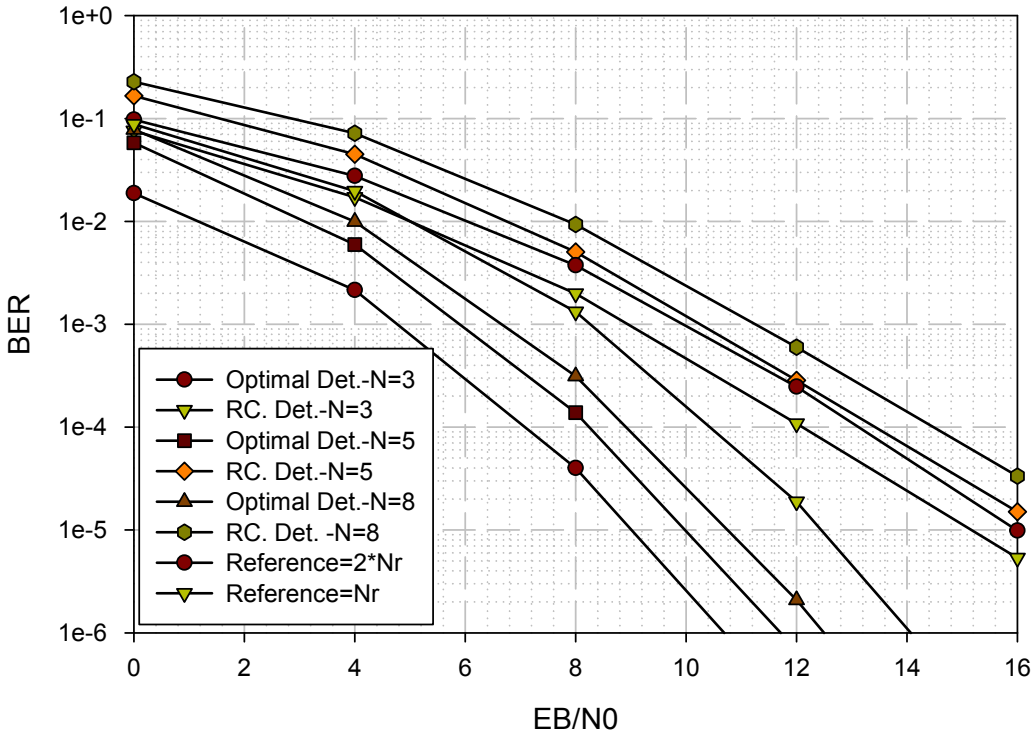

Fig. 6.8: BER of $(3, 5, 8) \times 4$ D-STBC-SM when the optimal ML and the RC decoder is used.

employ a multi-level optimization process. Also, a further reduced-complexity decoder is proposed. All of these claims are accompanied by numerical and theoretical evaluations.

6.8 Appendices

6.8.1 Rank of the constructed code

Following the steps of Algorithm 4, the constructed D-STBC-SM code based an STBC ($\mathcal{X}$), $\mathcal{X}$ is with rank of N^0, has the same rank of $\mathcal{X}$.

Proof: Let $\{\mathbf{X}\}$ denote the set of codewords for a codebook $\mathcal{X}_i$. The rank of the constructed code in Example 6.1, computed from $\mathbf{A}(X, \hat{X})$ of (6.6), is investigated to show that the maximum rate is preserved. There are two cases to consider, (1) when two codewords belong to the same codebook and (2) for the case of two different codebooks. In the first case, two codewords are present in the same codebook that used identical relays in its transmission. This results in

$$\mathbf{A}(\mathbf{X}, \hat{\mathbf{X}}) = \begin{bmatrix} \sum_{n=1}^{N^0} |x_{1n} - \hat{x}_{1n}|^2 & \sum_{n=1}^{N^0} (x_{1n} - \hat{x}_{1n})(x_{2n} - \hat{x}_{2n})^* & \dots & \sum_{n=1}^{N^0} (x_{1n} - \hat{x}_{1n})(x_{Ln} - \hat{x}_{Ln})^* \\ \sum_{n=1}^{N^0} (x_{2n} - \hat{x}_{2n})(x_{1n} - \hat{x}_{1n})^* & \sum_{n=1}^{N^0} |x_{2n} - \hat{x}_{2n}|^2 & \dots & \sum_{n=1}^{N^0} (x_{2n} - \hat{x}_{2n})(x_{Ln} - \hat{x}_{Ln})^* \\ \vdots & \vdots & \ddots & \vdots \\ \sum_{n=1}^{N^0} (x_{Ln} - \hat{x}_{Ln})(x_{1n} - \hat{x}_{1n})^* & \sum_{n=1}^{N^0} (x_{Ln} - \hat{x}_{Ln})(x_{2n} - \hat{x}_{2n})^* & \dots & \sum_{n=1}^{N^0} |x_{Ln} - \hat{x}_{Ln}|^2 \end{bmatrix}, \tag{6.28}$$

It can be noticed that $\mathbf{A}(\mathbf{X}, \hat{\mathbf{X}})$ of the constructed D-STBC-SM is equal to the original STBC used in the construction of the code. Therefore, it has a rank of N^0 if the used STBC has this rank.

In the second case, where two codewords belong to two different codebooks, the phase rotation between codebooks is used to mitigate rank deficiency among codebooks. The rank of N^0 is preserved even under the worst case among codewords combination possibilities. Without loss of generality, this concept is shown for Example 6.1 as

$$\mathbf{A}(\mathbf{X}, \hat{\mathbf{X}}) = \begin{bmatrix} |\mathbf{y}(1) - \hat{\mathbf{y}}(2)|^2 + |\mathbf{y}(2)|^2 + |\hat{\mathbf{y}}(1)|^2 & -(\mathbf{y}(1) - \hat{\mathbf{y}}(2))(\mathbf{y}(2) - \hat{\mathbf{y}}(1)) + \mathbf{y}(1)\mathbf{y}(2) - \hat{\mathbf{y}}(1)\hat{\mathbf{y}}(2) \\ -(\mathbf{y}(2) - \hat{\mathbf{y}}(1))^*(\mathbf{y}(1) - \hat{\mathbf{y}}(2))^* + \mathbf{y}^*(1)\mathbf{y}^*(2) - \hat{\mathbf{y}}^*(2)\hat{\mathbf{y}}^*(1) & -|\mathbf{y}(2) - \hat{\mathbf{y}}(1)|^2 + |\mathbf{y}(1)|^2 + |\hat{\mathbf{y}}(2)|^2 \end{bmatrix}. \tag{6.29}$$

It should be noted that if the phase θ is set to zero, then the code is rank deficient over several symbols, e.g. when $\{\mathbf{y}(1) = \hat{\mathbf{y}}(2), \mathbf{y}(2) = -\hat{\mathbf{y}}(1)\}$ and $\{\mathbf{y}(1) = \mathbf{y}(2) =$

$\hat{\mathbf{y}}(1) = -\hat{\mathbf{y}}(2)\}$. However, if θ is selected to mitigate this effect, then the rank is preserved. ■

Part III

Multi-user Interference in Wireless Relaying Networks

Part 3: Abstract

This part considers the multi-user interference of WRNs. Two transmission protocols with an interference cancellation scheme are proposed: the *concurrent*$_{S-R-D}$*-PIC*$_{R,D}$ protocol for DF WRNs and the *concurrent*$_{S-R-D}$*-PIC*$_{D}$ protocol for AF WRNs. Unlike existing protocols, these protocols allow the concurrent transmission in both phases of the transmission. Thus, high spectral efficiency is offered while maintaining low decoding complexity. This low decoding complexity is maintained due to the adaptation of the partial interference cancellation group decoding (PICGD) approach for WRNs, which was initially proposed by Guo, *et al.*, for point-to-point (P2P) communication link. For a WRN consisting of J users each equipped with J_a-antenna, a single half duplex (HD) R_a-antenna relay, and M-antenna destination, the *concurrent*$_{S-R-D}$*-PIC*$_{R,D}$ protocol achieves the *interference-free* diversity gain (i.e., $R_a \times \min\{J_a, M\}$) without imposing any conditions on a node's antenna number. The *interference-free* is the diversity gain achieved, assuming that each user in the network is transmitting solely without experiencing any interference from other users, hence it is considered as the natural natural upper bound of the diversity gain in multi-user WRNs. Similar to most exiting protocols, this protocol requires the CSI of the users-relay links at the relay. In contrast, the *concurrent*$_{S-R-D}$*-PIC*$_{R,D}$ protocol achieves a diversity gain of $J_a \times M$, given that $R_a > 8$, while the CSI is required only at the destination. Although the diversity's upper bound is not achieved, this protocol uses a simple relay as no CSI or encoding is required at the relay. In addition, and unlike the existing protocols, the achievable diversity gain is determined by both J_a and M and it is not sacrificed while J is increased. This part also establishes

sufficient conditions for an STBC to achieve the prior mentioned diversity gains, when the PICGD approach is employed by multi-users WRNs.

Part III: Publication List

Publications List

- El Astal, M.-T.; Ismail, A.; Alouini, M.-S. ; Olivier, J. C.: "Full-diversity partial interference cancellation for multi-user wireless relaying networks," in the **7th International Conference on Signal Processing and Communication Systems-ICSPCS 2013**, Gold coast, Australia, pp.1-6,16-18 Dec. 2013. URL: link.
- El Astal, M.-T.; Ismail, A.; Alouini, M.-S. ; Olivier, J. C.: "Low-Complexity and Full-Diversity Partial Interference Cancellation for Multi-User Wireless Relaying Networks," *re-submitted* in **IEEE Transactions on Vehicular Technology**.

7

Low-Complexity and Full-Diversity Partial Interference Cancellation for Multi-User WRNs

> *Man needs his difficulties because they are necessary to enjoy success.*
>
> **— A. P. J. Abdul Kalam**
> (Indian President)

7.1 Introduction

In the last decade, the demand for high capacity and reliable wireless communications networks has grown rapidly. This can be attributed mainly to the increasing need for high quality video streaming services via cellular networks. Compared with direct communications MIMO networks, relaying schemes are common for coverage extension purposes. These networks are referred to as WRNs where an intermediate node is used for relaying the information from the users to the destination. In these networks, the transmission is conducted in two phases. During the first phase, all users broadcast their information to the relaying node; and during the second phase, the relay processes and forwards the received signal to the destination. This process varies according to the relaying protocol adopted in the network.

Most of the related research that considers the multiple access channel (MAC) of WRNs limits their work in the case of assigning orthogonal channel resources to the active users [6, 7, 12, 35]. This avoids the expected multi-user interference. For example, the users in the *full-TDMA*$_{S-R-D}$ protocol have dedicated their time-slots

Protocol	S-R link.	R-D link.	Decoding @R	Decoding @D
concurrent$_{S-R}$-*IC*$_R$	concurrent	TDMA	IC+ML	ML
concurrent$_{R-D}$-*IC*$_D$	TDMA	concurrent	-	IC+ML
concurrent$_{S-R-D}$-*IC*$_D$	concurrent	concurrent	-	IC+ML
full-TDMA$_{S-R-D}$	concurrent	concurrent	-	ML
concurrent$_{S-R-D}$-*J. ML*$_D$	concurrent	concurrent	-	JML

Tab. 7.1: Protocol terms definitions

to avoid the interference. This protocol was shown to achieve the maximum diversity gain of WRNs, denoted as *interference-free* diversity gain. The *interference-free* is the diversity gain achieved assuming that each user in the network is transmitting solely without experiencing any interference from other users. This gain is considered to be the natural upper bound of the diversity gain in multi-user WRNs. Although the upper bound diversity is achieved using the *full-TDMA*$_{S-R-D}$ protocol, the spectral efficiency is significantly reduced due to the orthogonality among distinct users in the time domain. On the other hand, both the maximum spectral efficiency and diversity gain can be achieved using *concurrent*$_{S-R-D}$-*J.ML*$_D$ protocol, where concurrent transmission is allowed in both phases and the joint ML decoder is used at the destination. However, this protocol experiences the highest level of decoding complexity. This complexity order is considered to be the natural upper bound of complexity in multi-user WRNs.

Recently, the exploitation of the newly added dimension (i.e., space) to mitigate the multi-user interference was introduced. This is due to the merging of the MIMO techniques in wireless communication standards. The *space-based* interference cancellation (IC) schemes have the potential to significantly improve the system's spectral efficiency, especially when combined with the classical techniques. For the MAC over direct communication links, many IC schemes have been proposed to cancel the multi-user interference with affordable complexity, but this resulted in a reduced diversity gain [126–128]. The IC scheme, based on the partial interference cancellation group decoding (PICGD) of [129, 130], was initially proposed for direct communication link scenarios. Unlike [126–128], this IC scheme achieves full-diversity at an affordable detection complexity cost while retaining high spectral

efficiency [131, 132] . In order to cope with practical case scenarios, full-diversity, low-complexity IC schemes for more complex network models (e.g., relay-aided networks) need to be designed. The discussed protocols have been defined in Table 7.1 given below.

Contributions

In this chapter, a multi-user WRN with J users, a single R_a-antenna relay and a M-antenna destination is considered. The users are equipped each with J_a-antenna. The DF and AF relaying protocols are analysed. In the case of DF networks, it has been assumed that the perfect CSI is available only at the decoding nodes (the relay and the destination). On the other hand, it is available exclusively at the destination in the case of AF networks. In summary, and with respect to current literature, the contributions are

- Two transmission protocols are proposed: the *concurrent*$_{S-R-D}$-*PIC*$_{R,D}$ protocol for DF WRNs; and the *concurrent*$_{S-R-D}$-*PIC*$_D$ protocol for AF WRNs. Unlike [133] and *concurrent*$_{R-D}$-*IC*$_D$ of [134], the proposed protocols allow concurrent transmission in both phases of the transmission. Thus, higher spectral efficiency is offered while maintaining low decoding complexity. The low decoding complexity is maintained due to adapting the PICGD approach for multi-users WRNs. This approach was initially proposed by Guo, *et al.* for P2P communication links. The *concurrent*$_{S-R-D}$-*PIC*$_{R,D}$ protocol achieves the *interference-free* diversity gain without any condition on any nodes' antenna number. As with most exiting protocols, this protocol requires the CSI of the users-relay links at the relay. In contrast, the *concurrent*$_{S-R-D}$-*PIC*$_{R,D}$ protocol achieves a diversity of $J_a \times M$, given that $R_a > 8$, while the CSI is required only at the destination. Unlike the *concurrent*$_{S-R-D}$-*IC*$_D$ protocol of [133], the achievable diversity is determined by both the destination and user's antennas. This means that variant communications networks can be utilised.

- Assuming the PIC decoder, sufficient conditions are derived to achieve the mentioned achieved diversity gains of the proposed protocols.

The rest of the chapter is organised as follows: Section 7.4 introduces the network model and the proposed protocols. Then, diversity criteria of the protocols are derived in Section 7.5. Finally, the simulation results and the decoding complexity is discussed in Section 7.7 and 7.8, respectively.

7.2 Prior Work

In the literature, two multi-user WRN models are considered. In one model, multiple users are communicating with multiple destinations through a set of relaying nodes. In this model, each user is targeting one distinct destination through two hops of transmission. Two approaches have been discussed to resolve this interference. In [135, 136], an interference-aware relay selection scheme without interference mitigation has been introduced. In [137–139], the zero-forcing (ZF) method has been employed to mitigate the experienced multi-user interference; it uses scaling factors at the relaying nodes to null out the interference terms at the destinations. In [140, 141], schemes based on the minimum mean squared error (MMSE) have been introduced. Unlike [137–139], these schemes use factors that are designed to minimise the power of the interference-plus-noise at the destinations. In [142], an analysis has been presented for both the energy and spectral efficiency trade-off for schemes that use either the MMSE or the ZF method at their destinations. This analysis helped to identify the role of IC at the relaying nodes on realising the optimal power consumption-spectral efficiency trade-off. It shows how relaying schemes that do not attempt to mitigate the interference could yield a poor power consumption-spectral efficiency trade-off. There are two main drawbacks with these schemes: (1) they all require the global perfect CSI at one centralised node to calculate the gain factors and then fed them back to the relaying nodes; and (2) they cannot be applied directly to other multi-user WRN modelling, where non-parallel communication flows from multiple users to only one destination.

Afterwards, the multi-user interference of the other WRNs model has been considered. In this network model, multiple transmitting users are targeting one destination through a relaying node. In [143], ZF beam-formers have been determined to orthogonalize the users' signals that received at the destination. However, it still needs a feedback from a centralised node that has a global knowledge of CSI hence. Accordingly, high control overhead is induced. In [144], the IC schemes that were originally proposed for direct communications MIMO links have been adapted for WRNs. The achievable diversity of these schemes is sacrificed in favour of spectral efficiency. For example, a diversity gain of unity is achieved in WRN configurations of two single-antenna users, one double-antenna relay and a multi-antenna receiver, whereas the maximum diversity is two. In addition, these schemes require the IC process to be conducted at the relay, hence a relay of high computational capabilities is required. In [145], a protocol called *IC-Relay-TDMA* has been proposed for a WRN model consisted of two users, a double-antenna relay, and a single-antenna destination. The users can be single-, double- or quadruple-antenna nodes. This proposed protocol achieves the *interference-free* diversity gain only in the case of double and quadruple-antenna user nodes. It can be noted that in both [144] and [145], the destination's antenna number doesn't play a role in the achieved diversity. In [146], a protocol that denoted as *TDMA-ICRec* has been proposed. This protocol uses TDMA in the first phase while concurrent transmission is allowed only in the relaying phase. To achieve the *interference-free* diversity gain, the *TDMA-ICRec* protocol requires that both the destination and the relay are equipped with two or four antennas. Moreover, this protocol suffers from a spectral efficiency loss, especially when high number of users are utilised. This is as concurrent transmission is not allowed in the first phase of transmission where the user's data are multiplexed. In [134], the protocol of [145] has been generalised for J user WRNs, each user is equipped with J_a antennas. This protocol (denoted by *concurrent*$_{S-R}$IC$_R$) still requires the knowledge of CSI at the relays to achieve the *interference-free* diversity gain. This gain is achieved if the number of destination antennas (M) is less than $J_a(1 - \frac{J-1}{M})$. Otherwise, the gain is bounded by $\min\{(J_a(R_a - J + 1), R_a M\}$. As most other existing protocols, the *concurrent*$_{S-R}$IC$_R$ protocol has a low spectral

efficiency as concurrent transmission is only allowed in the users-relay link. Recently, a model of WRN with single-antenna users is considered under the assumption of linear complexity at both at both the relay node and the destination [133]. For this model, two protocols have been proposed, namely the *concurrent*$_{R-D}$IC$_D$ protocol and the *concurrent*$_{S-R-D}$IC$_D$ protocol. In the *concurrent*$_{R-D}IC_D$ protocol, the users have their own distinct time-slots in the first phase. Then, the relay transmits the user's data concurrently to the destination where the IC is conducted. Similar to [134, 146], this protocol has a low symbol rate of $\frac{1}{J+1}$ as concurrent transmission is allowed only in one phase of the transmission. Also, this protocol can achieve the *interference-free* diversity gain only if $M \geq 2J-1$ is held. Moreover, the CSI is also required at the relay. In contrast, the *concurrent*$_{S-R-D}$IC$_D$ protocol allows concurrent transmission over both $S-R$ and $R-D$ links and the IC is performed at the destination. Thus, a symbol rate of $\frac{1}{2}$ is offered. However, the *interference-free* diversity gain cannot be achieved and instead a gain of $R_a - J + 1$ is achieved. It can be seen that neither J_a nor M has a role in affecting the achievable diversity. Thus, this protocol suit specific communications systems where neither the users, nor the destination has multiple antennas. However, most modern communications systems standards assume the availability of multiple antenna nodes, which would be useless if this protocol is used.

Protocol	Diversity Gain	Rate	CSI Reqs.	Det. Comp.
concurrent$_{S-R}$-*IC*$_R$	$\min\{J_a(R_a - J + 1, R_a M\}$	$\frac{1}{J+1}$	R and D	$\mathcal{O}\left(\lvert\mathcal{A}\rvert^n\right)$
concurrent$_{R-D}$-*IC*$_D$	$\min\{M, \lfloor \frac{M}{J} \rfloor (N_a - J + 1)\}$	$\frac{1}{J+1}$	R and D	$\mathcal{O}\left(\lvert\mathcal{A}\rvert^n\right)$
concurrent$_{S-R-D}$-*IC*$_D$	$\leq R_a - J + 1$	$\frac{1}{2}$	D	$\mathcal{O}\left(\lvert\mathcal{A}\rvert^n\right)$
[1] *concurrent*$_{S-R-D}$-*PIC*$_{R,D}$	$\min\{J_a R_a, R_a M\}$	$\frac{1}{2}$	R and D	$\mathcal{O}\left(\lvert\mathcal{A}\rvert^{n/2}\right)$
[1] *concurrent*$_{S-R-D}$-*PIC*$_D$	$J_a \times M$	$\frac{1}{2}$	D	$\mathcal{O}\left(\lvert\mathcal{A}\rvert^{n/2}\right)$
[2] *full-TDMA*$_{S-R-D}$	$\min\{J_a R_a, R_a M\}$	$\frac{1}{2J}$	D	$\mathcal{O}\left(\lvert\mathcal{A}\rvert^{1}\right)$
[3] *concurrent*$_{S-R-D}$-*J. ML*$_D$	$\min\{J_a R_a, R_a M\}$	$\frac{1}{2}$	D	$\mathcal{O}\left(\lvert\mathcal{A}\rvert^{J\times n}\right)$

where $\mathcal{A}$ denotes the modulation constellation used.

Tab. 7.2: Comparison of main existing IC schemes in WRNs

To recapitulate, the existing protocols that can achieve the *interference-free* diversity gain are not allowed to use concurrent transmission in both phases and hence low spectral efficiency is imposed. Also, these protocols require the knowledge of

CSI at the relay and assume some strict conditions on nodes' antenna number. In contrast, the *concurrent*$_{S-R-D}$IC$_D$ protocol, which allows concurrent transmission and provides high spectral efficiency, cannot achieve the *interference-free* diversity gain. Instead, a gain of $R_a - J + 1$ is achieved, where neither J_a nor M has a role in affecting the achievable diversity. A brief comparison of main existing protocols is illustrated in Tab. 7.2, in terms of diversity gain, symbol rate and complexity-order.

7.3 Network Model

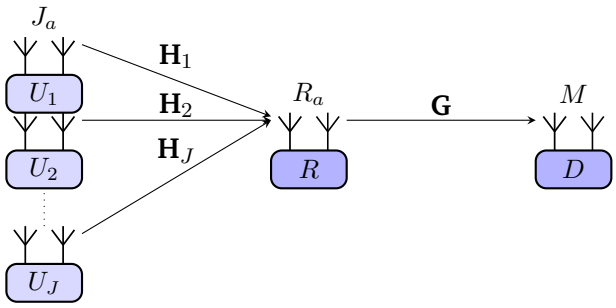

Fig. 7.1: multi-user MIMO wireless relay network

A coverage extension scenario is considered where the network is comprised of J users, a single R_a-antenna relay and a M-antenna destination (shown in Fig. 7.1). The users are equipped each with J_a-antenna. The communication through the network is conducted in two phases. During the first phase, all users broadcast their information to the relaying node simultaneously. During the second phase, the relay processes and forwards its received signal to the destination. The relay's process varies according to the relaying protocol adopted by the network. In the case of DF networks, it has been assumed that the perfect CSI is available only at the decoding nodes (the relay and the destination). However, it is available exclusively at the destination in the case of AF networks. The total transmission power dedicated for the entire network is denoted as P, and is evenly divided between the two transmission phases. Assuming that each user is equipped with J_a transmit antennas, the relay is equipped with R_a antennas and the destination is equipped with M receive antennas, this configuration is henceforth described by $\left(J_a^J, R_a, M\right)$.

7.4 The Proposed Protocols

7.4.1 Transmission Protocols Description

In this section, the proposed protocols are outlined. The *concurrent*$_{S-R-D}$*-PIC*$_{R,D}$ protocol is introduced for DF WRNs while the *concurrent*$_{S-R-D}$*-PIC*$_{D}$ protocol is introduced for AF WRNs. Assuming perfect time synchronization between the transmitting users, the baseband MIMO MAC uplink channel may be described by

$$\underset{T_1\times R_a}{\mathbf{Y}_r} = \sum_{j=1}^{J} \underset{T_1\times J_a}{\mathbf{X}_j}\,\underset{J_a\times R_a}{\mathbf{H}_j} + \underset{T_1\times R_a}{\mathbf{W}}, \tag{7.1}$$

where $\mathbf{Y}_r$ is the received signal at the relay, T_1 is the codeword signalling period of the broadcasting phase, $\mathbf{X}_j$ is the code matrix of the j^{th} user, $\mathbf{H}_j$ is the channel coefficients matrix from the j^{th} user to the relay with entries $h_{ik} \sim \mathcal{CN}(0,1)$, and $\mathbf{W}$ is the noise matrix at the relay with entries $w_{ik} \sim \mathcal{CN}(0, N_o)$. According to the above model, the n'th column of $\mathbf{X}_j$ denotes the symbols transmitted through the n'th transmit antenna of the j^{th} user during the signalling period T_1 while the t'th row of $\mathbf{X}_j$ denotes the symbols transmitted through the J_a transmit antennas of the j^{th} user during the t'th channel use.

In the second phase of a transmission, the relay is processing the received signal according to the relaying protocol used, then the resulting signal is forwarded to the destination. As mentioned, two relaying protocols are analysed:

- **DF relaying protocol**: As the name indicates, the relay here decodes its received signal (shown in (7.1)) and then, these estimated symbols ($\hat{s}_j, \forall j = 1,\ldots,J$) are encoded using linear dispersion code and forwarded to the destination. The decoding is conducted using the PICGD approach of Section 7.4.2. The second phase of transmission can be considered as an $R_a \times M$ P2P MIMO communication link. This can be modelled as

$$\underset{T_2\times M}{\mathbf{Y}_d} = \underset{T_2\times R_a}{\mathbf{X}}\,\underset{R_a\times M}{\mathbf{G}} + \underset{T_2\times M}{\mathbf{V}}, \tag{7.2}$$

where T_2 is the codeword signalling period of the relaying phase, $\mathbf{Y}_d$ is the received signal matrix at the destination and $\mathbf{X}$ is the code matrix used by the relay and $\mathbf{G}$ is the channel coefficients matrix for the link in between the relay and the destination with entries $g_{ij} \sim \mathcal{CN}(0,1)$. $\mathbf{V}$ is the noise matrix at the destination with entries $v_{ij} \sim \mathcal{CN}(0, N_o')$.

- **AF relaying protocol**: Here, the relay is simply amplified and then forward the received signal to the destination. This $R_a \times M$ MIMO P2P communication link can be modelled as

$$\underset{T_2\times M}{\mathbf{Y}_d} = \underset{T_2\times R_a}{\mathbf{Y}_r}\underset{R_a\times M}{\mathbf{G}} + \underset{T_2\times M}{\mathbf{V}}. \tag{7.3}$$

where $T_1 = T_2$ (as there is no encoding is being used).

The model of (7.3) can be simplified using (7.1) to

$$\underset{T_2\times M}{\mathbf{Y}_d} = \left(\sum_{j=1}^{J} \underset{T_1\times J_a}{\mathbf{X}_j}\ \underset{J_a\times R_a}{\mathbf{H}_j}\right)\underset{R_a\times M}{\mathbf{G}} + \underset{T_1\times R_a}{\mathbf{W}}\underset{R_a\times M}{\mathbf{G}} + \underset{T_2\times M}{\mathbf{V}}. \tag{7.4}$$

7.4.2 Interference Cancellation process

In the case of DF protocol, it is easy to see that the network is considered as two separated networks, namely the MAC part and the P2P part. This section shows the use of PICGD is provided at the relay and at the destination in the case of DF and AF WRNs, respectively. Due to similarity, the use of PICGD approach at the destination in the DF WRNs is omitted.

Toward this end, some algebraic manipulations are firstly required. Applying the vec(.) operator to the received signal leads to

$$\underbrace{\text{vec}\left(\mathbf{Y}_r\right)}_{\mathbf{y}} = \sum_{j=1}^{J} \underbrace{\mathbf{I}_{R_a} \otimes \mathbf{X}_j}_{\widetilde{\mathbf{X}}_j} \underbrace{\text{vec}\left(\mathbf{H}_j\right)}_{\mathbf{f}_j} + \underbrace{\text{vec}\left(\mathbf{V}\right)}_{\mathbf{n}} \tag{7.5}$$

in the case of DF WRNs and to

$$\underbrace{\mathrm{vec}\left(\mathbf{Y}_d\right)}_{\mathbf{y}} = \sum_{j=1}^{J} \underbrace{\mathbf{I}_M \otimes \mathbf{X}_j}_{\widetilde{\mathbf{X}}_j} \underbrace{\mathrm{vec}\left(\mathbf{H}_j\mathbf{G}\right)}_{\mathbf{f}_j} + \underbrace{\mathrm{vec}\left(\mathbf{WG}+\mathbf{V}\right)}_{\mathbf{n}}, \tag{7.6}$$

in the case of AF WRNs, where $\mathbf{I}_B$ is a $B \times B$ identity matrix as $B \in \{M, R_a\}$. For a large class of STBCs, the code matrices take the form of

$$\mathbf{X}_j = \sum_{i=1}^{n_j} \mathbf{A}_{j,i} s_{j,i}, \ \forall j = 1, 2 \ldots J, \tag{7.7}$$

where $\mathbf{A}_{j,i} \in \mathbb{C}^{T_1 \times R_a}$ and the $s_{j,i} \in \mathbb{C}$.

Using (7.7), the model of either (7.5) or (7.6) can be rewritten as

$$\mathbf{y} = \sum_{j=1}^{J} \sum_{i=1}^{n_j} \left(\mathbf{I}_B \otimes \mathbf{A}_{j,i}\right) \mathbf{f}_j s_{j,i} + \mathbf{n}, \tag{7.8}$$

where $B = R_a$ in the case of DF networks and $B = M$ in the case of AF networks.

This equation of (7.8) can be written equivalently as

$$\mathbf{y} = \sum_{j=1}^{J} \widetilde{\boldsymbol{\mathcal{H}}}_j \mathbf{s}_j + \mathbf{n}, \tag{7.9}$$

where

$$\widetilde{\boldsymbol{\mathcal{H}}}_j = \begin{bmatrix} \boldsymbol{\mathcal{H}}_{j,1} \\ \boldsymbol{\mathcal{H}}_{j,2} \\ \vdots \\ \boldsymbol{\mathcal{H}}_{j,B} \end{bmatrix}, \tag{7.10}$$

$\boldsymbol{\mathcal{H}}_{j,b} = \begin{bmatrix} \mathbf{A}_{j,1}\mathbf{f}_{j,b} & \ldots & \mathbf{A}_{j,n_j}\mathbf{f}_{j,b} \end{bmatrix}$ and $\mathbf{s}_j = \begin{bmatrix} s_{j,1} & \ldots & s_{j,n_j} \end{bmatrix}^{\mathsf{T}}$. $\mathbf{f}_{j,b}$ denotes the b^{th} column of $[\mathbf{H}_j\mathbf{G}]$ or the b^{th} column of $\mathbf{H}_j$ in the case of AF networks or the case of DF networks, respectively.

Now, the ultimate aim is to decode the users' data at the decoding node at a low complexity while trying to maintain the diversity gain offered by the network configurations. For this purpose, a multi-user relay-aided variant of the full-diversity

PICGD of [129, 130] is adopted. This approach was initially designed for P2P communication links and it is a decoding algorithm that generalises the zero-forcing receiver. Specifically, it separates the transmitted symbols into disjoint sets and hence decodes these sets independently. For instance, to decode the l^{th} set of transmitting symbols, the destination projects its signal into the subspace orthogonal to the one spanned by the rest of the symbol sets. Similarly, the users' symbols will correspond to the symbol sets. To illustrate the PICGD approach, the model of (7.9) should be rewritten as

$$\mathbf{y} = \widetilde{\boldsymbol{\mathcal{H}}}_l \mathbf{s}_l + \sum_{j=1, j\neq\ell}^{J} \widetilde{\boldsymbol{\mathcal{H}}}_j \mathbf{s}_j + \mathbf{n} \tag{7.11}$$

Now the decoding node needs to project its signal into the subspace orthogonal to the one spanned by interfering users. Let $\widetilde{\boldsymbol{\mathcal{H}}}_{\bar{l}}$ denote the basis of $\mathcal{M}\left(\widetilde{\boldsymbol{\mathcal{H}}}_j\right)$. Then the required projection matrix $\mathbf{P}_l$ needs to satisfy $\mathbf{P}_l \widetilde{\boldsymbol{\mathcal{H}}}_{\bar{l}} = \mathbf{0}$, which has a general solution as

$$\mathbf{P}_l = \mathbf{QM};\ \mathbf{M} = \left(\mathbf{I} - \widetilde{\boldsymbol{\mathcal{H}}}_{\bar{l}} \left(\widetilde{\boldsymbol{\mathcal{H}}}_{\bar{l}}\right)^{\dagger}\right). \tag{7.12}$$

It has been proved in [129, 130] that taking $\mathbf{Q} = \mathbf{I}$ minimizes the ML decoding probability of error. Thus, $\mathbf{P}_l = \mathbf{I} - \widetilde{\boldsymbol{\mathcal{H}}}_{\bar{l}} \left(\widetilde{\boldsymbol{\mathcal{H}}}_{\bar{l}}\right)^{\dagger}$. Left multiplying (7.11) by $\mathbf{P}_l$ results

$$\mathbf{P}_l \mathbf{y} = \mathbf{P}_l \widetilde{\boldsymbol{\mathcal{H}}}_l \mathbf{s}_l + \mathbf{P}_l \mathbf{n}. \tag{7.13}$$

7.4.3 Decoding Method

Note that although the noise term $\mathbf{P}_l\mathbf{n}$ is no longer a white Gaussian noise vector, it has been shown below that the minimum distance decision is still obtained through the ML decision. According to Section 7.4.2, $\mathbf{n} = \mathbf{WG} + \mathbf{V}$ in the case of AF WRNs while $\mathbf{n} = \mathbf{V}$ in the case of DF WRNs. Both that $\mathbf{W}$ and $\mathbf{V}$ are white Gaussian noise matrices. This section considers only the case of AF WRNs as the case of DF WRNs is implicitly contained.

The projection matrix $\mathbf{P}_l$ can be decomposed as

$$\mathbf{P}_l = \mathbf{U}^H \mathbf{D} \mathbf{U}, \tag{7.14}$$

where

$$\mathbf{D} = \begin{bmatrix} \mathbf{I}_{r\times r} & \mathbf{0}_{r\times(m-r)} \\ \mathbf{0}_{(m-r)\times r} & \mathbf{0}_{(m-r)\times(m-r)} \end{bmatrix}, \tag{7.15}$$

$\mathbf{U} \in \mathbb{C}^{m\times m}$ is unitary matrix with r =rank($\mathbf{P}_l$).

Multiplying (7.13) by **U**, this results in

$$\mathbf{U}\mathbf{P}_l\mathbf{y} = \mathbf{D}\mathbf{U}\widetilde{\boldsymbol{\mathcal{H}}}_l\mathbf{s}_l + \mathbf{D}\mathbf{U}\mathbf{n}, \tag{7.16}$$

It can be concluded that the effect of **D** in (7.16) is picking the first r entries and setting the others to zeros. This effect is denoted as $[.]_r$. Accordingly,

$$[\mathbf{U}\mathbf{P}_l\mathbf{y}]_r = \left[\mathbf{D}\mathbf{U}\widetilde{\boldsymbol{\mathcal{H}}}_l\mathbf{s}_l\right]_r + [\mathbf{D}\mathbf{U}\mathbf{n}]_r, \tag{7.17}$$

It can be observed that $\mathbf{n} = \mathbf{W}\mathbf{G} + \mathbf{V}$ is white a Gaussian noise vector if **G** is known to the destination. This is due to fact that states the summation of two Gaussian random variables ($w \in \mathcal{CN}(\mu_w, \sigma_w^2)$ and $v \in \mathcal{CN}(\mu_v, \sigma_v^2)$) is still Gaussian random variable with entries $\mathcal{CN}(\mu_w + \mu_v, \sigma_w^2 + \sigma_v^2)$ [6]. Accordingly, $[\mathbf{D}\mathbf{U}\mathbf{n}]_r$ is a vector with r Gaussian entries (similar to **n**) and $n - r$ zero entries. This is as the **U** is a unitary matrix.

Since $[\mathbf{D}\mathbf{U}\mathbf{n}]_r$ is a white Gaussian noise vector, the ML decision is given by

$$\hat{\mathbf{s}}_l = \underset{\bar{\mathbf{s}}\in\mathcal{A}^n}{\operatorname{argmin}} \| [\mathbf{U}\mathbf{P}_l\mathbf{y}]_r - \left[\mathbf{D}\mathbf{U}\widetilde{\boldsymbol{\mathcal{H}}}_l\bar{\mathbf{s}}\right]_r \|. \tag{7.18}$$

As the last $n - r$ entries have no effect on the distance, equation of (7.18) can be rewritten as

$$\hat{\mathbf{s}} = \underset{\bar{\mathbf{s}}\in\mathcal{A}^n}{\operatorname{argmin}} \|\mathbf{U}\mathbf{P}_l\mathbf{y} - \mathbf{D}\mathbf{U}\widetilde{\boldsymbol{\mathcal{H}}}_l\bar{\mathbf{s}}\|. \tag{7.19}$$

Thus,

$$\hat{\mathbf{s}} = \underset{\bar{\mathbf{s}}\in\mathcal{A}^n}{\operatorname{argmin}} \|\mathbf{P}_l\mathbf{y} - \mathbf{P}\widetilde{\boldsymbol{\mathcal{H}}}_l\bar{\mathbf{s}}\|. \tag{7.20}$$

This results as the $\mathbf{U}$ is a unitary matrix where $\mathbf{U}^H\mathbf{U} = \mathbf{I}$.

Accordingly, the minimum distance decision of the model described (7.13) can be made using

$$\mathbf{s}_l^{\text{ML-PICGD}} = \arg\min_{\mathbf{s}_l \in \mathcal{A}^{n_l}} \|\mathbf{P}_l\mathbf{y} - \mathbf{P}_l\widetilde{\boldsymbol{\mathcal{H}}}_l\mathbf{s}_l\|., \tag{7.21}$$

where $\mathcal{A}$ denotes the codebook spanned by $\mathbf{s}_l$ and assuming that $\widetilde{\mathcal{H}}_l$ is known to the decoder.

For the considered class of STBCs, one has $\widetilde{\mathbf{X}}_l\mathbf{f}_l = \widetilde{\boldsymbol{\mathcal{H}}}_l\mathbf{s}_l$. Therefore, the ML estimate under PICGD may be rewritten as

$$\widetilde{\mathbf{X}}_l^{\text{ML-PICGD}} = \underset{\widetilde{\mathbf{X}}_l \in \widetilde{\mathcal{C}}_l}{\text{argmin}} \|\mathbf{P}_l\mathbf{y} - \mathbf{P}_l\widetilde{\mathbf{X}}_l\mathbf{f}_l\|. \tag{7.22}$$

where $\widetilde{\mathcal{C}}_l$ denotes the code's book spanned by $\widetilde{\mathbf{X}}_l$.

7.5 Full-Diversity Criteria

As mentioned, the proposed *concurrent*$_{S-R-D}$*-PIC*$_{R,D}$ protocol and the *concurrent*$_{S-R-D}$*-PIC*$_D$ protocol can offer a diversity gain of $\min\{J_aR_a, R_aM\}$ and $J_a \times M$, respectively. Here, the sufficient conditions are derived to achieve the mentioned diversity gain in multi-user WRNs, either if AF or DF relaying protocol is adopted by the relay.

7.5.1 DF networks

Consider a multi-user DF WRNs that employs the proposed *concurrent*$_{S-R-D}$*-PIC*$_{R,D}$ protocol. In the MAC phase, this network's users use the STBCs $\mathbf{X}_l$, $\forall l = 1, \ldots, J$, and the STBC $\mathbf{X}$ is used by the relay in the P2P phase. Sufficient conditions needed to achieve the *interference free* diversity are given below:

The *concurrent*$_{S-R-D}$*-PIC*$_{R,D}$ multi-users WRN transmission protocol achieves the *interference free* diversity (defined by $\min(J_a \times R_a, R_a \times M)$) for each user if the following conditions are met

- Firstly, the STBCs $\mathbf{X}_l$, $\forall l = 1, \ldots, J$, that are used by the users in MAC phase are satisfying
  - $r(\mathbf{P}_l \Delta\mathbf{X}_l) \neq \{\mathbf{0}\}, \forall \mathbf{P}_l$, $\Delta\mathbf{X}_l \in \Delta\mathcal{C}_l \setminus 0$, $l = 1, \ldots, J$, where $\Delta\mathbf{X}_l$ is the codeword difference and $\Delta\mathcal{C}_l$ is the codeword difference codebook of the l^{th} user, respectively.
  - $\mathbf{P}_l \Delta\mathbf{X}_l$ is matrix of almost surely full column rank, $\forall \Delta\mathbf{X}_l \in \Delta\mathcal{C}_l \setminus \{\mathbf{0}\}$ and $l = 1, \ldots, J$.
- Secondly, the STBC $\mathbf{X}$ used by the relay in P2P phase is satisfying
  - for any two different codewords $\mathbf{X}$ and $\bar{\mathbf{X}} \in \boldsymbol{\mathcal{X}}$, $\triangle\mathbf{X} = \mathbf{X} - \bar{\mathbf{X}}$ is of full rank.
  - $\mathcal{M}(\mathbf{G}_{I_l}) \notin \mathcal{M}(\mathbf{G}_{I_{\bar{l}}})$, $\forall l = 1 \ldots J$, where $\mathbf{G}_{I_l}$ and $\mathbf{G}_{I_{\bar{l}}}$ are the corresponding columns of $\mathbf{G}$ of the l^{th} group and all the remaining columns, respectively.

Proof:

According to Definition 2.6, a system is said to achieve a diversity gain of d if the average error probability PEP can be upper-bounded in the high SNR range as $P_e \leq \alpha \text{SNR}^{-d}$, where α is a positive scalar independent of SNR. For this purpose, let the probability that $\mathbf{s}_i'$ is decoded while $\mathbf{s}_i$ was actually transmitted during the MAC-MIMO phase and the P2P phase be denoted by $\mathbb{P}_{\text{MAC}}(\mathbf{s}_i \to \mathbf{s}_i')$, and $\mathbb{P}_{\text{P2P}}(\mathbf{s}_i \to \mathbf{s}_i')$ respectively. Therefore, the pairwise error probability (PEP) for the i^{th} user can be bounded as

$$\begin{aligned}
\text{PEP} &\leq 1 - \mathbb{P}_{\text{MAC}}(\mathbf{s}_i \to \mathbf{s}_i)\, \mathbb{P}_{\text{P2P}}(\mathbf{s}_i \to \mathbf{s}_i) \\
&= 1 - \left(1 - \mathbb{P}_{\text{MAC}}\left(\mathbf{s}_i \to \mathbf{s}_i'\right)\right)\left(1 - \mathbb{P}_{\text{P2P}}\left(\mathbf{s}_i \to \mathbf{s}_i'\right)\right) \\
&= \mathbb{P}_{\text{MAC}}\left(\mathbf{s}_i \to \mathbf{s}_i'\right) + \mathbb{P}_{\text{P2P}}\left(\mathbf{s}_i \to \mathbf{s}_i'\right) \\
&\quad - \mathbb{P}_{\text{MAC}}\left(\mathbf{s}_i \to \mathbf{s}_i'\right)\mathbb{P}_{\text{P2P}}\left(\mathbf{s}_i \to \mathbf{s}_i'\right) \\
&\leq \mathbb{P}_{\text{MAC}}\left(\mathbf{s}_i \to \mathbf{s}_i'\right) + \mathbb{P}_{\text{P2P}}\left(\mathbf{s}_i \to \mathbf{s}_i'\right) \\
&\leq c_1\, \text{SNR}^{-J_a R_a} + c_2\, \text{SNR}^{-R_a M} \\
&\leq c\, \text{SNR}^{-R_a \min\{J_a, M\}}
\end{aligned} \tag{7.23}$$

where c_1, c_2 are positive numbers, and thus c is a positive value. Therefore, it can be concluded that the *concurrent*$_{S-R-D}$*-PIC*$_{R,D}$ protocol achieves the full diversity ($R_a \min\{J_a, M\}$). As seen this holds if the full-diversity is achieved in each phase individually. It has been proved in [147] that the outlined criteria of MAC part provide sufficient conditions to achieve full diversity while that P2P part was proved in [129, 130]. Thus, it can be concluded that the full diversity ($R_a \min\{J_a, M\}$) is achieved.

7.5.2 AF networks

The *concurrent*$_{S-R-D}$*-PIC*$_D$ multi-users WRN transmission protocol achieves a diversity gain of $J_a \times M$ for each user if the STBCs $\mathbf{X}_l$, $\forall l = 1, \ldots, J$ that structured as in (7.7) are satisfying

- $r(\mathbf{P}_l \Delta\mathbf{X}_l) \neq \{\mathbf{0}\}, \forall \mathbf{P}_l,\ \Delta\mathbf{X}_l \in \Delta\mathcal{C}_l \setminus 0,\ l = 1, \ldots, J$, where $\Delta\mathbf{X}_l$ is the codeword difference and $\Delta\mathcal{C}_l$ is the codeword difference codebook of the l^{th} user, respectively.

- The matrix $\mathbf{P}_l \Delta\mathbf{X}_l$ is almost surely of full column rank, $\forall \Delta\mathbf{X}_l \in \Delta\mathcal{C}_l \setminus \mathbf{0}$ and $l = 1, \ldots, J$.

- The number of relay antennas is $R_a > 8$.

Proof: According to (7.22), the conditional pairwise error probability (PEP) can be determined as

$$\mathbb{P}(\tilde{\mathbf{X}}_l \to \tilde{\mathbf{X}}_l | \mathbf{P}_l, \mathbf{f}_l) = Q\left(\sqrt{\frac{\mathrm{SNR}\|\mathbf{P}_l \Delta\mathbf{X}_l \mathbf{f}_l\|^2}{2}}\right) \tag{7.24}$$

where $\Delta\mathbf{X}_l = \tilde{\mathbf{X}}_l - \tilde{\mathbf{X}}_{\hat{l}}$.

Conditioning on $\mathbf{G}$, the average PEP can be simplified in two steps due to the independence between $\mathbf{P}_l$ and $\mathbf{f}_l$, namely by averaging over the $\mathbf{f}_l$ distribution for

a fixed $\mathbf{P}_l$ followed by averaging over the $\mathbf{P}_l$ distribution. Towards this end, the conditional expectation of the PEP can be expressed as

$$\begin{aligned}\mathbb{P}(\tilde{\mathbf{X}}_l \to \tilde{\mathbf{X}}_{\hat{l}}|\mathbf{P}_l, \mathbf{G}) &= \mathbb{E}_{\mathbf{f}_l|\mathbf{P}_l,\mathbf{G}}\left(Q\left(\sqrt{\frac{\mathrm{SNR}\,\tilde{\mathbf{f}}_l^H \Lambda_l \tilde{\mathbf{f}}_l}{2}}\right)\right) \\ &= \mathbb{E}_{\mathbf{f}_l|\mathbf{P}_l,\mathbf{G}}\left(Q\left(\sqrt{\frac{\mathrm{SNR}\sum_{i=1}^{r_l}\lambda_{l,i}^2\left|\tilde{\mathbf{f}}_l(i)\right|^2}{2}}\right)\right) \end{aligned} \tag{7.25}$$

where $\tilde{\mathbf{f}}_l = \mathbf{V}\mathbf{f}_l$,$\Lambda_l = \mathrm{diag}(\lambda_{l,i}^2, \ldots, \lambda_{l,J_a\times M}^2)$, $\lambda_{l,i}$ denote the singular values of $\mathbf{P}_l\Delta\tilde{\mathbf{X}}_l$ and r_l is the rank of $\mathbf{P}_l\Delta\tilde{\mathbf{X}}_l$.

Using Chernoff's bound, (7.25) can be rewritten as

$$\mathbb{P}(\tilde{\mathbf{X}}_l \to \tilde{\mathbf{X}}_{\hat{l}}|\mathbf{P}_l, \mathbf{G}) \le \mathbb{E}_{\mathbf{f}_l|\mathbf{P}_l,\mathbf{G}}\left(\exp\left(\frac{-\mathrm{SNR}\sum_{i=1}^{r_l}\lambda_{l,i}^2\left|\tilde{\mathbf{f}}_l(i)\right|^2}{4}\right)\right) \tag{7.26}$$

Assume $\mathbf{H}_j$ and $\mathbf{G}$ are $J_a \times R_a$ and $R_a \times M$ matrices with entries h_{ij} and $g_{ij} \sim \mathcal{CN}(0_{k\times 1}, \mathbf{1})$, respectively. Then, according to the proof given in Appendix A, the covariance matrix of $\mathbf{f}_j$, defined by $\mathbf{f}_j = \mathrm{vec}(H_j G)$, is given by

$$\mathbf{K}_{\mathbf{f}_l} = \mathrm{blkdiag}\left(\mathbf{I}_{J_a} \otimes \|\mathbf{g}_1\|^2, \ldots, \mathbf{I}_{J_a} \otimes \|\mathbf{g}_M\|^2\right), \tag{7.27}$$

assuming conditioning on G and that $\mathbf{K}_{\mathbf{H}_l} = \mathbf{I}_{J_a}$.

Accordingly, the averaging over $\mathbf{f}_l$ of (7.26) can be determined using the Lemma 1 of [148] as

$$\mathbb{P}(\tilde{\mathbf{X}}_l \to \tilde{\mathbf{X}}_{\hat{l}}|\mathbf{P}_l, \mathbf{G}) \le \prod_{i=1}^{r_l} \frac{1}{1 + \mathrm{SNR}\frac{\lambda_{l,i}^2}{4} \times \left\|\mathbf{g}_{\lfloor 1+\frac{i}{J_a}\rfloor}\right\|^2} \tag{7.28}$$

For a high SNR values range,

$$\mathbb{P}(\tilde{\mathbf{X}}_l \to \tilde{\mathbf{X}}_{\hat{l}} | \mathbf{P}_l, \mathbf{G}) \leq \left(\frac{4}{\text{SNR}}\right)^{r_l} \frac{1}{\prod_{i=1}^{r_l} \lambda_{l,i}^2 \left\| \mathbf{g}_{\lfloor 1+\frac{i}{J_a} \rfloor} \right\|^2} \tag{7.29}$$

Finally, the average PEP can be obtained by

$$\mathbb{P}(\tilde{\mathbf{X}}_l \to \tilde{\mathbf{X}}_{\hat{l}}) \leq \mathbb{E}_{\mathbf{G}} \left(\mathbb{E}_{\mathbf{P}_l | \mathbf{G}} \left(\left(\frac{4}{\text{SNR}}\right)^{r_l} \frac{1}{\prod_{i=1}^{r_l} \lambda_{l,i}^2 \left\| \mathbf{g}_{\lfloor 1+\frac{i}{J_a} \rfloor} \right\|^2} \right) \right) \tag{7.30}$$

Assuming that the first condition which implies that $r_l \neq 0, \forall \mathbf{P}_l$, $\Delta \mathbf{X}_l \in \Delta \mathcal{C}_l \setminus 0$, $l = 1, \ldots, J$ holds, then the second term of the R.H.S of (7.30) has a finite second moment under conditioning on $\mathbf{G}$. In addition, the fourth moment of $\mathbf{g}$ is finite, see Appendix C. Accordingly, the Cauchy-Schwartz inequality can be applied and results

$$\mathbb{P}(\tilde{\mathbf{X}}_l \to \tilde{\mathbf{X}}_{\hat{l}}) \leq \sqrt{\mathbb{E}_{r_l} \left(\frac{4}{\text{SNR}}\right)^{2r_l} \mathbb{E}_{\Lambda_l | \mathbf{G}} \left(\frac{1}{\prod_{i=1}^{r_l} \lambda_{l,i}^4 \left\| \mathbf{g}_{\lfloor 1+\frac{i}{J_a} \rfloor} \right\|^4} \right)} \tag{7.31}$$

According to Appendix B, the Cauchy-Schwartz inequality can be applied again to the $\mathbb{E}_{\Lambda_l | \mathbf{G}}$ term of (7.31), given that the third condition is satisfied, which results

$$\mathbb{P}(\tilde{\mathbf{X}}_l \to \tilde{\mathbf{X}}_{\hat{l}}) \leq \sqrt{\mathbb{E}_{r_l} \left(\frac{4}{\text{SNR}}\right)^{2r_l}} \sqrt[4]{\mathbb{E}_{\Lambda_l} \left(\frac{1}{\prod_{i=1}^{r_l} \lambda_{l,i}^8} \right) \mathbb{E}_{\mathbf{g}} \left(\frac{1}{\left\| \mathbf{g}_{\lfloor 1+\frac{i}{J_a} \rfloor} \right\|^8} \right)}. \tag{7.32}$$

Given that $r_l \overset{a.s.}{=} J_a \times M$, ($\overset{a.s.}{=}$ denotes almost sure equality) as a result of that the second condition is hold $\forall \Delta \mathbf{X}_l \in \Delta \mathcal{C}_l \setminus 0$ and $l = 1, \ldots, J$, the inequality of (7.32) can be written as

$$\mathbb{P}(\tilde{\mathbf{X}}_l \to \tilde{\mathbf{X}}_{\hat{l}}) \leq \alpha \left(\frac{4}{SNR}\right)^{r_l} \tag{7.33}$$

where α is a positive finite number.

Thus, a diversity gain of $r_l = J_a \times M$ is achieved if these listed conditions are held. As expected, achieving the full-diversity using ML for a particular STBC is a prerequisite to achieve the mentioned diversity using PICGD. This is implied by the second condition as $\Delta\mathbf{X}_l$ is not almost surely unless $\Delta\mathbf{X}_l$ is also full column rank $\forall \Delta\mathbf{X}_l \in \Delta\mathcal{C}_l \setminus 0$.

7.6 Proposed code structures

As mentioned, the STBC employed by the MAC part basically determines the rate of the network. Assuming that PICGD approach is used by the network, this code-rate is upper-bounded per user (R) by

$$R \leq \frac{1}{J-1}\left(1-\frac{J_a}{T}\right). \tag{7.34}$$

This bound results directly from the fact that $\begin{bmatrix} \boldsymbol{\mathcal{H}}_{\bar{l}} & \Delta\mathbf{X}_l \end{bmatrix}$ has to be almost surely of full column rank . Thus, by rearranging

$$(J-1)\,n + J_a \leq T,$$

the bound is obtained.

Except for the criterion of the number of a relay antenna, it can be noted that the conditions of DF (part 1) and AF WRNs are similar to the criteria derived for MIMO MAC P2P networks in [132]. Also, the conditions of DF (part 2) are similar to the criteria derived for MIMO P2P networks in [129, 130]. Accordingly, the code structures were proposed in [129, 130] and [132] can be used here for MAC part and P2P part respectively. Thus, only code instances structured according to these designs are listed. These instances are used in the simulation results section.

Example 7.1. *A code for two-users DF WRNs is given below. These users are double-antenna nodes and the relay is equipped with four antennas. The code matrices are given by*

$$\boldsymbol{X}_1 = \begin{bmatrix} s'_{1,1} & 0 \\ s'_{1,2} & s'_{1,2} \\ s'_{1,3} & s'_{1,3} \\ s'_{1,4} & s'_{1,4} \\ 0 & s'_{1,1} \\ 0 & 0 \end{bmatrix}, \boldsymbol{X}_2 = \begin{bmatrix} 0 & 0 \\ s'_{2,1} & 0 \\ s'_{2,2} & s'_{2,2} \\ s'_{2,3} & s'_{2,3} \\ s'_{2,4} & s'_{2,4} \\ 0 & s'_{2,1} \end{bmatrix} \text{ and } \boldsymbol{X} = \begin{bmatrix} \hat{s}'_{1,1} & 0 & 0 & 0 \\ \hat{s}'_{2,1} & \hat{s}'_{1,2} & 0 & 0 \\ 0 & \hat{s}'_{2,2} & s'_{1,3} & 0 \\ 0 & 0 & \hat{s}'_{2,3} & s'_{1,4} \\ 0 & 0 & 0 & \hat{s}'_{2,4} \end{bmatrix} \tag{7.35}$$

where $\begin{bmatrix} s'_{l,1} & s'_{l,2} & s'_{l,3} & s'_{l,4} \end{bmatrix}^T = \boldsymbol{U}_4 \begin{bmatrix} s_{l,1} & s_{l,2} & s_{l,3} & s_{l,4} \end{bmatrix}^T$ *and* $s_{l,i}$ $\forall l = 1, 2$, $i = 1, 2, 3, 4$ *are drawn from a conventional QAM constellation* $\mathcal{A}$. $\boldsymbol{U}_4$ *is* 4×4 *full-diversity rotation matrix shown in [149].*

In the case of AF WRNs, the following codes are used:

Example 7.2. *For a two-users AF WRNs where each user is double-antenna node, the 3/5-rate code is given by*

$$\boldsymbol{X}_1 = \begin{bmatrix} s'_{1,1} & 0 \\ s'_{1,2} & s'_{1,2} \\ s'_{1,3} & s'_{1,3} \\ 0 & s'_{1,1} \\ 0 & 0 \end{bmatrix}, \text{ and } \boldsymbol{X}_2 = \begin{bmatrix} 0 & 0 \\ s'_{2,1} & 0 \\ s'_{2,2} & s'_{2,2} \\ s'_{2,3} & s'_{2,3} \\ 0 & s'_{2,1} \end{bmatrix}, \tag{7.36}$$

where $\begin{bmatrix} s'_{l,1} & s'_{l,2} & s'_{l,3} \end{bmatrix}^T = \boldsymbol{U}_3 \begin{bmatrix} s_{l,1} & s_{l,2} & s_{l,3} \end{bmatrix}^T$ *and* $s_{l,i}$ $\forall l = 1, 2$, $i = 1, 2, 3$ *are drawn from a conventional QAM constellation* $\mathcal{A}$. $\boldsymbol{U}_3$ *is* 3×3 *full-diversity rotation matrix shown in [149].*

Example 7.3. *For a two-users AF WRNs where each user is triple-antenna node, the 1/2-rate code is given by*

$$\boldsymbol{X}_1 = \begin{bmatrix} s'_{1,1} & 0 & 0 \\ s'_{1,2} & s'_{1,2} & 0 \\ s'_{1,3} & s'_{1,3} & s'_{1,3} \\ 0 & s'_{1,1} & s'_{1,1} \\ 0 & 0 & s'_{1,1} \\ 0 & 0 & 0 \end{bmatrix}, \boldsymbol{X}_2 = \begin{bmatrix} 0 & 0 & 0 \\ s'_{2,1} & 0 & 0 \\ s'_{2,2} & s'_{2,2} & 0 \\ s'_{2,3} & s'_{2,3} & s'_{2,3} \\ 0 & s'_{2,1} & s'_{2,1} \\ 0 & 0 & s'_{2,1} \end{bmatrix} \tag{7.37}$$

where $\begin{bmatrix} s'_{l,1} & s'_{l,2} & s'_{l,3} \end{bmatrix}^T = \boldsymbol{U}_3 \begin{bmatrix} s_{l,1} & s_{l,2} & s_{l,3} \end{bmatrix}^T$ *and* $s_{l,i}$ $\forall l = 1, 2$, $i = 1, 2, 3$ *are drawn from a conventional QAM constellation* $\mathcal{A}$. $\boldsymbol{U}_3$ *is* 3×3 *full-diversity rotation matrix shown in [149].*

Example 7.4. *For a triple-users AF WRNs where each user is double-antenna node, the 3/8-rate code is given by*

$$\boldsymbol{X}_1 = \begin{bmatrix} s'_{1,1} & 0 \\ s'_{1,2} & s'_{1,2} \\ s'_{1,3} & s'_{1,3} \\ 0 & s'_{1,1} \\ 0 & 0 \\ 0 & 0 \\ 0 & 0 \\ 0 & 0 \end{bmatrix}, \boldsymbol{X}_2 = \begin{bmatrix} 0 & 0 \\ 0 & 0 \\ s'_{2,1} & 0 \\ s'_{2,2} & s'_{2,2} \\ s'_{2,3} & s'_{2,3} \\ 0 & s'_{2,1} \\ 0 & 0 \\ 0 & 0 \end{bmatrix}, \boldsymbol{X}_3 = \begin{bmatrix} 0 & 0 \\ 0 & 0 \\ 0 & 0 \\ 0 & 0 \\ s'_{3,1} & 0 \\ s'_{3,2} & s'_{3,2} \\ s'_{3,3} & s'_{3,3} \\ 0 & s'_{2,1} \end{bmatrix}, \tag{7.38}$$

where $\begin{bmatrix} s'_{l,1} & s'_{l,2} & s'_{l,3} \end{bmatrix}^T = \boldsymbol{U}_3 \begin{bmatrix} s_{l,1} & s_{l,2} & s_{l,3} \end{bmatrix}^T$ *and* $s_{l,i}$ $\forall l = 1, 2$, $i = 1, 2, 3$ *are drawn from a conventional QAM constellation* $\mathcal{A}$. $\boldsymbol{U}_3$ *is* 3×3 *full-diversity rotation matrix shown in [149].*

7.7 Decoding complexity Analysis

The decoding complexity is measured by the worst-case decoding complexity order. This order is defined as the minimum number of times that needed by the decoder to evaluate the ML metric in order to optimally detect the transmitted data. Due to the structure of the codes used (see Section 7.6), the detection of the transmitted symbols can be conducted on the real and imaginary parts of each user's data individually without performance degradation. This can be verified by noting that the QR decomposition of $\mathbf{P}_l\widetilde{\boldsymbol{\mathcal{H}}}_l = \mathbf{Q}_l\mathbf{R}_l$ results in a real upper triangular matrix $\mathbf{R}_l$. Therefore the ML decoding equation of (7.21) can be split into (7.39) and (7.40) shown below. Thus, the worst case decoding complexity at the destination in the case of AF WRNs, or at both of the relay and destination in the case of DF WRNs, has been reduced from $\mathcal{O}\left(|\mathcal{A}|^n\right)$ to $\mathcal{O}\left(|\mathcal{A}|^{n/2}\right)$.

$$\Re\left\{\begin{bmatrix}\hat{s}_{i,1} & \dots & \hat{s}_{i,n}\end{bmatrix}\right\} = \arg\min_{\hat{\mathbf{x}}\in\Re\{\mathcal{A}\}^n}\left\|\Re\left\{\left(\mathbf{Q}_i\right)^H\mathbf{P}_i\mathbf{y}\right\} - \mathbf{R}_i\hat{\mathbf{x}}\right\|^2 \tag{7.39}$$

$$\Im\left\{\begin{bmatrix}\hat{s}_{i,1} & \dots & \hat{s}_{i,n}\end{bmatrix}\right\} = \arg\min_{\hat{\mathbf{x}}\in\Im\{\mathcal{A}\}^n}\left\|\Im\left\{\left(\mathbf{Q}_i\right)^H\mathbf{P}_i\mathbf{y}\right\} - \mathbf{R}_i\hat{\mathbf{x}}\right\|^2, \tag{7.40}$$

7.8 Simulation Results

In this section, simulation results are provided to back up the theoretical claims of the proposed protocols. Thus, the two proposed protocols are simulated over different network configurations, namely $(2^2, 4, M)$, $(2^2, 9, M)$, $(2^3, 4, M)$ and $(3^2, 4, M)$, where $M \in \{2, 4\}$. In addition, slope references for the claimed diversity gains are included for comparison purposes. All simulations are conducted on a Rayleigh faded channel, and it is assumed that the total transmission power is evenly distributed between the transmission phases.

Fig. 7.2 shows the BER of the proposed *concurrent* $_{S-R-D}$*-PIC* $_{R,D}$ protocol, the *IC-Relay-TDMA* protocol of [134] and a diversity-gain reference curve of 8 are depicted. These results are of the $\left(2^2, 4, 4\right)$ network configurations. The *concurrent* $_{S-R-D}$*-PIC*

$_{R,D}$ protocol uses the codes of Example 7.1, with a rate of 2/3 in MAC phase and a rate of 4/5 in P2P phase. Therefore, the overall symbol rate of the proposed protocol is 4/11 per user. In contrast, the *IC-Relay-TDMA* protocol uses the Alamouti's STBC code of [12] in the MAC phase and the 3/4-rate STBC of [10] during the P2P phase. Clearly, there is a mismatch in the number of symbols available at the relay and which need to be transmitted; hence un-avoidable latency is introduced unless quasi-orthogonal STBCs are used. However, the use of QO-STBC leads to a higher decoding complexity at the destination [10]. For fair comparison, the proposed protocol draws its symbols from a rectangular 8-QAM constellation while the *IC-Relay-TDMA* protocol uses the 16-QAM constellation; this is because the former configurations of the *IC-Relay-TDMA* scheme have a symbol rate of 3/11 per user while the proposed protocol has a rate of 4/11. It can be observed from Fig. 7.2 that the proposed protocol achieves the *interference-free* diversity gain while the *IC-Relay-TDMA* protocol of [134] experiences a loss in the diversity gain. This is because the *IC-Relay-TDMA* protocol doesn't achieve the full diversity in the first phase. In contrast, the proposed protocol achieves the full diversity either in the users-relay or relay-destination link, unlike the existing *IC-Relay-TDMA* protocol.

Unlike the *concurrent*$_{S-R}$*-IC*$_R$ protocol of [134] and the *concurrent*$_{R-D}$*-IC*$_D$ protocol of [133], the proposed protocol (*concurrent* $_{S-R-D}$*-PIC* $_D$) requires the knowledge of CSI only at the destination. In addition, it achieves a diversity gain of $J_a \times M$, unlike the *concurrent*$_{S-R-D}$*-IC*$_D$ protocol of [133] where neither J_a nor M affect the achievable diversity. The simulation results are shown in Fig. 7.3 where the proposed protocol is simulated in $(2^2, 8, 2)$ and $(2^2, 8, 4)$. The proposed protocol uses the rate 3/5 code of Example 7.2 and hence the overall symbol rate is 3/10 per user. It has drawn the symbols from a rectangular 16-QAM constellation. From Fig. 7.3, it can be observed that the proposed protocol achieves a diversity of $2 \times 2 = 4$ and $2 \times 4 = 8$ as mentioned theoretically.

Other network configurations are simulated and shown in Fig. 7.4 assuming that the *concurrent* $_{S-R-D}$*-PIC* $_D$ protocol is used. These results consider the case of users equipped with triple transmitting antennas. The simulated protocol used the

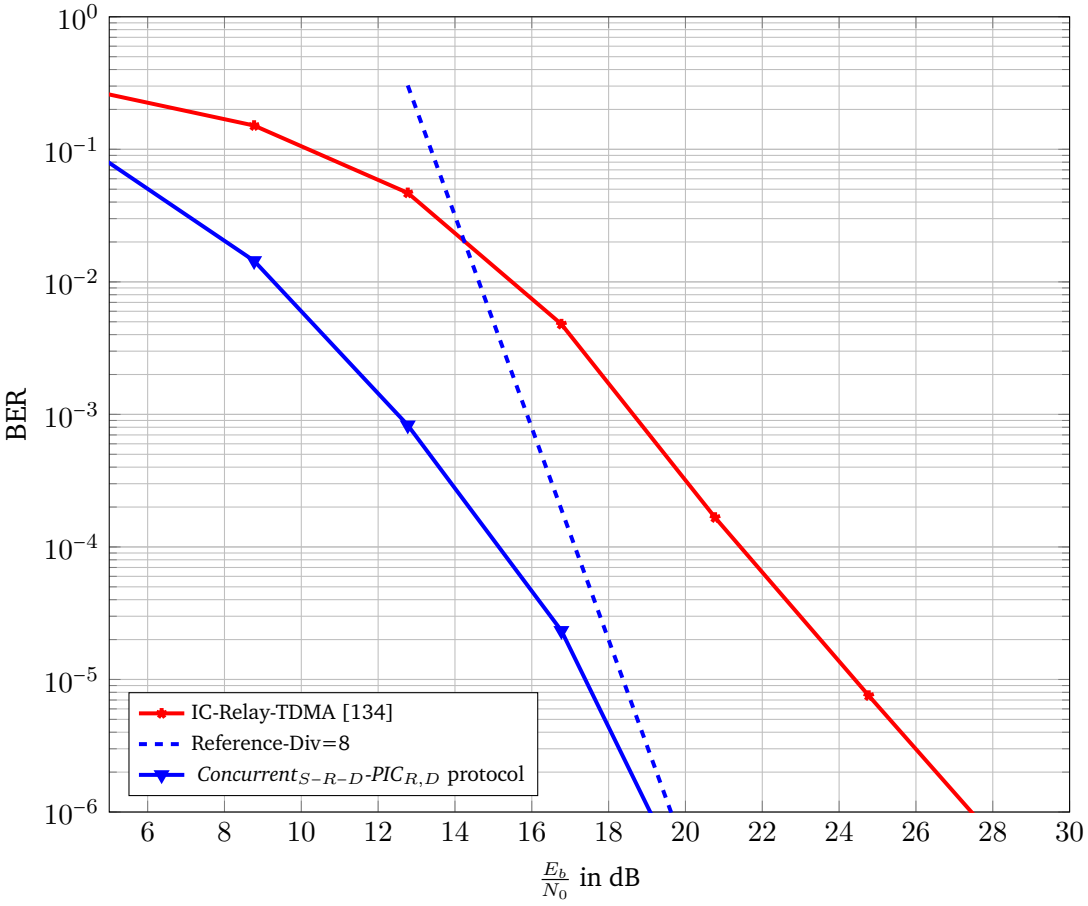

Fig. 7.2: BER performance for $\left(2^2, 4, 4\right)$ system

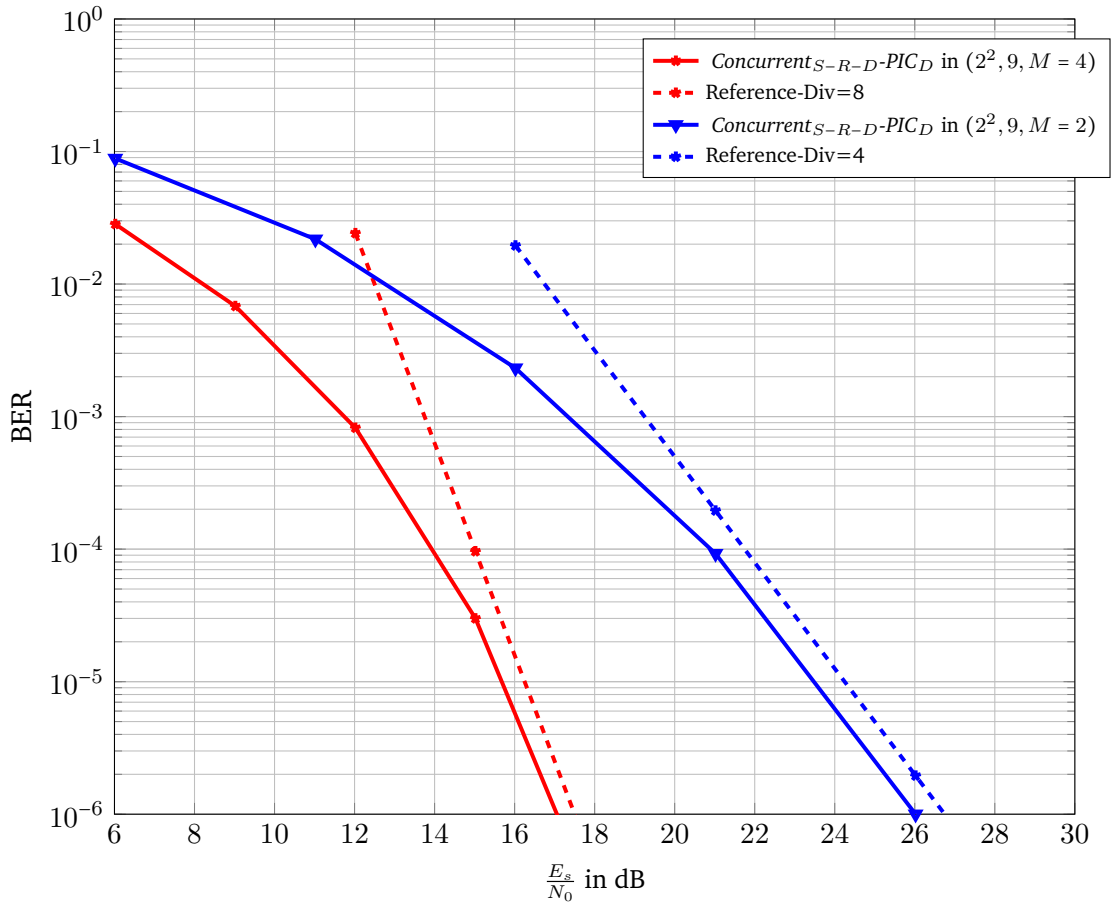

Fig. 7.3: BER performance for the proposed protocol, *Concurrent*$_{S-R-D}$ – PIC_D, in a network of $(2^2, 9, M)$.

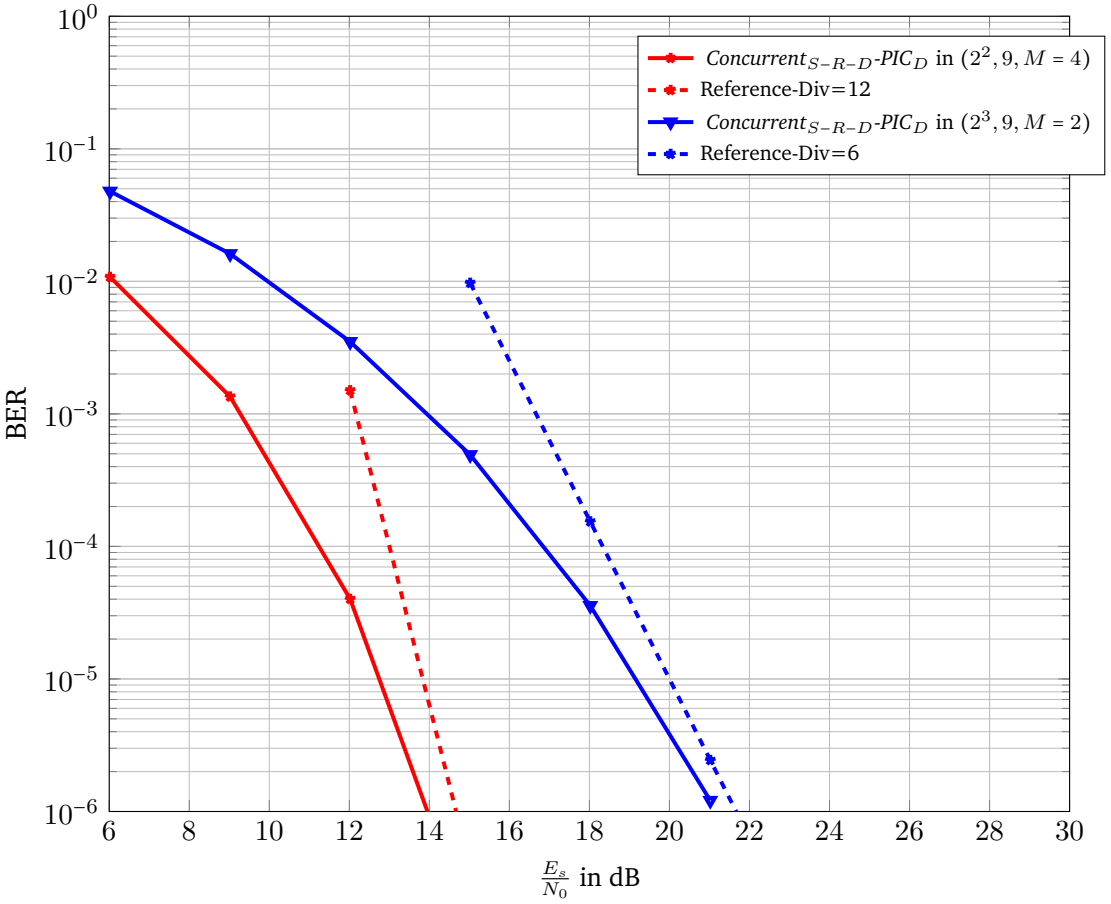

Fig. 7.4: BER performance for the proposed protocol, *Concurrent*$_{S-R-D}$ – PIC_D, in a network of $(2^3, 9, M)$.

code of Example 7.3. From Fig. 7.4, one can easily conclude that the proposed protocol achieves the mentioned diversity gain (6 and 12) and hence the theoretical assumption is numerically backed up.

In Fig. 7.5, the case of three transmitting users is considered. The network configurations of $(3^2, 9, 2)$ and $(3^2, 9, 2)$ are simulated. It can be observed that the claimed diversity gains are achieved.

7.9 Conclusion

This chapter focused on a full-diversity, low-complexity interference cancellation approach in multi-user WRNs. Two protocols are proposed: the *concurrent*$_{S-R-D}$-*PIC*$_{R,D}$ protocol for DF networks; and the *concurrent*$_{S-R-D}$-*PIC*$_D$ protocol for AF

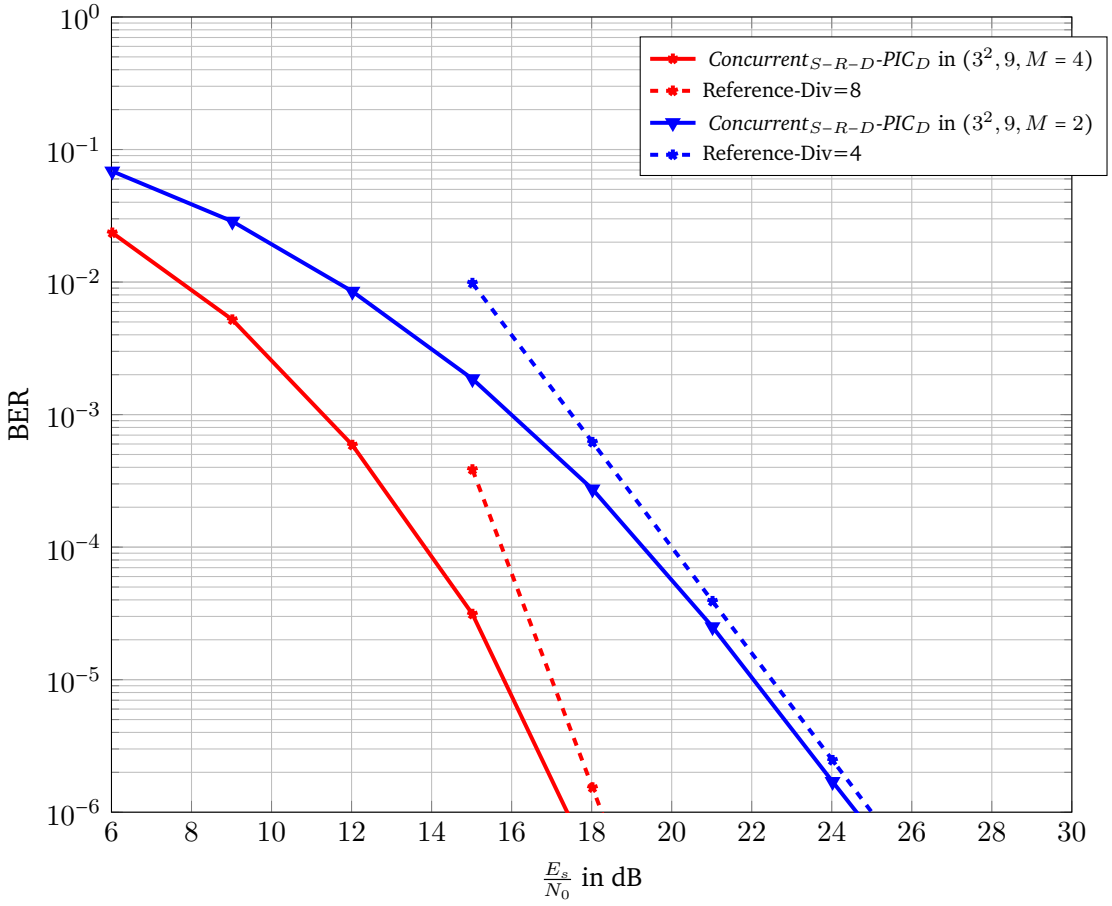

Fig. 7.5: BER performance for the proposed protocol, *Concurrent*$_{S-R-D}$ – PIC_D, in a network of $(3^2, 9, M)$.

networks. These protocols employ the PICGD approach for the decoding process. This leads to reduced decoding complexity. In addition, they both allow concurrent transmission in both phases of the communication through WRNs. Thus, higher spectral efficiency is offered. Unlike [133, 134], the *concurrent*$_{S-R-D}$*-PIC*$_{R,D}$ protocol achieves full-diversity on each transmission phase and hence the *interference-free* diversity gain is achieved. This is while no conditions on the node's antenna number has been imposed. Similar to [133], this protocol however requires the CSI at the relay. In contrast, the *concurrent*$_{S-R-D}$*-PIC*$_{R,D}$ protocol achieves a diversity of $J_a \times M$ while the CSI is required only at the destination. This chapter also derived sufficient conditions for an STBC to achieve the mentioned diversity gain, when the PICGD approach is employed by the network. By theoretical analysis and numerical simulations, it has been shown that the proposed protocols achieve the mentioned diversity gain and that they provide a higher symbol rate w.r.t *Full-TDMA* protocol and low decoding complexity w.r.t the *concurrent*$_{S-R-D}$*-J. ML*$_D$ protocol. Thanks to the used codes, the proposed protocols have further reduced the decoding complexity without performance degradation in the case of using rectangular modulation schemes.

7.10 Appendices

Appendix A

Assume $\mathbf{H}_j$ and $\mathbf{G}$ are $J_a \times R_a$ and $R_a \times M$ matrices with entries h_{ij} and $g_{ij} \sim \mathcal{CN}(0_{k\times 1}, \mathbf{1})$, respectively. Then, the covariance matrix of $\mathbf{f}_j$, defined by $\mathbf{f}_j = \text{vec}(H_j G)$, is given by

$$\mathbf{K}_{\mathbf{f}_l} = \text{blkdiag}\left(\mathbf{I}_{J_a} \otimes \|\mathbf{g}_1\|^2, \ldots, \mathbf{I}_{J_a} \otimes \|\mathbf{g}_M\|^2\right), \tag{7.41}$$

assuming conditioning on G and that $\mathbf{K}_{\mathbf{H}_l} = \mathbf{I}_{J_a}$.

Proof :

Conditioning on $\mathbf{G}$ and given that $\mathbf{K}(\mathbf{H}_l) = \mathbf{I}_{j_a}$

$$\begin{aligned}
\mathbf{K}_{\mathbf{f}_l} &= \text{blkdiag}\left(vec(\mathbf{H}_j\mathbf{G})\right) \\
&= \mathbf{K}\left(\underbrace{\mathbf{I}_M \otimes \mathbf{H}_k}_{\tilde{\mathbf{H}}_j} \underbrace{vec(\mathbf{G})}_{\mathbf{g}}\right) \\
&= \begin{bmatrix} \mathbf{I}_{J_a} \otimes \|\mathbf{g}_1\|^2 & \mathbf{0} & \mathbf{0} & \ldots & \mathbf{0} \\ \mathbf{0} & \mathbf{I}_{J_a} \otimes \|\mathbf{g}_2\|^2 & \mathbf{0} & \ldots & \mathbf{0} \\ \vdots & \vdots & \ddots & \vdots & \vdots \\ \mathbf{0} & \mathbf{0} & \mathbf{0} & \cdots & \mathbf{I}_{J_a} \otimes \|\mathbf{g}_M\|^2 \end{bmatrix} \qquad (7.42) \\
&= \text{blkdiag}\left(\mathbf{I}_{J_a} \otimes \|\mathbf{g}_1\|^2, \ldots, \mathbf{I}_{J_a} \otimes \|\mathbf{g}_M\|^2\right). \qquad (7.43)
\end{aligned}$$

Appendix B

Given that $\mathbf{G}$ is a $R_a \times M$ channel coefficients matrix, with entries $g_{ki} \sim \mathcal{CN}(0,1)$, the 8^{th} central moment $\mathbb{E}_{\mathbf{g}}\left(\frac{1}{\|\mathbf{g}_i\|^8}\right)$ is finite if $R_a > 8$ for $M \geq 1$.

Proof:

As $g_{ki} \sim \mathcal{CN}(0,1)$, then $\mathbf{Z} = \|\mathbf{g}\|^2$ is a chi-square random variable $\left(\chi^2(k)\right)$ with $k = N_a$ degree of freedom and $Z \sim (0,\infty)$. Therefore, $\mathbb{E}_{\mathbf{g}}\left(\frac{1}{\|\mathbf{g}\|^4}\right)^2$ can be evaluated as follow

$$\begin{aligned}
\mathbb{E}_{\mathbf{g}}\left(\frac{1}{\|\mathbf{g}\|^4}\right)^2 &= \mathbb{E}_{\mathbf{Z}}\left(\frac{1}{\mathbf{Z}^4}\right) \\
&= \int_0^\infty \frac{1}{Z^4}\gamma_Z(z)\,\mathrm{dz} \\
&= \int_0^\infty \frac{1}{Z^4}\frac{1}{2^{\frac{R_a}{2}}\Gamma\left(\frac{N_a}{2}\right)} Z^{\frac{R_a}{2}-1}e^{-\frac{Z}{2}}\,\mathrm{dz} \\
&= \frac{2^{\frac{R_a}{2}-4}\Gamma\left(\frac{R_a}{2}-4\right)}{2^{\frac{R_a}{2}}\Gamma\left(\frac{R_a}{2}\right)} \int_0^\infty \underbrace{\frac{Z^{\frac{R_a}{2}-5}e^{-\frac{Z}{2}}}{2^{\frac{R_a}{2}-4}\Gamma\left(\frac{R_a}{2}-4\right)}}_{\text{pdf of } \chi^2(k=R_a-8)}\mathrm{dz} \\
&= \frac{2^{\frac{R_a}{2}-4}\Gamma\left(\frac{R_a}{2}-4\right)}{2^{\frac{R_a}{2}}\Gamma\left(\frac{R_a}{2}\right)}
\end{aligned} \tag{7.44}$$

Using the recursion formula of $\Gamma(\alpha-1)$ [150]

$$\Gamma(\alpha) = (\alpha-1)\,\Gamma(\alpha-1), \tag{7.45}$$

then equation (7.44) can be simplified as shown below

$$\mathbb{E}_{\boldsymbol{g}}\left(\frac{1}{\|\boldsymbol{g}\|^4}\right)^2 = \frac{1}{(R_a-8)(R_a-6)(R_a-4)(R_a-2)} \tag{7.46}$$

Appendix C

Assume that $k > m$, $\mathbb{E}_{\mathbf{g}}\left(\frac{1}{\|\mathbf{g}_i\|^m}\right)$ is finite given that $\mathbb{E}_{\mathbf{g}}\left(\frac{1}{\|\mathbf{g}_i\|^k}\right)$ is finite.

Proof:

Let $\varphi\left(\frac{1}{\|\mathbf{g}_i\|}\right) = \left(\frac{1}{\|\mathbf{g}_i\|}\right)^{k/m}$. Since $k > m$, φ is a convex function and proceeding with the Jensen's inequality, this results

$$\left(\mathbb{E}_{\mathbf{g}}\left(\frac{1}{\|\mathbf{g}_i\|^m}\right)\right)^{k/m} \leq \mathbb{E}_{\mathbf{g}}\left(\left(\frac{1}{\|\mathbf{g}_i\|^m}\right)^{k/m}\right) = \mathbb{E}_{\mathbf{g}}\left(\frac{1}{\|\mathbf{g}_i\|^k}\right), \tag{7.47}$$

given that $\mathbb{E}_{\mathbf{g}}\left(\frac{1}{\|\mathbf{g}_i\|^k}\right)$ is finite, so $\mathbb{E}_{\mathbf{g}}\left(\frac{1}{\|\mathbf{g}_i\|^m}\right)$ is finite too.

Bibliography

[1]"IEEE Standard for Local and Metropolitan Area Networks - Part 20: Air Interface for Mobile Broadband Wireless Access Systems Supporting Vehicular Mobility – Physical and Media Access Control Layer Specification". In: *IEEE 802.20* (), pp. – (cit. on pp. 1, 21).

[2]David Tse and Pramod Viswanath. *Fundamentals of wireless communication*. Cambridge university press, 2005 (cit. on p. 1).

[3]Andrea Goldsmith. *Wireless communications*. Cambridge university press, 2005 (cit. on pp. 1, 9, 11, 13–16, 21–23).

[4]A. Sendonaris, E. Erkip, and B. Aazhang. "User Cooperation Diversity - Part I: System Description". In: *IEEE Transactions on Communications* 51.11 (2003), pp. 1927–1938 (cit. on pp. 2, 36).

[5]A. Sendonaris, E. Erkip, and B. Aazhang. "User Cooperation Diversity - Part II: Implementation Aspects and Performance Analysis". In: *IEEE Transactions on Communications* 51.11 (2003), pp. 1939–1948 (cit. on pp. 2, 36).

[6]J. N. Laneman and G. W. Wornell. "Distributed space-time-coded protocols for exploiting cooperative diversity in wireless networks". In: *IEEE Transactions on Information Theory* 49.10 (2003), pp. 2415–2425 (cit. on pp. 2, 29, 36, 45, 61, 91, 135, 146).

[7]J.N.a b Laneman, D.N.C.c Tse, and G.W.a Wornell. "Cooperative diversity in wireless networks: Efficient protocols and outage behavior". In: *IEEE Transactions on Information Theory* 50.12 (2004), pp. 3062–3080 (cit. on pp. 2, 9, 10, 36, 45, 61, 91, 107, 110, 114, 135).

[8]Rohit U Nabar, Helmut Bolcskei, and Felix W Kneubuhler. "Fading relay channels: Performance limits and space-time signal design". In: *IEEE Journal on Selected Areas in Communications* 22.6 (2004), pp. 1099–1109 (cit. on p. 2).

[9]Deqiang Chen and J Nicholas Laneman. "Modulation and demodulation for cooperative diversity in wireless systems". In: *IEEE Transactions on Wireless Communications* 5.7 (2006), pp. 1785–1794 (cit. on p. 2).

[10]Y. Jing and H. Jafarkhani. "Using orthogonal and quasi-orthogonal designs in wireless relay networks". In: *IEEE Transactions on Information Theory* 53.11 (2007), pp. 4106–4118 (cit. on pp. 2, 30, 31, 45, 64, 72, 110, 114, 118, 123, 156).

[11]Claude Oestges and Bruno Clerckx. *MIMO Wireless Communications: From Real-World Propagation to Space-Time Code Design*. 1st edition. Academic Press, 2007 (cit. on pp. 2, 45).

[12]S. M. Alamouti. “A simple transmit diversity technique for wireless communications”. In: *IEEE Journal on Selected Areas in Communications* 16.8 (1998), pp. 1451–1458 (cit. on pp. 2, 29, 34, 69, 78, 135, 156).

[13]KJ Ray Liu. *Cooperative communications and networking*. Cambridge University Press, 2009 (cit. on pp. 2, 9, 24, 27, 45).

[14]Y. Jia, C. Andrieu, R. J. Piechocki, and M. Sandell. “Gaussian approximation based mixture reduction for near optimum detection in MIMO systems”. In: *IEEE Communications Letters* 9.11 (2005), pp. 997–999 (cit. on pp. 3, 45, 51).

[15]S. Wei, D. L. Goeckel, and M. C. Valenti. “Asynchronous cooperative diversity”. In: *IEEE Transactions on Wireless Communications* 5.6 (2006), pp. 1547–1556 (cit. on pp. 3, 45, 51).

[16]Andreas F. Molisch. *Wireless communications*. A John Wiley and Sons, 2012 (cit. on pp. 9, 14, 15).

[17]E. Telatar. “Capacity of multi-antenna Gaussian channels”. In: *European Transactions on Telecommunications* 10.6 (1999), pp. 585–595 (cit. on p. 9).

[18]G. J. Foschini and M. J. Gans. “On Limits of Wireless Communications in a Fading Environment when Using Multiple Antennas”. In: *Wireless Personal Communications* 6.3 (1998), pp. 311–335 (cit. on p. 9).

[19]V. Tarokh, N. Seshadri, and A. R. Calderbank. “Space-time codes for high data rate wireless communication: Performance criterion and code construction”. In: *IEEE Transactions on Information Theory* 44.2 (1998), pp. 744–765 (cit. on p. 9).

[20]V. Tarokh, H. Jafarkhani, and A. R. Calderbank. “Space-time block codes from orthogonal designs”. In: *IEEE Transactions on Information Theory* 45.5 (1999), pp. 1456–1467 (cit. on p. 9).

[21]V. Tarokh, H. Jafarkhani, and A. R. Calderbank. “Space-time block coding for wireless communications: Performance results”. In: *IEEE Journal on Selected Areas in Communications* 17.3 (1999), pp. 451–460 (cit. on p. 9).

[22]J. Nicholas Laneman and G. W. Wornell. “Energy-efficient antenna sharing and relaying for wireless networks”. In: *2000 IEEE Wireless Communications and Networking Conference*. 2000, pp. 7–12 (cit. on pp. 10, 36).

[23]D. Soldani and S. Dixit. “Wireless relays for broadband access [radio communications series]”. In: *IEEE Communications Magazine* 46.3 (Mar. 2008), pp. 58–66. ISSN: 0163-6804. DOI: 10.1109/MCOM.2008.4463772 (cit. on p. 10).

[24]Theodore S Rappaport et al. *Wireless communications: principles and practice*. Vol. 2. prentice hall PTR New Jersey, 1996 (cit. on pp. 13–16, 21, 23).

[25]M.-T.O.a El Astal and A.M.b Abu-Hudrouss. *Distributed Space Time BLock codes for Asynchronous Cooperative Networks : Imperfect Synchronization problem and proposed solutions*. LAP, 2011 (cit. on pp. 15, 18).

[26]Marvin K. Simon and Mohamed-Slim Alouini. *Digital Communication over Fading Channels*. 2nd. Wiley-IEEE Press, 2004 (cit. on pp. 17, 119).

[27]Wikipedia. *Rayleigh fading*. Aug. 2014. URL: http://en.wikipedia.org/wiki/Rayleigh_fading (cit. on p. 18).

[28]John G Proakis, Masoud Salehi, Ning Zhou, and Xiaofeng Li. *Communication systems engineering*. Vol. 2. Prentice-hall Englewood Cliffs, 1994 (cit. on pp. 18–20).

[29]Andrew J Viterbi and Jim K Omura. *Principles of digital communication and coding*. Courier Corporation, 2013 (cit. on pp. 18, 19).

[30]L. Hanzo, S. Ng, T. Keller, and W. Webb. "Quadrature Amplitude Modulation:From Basics to Adaptive Trellis-Coded, Turbo-Equalised and Space-Time Coded OFDM, CDMA and MC-CDMA Systems". In: Wiley-IEEE Press, 2004. Chap. Star QAM Schemes for Rayleigh Fading Channels, pp. 307 –335 (cit. on p. 20).

[31]Branka and Vucetic. *Space-Time Block Codes*. 1st. John Wiley and Sons, 2003 (cit. on pp. 21, 27).

[32]Jean-Benoit Larouche. *Alamouti Space-Time Block Coding*. June 2013. URL: `http://nutaq.com/en/blog/alamouti-space-time-block-coding` (cit. on p. 23).

[33]Y. Jing and B. Hassibi. "Distributed space-time coding in wireless relay networks". In: *IEEE Transactions on Wireless Communications* 5.12 (2006), pp. 3524–3536 (cit. on pp. 24, 92, 106).

[34]Hamid Jafarkhani. *Space-time coding: theory and practice*. Cambridge university press, 2005 (cit. on p. 27).

[35]M. Dohler, M. Hussain, A. Desai, and H. Aghvami. "Performance of distributed space-time block codes". In: *IEEE Vehicular Technology Conference*. Vol. 59. 2004. Chap. 2, pp. 742–746 (cit. on pp. 29, 91, 135).

[36]F. . Zheng, A. G. Burr, and S. Olafsson. "Signal detection for distributed space-time block coding: 4 relay nodes under quasi-synchronisation". In: *IEEE Transactions on Communications* 57.5 (2009), pp. 1250–1255 (cit. on pp. 29, 45, 51, 52, 56, 62, 64, 71, 73, 80, 83, 105).

[37]M.-T.O El Astal and A.M Abu-Hudrouss. "SIC detector for 4 relay distributed space-time block coding under quasi-synchronization". In: *IEEE Communications Letters* 15.10 (2011), pp. 1056–1058 (cit. on pp. 29, 45, 47, 51, 56, 62, 64, 71, 73, 80, 83, 105).

[38]X. . Liang and X. . Xia. "On the Nonexistence of Rate-One Generalized Complex Orthogonal Designs". In: *IEEE Transactions on Information Theory* 49.11 (2003), pp. 2984–2989 (cit. on p. 30).

[39]Y. Yu, S. Keroueden, and J. Yuan. "Closed-loop extended orthogonal space-time block codes for three and four transmit antennas". In: *IEEE Signal Processing Letters* 13.5 (2006), pp. 273–276 (cit. on p. 31).

[40]F. . Gong, J. . Zhang, and J. . Ge. "Novel distributed quasi-orthogonal space-time block codes for two-way two-antenna relay networks". In: *IEEE Transactions on Wireless Communications* 12.9 (2013), pp. 4338–4349 (cit. on pp. 32, 61, 63, 67, 78).

[41]Van Der Meulen Ec. "Three terminal communication channels". In: *Advances in Applied Probability* 1.11 (1971), pp. 120–154 (cit. on p. 36).

[42]Thomas M. Cover and Abbas A. E. Gamal. "CAPACITY THEOREMS FOR THE RELAY CHANNEL." In: *IEEE Transactions on Information Theory* IT-25.5 (1979), pp. 572–584 (cit. on p. 36).

[43]A. Sendonaris, E. Erkip, and B. Aazhang. “Increasing uplink capacity via user cooperation diversity”. In: *IEEE International Symposium on Information Theory - Proceedings*. 1998, p. 156 (cit. on p. 36).

[44]B. Zhao and M. C. Valenti. “Distributed turbo coded diversity for relay channel”. In: *Electronics Letters* 39.10 (2003), pp. 786–787 (cit. on p. 36).

[45]Y. Cao and B. Vojcic. “Cooperative coding using serial concatenated convolutional codes”. In: *IEEE Wireless Communications and Networking Conference (WCNC)*. Vol. 2. 2005, pp. 1001–1006 (cit. on p. 36).

[46]A. Chakrabarti, A. De Baynast, A. Sabharwal, and B. Aazhang. “Low density parity check codes for the relay channel”. In: *IEEE Journal on Selected Areas in Communications* 25.2 (2007), pp. 280–290 (cit. on p. 36).

[47]A. Nosratinia, T. E. Hunter, and A. Hedayat. “Cooperative communication in wireless networks”. In: *IEEE Communications Magazine* 42.10 (2004), pp. 74–80 (cit. on p. 36).

[48]T.E. Hunter and A. Nosratinia. “Diversity through coded cooperation”. In: *IEEE Transactions o Wireless Communications* 5.2 (Feb. 2006), pp. 283–289. ISSN: 1536-1276. DOI: 10.1109/TWC.2006.1611050 (cit. on p. 36).

[49]M. Janani, A. Hedayat, T. E. Hunter, and A. Nosratinia. “Coded cooperation in wireless communications: Space-time transmission and iterative decoding”. In: *IEEE Transactions on Signal Processing* 52.2 (2004), pp. 362–371 (cit. on p. 36).

[50]S. Yiu, R. Schober, and L. Lampe. “Distributed space - Time block coding”. In: *IEEE Transactions on Communications* 54.7 (2006), pp. 1195–1206 (cit. on p. 45).

[51]T. . Nguyen, O. Berder, and O. Sentieys. “Impact of transmission synchronization error and cooperative reception techniques on the performance of cooperative MIMO systems”. In: *IEEE International Conference on Communications*. 2008, pp. 4601–4605 (cit. on p. 45).

[52]M-T EL Astal, AM Abu-Hudrouss, and JC Olivier. “Improved Signal Detection of Wireless Relaying Networks Employing Space-Time Block Codes Under Imperfect Synchronization”. In: *Wireless Personal Communications* 82.1 (2015), pp. 533–550 (cit. on p. 46).

[53]O. . Shin, A. M. Chan, H. T. Kung, and V. Tarokh. “Design of an OFDM cooperative space-time diversity system”. In: *IEEE Transactions on Vehicular Technology* 56.4 II (2007), pp. 2203–2215 (cit. on p. 47).

[54]F. T. Alotaibi and J. A. Chambers. “Full-rate and full-diversity extended orthogonal space-time block coding in cooperative relay networks with imperfect synchronization”. In: *IEEE International Conference on Acoustics, Speech and Signal Processing (ICASSP)*. 2010, pp. 2882–2885 (cit. on pp. 47, 83).

[55]A. M. Elazreg and J. A. Chambers. “Closed-loop extended orthogonal space time block coding for four relay nodes under imperfect synchronization”. In: *IEEE Workshop on Statistical Signal Processing Proceedings*. 2009, pp. 545–548 (cit. on pp. 47, 56, 73, 83).

[56]F. Ng and X. Li. “Cooperative STBC-OFDM transmissions with imperfect synchronization in time and frequency”. In: *Conference Record - Asilomar Conference on Signals, Systems and Computers*. Vol. 2005. 2005, pp. 524–528 (cit. on pp. 48, 83).

[57]A. Yadav, M. Juntti, and J. Karjalainen. “Combating timing asynchronism in relay transmission for 3GPP LTE uplink”. In: *IEEE Wireless Communications and Networking Conference (WCNC)*. 2009 (cit. on pp. 48, 83).

[58]T. Hwang and Y. Li. “Iterative cyclic prefix reconstruction for coded single-carrier systems with frequency-domain equalization(SC-FDE)”. In: *IEEE Vehicular Technology Conference*. Vol. 57. 2003. Chap. 3, pp. 1841–1845 (cit. on p. 48).

[59]F. . Zheng, A. G. Burr, and S. Olafsson. “Near-optimum detection for distributed space-time block coding under imperfect synchronization”. In: *IEEE Transactions on Communications* 56.11 (2008), pp. 1795–1799 (cit. on pp. 48, 50, 51, 83).

[60]X. Li. “Space-time coded multi-transmission among distributed transmitters without perfect synchronization”. In: *IEEE Signal Processing Letters* 11.12 (2004), pp. 948–951 (cit. on pp. 49, 83).

[61]F. T. Alotaibi, F. Abdurahman, U. Mannai, and J. A. Chambers. “Extended orthogonal space-time block coding scheme in asynchronous two-way cooperative relay networks over frequency-selective fading channels”. In: *17th DSP 2011 International Conference on Digital Signal Processing, Proceedings*. 2011 (cit. on pp. 51, 62, 83).

[62]U. N. Mannai, F. M. Abdurahman, A. M. Elazreg, and J. A. Chambers. “Orthogonal space time block coding for two-way wireless relay networks under imperfect synchronization”. In: *IWCMC 2011 - 7th International Wireless Communications and Mobile Computing Conference*. 2011, pp. 1694–1697 (cit. on pp. 51, 62, 83).

[63]T. Cui, F. Gao, T. Ho, and A. Nallanathan. “Distributed space-time coding for two-way wireless relay networks”. In: *IEEE Transactions on Signal Processing* 57.2 (2009), pp. 658–671 (cit. on p. 61).

[64]F. . Gong, J. . Zhang, and J. . Ge. “Distributed concatenated alamouti codes for two-way relaying networks”. In: *IEEE Wireless Communications Letters* 1.3 (2012), pp. 197–200 (cit. on p. 61).

[65]Miao Wang, Fanggang Wang, and Zhangdui Zhong. “Wireless MIMO switching: distributed zero-forcing and MMSE relaying using network coding”. In: *EURASIP Journal on Advances in Signal Processing* 2013.1 (2013), p. 130. ISSN: 1687-6180 (cit. on p. 61).

[66]M.-T.O El Astal, B. Salmon, and J.C. Olivier. “Distributed Space-Time Block Coding for Two-Way Wireless Relaying Networks: Improved Performance under Imperfect Synchronization”. In: *IEEE Wireless Communications and Networking Conference (WCNC): 6-9 April; Istanbul*. 2014 (cit. on pp. 61, 78).

[67]F. Abdurahman, A. Elazreg, and J. A. Chambers. “Distributed quasi-orthogonal space-time coding for two-way wireless relay networks”. In: *Proceedings of the 2010 7th International Symposium on Wireless Communication Systems, ISWCS’10*. 2010, pp. 413–416 (cit. on pp. 61, 78).

[68]Shengli Zhang, Soung-Chang Liew, and P.P. Lam. “On the Synchronization of Physical-Layer Network Coding”. In: *IEEE Information Theory Workshop (ITW)*. 2006, pp. 404–408 (cit. on p. 62).

[69]S. Chang and B. Kelley. “An efficient time synchronization scheme for broadband two-way relaying networks based on physical-layer network coding”. In: *IEEE Communications Letters* 16.9 (2012), pp. 1416–1419 (cit. on p. 62).

[70]Z. Zhong, S. Zhu, and A. Nallanathan. “Distributed space-time trellis code for asynchronous cooperative communications under frequency-selective channels”. In: *IEEE Transactions on Wireless Communications* 8.2 (2009), pp. 796–805 (cit. on p. 62).

[71]Z. Li, X. . Xia, and B. Li. “Achieving full diversity and fast ML decoding via simple analog network coding for asynchronous two-way relay networks”. In: *IEEE Transactions on Communications* 57.12 (2009), pp. 3672–3681 (cit. on p. 62).

[72]Y. Liu, X. . Xia, and H. Zhang. “Distributed linear convolutional space-time coding for two-relay full-duplex asynchronous cooperative networks”. In: *IEEE Transactions on Wireless Communications* 12.12 (2013), pp. 6406–6417 (cit. on p. 62).

[73]Z. Zhong, S. Zhu, and G. Lv. “Distributed space-time code for asynchronous two-way wireless relay networks under frequency-selective channels”. In: *IEEE International Conference on Communications (ICC)*. 2009 (cit. on p. 62).

[74]F. . Zheng, A. G. Burr, and S. Olafsson. “Distributed space-time block coding with incremental relay: Performance improvement under imperfect synchronisation”. In: *2007 16th IST Mobile and Wireless Communications Summit*. 2007 (cit. on pp. 73, 83).

[75]A.M. Elazreg, U.N. Mannai, and J.A. Chambers. “Distributed cooperative space-time coding with parallel interference cancellation for asynchronous wireless relay networks”. In: 2010, pp. 360–364 (cit. on pp. 73, 83).

[76]M.O. El Astal and A.M. Abu-Hudrouss. “Generalized PIC Detector for Distributed STBC under Quasi-Synchronization”. In: *Wireless Engineering and Technology* 3.1 (2012), pp. 25 –29. ISSN: 2152-2294. DOI: 10.4236/wet.2012.31004 (cit. on pp. 73, 83).

[77]S. Zhang, F. Gao, and C. . Pei. “Optimal training design for individual channel estimation in two-way relay networks”. In: *IEEE Transactions on Signal Processing* 60.9 (2012), pp. 4987–4991 (cit. on p. 76).

[78]X. Xu, J. Wu, S. Ren, X. Luan, and H. Xiang. “Superimposed training and channel estimation for two-way relay networks”. In: *International Conference on Advanced Communication Technology, ICACT*. 2014, pp. 1050–1054 (cit. on p. 76).

[79]M. Biguesh and A. B. Gershman. “Training-based MIMO channel estimation: A study of estimator tradeoffs and optimal training signals”. In: *IEEE Transactions on Signal Processing* 54.3 (2006), pp. 884–893 (cit. on p. 76).

[80]T. F. Wong and B. Park. “Training sequence optimization in MIMO systems with colored interference”. In: *IEEE Transactions on Communications* 52.11 (2004), pp. 1939–1947 (cit. on p. 76).

[81]F. . Zheng, A. G. Burr, and S. Olafsson. “A simple optimum detector for distributed space-time block coding under imperfect synchronisation”. In: *IEEE Workshop on Signal Processing Advances in Wireless Communications, SPAWC*. 2007 (cit. on p. 83).

[82]F. . Zheng, A. G. Burr, and S. Olafsson. “PIC detector for distributed space-time block coding under imperfect synchronisation”. In: *Electronics Letters* 43.10 (2007), pp. 580–582 (cit. on p. 83).

[83]F.-C.a b Zheng, A.G.a Burr, and S.c d Olafsson. “Distributed space-time block coding for 3 and 4 relay nodes: Imperfect synchronisation and a solution”. In: 2007 (cit. on p. 83).

[84]A. M. Elazreg, F. M. Abdurahman, and J. A. Chambers. “Distributed closed-loop quasi-orthogonal space time block coding with four relay nodes: Overcoming imperfect synchronization”. In: *5th IEEE International Conference on Wireless and Mobile Computing Networking and Communication (WiMob)*. 2009, pp. 320–325 (cit. on p. 83).

[85]W. Xin and W. Zhuo. “PIC detector for joint distributed STBC under imperfect synchronization”. In: *Proceedings - 5th International Conference on Wireless Communications, Networking and Mobile Computing, WiCOM 2009*. 2009 (cit. on p. 83).

[86]X. Wang and Z. Wu. “Interference cancellation technique under imperfect synchronization in cellular systems”. In: *Journal of Shanghai University* 13.5 (2009), pp. 379–383 (cit. on p. 83).

[87]Gordhan Menghwar, Akhtar Jalbani, Mukhtiar Memon, Mansoor Hyder1, and Christoph Mecklenbrauker. “Cooperative space-time codes with network coding”. In: *EURASIP Journal on Wireless Communications and Networking* 2012.1 (2012), p. 205. ISSN: 1687-1499. DOI: 10.1186/1687-1499-2012-205 (cit. on p. 91).

[88]Y. Jing and B. Hassibi. “Diversity analysis of distributed space-time codes in relay networks with multiple transmit/receive antennas”. In: *Eurasip Journal on Advances in Signal Processing* 2008 (2008) (cit. on p. 91).

[89]S. S. Ikki and M. H. Ahmed. “Performance analysis of generalized selection combining for decode-and-forward cooperative-diversity networks”. In: *IEEE Vehicular Technology Conference*. 2010 (cit. on p. 91).

[90]Qingxiong Deng and Andrew Klein. “Relay selection in cooperative networks with frequency selective fading”. In: *EURASIP Journal on Wireless Communications and Networking* 2011.1 (2011), p. 171. ISSN: 1687-1499. DOI: 10.1186/1687-1499-2011-171 (cit. on p. 91).

[91]George K Karagiannidis, Chintha Tellambura, Sayandev Mukherjee, and Abraham O Fapojuwo. “Multiuser Cooperative Diversity for Wireless Networks”. In: *EURASIP Journal on Wireless Communications and Networking* 2006.1 (2006), p. 017202. ISSN: 1687-1499. DOI: 10.1155/WCN/2006/17202 (cit. on p. 91).

[92]Yasser Izi and Abolfazl Falahati. “Amplify-forward relaying for multiple-antenna multiple relay networks under individual power constraint at each relay”. In: *EURASIP Journal on Wireless Communications and Networking* 2012.1 (2012), p. 50. ISSN: 1687-1499. DOI: 10.1186/1687-1499-2012-50 (cit. on p. 91).

[93]H. Tomeba, K. Takeda, and F. Adachi. “Space-time block coded-joint transmit/receive antenna diversity using more than 4 receive antennas”. In: *IEEE Vehicular Technology Conference*. 2008 (cit. on pp. 91, 95, 101).

[94]H. Tomeba, K. Takeda, and F. Adachi. “Space-time block coded joint transmit/receive diversity in a frequency-nonselective Rayleigh fading channel”. In: *IEICE Trans. on Commun.* E89-B.8 (2006) (cit. on pp. 91, 95, 101).

[95]G. S. Rajan and B. S. Rajan. “Multigroup ML decodable collocated and distributed space-time block codes”. In: *IEEE Transactions on Information Theory* 56.7 (2010), pp. 3221–3247 (cit. on pp. 92, 106).

[96]Z. Yi and I. . Kim. “Single-symbol ML decodable distributed STBCs for cooperative networks”. In: *IEEE Transactions on Information Theory* 53.8 (2007), pp. 2977–2985 (cit. on pp. 92, 105, 106).

[97]A. Sreedhar D. Chockalingam and B. Rajan. “Single-symbol ml decodable distributed stbcs for partially-coherent cooperative networks”. In: *IEEE Transaction on Wireless Communications* 8.5 (2009), pp. 2672–2681 (cit. on pp. 92, 105, 106).

[98]K. Pavan Srinath and B. Sundar Rajan. “Single real-symbol decodable, high-rate, distributed space-time block codes”. In: *IEEE Information Theory Workshop (ITW)*. 2010 (cit. on pp. 92, 98, 99, 107).

[99]T. Peng, R. C. de Lamare, and A. Schmeink. “Adaptive Distributed Space-Time Coding Based on Adjustable Code Matrices for Cooperative MIMO Relaying Systems”. In: *IEEE Transactions on Communications* (2013) (cit. on pp. 92, 107).

[100]B. Maham and A. Hjørungnes. “Distributed GABBA space-time codes in amplify-and-forward cooperation”. In: *Proceedings of the 2007 IEEE Information Theory Workshop on Information Theory for Wireless Networks, ITW*. 2007, pp. 189–193 (cit. on pp. 92, 105, 107).

[101]B. Maham, A. Hjørungnes, and G. Abreu. “Distributed GABBA space-time codes with complex signal constellations”. In: *SAM 2008 - 5th IEEE Sensor Array and Multichannel Signal Processing Workshop*. 2008, pp. 118–121 (cit. on pp. 92, 105, 107).

[102]B. Maham, A. Hjørungnes, and G. Abreu. “Distributed GABBA space-time codes in amplify-and-forward relay networks”. In: *IEEE Transactions on Wireless Communications* 8.4 (2009), pp. 2036–2045 (cit. on pp. 92, 101, 105, 107, 123, 124).

[103]T. Giuseppe and D. Freitas. “Generalized ABBA Space-Time Block Codes”. In: *CoRR* abs/cs/0510003 (2005) (cit. on pp. 92, 101, 107).

[104]Md Z. A. Khan and B. S. Rajan. “Single-symbol maximum likelihood decodable linear STBCs”. In: *IEEE Transactions on Information Theory* 52.5 (2006), pp. 2062–2091 (cit. on pp. 98, 99).

[105]Y. Chang and Y. Hua. “Diversity analysis of orthogonal space-time modulation for distributed wireless relays”. In: *IEEE International Conference on Acoustics, Speech and Signal Processing (ICASSP)*. Vol. 4. 2004, pp. IV–561–IV–564 (cit. on p. 99).

[106]M. C. Ju, H. . Song, and I. . Kim. “Exact BER analysis of distributed alamouti’s code for cooperative diversity networks”. In: *IEEE Transactions on Communications* 57.8 (2009), pp. 2380–2390 (cit. on pp. 100, 119, 123).

[107]E. Basar, U. Aygolu, E. Panayirci, and H.V. Poor. “Space-Time Block Coded Spatial Modulation”. In: *IEEE Transactions on Communications* 59.3 (Mar. 2011), pp. 823–832. ISSN: 0090-6778. DOI: 10.1109/TCOMM.2011.121410.100149 (cit. on pp. 105, 111–113, 121, 124).

[108]L. Wang, Z. Chen, and X. Wang. “A space-time block coded spatial modulation from (n,k) error correcting code”. In: *IEEE Wireless Communications Letters* 3.1 (2014), pp. 54–57 (cit. on pp. 105, 111, 112).

[109]X. Li and L. Wang. “High rate space-time block coded spatial modulation with cyclic structure”. In: *IEEE Communications Letters* 18.4 (2014), pp. 532–535 (cit. on pp. 105, 111, 112).

[110]H. . Mai, T. . Dinh, X. . Tran, M. . Le, and V. . Ngo. “A novel spatially-modulated orthogonal space-time block code for 4 transmit antennas”. In: *IEEE International Symposium on Signal Processing and Information Technology (ISSPIT)*. 2012, pp. 119–123 (cit. on pp. 105, 111, 112).

[111]M. . Le, V. . Ngo, H. . Mai, X. N. Tran, and M. Di Renzo. “Spatially modulated orthogonal space-time block codes with non-vanishing determinants”. In: *IEEE Transactions on Communications* 62.1 (2014), pp. 85–99 (cit. on pp. 105, 111, 112).

[112]M.-T. El Astal, B. Salmon, and J.C. Olivier. “Full-space diversity and full-rate distributed space-time block codes for amplify-and-forward relaying networks”. English. In: *IET, The Journal of Engineering* 1 (1 Feb. 2009), –(0) (cit. on p. 107).

[113]R.Y. Mesleh, H. Haas, S. Sinanovic, Chang Wook Ahn, and Sangboh Yun. “Spatial Modulation”. In: *IEEE Transactions on Vehicular Technology* 57.4 (July 2008), pp. 2228–2241. ISSN: 0018-9545. DOI: 10.1109/TVT.2007.912136 (cit. on pp. 107, 123, 124).

[114]P. Yang, B. Zhang, Y. Xiao, et al. “Detect-and-forward relaying aided cooperative spatial modulation for wireless networks”. In: *IEEE Transactions on Communications* 61.11 (2013), pp. 4500–4511 (cit. on p. 107).

[115]R. Mesleh, S. Ikki, and M. Alwakeel. “Performance analysis of space shift keying with amplify and forward relaying”. In: *IEEE Communications Letters* 15.12 (2011), pp. 1350–1352 (cit. on p. 107).

[116]S. Sugiura, S. Chen, H. Haas, P. M. Grant, and L. Hanzo. “Coherent versus non-coherent decode-and-forward relaying aided cooperative space-time shift keying”. In: *IEEE Transactions on Communications* 59.6 (2011), pp. 1707–1719 (cit. on p. 107).

[117]Raed Mesleh, Salama Ikki, El-Hadi Aggoune, and Ali Mansour. “Performance analysis of space shift keying (SSK) modulation with multiple cooperative relays”. In: *EURASIP Journal on Advances in Signal Processing* 2012.1 (2012), p. 201. ISSN: 1687-6180. DOI: 10.1186/1687-6180-2012-201 (cit. on p. 107).

[118]R. Mesleh and S. S. Ikki. “Performance analysis of spatial modulation with multiple decode and forward relays”. In: *IEEE Wireless Communications Letters* 2.4 (2013), pp. 423–426 (cit. on p. 107).

[119]Y. Yang and S. Aïssa. “Information-guided transmission in decode-and-forward relaying systems: Spatial exploitation and throughput enhancement”. In: *IEEE Transactions on Wireless Communications* 10.7 (2011), pp. 2341–2351 (cit. on p. 107).

[120]D. Yang, C. Xu, L. . Yang, and L. Hanzo. “Transmit-diversity-assisted space-shift keying for colocated and distributed/cooperative MIMO elements”. In: *IEEE Transactions on Vehicular Technology* 60.6 (2011), pp. 2864–2869 (cit. on p. 107).

[121]Sergey Kitaev. *Patterns in permutations and words*. Springer, 2011 (cit. on p. 114).

[122]Carla Savage. “A survey of combinatorial Gray codes”. In: *SIAM review* 39.4 (1997), pp. 605–629 (cit. on p. 114).

[123]T. Hough and F. Ruskey. “An efficient implementation of the Eades, Hickey, Read adjacent interchange combination generation algorithm”. In: *J. Comb. Math. and Comb. Comp.* 4 (1988), pp. 79–86 (cit. on p. 114).

[124]Al-Tous Hanan and Barhumi Imad. “Performance analysis of relay selection in cooperative networks over Rayleigh flat fading channels”. In: *EURASIP Journal on Wireless Communications and Networking* 2012.10 (2012), p. 224. ISSN: 1687-1499. DOI: 10.1186/1687-1499-2012-224 (cit. on p. 123).

[125]S. Narayanan, M. Di Renzo, F. Graziosi, and H. Haas. “Distributed spatial modulation for relay networks”. In: *IEEE Vehicular Technology Conference*. 2013 (cit. on pp. 123, 124).

[126]A.F. Naguib, N. Seshadri, and A.R. Calderbank. “Applications of Space-Time Block Codes and Interference Suppression for High Capacity and High Data Rate Wireless Systems”. In: *Proc. 1998 Asilomar Conference on on Signals, Systems, and Computers, Pacific Grove, CA, USA, (Asilomar’98)*. DOI: 10.1109/ACSSC.1998.751635 (cit. on p. 136).

[127]A. Stamoulis, N. Al-Dhahir, and A. R. Calderbank. “Further results on interference cancellation and space-time block codes”. In: *Conference Record of the Asilomar Conference on Signals, Systems and Computers*. Vol. 1. 2001, pp. 257–261 (cit. on p. 136).

[128]J. Kazemitabar and H. Jafarkhani. “Multiuser interference cancellation and detection for users with more than two transmit antennas”. In: *IEEE Transactions on Communications* 56.4 (2008), pp. 574–583 (cit. on p. 136).

[129]X. Guo and X. . Xia. “On full diversity space-time block codes with partial interference cancellation group decoding”. In: *IEEE Transactions on Information Theory* 55.10 (2009), pp. 4366–4385 (cit. on pp. 136, 145, 149, 153).

[130]X. Guo and Xiang-Gen Xia. “Correction to ";On Full Diversity Space-Time Block Codes With Partial Interference Cancellation Group Decoding”. In: *IEEE Transactions on Information Theory* 56.7 (2010), pp. 3635–3636. ISSN: 0018-9448. DOI: 10.1109/TIT.2010.2048465 (cit. on pp. 136, 145, 149, 153).

[131]Long Shi, Wei Zhang, and Xiang-Gen Xia. “On Designs of Full Diversity Space-Time Block Codes for Two-User MIMO Interference Channels”. In: *IEEE Transactions on Wireless Communications* 11.11 (2012), pp. 4184–4191. ISSN: 1536-1276. DOI: 10.1109/TWC.2012.101112.120462 (cit. on p. 137).

[132]Amr Ismail and Mohamed-Slim Alouini. “On Low-Complexity Full-diversity Detection of Multi-User Space-Time Coding”. In: *IEEE International Conference on Communications*. 2013 (cit. on pp. 137, 153).

[133]L. Li, Y. Jing, and H. Jafarkhani. “Multisource transmission for wireless relay networks with linear complexity”. In: *IEEE Transactions on Signal Processing* 59.6 (2011), pp. 2898–2912 (cit. on pp. 137, 140, 157, 161).

[134]L. Li, Y. Jing, and H. Jafarkhani. “Interference cancellation at the relay for multi-user wireless cooperative networks”. In: *IEEE Transactions on Wireless Communications* 10.3 (2011), pp. 930–939 (cit. on pp. 137, 139, 140, 156, 157, 161).

[135]J. Xu, S. Zhou, and Z. Niu. “Interference-aware relay selection for multiple source-destination cooperative networks”. In: *2009 15th Asia-Pacific Conference on Communications, APCC 2009*. 2009, pp. 338–341 (cit. on p. 138).

[136]N. Yang, M. Elkashlan, and J. Yuan. “Cooperative selection diversity in wireless multiuser relay networks”. In: *IEEE Vehicular Technology Conference*. 2010 (cit. on p. 138).

[137]A. Wittneben and B. Rankov. “Distributed antenna systems and linear relaying for gigabit MIMO wireless”. In: *IEEE Vehicular Technology Conference*. Vol. 60. 2004. Chap. 5, pp. 3624–3630 (cit. on p. 138).

[138]A. Wittneben. “Coherent multiuser relaying with partial relay cooperation”. In: *IEEE Wireless Communications and Networking Conference (WCNC)*. Vol. 2. 2006, pp. 1027–1033 (cit. on p. 138).

[139]B. Niu, O. Simeone, O. Somekh, and A.M. Haimovich. “Throughput of two-hop wireless networks with relay cooperation”. In: *Allerton Conference*. 2007 (cit. on p. 138).

[140]S. Berger and A. Wittneben. “Cooperative distributed multiuser MSE relaying in wireless ad-hoc networks”. In: *Conference Record - Asilomar Conference on Signals, Systems and Computers*. Vol. 2005. 2005, pp. 1072–1076 (cit. on p. 138).

[141]A. El-Keyi and B. Champagne. “Cooperative MIMO-beamforming for multiuser relay networks”. In: *IEEE International Conference on Acoustics, Speech and Signal Processing (ICSSP*. 2008, pp. 2749–2752 (cit. on p. 138).

[142]Ö. Oyman and A. J. Paulraj. “Power-bandwidth tradeoff in dense multi-antenna relay networks”. In: *IEEE Transactions on Wireless Communications* 6.6 (2007), pp. 2282–2293 (cit. on p. 138).

[143]A. Ö. Yilmaz. “Cooperative multiple-access in fading relay channels”. In: *IEEE International Conference on Communications*. Vol. 10. 2006, pp. 4532–4537 (cit. on p. 139).

[144]Y. Jing and H. Jafarkhani. “Interference cancellation in distributed space-time coded wireless relay networks”. In: *IEEE International Conference on Communications*. 2009 (cit. on p. 139).

[145]L. Li, Y. Jing, and H. Jafarkhani. “Interference cancellation at the relay in two user wireless relay networks”. In: *IEEE Wireless Communications and Networking Conference (WCNC)*. 2010 (cit. on p. 139).

[146]L. Li, Y. Jing, and H. Jafarkhani. “Transmission schemes for two-user linear multi-access relay networks”. In: *IEEE Global Telecommunications Conference (GLOBECOM)*. 2010 (cit. on pp. 139, 140).

[147]A. Ismail and M.-S. Alouini. “On Low-Complexity Full-diversity Detection In Multi-User MIMO Multiple-Access Channels”. In: *ArXiv e-prints* (Jan. 2014). arXiv: 1401.4834 [cs.IT] (cit. on p. 149).

[148]M. C. Ju, H. . Song, and I. . Kim. “Exact BER nalysis of distributed alamouti’s code for cooperative diversity networks”. In: *IEEE Transactions on Communications* 57.8 (2009), pp. 2380–2390 (cit. on p. 151).

[149]Emanuele Viterbo. *Table of best known full diversity algebraic rotations*. Monash University. Mar. 2005. URL: http://www.ecse.monash.edu.au/staff/eviterbo/rotations/rotations.html (cit. on pp. 153–155).

[150]Sharon L. Ronald E. Walpole Raymond H. Myers and Myers Keying Ye. *Probability & Statistics for Engineers & Scientists*. 9th edition. Prentice Hall, 2011 (cit. on p. 163).